
Quantum Electrodynamic Bound–State Calculations and Large–Order Perturbation Theory

based on a

Habilitation Thesis
Dresden University of Technology

by

Ulrich Jentschura

1st Edition June 2002

2nd Edition April 2003

[with hypertext references and updates]

3rd Edition April 2004

E–Mail:

jentschura@physik.uni-freiburg.de and ulj@nist.gov

This manuscript is also available – in the form of a book – from

Shaker Verlag GmbH, Postfach 101818, 52018 Aachen, Germany,
world-wide web address: <http://www.shaker.de>,
electronic-mail address: info@shaker.de.

It has been posted in the online archives with permission of the publisher.

Contents

| | | |
|----------|--|-----------|
| I | Quantum Electrodynamic Bound–State Calculations | 7 |
| 1 | Numerical Calculation of the One–Loop Self Energy (Excited States) | 8 |
| 1.1 | Orientation | 8 |
| 1.2 | Introduction to the Numerical Calculation of Radiative Corrections | 8 |
| 1.3 | Method of Evaluation | 9 |
| 1.3.1 | Status of Analytic Calculations | 9 |
| 1.3.2 | Formulation of the Numerical Problem | 12 |
| 1.3.3 | Treatment of the divergent terms | 15 |
| 1.4 | The Low-Energy Part | 17 |
| 1.4.1 | The Infrared Part | 17 |
| 1.4.2 | The Middle-Energy Subtraction Term | 21 |
| 1.4.3 | The Middle-Energy Remainder | 22 |
| 1.5 | The High-Energy Part | 25 |
| 1.5.1 | The High-Energy Subtraction Term | 25 |
| 1.5.2 | The High-Energy Remainder | 27 |
| 1.5.3 | Results for the High-Energy Part | 29 |
| 1.6 | Comparison to Analytic Calculations | 29 |
| 2 | Analytic Self–Energy Calculations for Excited States | 34 |
| 2.1 | Orientation | 34 |
| 2.2 | The epsilon-Method | 35 |
| 2.3 | Results for High– and Low–Energy Contributions | 37 |
| 2.3.1 | P _{1/2} states ($\kappa = 1$) | 37 |
| 2.3.2 | P _{3/2} states ($\kappa = -2$) | 38 |
| 2.3.3 | D _{3/2} states ($\kappa = 2$) | 39 |
| 2.3.4 | D _{5/2} states ($\kappa = -3$) | 39 |
| 2.3.5 | F _{5/2} states ($\kappa = 3$) | 40 |
| 2.3.6 | F _{7/2} states ($\kappa = -4$) | 40 |
| 2.3.7 | G _{7/2} states ($\kappa = 4$) | 41 |
| 2.3.8 | G _{9/2} states ($\kappa = -5$) | 41 |
| 2.4 | Summary of Results | 41 |
| 2.5 | Typical Cancellations | 41 |
| 2.6 | Observations | 42 |

| | | |
|-----------|---|------------|
| 3 | The Two-Loop Self-Energy | 45 |
| 3.1 | Orientation | 45 |
| 3.2 | Introduction to the Two-Loop Self-Energy | 45 |
| 3.3 | Two-loop Form Factors | 47 |
| 3.4 | High-Energy Part | 50 |
| 3.5 | Low-Energy Part | 52 |
| 3.6 | Results for the Two-Loop Corrections | 55 |
| 4 | Spinless Particles in Bound-State Quantum Electrodynamics | 56 |
| 4.1 | Orientation | 56 |
| 4.2 | Introduction to Spinless QED and Pionium | 56 |
| 4.3 | Breit hamiltonian for Spinless Particles | 56 |
| 4.4 | Vacuum Polarization Effects | 60 |
| 4.5 | Effects due to Scalar QED | 60 |
| 5 | QED Calculations: A Summary | 63 |
| II | Convergence Acceleration and Divergent Series | 67 |
| 6 | Introduction to Convergence Acceleration and Divergent Series in Physics | 68 |
| 7 | Convergence Acceleration | 71 |
| 7.1 | The Concept of Convergence Acceleration | 71 |
| 7.1.1 | A Brief Survey | 71 |
| 7.1.2 | The Forward Difference Operator | 72 |
| 7.1.3 | Linear and Logarithmic Convergence | 72 |
| 7.1.4 | The Standard Tool: Padé Approximants | 73 |
| 7.1.5 | Nonlinear Sequence Transformations | 74 |
| 7.1.6 | The Combined Nonlinear-Condensation Transformation (CNCT) | 77 |
| 7.2 | Applications of Convergence Acceleration Methods | 79 |
| 7.2.1 | Applications in Statistics and Applied Biophysics | 79 |
| 7.2.2 | An Application in Experimental Mathematics | 80 |
| 7.2.3 | Other Applications of the CNCT | 84 |
| 7.3 | Conclusions and Outlook for Convergence Acceleration | 84 |
| 8 | Divergent Series | 86 |
| 8.1 | Introduction to Divergent Series in Physics | 86 |
| 8.2 | The Stark Effect: A Paradigmatic Example | 87 |
| 8.2.1 | Perturbation Series for the Stark Effect | 87 |
| 8.2.2 | Borel-Padé Resummation | 88 |
| 8.2.3 | Doubly-Cut Borel Plane | 90 |
| 8.2.4 | Numerical Calculations for the Stark Effect | 92 |
| 8.3 | Further Applications of Resummation Methods | 95 |
| 8.3.1 | Zero-Dimensional Theories with Degenerate Minima | 95 |
| 8.3.2 | The Effective Action as a Divergent Series | 98 |
| 8.3.3 | The Double-Well Problem | 103 |
| 8.4 | Divergent Series: Some Conclusions | 108 |
| 9 | Conclusions | 111 |

Abstract

This Thesis is based on quantum electrodynamic (QED) bound-state calculations [1, 2, 3, 4, 5, 6, 7, 8, 9, 10, 11, 12, 13, 14, 15, 16, 17, 18, 19, 20, 21, 22], as well as on investigations related to divergent series, convergence acceleration and applications of these concepts to physical problems [23, 24, 25, 26, 27, 28, 29, 30, 31].

The subjects which are discussed in this Thesis include: the self energy of a bound electron and the spin-dependence of QED corrections in bound systems (Chs. 1 – 5), convergence acceleration techniques (Chs. 6 and 7), and resummation methods for divergent series with an emphasis on physical applications (Ch. 8).

In **Chapter 1**, we present numerical results [12], accurate to the level of 1 Hz for atomic hydrogen, for the energy correction to the K and L shell states due to the one-loop self energy. We investigate hydrogenlike systems with low nuclear charge number $Z = 1-5$. Calculations are carried out using on-mass shell renormalization, which guarantees that the final result is written in terms of the physical electron charge. The purpose of the calculation is twofold: first, we provide accurate theoretical predictions for the one-loop self energy of K and L shell states. Second, the comparison of the analytic and numerical approaches to the Lamb shift calculations, which have followed separate paths for the past few decades, is demonstrated by comparing the numerical values with analytic data obtained using the $Z\alpha$ -expansion [1, 2, 32]. Our calculation essentially eliminates the uncertainty due to the truncation of the $Z\alpha$ -expansion, and it demonstrates the consistency of the numerical and analytic approaches which have attracted attention for more than five decades, beginning with the seminal paper [33]. The most important numerical results are summarized in Table 1.5.

In **Chapter 2**, we investigate higher-order analytic calculations of the one-photon self energy for excited atomic states. These calculations rely on mathematical methods described in Sec. 2.2 which, in physical terms, lead to a separation of the calculation into a high- and a low-energy part for the virtual photon. This separation does not only permit adequate simplifications for the two energy regions [1, 2], but also an adequate treatment of the infrared divergences which plague all bound-state calculations (see also Ch. 7 of [34]). The investigation represents a continuation of previous work on the subject [1, 2, 32]. The calculations are relevant for transitions to highly excited states, which are relevant for the extraction of fundamental constants from the high-precision measurements in atomic hydrogen [35], and for the estimation of QED effects in more complex atomic systems where some of the electrons occupy highly excited states.

Chapter 3. We investigate the two-loop self energy. The calculation is based on a generalization of the methods introduced in Sec. 2.2. Historically, the two-loop self energy for bound states has represented a major task for theoretical evaluations. We present an analytic calculation [16] of the fine-structure difference of the two-loop self energy for P states in atomic hydrogen in the order $\alpha^2 (Z\alpha)^6 m_e c^2$. This energy difference can be parameterized by two analytic coefficients, known as B_{61} and B_{60} (see Sec. 3.2). These coefficients describe the two-loop self energy in the sixth order in $Z\alpha$, with an additional enhancement due to a large logarithm $\ln[(Z\alpha)^{-2}]$ (in the case of the B_{61} -coefficient). The calculations are relevant for an improved theoretical understanding of the fine-structure in hydrogenlike systems. They are also in part relevant for current experiments on atomic helium [36, 37, 38, 39], whose motivation is the determination of the fine-structure constant with improved accuracy. Finally, it is hoped that numerical calculations of the two-loop effect will be carried out in the near future for which the current analytic evaluation will be an important consistency check. The calculation of the analytic corrections discussed in Sec. 3 represents a solution for the most problematic set of diagrams on the way to advance our understanding of the fine-structure in atomic hydrogen to the few-Hz level. Explicit results for the fine-structure difference of

the B_{61} - and B_{60} -coefficients can be found in Eqs. (3.59) – (3.64).

In **Chapter 4**, We investigate the spin-dependence of the Breit hamiltonian and quantum electrodynamic effects in general. Specifically, we consider a bound system of two spinless particles. The calculation is motivated in part by current experiments (DIRAC at CERN) whose aim is the experimental study of pionium, which is the bound system of two (spinless) oppositely charged pions. The evaluation of the two-body relativistic corrections of order $(Z\alpha)^4$ leads to a different result [17] than expected for a system of two spin-1/2 particles of equal mass, e.g. positronium. In particular, we conclude in Sec. 4.3 that the so-called zitterbewegung term is absent for a system of two spinless particles (the absence of the zitterbewegung term in a bound system consisting of a spinless and a spin-1/2 particle was previously pointed out in [40]). Final results for the relativistic correction, the vacuum polarization, and the self energy of a system of two scalar particles can be found in Eqs. (4.15), (4.21) and (4.31). A summary of the QED calculations is provided in **Chapter 5**.

In the second part of this Thesis, we discuss methods for *accelerating the convergence* of series, and for the *resummation of divergent series*. As discussed in **Chapter 6** and Sec. 7.1.1, convergence acceleration is essentially based on the idea that information hidden in trailing digits of elements of the sequence can be used in order to make “educated guesses” regarding the remainder term, which can be used for the construction of powerful sequence transformations (see Sec. 7.1.5). In **Chapter 7**, we discuss convergence acceleration in detail. After a short overview of relevant mathematical methods (Sec. 7.1), we discuss applications in applied biophysics (Sec. 7.2.1), in experimental mathematics (Sec. 7.2.2), and other applications, mainly in the evaluation of special functions (Sec. 7.2.3). In particular, Secs. 7.2.1 – 7.2.3 illustrate how the combined nonlinear-condensation transformation (CNCT) described in Sec. 7.1.6 can be used for the accelerated evaluation of nonalternating series, with an emphasis to applications of practical significance (Sec. 7.2.1).

The discussion on convergence acceleration in Ch. 7 is complemented in **Chapter 8** by an overview of resummation techniques and relevant applications. Using the Stark effect and the associated autoionization width as a paradigmatic example, we discuss basic concepts like the Borel resummation method and its generalizations (Sec. 8.2.2), and the conformal mapping of the complex plane (Sec. 8.4). We then proceed to discuss further applications of resummation methods like zero-dimensional model theories (Sec. 8.3.1), the QED effective action (expressed as a perturbation series in the fine structure constant, see Sec. 8.3.2), and the quantum-mechanical double-well problem (Sec. 8.3.3). Within the context of the double-well problem, we perform an analytic evaluation of higher-order corrections to the two-instanton effect and demonstrate the consistency of numerically determined energy levels with the instanton expansion.

We conclude with a summary of the results in **Chapter 9**, where we also explain the interrelations and connections between the different subjects treated in this Thesis.

Part I

Quantum Electrodynamic Bound–State Calculations

Chapter 1

Numerical Calculation of the One-Loop Self Energy (Excited States)

1.1 Orientation

A nonperturbative numerical evaluation of the one-photon electron self energy for the K- and L-shell states of hydrogenlike ions with nuclear charge numbers $Z = 1$ to 5 is described. Our calculation for the $1S_{1/2}$ state has a numerical uncertainty of 0.8 Hz in atomic hydrogen, and for the L-shell states ($2S_{1/2}$, $2P_{1/2}$, and $2P_{3/2}$) the numerical uncertainty is 1.0 Hz. The method of evaluation for the ground state and for the excited states is described in detail. The numerical results are compared to results based on known terms in the expansion of the self energy in powers of $Z\alpha$.

1.2 Introduction to the Numerical Calculation of Radiative Corrections

The nonperturbative numerical evaluation of radiative corrections to bound-state energy levels is interesting for two reasons. First, the recent dramatic increase in the accuracy of experiments that measure the transition frequencies in hydrogen and deuterium [35, 41, 42] necessitates a numerical evaluation (nonperturbative in the binding Coulomb field) of the radiative corrections to the spectrum of atomic systems with low nuclear charge Z . Second, the numerical calculation serves as an independent test of analytic evaluations which are based on an expansion in the binding field with an expansion parameter $Z\alpha$.

In order to address both issues, a high-precision numerical evaluation of the self energy of an electron in the ground state in hydrogenlike ions has been performed [9, 12, 43]. The approach outlined in [9] is generalized here to the L shell, and numerical results are obtained for the ($n = 2$) states $2S_{1/2}$, $2P_{1/2}$ and $2P_{3/2}$. Results are provided for atomic hydrogen, He^+ , Li^{2+} , Be^{3+} , and B^{4+} .

It has been pointed out in [9, 43] that the nonperturbative effects (in $Z\alpha$) can be large even for low nuclear charge and exceed the current experimental accuracy for atomic transitions. For example, the difference between the sum of the analytically evaluated terms up to the order of $\alpha(Z\alpha)^6$ and the final numerical result for the ground state is roughly 27 kHz for atomic hydrogen and about 3200 kHz for He^+ . For the 2S state the difference is 3.5 kHz for atomic hydrogen and 412 kHz for He^+ . The large difference between the result obtained by an expansion in $Z\alpha$ persists even after the inclusion of a result recently obtained in [44] for the logarithmic term of order $\alpha(Z\alpha)^7 \ln(Z\alpha)^{-2}$. For the ground state, the difference between the all-order numerical result and the sum of the perturbative terms is still 13 kHz for atomic hydrogen and 1600 kHz for He^+ . For the 2S state, the difference amounts to 1.6 kHz for atomic hydrogen and to 213 kHz for He^+ .

These figures should be compared to the current experimental precision. The most accurately measured transition to date is the 1S–2S frequency in hydrogen; it has been measured with to a relative accuracy of 1.8 parts in 10^{14} or 46 Hz [42]. This experimental progress is due in part to the use of frequency chains that bridge the range between optical frequencies and the microwave cesium time standard. The accuracy of the measurement is likely to be improved by an order of magnitude in the near future [42, 45]. With trapped hydrogen atoms, it should be feasible to observe the 1S–2S frequency with an experimental linewidth that approaches the 1.3 Hz natural width of the 2S level [46, 47].

The apparent convergence of the perturbation series in $Z\alpha$ is slow. Our all-order numerical calculation presented here essentially eliminates the uncertainty from unevaluated higher-order analytic terms, and we obtain results for the self energy remainder function G_{SE} with a precision of roughly $0.8 \times Z^4$ Hz for the ground state of atomic hydrogen and $1.0 \times Z^4$ Hz for the 2S state.

In the evaluation, we take advantage of resummation and convergence acceleration techniques. The resummation techniques provide an efficient method of evaluation of the Dirac-Coulomb Green function to a relative accuracy of 10^{-24} over a wide parameter range [43]. The convergence acceleration techniques remove the principal numerical difficulties associated with the singularity of the relativistic propagators for nearly equal radial arguments [23].

The one-photon self energy is about two orders of magnitude larger than the other contributions to the Lamb shift in atomic hydrogen. Comprehensive reviews of the various contributions to the Lamb shift in hydrogenlike atoms in the full range of nuclear charge numbers $Z = 1$ –110 have been given in Refs. [48, 49, 50, 51].

1.3 Method of Evaluation

1.3.1 Status of Analytic Calculations

The (real part of the) energy shift ΔE_{SE} due to the electron self energy radiative correction is usually written as

$$\Delta E_{\text{SE}} = \frac{\alpha}{\pi} \frac{(Z\alpha)^4}{n^3} F(nl_j, Z\alpha) m_e c^2 \quad (1.1)$$

where F is a dimensionless quantity. In the following, the natural unit system with $\hbar = c = m_e = 1$ and $e^2 = 4\pi\alpha$ is employed. Note that $F(nl_j, Z\alpha)$ is a dimensionless function which depends for a given atomic state with quantum numbers n , l and j on only one argument (the coupling $Z\alpha$). For excited states, the (nonvanishing) imaginary part of the self energy is proportional to the (spontaneous) decay width of the state. We will denote here the *real* part of the self energy by ΔE_{SE} , exclusively. The semi-analytic expansion of $F(nl_j, Z\alpha)$ about $Z\alpha = 0$ for a general atomic state with quantum numbers n , l and j gives rise to the expression,

$$\begin{aligned} F(nl_j, Z\alpha) &= A_{41}(nl_j) \ln(Z\alpha)^{-2} \\ &+ A_{40}(nl_j) + (Z\alpha) A_{50}(nl_j) \\ &+ (Z\alpha)^2 [A_{62}(nl_j) \ln^2(Z\alpha)^{-2} \\ &+ A_{61}(nl_j) \ln(Z\alpha)^{-2} + G_{\text{SE}}(nl_j, Z\alpha)] . \end{aligned} \quad (1.2)$$

For particular states, some of the coefficients may vanish. Notably, this is the case for P states, which are less singular than S states at the origin [see Eq. (1.4) below]. For the $nS_{1/2}$ state ($l = 0$, $j = 1/2$), none

of the terms in Eq. (1.2) vanishes, and we have,

$$\begin{aligned}
F(nS_{1/2}, Z\alpha) &= A_{41}(nS_{1/2}) \ln(Z\alpha)^{-2} \\
&+ A_{40}(nS_{1/2}) + (Z\alpha) A_{50}(nS_{1/2}) \\
&+ (Z\alpha)^2 [A_{62}(nS_{1/2}) \ln^2(Z\alpha)^{-2} \\
&+ A_{61}(nS_{1/2}) \ln(Z\alpha)^{-2} + G_{\text{SE}}(nS_{1/2}, Z\alpha)] .
\end{aligned} \tag{1.3}$$

The A coefficients have two indices, the first of which denotes the power of $Z\alpha$ [including those powers implicitly contained in Eq. (1.1)], while the second index denotes the power of the logarithm $\ln(Z\alpha)^{-2}$. For P states, the coefficients A_{41} , A_{50} and A_{62} vanish, and we have

$$F(nP_j, Z\alpha) = A_{40}(nP_j) + (Z\alpha)^2 [A_{61}(nP_j) \ln(Z\alpha)^{-2} + G_{\text{SE}}(nP_j, Z\alpha)] . \tag{1.4}$$

For S states, the self energy remainder function G_{SE} can be expanded semi-analytically as

$$G_{\text{SE}}(nS_{1/2}, Z\alpha) = A_{60}(nS_{1/2}) + (Z\alpha) [A_{71}(nS_{1/2}) \ln(Z\alpha)^{-2} + A_{70}(nS_{1/2}) + o(Z\alpha)] . \tag{1.5}$$

For the “order” symbols o and O we follow the usual convention [52, 53]: the requirement is $O(x)/x \rightarrow \text{const.}$ as $x \rightarrow 0$, whereas $o(x)$ fulfills the *weaker* requirement $o(x) \rightarrow 0$ as $x \rightarrow 0$. For example, the expression $[(Z\alpha) \ln(Z\alpha)]$ is $o(Z\alpha)$ but *not* $O(Z\alpha)$. Because logarithmic terms corresponding to a nonvanishing A_{83} -coefficient must be expected in Eq. (1.5), the symbol $o(Z\alpha)$ should be used to characterize the remainder, *not* $O(Z\alpha)$.

For P states, the semi-analytic expansion of G_{SE} reads

$$G_{\text{SE}}(nP_j, Z\alpha) = A_{60}(nP_j)(Z\alpha) [A_{70}(nP_j) + o(Z\alpha)] . \tag{1.6}$$

The fact that $A_{71}(nP_j)$ vanishes has been pointed out in [44]. We list below the analytic coefficients and the Bethe logarithms relevant to the atomic states under investigation. For the ground state, the coefficients A_{41} and A_{40} were obtained in [33, 54, 55, 56, 57, 58, 59], the correction term A_{50} was found in [60, 61, 62], and the higher-order binding corrections A_{62} and A_{61} were evaluated in [32, 63, 64, 65, 66, 67, 68, 69, 70, 71]. The results are,

$$\begin{aligned}
A_{41}(1S_{1/2}) &= \frac{4}{3} , \\
A_{40}(1S_{1/2}) &= \frac{10}{9} - \frac{4}{3} \ln k_0(1S) , \\
A_{50}(1S_{1/2}) &= 4\pi \left[\frac{139}{128} - \frac{1}{2} \ln 2 \right] , \\
A_{62}(1S_{1/2}) &= -1 , \\
A_{61}(1S_{1/2}) &= \frac{28}{3} \ln 2 - \frac{21}{20} .
\end{aligned} \tag{1.7}$$

The Bethe logarithm $\ln k_0(1S)$ has been evaluated in [72] and [73, 74, 75, 76, 77] as

$$\ln k_0(1S) = 2.984\,128\,555\,8(3) . \tag{1.8}$$

For the 2S state, we have

$$\begin{aligned}
A_{41}(2S_{1/2}) &= \frac{4}{3}, \\
A_{40}(2S_{1/2}) &= \frac{10}{9} - \frac{4}{3} \ln k_0(2S), \\
A_{50}(2S_{1/2}) &= 4\pi \left[\frac{139}{128} - \frac{1}{2} \ln 2 \right], \\
A_{62}(2S_{1/2}) &= -1, \\
A_{61}(2S_{1/2}) &= \frac{16}{3} \ln 2 + \frac{67}{30}.
\end{aligned} \tag{1.9}$$

The Bethe logarithm $\ln k_0(2S)$ has been evaluated (see [72, 73, 74, 75, 76, 77], the results exhibit varying accuracy) as

$$\ln k_0(2S) = 2.811\,769\,893(3). \tag{1.10}$$

It might be worth noting that the value for $\ln k_0(2S)$ given in [78] evidently contains a typographical error. Our independent re-evaluation confirms the result given in Eq. (1.10), which was originally obtained in [72] to the required precision. For the $2P_{1/2}$ state we have

$$\begin{aligned}
A_{40}(2P_{1/2}) &= -\frac{1}{6} - \frac{4}{3} \ln k_0(2P), \\
A_{61}(2P_{1/2}) &= \frac{103}{108}.
\end{aligned} \tag{1.11}$$

Note that a general analytic result for the logarithmic correction A_{61} as a function of the bound state quantum numbers n , l and j can be inferred from Eq. (4.4a) of [68, 69] upon subtraction of the vacuum polarization contribution implicitly contained in the quoted equation. The Bethe logarithm for the 2P states reads [72, 79]

$$\ln k_0(2P) = -0.030\,016\,708\,9(3). \tag{1.12}$$

Because the Bethe logarithm is an inherently nonrelativistic quantity, it is spin-independent and therefore independent of the total angular momentum j for a given orbital angular momentum l . For the $2P_{3/2}$ state the analytic coefficients are

$$\begin{aligned}
A_{40}(2P_{3/2}) &= \frac{1}{12} - \frac{4}{3} \ln k_0(2P), \\
A_{61}(2P_{3/2}) &= \frac{29}{90}.
\end{aligned} \tag{1.13}$$

We now consider the limit of the function $G_{SE}(Z\alpha)$ as $Z\alpha \rightarrow 0$. The higher-order terms in the potential expansion (see Fig. 1.3 below) and relativistic corrections to the wavefunction both generate terms of higher order in $Z\alpha$ which are manifest in Eq. (1.2) in the form of the nonvanishing function $G_{SE}(Z\alpha)$ which summarizes the effects of the relativistic corrections to the bound electron wave function and of higher-order terms in the potential expansion. For very soft virtual photons, the potential expansion fails and generates an infrared divergence which is cut off by the atomic momentum scale, $Z\alpha$. This cut-off for the *infrared* divergence is one of the mechanisms which lead to the logarithmic terms in Eq. (1.2). Some of the nonlogarithmic terms in relative order $(Z\alpha)^2$ in Eq. (1.2) are generated by the relativistic corrections to the wave function. The function G_{SE} does not vanish, but approaches a constant in the limit $Z\alpha \rightarrow 0$. This constant can be determined by analytic or semi-analytic calculations; it is referred to as the A_{60} coefficient, i.e.

$$A_{60}(nl_j) = G_{SE}(nl_j, 0). \tag{1.14}$$

The evaluation of the coefficient $A_{60}(1S_{1/2})$ has drawn a lot of attention for a long time [32, 68, 69, 70, 71]. For the 2S state, there is currently only one accurate analytic result available,

$$A_{60}(2S_{1/2}) = -31.840\,47(1) \quad (\text{see Ref. [32]}). \quad (1.15)$$

For the $2P_{1/2}$ state, the analytically obtained result is

$$A_{60}(2P_{1/2}) = -0.998\,91(1) \quad (\text{see Ref. [1]}), \quad (1.16)$$

and for the $2P_{3/2}$ state, we have

$$A_{60}(2P_{3/2}) = -0.503\,37(1) \quad (\text{see Ref. [1]}), \quad (1.17)$$

The analytic evaluations essentially rely on an expansion of the relativistic Dirac-Coulomb propagator in powers of the binding field, i.e. in powers of Coulomb interactions of the electron with the nucleus. In numerical evaluations, the binding field is treated nonperturbatively, and no expansion is performed.

1.3.2 Formulation of the Numerical Problem

Numerical cancellations are severe for small nuclear charges. In order to understand the origin of the numerical cancellations it is necessary to consider the renormalization of the self energy. The renormalization procedure postulates that the self energy is essentially the effect on the bound electron due to the self interaction with its own radiation field, minus the same effect on a free electron which is absorbed in the mass of the electron and therefore not observable. The self energy of the bound electron is the residual effect obtained after the subtraction of two large quantities. Terms associated with renormalization counterterms are of order 1 in the $Z\alpha$ -expansion, whereas the residual effect is of order $(Z\alpha)^4$ [see Eq. (1.1)]. This corresponds to a loss of roughly 9 significant digits at $Z = 1$. Consequently, even the precise evaluation of the one-photon self energy in a Coulomb field presented in [80] extends only down to $Z = 5$. Among the self energy corrections in one-loop and higher-loop order, numerical cancellations in absolute terms are most severe for the *one*-loop problem because of the large size of the effect of the one-loop self energy correction on the spectrum.

For our high-precision numerical evaluation, we start from the regularized and renormalized expression for the one-loop self energy of a bound electron,

$$\begin{aligned} \Delta E_{\text{SE}} &= \lim_{\Lambda \rightarrow \infty} \left\{ i e^2 \text{Re} \int_{C_F} \frac{d\omega}{2\pi} \int \frac{d^3\mathbf{k}}{(2\pi)^3} D_{\mu\nu}(k^2, \Lambda) \right. \\ &\quad \times \left\langle \bar{\psi} \left| \gamma^\mu \frac{1}{\not{p} - \not{k} - 1 - \gamma^0 V} \gamma^\nu \right| \psi \right\rangle - \Delta m \Big\} \\ &= \lim_{\Lambda \rightarrow \infty} \left\{ -i e^2 \text{Re} \int_C \frac{d\omega}{2\pi} \int \frac{d^3\mathbf{k}}{(2\pi)^3} D_{\mu\nu}(k^2, \Lambda) \right. \\ &\quad \times \left\langle \psi \left| \alpha^\mu e^{i\mathbf{k}\cdot\mathbf{x}} G(E_n - \omega) \alpha^\nu e^{-i\mathbf{k}\cdot\mathbf{x}} \right| \psi \right\rangle - \Delta m \Big\}, \end{aligned} \quad (1.18)$$

where G denotes the Dirac-Coulomb propagator,

$$G(z) = \frac{1}{\boldsymbol{\alpha} \cdot \mathbf{p} + \beta + V - z}, \quad (1.19)$$

and Δm is the Λ -dependent (cutoff-dependent) one-loop mass-counter term,

$$\Delta m = \frac{\alpha}{\pi} \left(\frac{3}{4} \ln \Lambda^2 + \frac{3}{8} \right) \langle \beta \rangle. \quad (1.20)$$

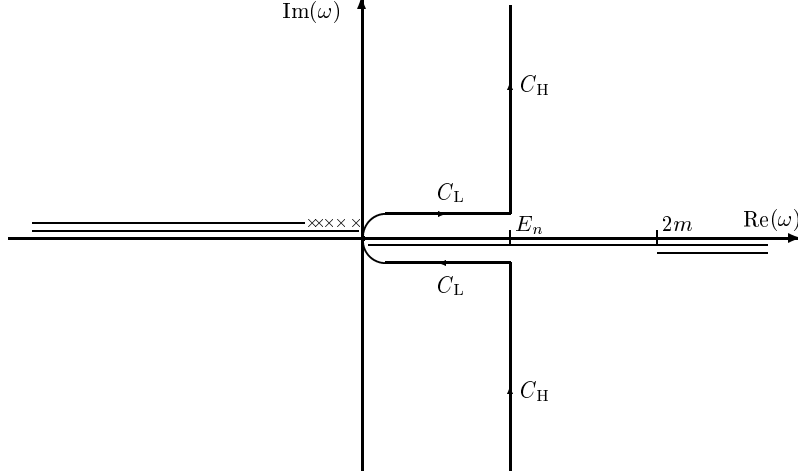


Figure 1.1: Integration contour \mathcal{C} for the integration over the energy $\omega = E_n - z$ of the virtual photon. The contour \mathcal{C} consists of the low-energy contour C_L and the high-energy contour C_H . Lines shown displaced directly below and above the real axis denote branch cuts from the photon and electron propagator. Crosses denote poles originating from the discrete spectrum of the electron propagator. The contour used in this work corresponds to the one used in [81].

The photon propagator $D_{\mu\nu}(k^2, \Lambda)$ in Eq. (1.18) in Feynman gauge reads

$$D_{\mu\nu}(k^2, \Lambda) = - \left(\frac{g_{\mu\nu}}{k^2 + i\epsilon} - \frac{g_{\mu\nu}}{k^2 - \Lambda^2 + i\epsilon} \right). \quad (1.21)$$

The contour C_F in Eq. (1.18) is the Feynman contour, whereas the contour \mathcal{C} is depicted in Fig. 1.1. The contour \mathcal{C} is employed for the ω -integration in the current evaluation [see the last line of Eq. (1.18)]. The energy variable z in Eq. (1.19) therefore assumes the value

$$z = E_n - \omega, \quad (1.22)$$

where E_n is the Dirac energy of the atomic state, and ω denotes the complex-valued energy of the virtual photon. It is understood that the limit $\Lambda \rightarrow \infty$ is taken *after* all integrals in Eq. (1.18) are evaluated.

The integration contour for the complex-valued energy of the virtual photon ω in this calculation is the contour \mathcal{C} employed in [80, 81, 82, 83] and depicted in Fig. 1.1. The integrations along the low-energy contour C_L and the high-energy contour C_H in Fig. 1.1 give rise to the low- and the high-energy contributions ΔE_L and ΔE_H to the self energy, respectively. Here, we employ a further separation of the low-energy integration contour C_L into an infrared contour C_{IR} and a middle-energy contour C_M shown in Fig. 1.2. This separation gives rise to a separation of the low-energy part ΔE_L into the infrared part ΔE_{IR} and the middle-energy part ΔE_M ,

$$\Delta E_L = \Delta E_{\text{IR}} + \Delta E_M. \quad (1.23)$$

For the low- Z systems discussed here, all complications which arise for excited states due to the decay into the ground state are relevant only for the infrared part. Except for the further separation into the infrared and the middle-energy part, the same basic formulation of the self energy problem as in [81] is

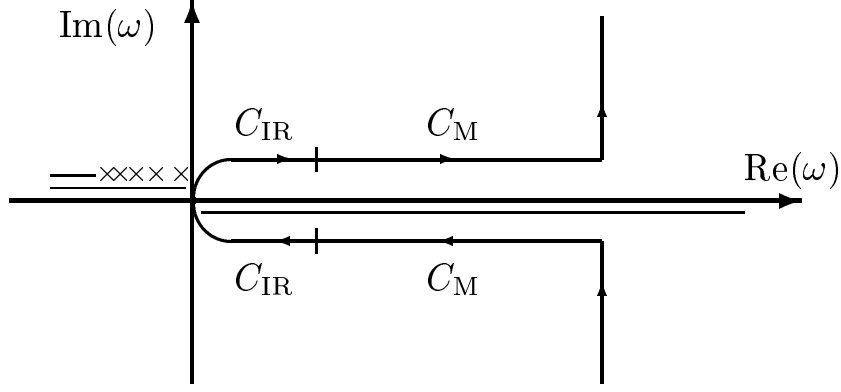


Figure 1.2: Separation of the low-energy contour C_L into the infrared part C_{IR} and the middle-energy part C_M . As in Fig. 1.1, the lines directly above and below the real axis denote branch cuts from the photon and electron propagator. Strictly speaking, the figure is valid only for the ground state. For excited states, some of the crosses, which denote poles originating from the discrete spectrum of the electron propagator, are positioned to the right of the line $\text{Re } \omega = 0$. These poles are subtracted in the numerical evaluation.

used. This leads to the following separation,

$$\begin{aligned} \omega \in (0, \frac{1}{10} E_n) \pm i\epsilon & : \text{infrared part } \Delta E_{\text{IR}}, \\ \omega \in (\frac{1}{10} E_n, E_n) \pm i\epsilon & : \text{middle-energy part } \Delta E_{\text{M}}, \\ \omega \in E_n + i(-\infty, +\infty) & : \text{high-energy part } \Delta E_{\text{H}}. \end{aligned}$$

Integration along these contours gives rise to the infrared, the middle-energy, and the high-energy contributions to the energy shift. For all of these contributions, lower-order terms are subtracted in order to obtain the contribution to the self energy of order $(Z\alpha)^4$. We obtain for the infrared part,

$$\Delta E_{\text{IR}} = \frac{\alpha}{\pi} \left[\frac{21}{200} \langle \beta \rangle + \frac{43}{600} \langle V \rangle + \frac{(Z\alpha)^4}{n^3} F_{\text{IR}}(nl_j, Z\alpha) \right], \quad (1.24)$$

where $F_{\text{IR}}(nl_j, Z\alpha)$ is a dimensionless function of order one. The middle-energy part is recovered as

$$\Delta E_{\text{M}} = \frac{\alpha}{\pi} \left[\frac{279}{200} \langle \beta \rangle + \frac{219}{200} \langle V \rangle + \frac{(Z\alpha)^4}{n^3} F_{\text{M}}(nl_j, Z\alpha) \right], \quad (1.25)$$

and the high-energy part reads [81, 82]

$$\Delta E_{\text{H}} = \Delta m + \frac{\alpha}{\pi} \left[-\frac{3}{2} \langle \beta \rangle - \frac{7}{6} \langle V \rangle + \frac{(Z\alpha)^4}{n^3} F_{\text{H}}(nl_j, Z\alpha) \right]. \quad (1.26)$$

The infrared part is discussed in Sec. 1.4.1. The middle-energy part is divided into a middle-energy subtraction term F_{MA} and a middle-energy remainder F_{MB} . The subtraction term F_{MA} is discussed in Sec. 1.4.2, the remainder term F_{MB} is treated in Sec. 1.4.3. We recover the middle-energy term as the sum

$$F_{\text{M}}(nl_j, Z\alpha) = F_{\text{MA}}(nl_j, Z\alpha) + F_{\text{MB}}(nl_j, Z\alpha). \quad (1.27)$$

A similar separation is employed for the high-energy part. The high-energy part is divided into a subtraction term F_{HA} , which is evaluated in Sec. 1.5.1, and the high-energy remainder F_{HB} , which is discussed

in Sec. 1.5.2. The sum of the subtraction term and the remainder is

$$F_{\text{H}}(nl_j, Z\alpha) = F_{\text{HA}}(nl_j, Z\alpha) + F_{\text{HB}}(nl_j, Z\alpha). \quad (1.28)$$

The total energy shift is given as

$$\begin{aligned} \Delta E_{\text{SE}} &= \Delta E_{\text{IR}} + \Delta E_{\text{M}} + E_{\text{H}} - \Delta m \\ &= \frac{\alpha (Z\alpha)^4}{\pi n^3} [F_{\text{IR}}(nl_j, Z\alpha) + F_{\text{M}}(nl_j, Z\alpha) + F_{\text{H}}(nl_j, Z\alpha)]. \end{aligned} \quad (1.29)$$

The scaled self energy function F defined in Eq. (1.1) is therefore obtained as

$$F(nl_j, Z\alpha) = F_{\text{IR}}(nl_j, Z\alpha) + F_{\text{M}}(nl_j, Z\alpha) + F_{\text{H}}(nl_j, Z\alpha). \quad (1.30)$$

In analogy to the approach described in [80, 81, 83], we define the low-energy part as the sum of the infrared part and the middle-energy part,

$$\begin{aligned} \Delta E_{\text{L}} &= \Delta E_{\text{IR}} + \Delta E_{\text{M}} \\ &= \frac{\alpha}{\pi} \left[\frac{3}{2} \langle \beta \rangle + \frac{7}{6} \langle V \rangle + \frac{(Z\alpha)^4}{n^3} F_{\text{L}}(nl_j, Z\alpha) \right], \end{aligned} \quad (1.31)$$

where

$$F_{\text{L}}(nl_j, Z\alpha) = F_{\text{IR}}(nl_j, Z\alpha) + F_{\text{M}}(nl_j, Z\alpha). \quad (1.32)$$

The limits for the functions $F_{\text{L}}(nl_j, Z\alpha)$ and $F_{\text{H}}(nl_j, Z\alpha)$ as $Z\alpha \rightarrow 0$ were obtained in [43, 82, 84].

1.3.3 Treatment of the divergent terms

The free electron propagator,

$$F = \frac{1}{\boldsymbol{\alpha} \cdot \mathbf{p} + \beta - z}, \quad (1.33)$$

and the full electron propagator G defined in Eq. (1.19), fulfill the following identity which is of particular importance for the validity of the method used in the numerical evaluation of the all-order binding correction to the Lamb shift,

$$G = F - F V F + F V G V F. \quad (1.34)$$

This identity leads naturally to a separation of the one-photon self energy into a zero-vertex, a single-vertex and a many-vertex term. This is represented diagrammatically in Fig. 1.3.

All ultraviolet divergences which occur in the one-photon problem (mass counter term and vertex divergence) are generated by the zero-vertex and the single-vertex terms. The many-vertex term is ultraviolet safe. Of crucial importance is the observation that one may additionally simplify the problem by replacing the one-potential term with an approximate expression in which the potential is “commuted to the outside”. The approximate expression generates all divergences and all terms of lower order than $\alpha (Z\alpha)^4$ present in the one-vertex term. Unlike the raw one-potential term, it is amenable to significant further simplification and can be reduced to *one*-dimensional numerical integrals which can be evaluated easily (a straightforward formulation of the self energy problem requires a *three*-dimensional numerical integration). Without this significant improvement, an all-order calculation would be much more difficult at low nuclear charge, because the lower-order terms would introduce significant further numerical cancellations.

Furthermore, the special approximate resolvent can be used effectively for an efficient subtraction scheme in the middle-energy part of the calculation. In the infrared part, such a subtraction is not used because it would introduce infrared divergences.

We now turn to the construction of the special approximate resolvent, which will be referred to as G_{A} and will be used in this calculation to isolate the ultraviolet divergences in the high-energy part (and to provide subtraction terms in the middle-energy part). It is based on an approximation to the first

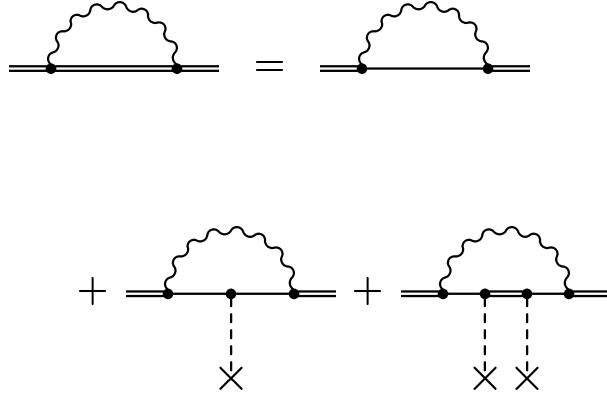


Figure 1.3: The exact expansion of the bound electron propagator in powers of the binding field leads to a zero-potential, a one-potential and a many-potential term. The dashed lines denote Coulomb photons, the crosses denote the interaction with the (external) binding field.

two terms on the right-hand side of Eq. (1.34). The so-called one-potential term FVF in Eq. (1.34) is approximated by an expression in which the potential terms V are commuted to the outside,

$$-FVF \approx -\frac{1}{2} \{V, F^2\}. \quad (1.35)$$

Furthermore, the following identity is used,

$$\begin{aligned} F^2 &= \left(\frac{1}{\boldsymbol{\alpha} \cdot \mathbf{p} + \beta - z} \right)^2 \\ &= \frac{1}{\mathbf{p}^2 + 1 - z^2} + \frac{2z(\beta + z)}{(\mathbf{p}^2 + 1 - z^2)^2} \\ &\quad + \frac{2z(\boldsymbol{\alpha} \cdot \mathbf{p})}{(\mathbf{p}^2 + 1 - z^2)^2}. \end{aligned} \quad (1.36)$$

In 2×2 spinor space, this expression may be divided into a diagonal and a non-diagonal part. The diagonal part is

$$\text{diag}(F^2) = \frac{1}{\mathbf{p}^2 + 1 - z^2} + \frac{2z(\beta + z)}{(\mathbf{p}^2 + 1 - z^2)^2}. \quad (1.37)$$

The off-diagonal part is given by

$$F^2 - \text{diag}(F^2) = \frac{2z(\boldsymbol{\alpha} \cdot \mathbf{p})}{(\mathbf{p}^2 + 1 - z^2)^2}.$$

We define the resolvent G_A as

$$G_A = F - \frac{1}{2} \{V, \text{diag}(F^2)\}. \quad (1.38)$$

All divergences which occur in the self energy are generated by the simplified propagator G_A . We define

the propagator G_B as the difference of G and G_A ,

$$\begin{aligned} G_B &= G - G_A \\ &= \frac{1}{2} \{V, \text{diag}(F^2)\} - F V F + F V G V F. \end{aligned} \quad (1.39)$$

G_B does not generate any divergences and leads to the middle-energy remainder discussed in Sec. 1.4.3 and the high-energy remainder (Sec. 1.5.2).

1.4 The Low-Energy Part

1.4.1 The Infrared Part

The infrared part is given by

$$\begin{aligned} \Delta E_{\text{IR}} &= -i e^2 \text{Re} \int_{C_{\text{IR}}} \frac{d\omega}{2\pi} \int \frac{d^3 \mathbf{k}}{(2\pi)^3} D_{\mu\nu}(k^2) \\ &\quad \times \langle \psi | \alpha^\mu e^{i\mathbf{k}\cdot\mathbf{x}} G(E_n - \omega) \alpha^\nu e^{-i\mathbf{k}\cdot\mathbf{x}} | \psi \rangle, \end{aligned} \quad (1.40)$$

where relevant definitions of the symbols can be found in Eqs. (1.18–1.21), the contour C_{IR} is as shown in Fig. 1.2, and the unregularized version of the photon propagator

$$D_{\mu\nu}(k^2) = -\frac{g_{\mu\nu}}{k^2 + i\epsilon} \quad (1.41)$$

may be used. The infrared part comprises the following integration region for the virtual photon (contour C_{IR} in Fig. 1.2),

$$\left. \begin{aligned} \omega &\in (0, 1/10 E_n) \pm i\epsilon \\ z &\in (9/10 E_n, E_n) \pm i\epsilon \end{aligned} \right\} \text{infrared part } \Delta E_{\text{IR}}. \quad (1.42)$$

Following Secs. 2 and 3 of [81], we write ΔE_{IR} as a three-dimensional integral [see, e.g., Eqs. (3.4), (3.11) and (3.14) *ibid.*]

$$\Delta E_{\text{IR}} = \frac{\alpha}{\pi} \frac{E_n}{10} - \frac{\alpha}{\pi} (\text{P.V.}) \int_{9/10 E_n}^{E_n} dz \int_0^\infty dx_1 x_1^2 \int_0^\infty dx_2 x_2^2 \mathcal{M}_{\text{IR}}(x_2, x_1, z), \quad (1.43)$$

where

$$\mathcal{M}_{\text{IR}}(x_2, x_1, z) = \sum_{\kappa} \sum_{i,j=1}^2 f_i(x_2) G_{\kappa}^{ij}(x_2, x_1, z) f_{\bar{j}}(x_1) A_{\kappa}^{ij}(x_2, x_1). \quad (1.44)$$

Here, the quantum number κ is the Dirac angular quantum number of the intermediate state,

$$\kappa = 2(l - j)(j + 1/2), \quad (1.45)$$

where l is the orbital angular momentum quantum number and j is the total angular momentum of the bound electron. The functions $f_i(x_2)$ ($i = 1, 2$) are the radial wave functions defined in Eq. (A.4) in [81] for an arbitrary bound state (and in Eq. (A.8) in [81] for the 1S state). We define $\bar{i} = 3 - i$. The functions $G_{\kappa}^{ij}(x_2, x_1, z)$ ($i, j = 1, 2$) are the radial Green functions, which result from a decomposition of the electron Green function defined in Eq. (1.19) into partial waves. The explicit formulas are given in Eq. (A.16) in [81], and we do not discuss them in any further detail, here.

The photon angular functions A_{κ}^{ij} ($i, j = 1, 2$) are defined in Eq. (3.15) of Ref. [81] for an arbitrary bound state. In Eq. (3.17) in [81], specific formulas are given for the 1S state. In Eqs. (2.2), (2.3) and (2.4) of [83], the special cases of $S_{1/2}$, $P_{1/2}$ and $P_{3/2}$ states are considered. Further relevant formulas for

excited states can be found in [85]. The photon angular functions depend on the energy argument z , but this dependence is usually suppressed. The summation over κ in Eq. (1.44) extends over all negative and all positive integers, excluding zero. We observe that the integral is symmetric under the interchange of the radial coordinates x_2 and x_1 , so that

$$\Delta E_{\text{IR}} = \frac{\alpha}{\pi} \frac{E_n}{10} - \frac{2\alpha}{\pi} (\text{P.V.}) \int_{9/10}^{E_n} dz \int_0^\infty dx_1 x_1^2 \int_0^{x_1} dx_2 x_2^2 \mathcal{M}_{\text{IR}}(x_2, x_1, z). \quad (1.46)$$

The following variable substitution,

$$r = x_2/x_1, \quad y = a x_1, \quad (1.47)$$

is made, so that $r \in (0, 1)$ and $y \in (0, \infty)$. The scaling variable a is defined as

$$a = 2 \sqrt{1 - E_n^2}. \quad (1.48)$$

The Jacobian is

$$\left| \frac{\partial(x_2, x_1)}{\partial(r, y)} \right| = \left| \begin{array}{cc} \frac{\partial x_2}{\partial r} & \frac{\partial x_1}{\partial r} \\ \frac{\partial x_2}{\partial y} & \frac{\partial x_1}{\partial y} \end{array} \right| = \frac{y}{a^2}. \quad (1.49)$$

The function S_{IR} is given by,

$$\begin{aligned} S_{\text{IR}}(r, y, z) &= -\frac{2r^2 y^5}{a^6} \mathcal{M}_{\text{IR}}\left(\frac{r y}{a}, \frac{y}{a}, z\right) \\ &= -\frac{2r^2 y^5}{a^6} \sum_{|\kappa|=1}^\infty \sum_{\kappa=\pm|\kappa|} \sum_{i,j=1}^2 f_i\left(\frac{r y}{a}\right) \\ &\quad \times G_\kappa^{ij}\left(\frac{r y}{a}, \frac{y}{a}, z\right) f_{\bar{j}}\left(\frac{y}{a}\right) A_\kappa^{ij}\left(\frac{r y}{a}, \frac{y}{a}\right) \\ &= -\frac{2r^2 y^5}{a^6} \sum_{|\kappa|=1}^\infty T_{\text{IR},|\kappa|}(r, y, z), \end{aligned} \quad (1.50)$$

where in the last line we define implicitly the terms $T_{\text{IR},|\kappa|}$ for $|\kappa| = 1, \dots, \infty$ as

$$\begin{aligned} T_{\text{IR},|\kappa|}(r, y, z) &= \sum_{\kappa=\pm|\kappa|} \sum_{i,j=1}^2 \\ &\quad f_i\left(\frac{r y}{a}\right) G_\kappa^{ij}\left(\frac{r y}{a}, \frac{y}{a}, z\right) f_{\bar{j}}\left(\frac{y}{a}\right) A_\kappa^{ij}\left(\frac{r y}{a}, \frac{y}{a}\right). \end{aligned} \quad (1.51)$$

Using the definition (1.50), we obtain for ΔE_{IR} ,

$$\begin{aligned} \Delta E_{\text{IR}} &= \frac{\alpha}{\pi} \frac{E_n}{10} + \frac{\alpha}{\pi} (\text{P.V.}) \int_{9/10}^{E_n} dz \\ &\quad \int_0^1 dr \int_0^\infty dy S_{\text{IR}}(r, y, z). \end{aligned} \quad (1.52)$$

The specification of the principal value (P.V.) is necessary for the excited states of the L shell, because of the poles along the integration contour which correspond to the spontaneous decay into the ground state. Here we are exclusively concerned with the real part of the energy shift, as specified in Eq. (1.40), which is equivalent to the specification of the principal value in (1.52). Evaluation of the integral over

z is facilitated by the subtraction of those terms which generate the singularities along the integration contour (for higher excited states, there can be numerous bound state poles, as pointed out in [2, 85]). For the 2S and $2P_{1/2}$ states, only the pole contribution from the ground state must be subtracted. For the $2P_{3/2}$ state, pole contributions originating from the 1S, the 2S and the $2P_{1/2}$ states must be taken into account. The numerical evaluation of the subtracted integrand proceeds along ideas outlined in [83, 85] and is not discussed here in any further detail.

The scaling parameter a for the integration over y is chosen to simplify the exponential dependence of the function S defined in Eq. (1.50). The main exponential dependence is given by the relativistic radial wave functions (upper and lower components). Both components $[f_1(x)$ and $f_2(x)]$ vary approximately as (neglecting relatively slowly varying factors)

$$\exp(-a x/2) \quad (\text{for large } x).$$

The scaling variable a , expanded in powers of $Z\alpha$, is

$$\begin{aligned} a &= 2\sqrt{1 - E_n^2} \\ &= 2\sqrt{1 - \left(1 - \frac{(Z\alpha)^2}{2n^2} + \mathcal{O}[(Z\alpha)^4]\right)^2} \\ &= 2\frac{Z\alpha}{n} + \mathcal{O}[(Z\alpha)^3]. \end{aligned} \quad (1.53)$$

Therefore, a is just twice the *inverse* of the Bohr radius $n/(Z\alpha)$ in the nonrelativistic limit. The product

$$f_{\bar{i}}\left(\frac{ry}{a}\right) \times f_{\bar{j}}\left(\frac{y}{a}\right) \quad \text{for arbitrary } \bar{i}, \bar{j} \in \{1, 2\}$$

[which occurs in Eq. (1.50)] depends on the radial arguments approximately as

$$e^{-y} \times \exp\left[\frac{1}{2}(1-r)y\right] \quad (\text{for large } y).$$

Note that the main dependence as given by the term $\exp(-y)$ is exactly the weight factor of the Gauß-Laguerre integration quadrature formula. The deviation from the exact $\exp(-y)$ -type behavior becomes smaller as $r \rightarrow 1$. This is favorable because the region near $r = 1$ gives a large contribution to the integral in (1.52).

| Z | $F_{\text{IR}}(1S_{1/2}, Z\alpha)$ | $F_{\text{IR}}(2S_{1/2}, Z\alpha)$ | $F_{\text{IR}}(2P_{1/2}, Z\alpha)$ | $F_{\text{IR}}(2P_{3/2}, Z\alpha)$ |
|-----|------------------------------------|------------------------------------|------------------------------------|------------------------------------|
| 1 | 7.236 623 736 8(1) | 7.479 764 180(1) | 0.085 327 852(1) | 0.082 736 497(1) |
| 2 | 5.539 002 119 1(1) | 5.782 025 637(1) | 0.086 073 669(1) | 0.083 279 461(1) |
| 3 | 4.598 155 821 8(1) | 4.840 923 962(1) | 0.087 162 510(1) | 0.084 091 830(1) |
| 4 | 3.963 124 140 6(1) | 4.205 501 798(1) | 0.088 543 188(1) | 0.085 140 788(1) |
| 5 | 3.493 253 319 4(1) | 3.735 114 958(1) | 0.090 180 835(1) | 0.086 403 178(1) |

Table 1.1: Infrared part for the K and L shell states, $F_{\text{IR}}(1S_{1/2}, Z\alpha)$, $F_{\text{IR}}(2S_{1/2}, Z\alpha)$, $F_{\text{IR}}(2P_{1/2}, Z\alpha)$, and $F_{\text{IR}}(2P_{3/2}, Z\alpha)$, evaluated for low- Z hydrogen(-like) ions. The calculations are performed with the numerical value of $\alpha^{-1} = 137.036$ for the fine structure constant.

The sum over $|\kappa|$ in Eq. (1.50) is carried out locally, i.e. for each set of arguments r, y, z . The sum over $|\kappa|$ is absolutely convergent. For $|\kappa| \rightarrow \infty$, the convergence of the sum is governed by the asymptotic behavior of the Bessel functions which occur in the photon functions A_{κ}^{ij} ($i, j = 1, 2$) [see Eqs. (3.15) and (3.16) in [81]]. The photon functions contain products of two Bessel functions of the form $\mathcal{J}_l(\rho_{2/1})$ where

\mathcal{J}_l stands for either j_l or j'_l , the index l is in the range $l \in \{|\kappa| - 1, |\kappa|, |\kappa| + 1\}$. The argument is either $\rho_2 = (E_n - z) x_2$ or $\rho_1 = (E_n - z) x_1$. The asymptotic behavior of the two relevant Bessel functions for large l (and therefore large $|\kappa|$) is

$$j'_l(x) = \frac{l}{x} \frac{x^l}{(2l+1)!!} \left[1 + \mathcal{O}\left(\frac{1}{l}\right) \right] \quad \text{and} \quad (1.54)$$

$$j_l(x) = \frac{x^l}{(2l+1)!!} \left[1 + \mathcal{O}\left(\frac{1}{l}\right) \right]. \quad (1.55)$$

This implies that when $\min\{\rho_2, \rho_1\} = \rho_2 < l$, the function $\mathcal{J}_l(\rho_2)$ vanishes with increasing l approximately as $(e \rho_2 / 2l)^l$. This rapidly converging asymptotic behavior sets in as soon as $l \approx |\kappa| > \rho_2 = r \omega y / a$ [see Eqs. (1.22) and (1.51)]. Due to the rapid convergence for $|\kappa| > \rho_2$, the maximum angular momentum quantum number $|\kappa|$ in the numerical calculation of the infrared part is less than 3 000. Note that because $z \in ({}^9/_{10} E_n, E_n)$ in the infrared part, $\omega < {}^1/_{10} E_n$.

The integration scheme is based on a crude estimate of the dependence of the integrand $S_{\text{IR}}(r, y, z)$ defined in Eq. (1.50) on the integration variables r , y and z . The main contribution to the integral is given by the region where the arguments of the Whittaker functions as they occur in the Green function [see Eq. (A.16) in [81]] are much larger than the Dirac angular momentum,

$$2c \frac{y}{a} \gg |\kappa|$$

(see also p. 56 of [82]). We assume the asymptotic form of the Green function given in Eq. (A.3) in [82] applies and attribute a factor

$$\exp[-(1-r)cy/a]$$

to the radial Green functions G_{κ}^{ij} as they occur in Eq. (1.50). Note that relatively slowly varying factors are replaced by unity. The products of the radial wave functions $f_{\bar{i}}$ and $f_{\bar{j}}$, according to the discussion following Eq. (1.53), behave as

$$e^{-y} \exp\left[\frac{1}{2}(1-r)y\right]$$

for large y . The photon functions A_{κ}^{ij} in Eq. (1.50) give rise to an approximate factor

$$\frac{\sin[(1-r)(E_n - z)y/a]}{(1-r)}. \quad (1.56)$$

Therefore [see also Eq. (2.12) in [82]], we base our choice of the integration routine on the approximation

$$e^{-y} \exp\left[-\left(\frac{c}{a} - \frac{1}{2}\right)(1-r)y\right] \times \frac{\sin[(1-r)\{(E_n - z)y/a\}]}{(1-r)} \quad (1.57)$$

for S_{IR} . The three-dimensional integral in (1.52) is evaluated by successive Gaussian quadrature. Details of the integration procedure can be found in [43].

In order to check the numerical stability of the results, the calculations are repeated with three different values of the fine structure constant α ,

$$\begin{aligned} \alpha_{<} &= 1/137.036\,000\,5, \\ \alpha_0 &= 1/137.036\,000\,0 \quad \text{and} \\ \alpha_{>} &= 1/137.035\,999\,5. \end{aligned} \quad (1.58)$$

These values of the fine-structure constant are close to the 1998 CODATA recommended value of $\alpha^{-1} = 137.035\,999\,76(50)$ [86]. The calculation was parallelized using the Message Passing Interface (MPI) and carried out on a cluster of Silicon Graphics workstations and on an IBM 9276 SP/2 multiprocessor system. The results for the infrared part, F_{IR} defined in Eq. (1.24), are given in Table 1.1 for a value of $\alpha^{-1} = \alpha_0^{-1} = 137.036$. This value of α will be used exclusively in the numerical evaluations presented here. For numerical results obtained by employing the values of $\alpha_{<}$ and $\alpha_{>}$ [see Eq. (1.58)] we refer to [43].

1.4.2 The Middle-Energy Subtraction Term

The middle-energy part is given by

$$\begin{aligned} \Delta E_M = & -i e^2 \int_{C_M} \frac{d\omega}{2\pi} \int \frac{d^3 \mathbf{k}}{(2\pi)^3} D_{\mu\nu}(k^2) \\ & \times \langle \psi | \alpha^\mu e^{i\mathbf{k}\cdot\mathbf{x}} G(E_n - \omega) \alpha^\nu e^{-i\mathbf{k}\cdot\mathbf{x}} | \psi \rangle, \end{aligned} \quad (1.59)$$

where relevant definitions of the symbols can be found in Eqs. (1.18)–(1.21) and in Eq. (1.41). The middle-energy part comprises the following integration region for the virtual photon (contour C_M in Fig. 1.2),

$$\left. \begin{aligned} \omega & \in ({}^{1/10} E_n, E_n) \pm i\epsilon \\ z & \in (0, {}^{9/10} E_n) \pm i\epsilon \end{aligned} \right\} \text{middle-energy part } \Delta E_M. \quad (1.60)$$

The numerical evaluation of the middle-energy part is simplified considerably by the decomposition of the relativistic Dirac-Coulomb Green function G as

$$G = G_A + G_B, \quad (1.61)$$

where G_A is defined in (1.38) and represents the sum of an approximation to the so-called zero- and one-potential terms generated by the expansion of the Dirac-Coulomb Green function G in powers of the binding field V . We define the middle-energy subtraction term F_{MA} as the expression obtained upon substitution of the propagator G_A for G in Eq. (1.59). The propagator G_B is simply calculated as the difference of G and G_A [see Eq. (1.39)]. A substitution of the propagator G_B for G in Eq. (1.59) leads to the middle-energy remainder F_{MB} which is discussed in Sec. 1.4.3. We provide here the explicit expressions

$$\begin{aligned} \Delta E_{MA} = & -i e^2 \int_{C_M} \frac{d\omega}{2\pi} \int \frac{d^3 \mathbf{k}}{(2\pi)^3} D_{\mu\nu}(k^2) \\ & \times \langle \psi | \alpha^\mu e^{i\mathbf{k}\cdot\mathbf{x}} G_A(E_n - \omega) \alpha^\nu e^{-i\mathbf{k}\cdot\mathbf{x}} | \psi \rangle \end{aligned} \quad (1.62)$$

and

$$\begin{aligned} \Delta E_{MB} = & -i e^2 \int_{C_M} \frac{d\omega}{2\pi} \int \frac{d^3 \mathbf{k}}{(2\pi)^3} D_{\mu\nu}(k^2) \\ & \times \langle \psi | \alpha^\mu e^{i\mathbf{k}\cdot\mathbf{x}} G_B(E_n - \omega) \alpha^\nu e^{-i\mathbf{k}\cdot\mathbf{x}} | \psi \rangle. \end{aligned} \quad (1.63)$$

Note that the decomposition of the Dirac-Coulomb Green function as in (1.61) is not applicable in the infrared part, because of numerical problems for ultra-soft photons (infrared divergences). Rewriting (1.62) appropriately into a three-dimensional integral [43, 81, 82], we have

$$\begin{aligned} \Delta E_{MA} = & \frac{\alpha}{\pi} \frac{9}{10} E_n - \frac{2\alpha}{\pi} \int_0^{{}^{9/10} E_n} dz \\ & \int_0^\infty dx_1 x_1^2 \int_0^{x_1} dx_2 x_2^2 \mathcal{M}_{MA}(x_2, x_1, z). \end{aligned} \quad (1.64)$$

The function $\mathcal{M}_{MA}(x_2, x_1, z)$ is defined in analogy to the function $\mathcal{M}_{IR}(x_2, x_1, z)$ defined in Eq. (1.44) for the infrared part. Also, we define a function $\mathcal{S}_{MA}(x_2, x_1, z)$ in analogy to the function $\mathcal{S}_{IR}(x_2, x_1, z)$

given in Eq. (1.50) for the infrared part, which will be used in Eq. (1.67) below. We have,

$$\begin{aligned}
S_{\text{MA}}(r, y, z) &= -\frac{2r^2 y^5}{a^6} \mathcal{M}_{\text{MA}}\left(\frac{ry}{a}, \frac{y}{a}, z\right) \\
&= -\frac{2r^2 y^5}{a^6} \sum_{|\kappa|=1} \sum_{\kappa=\pm|\kappa|} \sum_{i,j=1}^2 f_{\bar{i}}\left(\frac{ry}{a}\right) \\
&\quad \times G_{\text{A},\kappa}^{ij}\left(\frac{ry}{a}, \frac{y}{a}, z\right) f_{\bar{j}}\left(\frac{y}{a}\right) A_{\kappa}^{ij}\left(\frac{ry}{a}, \frac{y}{a}\right) \\
&= -\frac{2r^2 y^5}{a^6} \sum_{|\kappa|=1}^{\infty} T_{\text{MA},|\kappa|}(r, y, z). \tag{1.65}
\end{aligned}$$

The expansion of the propagator G_{A} into partial waves is given in Eqs. (5.4) and (A.20) in [81] and in Eqs. (D.37) and (D.42) in [43]. This expansion leads to the component functions $G_{\text{A},\kappa}^{ij}$. The terms $T_{\text{MA},|\kappa|}$ in the last line of Eq. (1.65) read

$$T_{\text{MA},|\kappa|}(r, y, z) = \sum_{\kappa=\pm|\kappa|} \sum_{i,j=1}^2 f_{\bar{i}}\left(\frac{ry}{a}\right) G_{\text{A},\kappa}^{ij}\left(\frac{ry}{a}, \frac{y}{a}, z\right) f_{\bar{j}}\left(\frac{y}{a}\right) A_{\kappa}^{ij}\left(\frac{ry}{a}, \frac{y}{a}\right). \tag{1.66}$$

With these definitions, the middle-energy subtraction term ΔE_{MA} can be written as

$$\Delta E_{\text{MA}} = \frac{\alpha}{\pi} \frac{9}{10} E_n + \frac{\alpha}{\pi} \int_0^{9/10 E_n} dz \int_0^{\infty} dy \int_0^1 dr S_{\text{MA}}(r, y, z). \tag{1.67}$$

The subtracted lower-order terms yield,

$$\Delta E_{\text{MA}} = \frac{\alpha}{\pi} \left[\frac{279}{200} \langle \beta \rangle + \frac{219}{200} \langle V \rangle + \frac{(Z\alpha)^4}{n^3} F_{\text{MA}}(nl_j, Z\alpha) \right]. \tag{1.68}$$

The three-dimensional integral (1.67) is evaluated by successive Gaussian quadrature. Details of the integration procedure can be found in [43]. The numerical results are summarized in the Table 1.2.

1.4.3 The Middle-Energy Remainder

The remainder term in the middle-energy part involves the propagator G_{B} defined in Eq. (1.39), $G_{\text{B}} = G - G_{\text{A}}$, where G is defined in (1.19) and G_{A} is given in (1.38). In analogy to the middle-energy subtraction term, the middle-energy remainder can be rewritten as a three-dimensional integral,

$$\Delta E_{\text{MB}} = \frac{\alpha}{\pi} \int_0^{9/10 E_n} dz \int_0^1 dr \int_0^{\infty} dy S_{\text{MB}}(r, y, z), \tag{1.69}$$

where

$$\begin{aligned}
S_{\text{MB}}(r, y, z) &= -\frac{2r^2 y^5}{a^6} \sum_{|\kappa|=1} \sum_{\kappa=\pm|\kappa|} \sum_{i,j=1}^2 f_{\bar{i}}\left(\frac{ry}{a}\right) G_{\text{B},\kappa}^{ij}\left(\frac{ry}{a}, \frac{y}{a}, z\right) f_{\bar{j}}\left(\frac{y}{a}\right) A_{\kappa}^{ij}\left(\frac{ry}{a}, \frac{y}{a}\right) \\
&= -\frac{2r^2 y^5}{a^6} \sum_{|\kappa|=1}^{\infty} T_{\text{MB},|\kappa|}(r, y, z), \tag{1.70}
\end{aligned}$$

| Z | $F_{\text{MA}}(1S_{1/2}, Z\alpha)$ | $F_{\text{MA}}(2S_{1/2}, Z\alpha)$ | $F_{\text{MA}}(2P_{1/2}, Z\alpha)$ | $F_{\text{MA}}(2P_{3/2}, Z\alpha)$ |
|-----|------------------------------------|------------------------------------|------------------------------------|------------------------------------|
| 1 | 2.699 379 904 5(1) | 2.720 878 318(1) | 0.083 207 314(1) | 0.701 705 240(1) |
| 2 | 2.659 561 381 1(1) | 2.681 820 660(1) | 0.084 208 832(1) | 0.701 850 024(1) |
| 3 | 2.623 779 453 0(1) | 2.647 262 568(1) | 0.085 831 658(1) | 0.702 091 147(1) |
| 4 | 2.591 151 010 1(1) | 2.616 290 432(1) | 0.088 040 763(1) | 0.702 426 850(1) |
| 5 | 2.561 096 522 1(1) | 2.588 297 638(1) | 0.090 803 408(1) | 0.702 854 461(1) |

| Z | $F_{\text{MB}}(1S_{1/2}, Z\alpha)$ | $F_{\text{MB}}(2S_{1/2}, Z\alpha)$ | $F_{\text{MB}}(2P_{1/2}, Z\alpha)$ | $F_{\text{MB}}(2P_{3/2}, Z\alpha)$ |
|-----|------------------------------------|------------------------------------|------------------------------------|------------------------------------|
| 1 | 1.685 993 923 2(1) | 1.784 756 705(2) | 0.771 787 771(2) | -0.094 272 681(2) |
| 2 | 1.626 842 294 5(1) | 1.725 583 798(2) | 0.770 778 394(2) | -0.094 612 071(2) |
| 3 | 1.571 406 090 7(1) | 1.670 086 996(2) | 0.769 153 314(2) | -0.095 165 248(2) |
| 4 | 1.519 082 768 6(1) | 1.617 650 004(2) | 0.766 954 435(2) | -0.095 922 506(2) |
| 5 | 1.469 482 409 0(1) | 1.567 873 140(2) | 0.764 220 149(2) | -0.096 874 556(2) |

| Z | $F_{\text{M}}(1S_{1/2}, Z\alpha)$ | $F_{\text{M}}(2S_{1/2}, Z\alpha)$ | $F_{\text{M}}(2P_{1/2}, Z\alpha)$ | $F_{\text{M}}(2P_{3/2}, Z\alpha)$ |
|-----|-----------------------------------|-----------------------------------|-----------------------------------|-----------------------------------|
| 1 | 4.385 373 827 7(1) | 4.505 635 023(2) | 0.854 995 085(2) | 0.607 432 559(2) |
| 2 | 4.286 403 675 7(1) | 4.407 404 458(2) | 0.854 987 226(2) | 0.607 237 953(2) |
| 3 | 4.195 185 543 6(1) | 4.317 349 564(2) | 0.854 984 972(2) | 0.606 925 899(2) |
| 4 | 4.110 233 778 8(1) | 4.233 940 436(2) | 0.854 995 198(2) | 0.606 504 344(2) |
| 5 | 4.030 578 931 1(1) | 4.156 170 778(2) | 0.855 023 557(2) | 0.605 979 905(2) |

Table 1.2: Numerical results for the middle-energy subtraction term F_{MA} , the middle-energy remainder term F_{MB} and the middle-energy term F_{M} . The middle-energy term F_{M} is given as the sum $F_{\text{M}}(nl_j, Z\alpha) = F_{\text{MA}}(nl_j, Z\alpha) + F_{\text{MB}}(nl_j, Z\alpha)$ [see also Eqs.(1.25), (1.68) and (1.72)].

where we implicitly define the terms $T_{\text{MB},|\kappa|}(r, y, z)$ in analogy with the infrared part Eq. (1.50). The functions $G_{\text{B},\kappa}^{ij}$ are obtained as the difference of the expansion of the full propagator G and the simplified propagator G_{A} into angular momenta,

$$G_{\text{B},\kappa}^{ij} = G_{\kappa}^{ij} - G_{\text{A},\kappa}^{ij} \quad (1.71)$$

where the G_{κ}^{ij} are listed in Eq. (A.16) in [81] and in Eq. (D.43) in [43], and the $G_{\text{A},\kappa}^{ij}$ have already been defined in Eqs. (5.4) and (A.20) in [81] and in Eqs. (D.37) and (D.42) in [43]. There are no lower-order terms to subtract, and therefore

$$\Delta E_{\text{MB}} = \frac{\alpha}{\pi} \frac{(Z\alpha)^4}{n^3} F_{\text{MB}}(nl_j, Z\alpha). \quad (1.72)$$

The three-dimensional integral (1.69) is evaluated by successive Gaussian quadrature. Details of the integration procedure are provided in [43]. Numerical results for the middle-energy remainder F_{MB} , are summarized in Table 1.2 for the K- and L-shell states.

For the middle-energy part, the separation into a subtraction and a remainder term has considerable computational advantages which become obvious upon inspection of Eqs. (1.68) and (1.72). The subtraction involves a propagator whose angular components can be evaluated by recursion [43, 82], which is computationally time-consuming. Because the subtraction term involves lower-order components [see Eq. (1.25)], it has to be evaluated to high precision numerically (in a typical case, a relative accuracy of 10^{-19} is required). This high precision requires in turn a large number of integration points for the Gaussian quadratures, which is possible only if the numerical evaluation of the integrand is not computationally time-consuming. For the remainder term, no lower-order terms have to be subtracted, and the relative accuracy required of the integrals is in the range of $10^{-11} \dots 10^{-9}$. A numerical evaluation to this

smaller level of precision is feasible although the calculation of the Green function G_B is computationally more expensive than that of G_A [43, 81, 82]. The separation of the high-energy part into a subtraction term and a remainder term, which is discussed in Sec. 1.5, is motivated by analogous considerations as for the middle-energy part. In the high-energy part, this separation is even more important than in the middle-energy part, because of the occurrence of infinite terms which need to be subtracted analytically before a numerical evaluation can proceed [see Eq. (1.82) below].

We now summarize the results for the middle-energy part. The middle-energy part is the sum of the middle-energy subtraction term F_{MA} and the middle-energy remainder F_{MB} [see also Eq. (1.27)]. Numerical results are summarized in Table 1.2 for the K- and L-shell states. The low-energy part F_L is defined as the sum of the infrared contribution F_{IR} and the middle-energy contribution F_M [see Eq. (1.32)]. The results for F_L are provided in the Table 1.3 for the K- and L-shell states. The limits for the low-energy part as a function of the bound state quantum numbers can be found in Eq. (7.80) of [43],

$$\begin{aligned}
F_L(nl_j, Z\alpha) = & \frac{4}{3} \delta_{l,0} \ln(Z\alpha)^{-2} - \frac{4}{3} \ln k_0(n, l) + \left(\ln 2 - \frac{11}{10} \right) \frac{1}{n} \\
& + \left(2 \ln 2 - \frac{16}{15} \right) \frac{1}{2l+1} + \left(\frac{3}{2} \ln 2 - \frac{7}{4} \right) \frac{1}{\kappa(2l+1)} \\
& + \left(-\frac{3}{2} \ln 2 + \frac{9}{4} \right) \frac{1}{|\kappa|} + \left(\frac{4}{3} \ln 2 - \frac{1}{3} \right) \delta_{l,0} \\
& + \left(\ln 2 - \frac{5}{6} \right) \frac{n-2l-1}{n(2l+1)} + O(Z\alpha). \tag{1.73}
\end{aligned}$$

The leadings asymptotics for the states under investigation are,

$$\begin{aligned}
F_L(1S_{1/2}, Z\alpha) &= (4/3) \ln(Z\alpha)^{-2} - 1.554\,642 + O(Z\alpha), \\
F_L(2S_{1/2}, Z\alpha) &= (4/3) \ln(Z\alpha)^{-2} - 1.191\,497 + O(Z\alpha), \\
F_L(2P_{1/2}, Z\alpha) &= 0.940\,023 + O(Z\alpha), \\
F_L(2P_{3/2}, Z\alpha) &= 0.690\,023 + O(Z\alpha). \tag{1.74}
\end{aligned}$$

These asymptotics are consistent with the numerical data in Table 1.3. For S states, the low-energy contribution F_L diverges logarithmically as $Z\alpha \rightarrow 0$, whereas for P states, F_L approaches a constant as $Z\alpha \rightarrow 0$. The leading logarithm is a consequence of an infrared divergence cut off by the atomic

| Z | $F_L(1S_{1/2}, Z\alpha)$ | $F_L(2S_{1/2}, Z\alpha)$ | $F_L(2P_{1/2}, Z\alpha)$ | $F_L(2P_{3/2}, Z\alpha)$ |
|-----|--------------------------|--------------------------|--------------------------|--------------------------|
| 1 | 11.621 997 564 5(1) | 11.985 399 203(2) | 0.940 322 937(2) | 0.690 169 056(2) |
| 2 | 9.825 405 794 7(1) | 10.189 430 095(2) | 0.941 060 895(2) | 0.690 517 414(2) |
| 3 | 8.793 341 365 4(1) | 9.158 273 526(2) | 0.942 147 482(2) | 0.691 017 729(2) |
| 4 | 8.073 357 919 4(1) | 8.439 442 234(2) | 0.943 538 386(2) | 0.691 645 132(2) |
| 5 | 7.523 832 250 6(1) | 7.891 285 736(2) | 0.945 204 392(2) | 0.692 383 083(2) |

Table 1.3: Low-energy part F_L for the K- and L-shell states $F_L(1S_{1/2}, Z\alpha)$, $F_L(2S_{1/2}, Z\alpha)$, $F_L(2P_{1/2}, Z\alpha)$, and $F_L(2P_{3/2}, Z\alpha)$, evaluated for low- Z hydrogenlike ions.

momentum scale. It is a nonrelativistic effect which is generated by the nonvanishing probability density of S waves at the origin in the nonrelativistic limit. The presence of the logarithmic behavior for S states [nonvanishing A_{41} -coefficient, see Eqs. (1.2) and (1.3)] and its absence for P states is reproduced consistently by the data in Table 1.3.

1.5 The High-Energy Part

1.5.1 The High-Energy Subtraction Term

The high-energy part is given by

$$\begin{aligned} \Delta E_H &= - \lim_{\Lambda \rightarrow \infty} i e^2 \int_{C_H} \frac{d\omega}{2\pi} \int \frac{d^3 \mathbf{k}}{(2\pi)^3} D_{\mu\nu}(k^2, \Lambda) \\ &\quad \times \langle \psi | \alpha^\mu e^{i\mathbf{k} \cdot \mathbf{x}} G(E_n - \omega) \alpha^\nu e^{-i\mathbf{k} \cdot \mathbf{x}} | \psi \rangle, \end{aligned} \quad (1.75)$$

where relevant definitions of the symbols can be found in Eqs. (1.18)–(1.21), and the contour C_H is as shown in Fig. 1.1. The high-energy part comprises the following integration region for the virtual photon,

$$\left. \begin{aligned} \omega &\in (E_n - i\infty, E_n + i\infty) \\ z &\in (-i\infty, i\infty) \end{aligned} \right\} \text{high-energy part } \Delta E_H. \quad (1.76)$$

The separation of the high-energy part into a subtraction term and a remainder is accomplished as in the middle-energy part [see Eq. (1.61)] by writing the full Dirac-Coulomb Green function G [Eq. (1.19)] as $G = G_A + G_B$. We define the high-energy subtraction term F_{HA} as the expression obtained upon substitution of the propagator G_A for G in Eq. (1.75), and a substitution of the propagator G_B for G in Eq. (1.75) leads to the high-energy remainder F_{HB} which is discussed in Sec. 1.5.2. The subtraction term (including all divergent contributions) is generated by G_A , the high-energy remainder term corresponds to G_B . We have

$$\begin{aligned} \Delta E_{HA} &= - \lim_{\Lambda \rightarrow \infty} i e^2 \int_{C_H} \frac{d\omega}{2\pi} \int \frac{d^3 \mathbf{k}}{(2\pi)^3} D_{\mu\nu}(k^2, \Lambda) \\ &\quad \times \langle \psi | \alpha^\mu e^{i\mathbf{k} \cdot \mathbf{x}} G_A(E_n - \omega) \alpha^\nu e^{-i\mathbf{k} \cdot \mathbf{x}} | \psi \rangle \end{aligned} \quad (1.77)$$

and

$$\begin{aligned} \Delta E_{HB} &= -i e^2 \int_{C_H} \frac{d\omega}{2\pi} \int \frac{d^3 \mathbf{k}}{(2\pi)^3} D_{\mu\nu}(k^2) \\ &\quad \times \langle \psi | \alpha^\mu e^{i\mathbf{k} \cdot \mathbf{x}} G_B(E_n - \omega) \alpha^\nu e^{-i\mathbf{k} \cdot \mathbf{x}} | \psi \rangle. \end{aligned} \quad (1.78)$$

The contribution ΔE_{HA} corresponding to G_A can be separated further into a term $\Delta E_{HA}^{(1)}$, which contains all divergent contributions, and a term $\Delta E_{HA}^{(2)}$, which comprises contributions of lower order than $(Z\alpha)^4$, but is convergent as $\Lambda \rightarrow \infty$. This separation is described in detail in [81, 84]. We have

$$\Delta E_{HA} = \Delta E_{HA}^{(1)} + \Delta E_{HA}^{(2)}. \quad (1.79)$$

We obtain for $\Delta E_{HA}^{(1)}$, which contains a logarithmic divergence as $\Lambda \rightarrow \infty$,

$$\Delta E_{HA}^{(1)} = \frac{\alpha}{\pi} \left[\left(\frac{3}{4} \ln \Lambda^2 - \frac{9}{8} \right) \langle \beta \rangle + \left(\frac{1}{2} \ln 2 - \frac{17}{12} \right) \langle V \rangle + \frac{(Z\alpha)^4}{n^3} F_{HA}^{(1)}(nl_j, Z\alpha) \right]. \quad (1.80)$$

For the contribution $F_{\text{HA}}^{(1)}$, an explicit analytic result is obtained in Eq. (4.15) in [81]. This contribution is therefore not discussed in any further detail, here. The contribution $\Delta E_{\text{HA}}^{(2)}$ contains lower-order terms,

$$\Delta E_{\text{HA}}^{(2)} = \frac{\alpha}{\pi} \left[\left(-\frac{1}{2} \ln 2 + \frac{1}{4} \right) \langle V \rangle + \frac{(Z\alpha)^4}{n^3} F_{\text{HA}}^{(2)}(nl_j, Z\alpha) \right]. \quad (1.81)$$

Altogether we have

$$\begin{aligned} \Delta E_{\text{HA}} &= \Delta E_{\text{HA}}^{(1)} + \Delta E_{\text{HA}}^{(2)} \\ &= \frac{\alpha}{\pi} \left[\left(\frac{3}{4} \ln \Lambda^2 - \frac{9}{8} \right) \langle \beta \rangle - \frac{7}{6} \langle V \rangle + \frac{(Z\alpha)^4}{n^3} F_{\text{HA}}(nl_j, Z\alpha) \right]. \end{aligned} \quad (1.82)$$

The scaled function $F_{\text{HA}}(nl_j, Z\alpha)$ is given as

$$F_{\text{HA}}(nl_j, Z\alpha) = F_{\text{HA}}^{(1)}(nl_j, Z\alpha) + F_{\text{HA}}^{(2)}(nl_j, Z\alpha). \quad (1.83)$$

The term $\Delta E_{\text{HA}}^{(2)}$ falls naturally into a sum of four contributions [81],

$$\Delta E_{\text{HA}}^{(2)} = T_1 + T_2 + T_3 + T_4 \quad (1.84)$$

where

$$\begin{aligned} T_1 &= -\frac{1}{10} \langle V \rangle + \frac{(Z\alpha)^4}{n^3} h_1(nl_j, Z\alpha), \\ T_2 &= \left(\frac{7}{20} - \frac{1}{2} \ln 2 \right) \langle V \rangle + \frac{(Z\alpha)^4}{n^3} h_2(nl_j, Z\alpha), \\ T_3 &= \frac{(Z\alpha)^4}{n^3} h_3(nl_j, Z\alpha), \\ T_4 &= \frac{(Z\alpha)^4}{n^3} h_4(nl_j, Z\alpha). \end{aligned} \quad (1.85)$$

The functions h_i ($i = 1, 2, 3, 4$) are defined in Eqs. (4.18), (4.19) and (4.21) in [81] (see also Eq. (3.6) in [83]). The evaluation of the high-energy subtraction term proceeds as outlined in [81, 82, 83], albeit with an increased accuracy and improved calculational methods in intermediate steps of the calculation in order to overcome the severe numerical cancellations in the low- Z region. We recover $F_{\text{HA}}^{(2)}$ as the sum

$$F_{\text{HA}}^{(2)}(nl_j, Z\alpha) = h_1(nl_j, Z\alpha) + h_2(nl_j, Z\alpha) + h_3(nl_j, Z\alpha) + h_4(nl_j, Z\alpha). \quad (1.86)$$

The scaled function $F_{\text{HA}}(nl_j, Z\alpha)$ [see also Eqs. (1.26) and (1.28)] is obtained as

$$F_{\text{HA}}(nl_j, Z\alpha) = F_{\text{HA}}^{(1)}(nl_j, Z\alpha) + F_{\text{HA}}^{(2)}(nl_j, Z\alpha). \quad (1.87)$$

The limits of the contributions $F_{\text{HA}}^{(1)}(nl_j, Z\alpha)$ and $F_{\text{HA}}^{(2)}(nl_j, Z\alpha)$ as $(Z\alpha) \rightarrow 0$ have been investigated in [81, 83, 84]. For the contribution $F_{\text{HA}}^{(1)}(nl_j, 0)$, the result can be found in Eq. (3.5) in [83]. The limits of the functions $h_i(nl_j, Z\alpha)$ ($i = 1, 2, 3, 4$) as $Z\alpha \rightarrow 0$ are given as a function of the atomic state quantum numbers in Eq. (3.8) in [83]. For the scaled high-energy subtraction term F_{HA} , the limits read (see Eq. (3.9) in [83])

$$\begin{aligned} F_{\text{HA}}(nl_j, Z\alpha) &= \left(\frac{11}{10} - \ln 2 \right) \frac{1}{n} + \left(\frac{16}{15} - 2 \ln 2 \right) \frac{1}{2l+1} \\ &\quad + \left(\frac{1}{2} \ln 2 - \frac{1}{4} \right) \frac{1}{\kappa(2l+1)} + \left(\frac{3}{2} \ln 2 - \frac{9}{4} \right) \frac{1}{|\kappa|} + \mathcal{O}(Z\alpha). \end{aligned} \quad (1.88)$$

Therefore, the explicit forms of the limits for the states under investigation are,

$$F_{\text{HA}}(1\text{S}_{1/2}, Z\alpha) = -1.219\,627 + \mathcal{O}(Z\alpha),$$

$$F_{\text{HA}}(2\text{S}_{1/2}, Z\alpha) = -1.423\,054 + \mathcal{O}(Z\alpha),$$

$$F_{\text{HA}}(2\text{P}_{1/2}, Z\alpha) = -1.081\,204 + \mathcal{O}(Z\alpha),$$

$$F_{\text{HA}}(2\text{P}_{3/2}, Z\alpha) = -0.524\,351 + \mathcal{O}(Z\alpha). \quad (1.89)$$

Numerical results for F_{HA} , which are presented in Table 1.4, exhibit consistency with the limits in Eq. (1.89).

| Z | $F_{\text{HA}}(1\text{S}_{1/2}, Z\alpha)$ | $F_{\text{HA}}(2\text{S}_{1/2}, Z\alpha)$ | $F_{\text{HA}}(2\text{P}_{1/2}, Z\alpha)$ | $F_{\text{HA}}(2\text{P}_{3/2}, Z\alpha)$ |
|-----|---|---|---|---|
| 1 | -1.216 846 660 6(1) | -1.420 293 291(1) | -1.081 265 954(1) | -0.524 359 802(1) |
| 2 | -1.214 322 536 9(1) | -1.417 829 864(1) | -1.081 451 269(1) | -0.524 385 053(1) |
| 3 | -1.212 026 714 1(1) | -1.415 635 310(1) | -1.081 760 224(1) | -0.524 427 051(1) |
| 4 | -1.209 942 847 4(1) | -1.413 693 422(1) | -1.082 192 995(1) | -0.524 485 727(1) |
| 5 | -1.208 059 033 6(1) | -1.411 992 480(1) | -1.082 749 845(1) | -0.524 561 017(1) |
| Z | $F_{\text{HB}}(1\text{S}_{1/2}, Z\alpha)$ | $F_{\text{HB}}(2\text{S}_{1/2}, Z\alpha)$ | $F_{\text{HB}}(2\text{P}_{1/2}, Z\alpha)$ | $F_{\text{HB}}(2\text{P}_{3/2}, Z\alpha)$ |
| 1 | -0.088 357 254(1) | -0.018 280 727(5) | 0.014 546 64(1) | -0.042 310 69(1) |
| 2 | -0.082 758 206(1) | -0.012 729 99(1) | 0.014 574 21(1) | -0.042 296 81(1) |
| 3 | -0.076 811 229(1) | -0.006 861 02(1) | 0.014 620 51(1) | -0.042 273 58(1) |
| 4 | -0.070 590 991(1) | -0.000 746 40(1) | 0.014 685 82(1) | -0.042 240 92(1) |
| 5 | -0.064 146 139(1) | 0.005 567 16(1) | 0.014 770 52(1) | -0.042 198 76(1) |
| Z | $F_{\text{H}}(1\text{S}_{1/2}, Z\alpha)$ | $F_{\text{H}}(2\text{S}_{1/2}, Z\alpha)$ | $F_{\text{H}}(2\text{P}_{1/2}, Z\alpha)$ | $F_{\text{H}}(2\text{P}_{3/2}, Z\alpha)$ |
| 1 | -1.305 203 915(1) | -1.438 574 018(5) | -1.066 719 31(1) | -0.566 670 50(1) |
| 2 | -1.297 080 743(1) | -1.430 559 85(1) | -1.066 877 06(1) | -0.566 681 86(1) |
| 3 | -1.288 837 943(1) | -1.422 496 33(1) | -1.067 139 72(1) | -0.566 700 63(1) |
| 4 | -1.280 533 839(1) | -1.414 439 82(1) | -1.067 507 18(1) | -0.566 726 65(1) |
| 5 | -1.272 205 173(1) | -1.406 425 32(1) | -1.067 979 33(1) | -0.566 759 78(1) |

Table 1.4: Numerical results for the high-energy subtraction term F_{HA} and the high-energy remainder term F_{HB} . The high-energy term F_{H} is given as the sum $F_{\text{H}}(nl_j, Z\alpha) = F_{\text{HA}}(nl_j, Z\alpha) + F_{\text{HB}}(nl_j, Z\alpha)$.

1.5.2 The High-Energy Remainder

The remainder term in the high-energy part involves the propagator G_{B} defined in Eq. (1.39), $G_{\text{B}} = G - G_{\text{A}}$, where G is defined in (1.19) and G_{A} is given in (1.38). The evaluation proceeds in complete analogy to the calculation of the middle-energy remainder term (Sec. 1.4.3). The only difference lies in the different integration region for the photon energy, which is given – for the high-energy part – in

Eq. (1.76). The photon energy integration variable z is conveniently expressed as

$$z \rightarrow i u \quad \text{where} \quad u = \frac{1}{2} \left(\frac{1}{t} - t \right). \quad (1.90)$$

The method of integration is described in [12, 43], and we do not discuss any further details, here. We focus instead on the convergence acceleration technique used in the evaluation.

In analogy with the middle-energy remainder, we may write the integrand S_{HB} which is defined in complete analogy to (1.70) as a sum over angular momenta (“partial waves”)

$$S_{\text{HB}} \propto \sum_{|\kappa|=1}^{\infty} T_{\text{HB},|\kappa|}, \quad (1.91)$$

where the $T_{\text{HB},|\kappa|}$ are defined in analogy to Eq. (1.70). Here, $|\kappa|$ represents the modulus of the Dirac angular momentum quantum number of the virtual intermediate state. The asymptotic behaviour of the $T_{\text{HB},|\kappa|}$ for large $|\kappa|$ is [see Eq. (4.7) in [82]]

$$T_{\text{HB},|\kappa|} = \frac{r^{2|\kappa|}}{|\kappa|} \left[\text{const.} + \mathcal{O}\left(\frac{1}{|\kappa|}\right) \right], \quad (1.92)$$

where “const.” is independent of $|\kappa|$. The series in Eq. (1.91) is slowly convergent for r close to one, and the region near $r = 1$ is known to be problematic in numerical evaluations.

It is found that the convergence of the series (1.92) series near $r = 1$ can be accelerated very efficiently using the combined nonlinear-condensation transformation (see [23] and Sec. 7.1.6) applied to the series $\sum_{k=0}^{\infty} t_k$ where $t_k = T_{\text{HB},k+1}$ [see Eqs. (1.91) and (1.92)]. The combined transformation (combination of the condensation transformation and the Weniger transformation) was found to be applicable to a wide range of slowly convergent monotone series (series whose terms have the same sign), and many examples for its application were given in Ref. [23, 31]. For the numerical treatment of radiative corrections in low- Z systems, the transformation has the advantage of removing the principal numerical difficulties associated with the slow convergence of angular momentum decompositions of the propagators near their singularity for equal radial arguments.

All that remains to be discussed in the current section is the low- Z limit of the energy shift

$$\Delta E_{\text{HB}} = \frac{\alpha}{\pi} \frac{(Z\alpha)^4}{n^3} F_{\text{HB}}(nl_j, Z\alpha). \quad (1.93)$$

For the high-energy remainder F_{HB} , the limits as $Z\alpha \rightarrow 0$ read [see Eq. (4.15) in [83]]

$$\begin{aligned} F_{\text{HB}}(nl_j, Z\alpha) &= \frac{1}{2l+1} \left[\left(\frac{17}{18} - \frac{4}{3} \ln 2 \right) \delta_{l,0} + \left(\frac{3}{2} - 2 \ln 2 \right) \frac{1}{\kappa} \right. \\ &\quad \left. + \left(\frac{5}{6} - \ln 2 \right) \frac{n-2l-1}{n} \right] + \mathcal{O}(Z\alpha). \end{aligned} \quad (1.94)$$

For the atomic states under investigation, this leads to

$$\begin{aligned} F_{\text{HB}}(1S_{1/2}, Z\alpha) &= -0.093\,457 + \mathcal{O}(Z\alpha), \\ F_{\text{HB}}(2S_{1/2}, Z\alpha) &= -0.023\,364 + \mathcal{O}(Z\alpha), \\ F_{\text{HB}}(2P_{1/2}, Z\alpha) &= 0.014\,538 + \mathcal{O}(Z\alpha), \\ F_{\text{HB}}(2P_{3/2}, Z\alpha) &= -0.042\,315 + \mathcal{O}(Z\alpha). \end{aligned} \quad (1.95)$$

1.5.3 Results for the High-Energy Part

The limit of the function F_H as $Z\alpha \rightarrow 0$ can be derived easily from the Eqs. (1.88), (1.94) as a function of the bound state quantum numbers. It reads

$$\begin{aligned}
F_H(nl_j, Z\alpha) = & \left(\frac{11}{10} - \ln 2 \right) \frac{1}{n} + \left(\frac{16}{15} - 2 \ln 2 \right) \frac{1}{2l+1} \\
& + \left(-\frac{3}{2} \ln 2 + \frac{5}{4} \right) \frac{1}{\kappa(2l+1)} + \left(\frac{3}{2} \ln 2 - \frac{9}{4} \right) \frac{1}{|\kappa|} \\
& + \left(\frac{17}{18} - \frac{4}{3} \ln 2 \right) \delta_{l,0} + \left(\frac{5}{6} - \ln 2 \right) \frac{n-2l-1}{n(2l+1)} + O(Z\alpha). \tag{1.96}
\end{aligned}$$

For the atomic states investigated here, this expression yields the numerical values,

$$\begin{aligned}
F_H(1S_{1/2}, Z\alpha) &= -1.313\,085 + O(Z\alpha), \\
F_H(2S_{1/2}, Z\alpha) &= -1.446\,418 + O(Z\alpha), \\
F_H(2P_{1/2}, Z\alpha) &= -1.066\,667 + O(Z\alpha), \\
F_H(2P_{3/2}, Z\alpha) &= -0.566\,667 + O(Z\alpha). \tag{1.97}
\end{aligned}$$

Numerical results for the high-energy part

$$F_H(nl_j, Z\alpha) = F_{HA}(nl_j, Z\alpha) + F_{HB}(nl_j, Z\alpha) \tag{1.98}$$

are summarized in Table 1.4. Note the apparent consistency of the numerical results in Table 1.4 with their analytically obtained low- Z limits in Eq. (1.97).

1.6 Comparison to Analytic Calculations

The numerical results for the scaled function $F(nl_j, Z\alpha)$ describing the self energy defined in Eq. (1.1) are given in Table 1.5, together with the results for the nonperturbative function $G_{SE}(nl_j, Z\alpha)$, which is implicitly defined in Eq. (1.2). Results are provided for K and L shell states. The numerical results for the remainder G_{SE} are obtained by subtracting the analytic lower-order terms listed in Eq. (1.2) from the complete numerical result for the scaled function $F(nl_j, Z\alpha)$. No additional fitting is performed.

Analytic and numerical results at low Z can be compared by considering the remainder function G_{SE} . Note that an inconsistency in any of the analytically obtained lower-order terms would be likely to manifest itself in a grossly inconsistent dependence of $G_{SE}(nl_j, Z\alpha)$ on its argument $Z\alpha$; this is not observed. For S states, the following analytic model for G_{SE} is commonly assumed, which is motivated in part by a renormalization-group analysis [87] and is constructed in analogy with the pattern of the analytic coefficients A_{ij} in Eq. (1.2) and (1.3),

$$\begin{aligned}
G_{SE}(nS_{1/2}, Z\alpha) = & A_{60}(nS_{1/2}) + (Z\alpha) [A_{71}(nS_{1/2}) \ln(Z\alpha)^{-2} + A_{70}(nS_{1/2})] \\
& + (Z\alpha)^2 [A_{83}(nS_{1/2}) \ln^3(Z\alpha)^{-2} + A_{82}(nS_{1/2}) \ln^2(Z\alpha)^{-2} \\
& + A_{81}(nS_{1/2}) \ln(Z\alpha)^{-2} + A_{80}(nS_{1/2})] . \tag{1.99}
\end{aligned}$$

The (probably nonvanishing) A_{83} coefficient, which introduces a triple logarithmic singularity at $Z\alpha = 0$, hinders an accurate comparison of numerical and analytic data for G_{SE} . A somewhat less singular behavior is expected of the difference

$$\Delta G_{\text{SE}}(Z\alpha) = G_{\text{SE}}(2S_{1/2}, Z\alpha) - G_{\text{SE}}(1S_{1/2}, Z\alpha), \quad (1.100)$$

because the leading logarithmic coefficients in any given order of $Z\alpha$ are generally assumed to be equal for all S states, which would mean in particular

$$A_{71}(1S_{1/2}) = A_{71}(2S_{1/2}) \quad (1.101)$$

and

$$A_{83}(1S_{1/2}) = A_{83}(2S_{1/2}). \quad (1.102)$$

Now we define ΔA_{kl} as the difference of the values of the analytic coefficients for the two lowest S states,

$$\Delta A_{kl} = A_{kl}(2S_{1/2}) - A_{kl}(1S_{1/2}). \quad (1.103)$$

The function ΔG_{SE} defined in Eq. (1.100) can be assumed to have the following semi-analytic expansion around $Z\alpha = 0$,

$$\begin{aligned} \Delta G_{\text{SE}}(Z\alpha) = & \Delta A_{60} + (Z\alpha) \Delta A_{70} + (Z\alpha)^2 [\Delta A_{82} \ln^2(Z\alpha)^{-2} \\ & + \Delta A_{81} \ln(Z\alpha)^{-2} + \Delta A_{80} + o(Z\alpha)] . \end{aligned} \quad (1.104)$$

In order to detect possible inconsistencies in the numerical and analytic data for G_{SE} , we difference the data for ΔG_{SE} , i.e., we consider the following finite difference approximation to the derivative of the function ΔG_{SE} ,

$$g(Z) = \Delta G_{\text{SE}}((Z+1)\alpha) - \Delta G_{\text{SE}}(Z\alpha). \quad (1.105)$$

It is perhaps not *a priori* obvious why this combination leads to a sensible comparison of numerical and analytic data. This will be explained in the sequel.

We denote the analytic and numerical limits of $\Delta G_{\text{SE}}(Z\alpha)$ as $Z\alpha \rightarrow 0$ as $\Delta A_{60}^{\text{ana}}$ and $\Delta A_{60}^{\text{num}}$, respectively. Of course, we hope that these will turn out to be equal. However, we temporarily leave open the possibility of an inconsistency between numerical and analytic data by keeping $\Delta A_{60}^{\text{num}}$ and $\Delta A_{60}^{\text{ana}}$ as distinct variables. In order to illustrate how a discrepancy could be detected by investigating the function $g(Z)$, we consider special cases of the function $\Delta G_{\text{SE}}(Z\alpha)$ and $g(Z)$. For $Z = 0$, the exact result can be inferred exclusively and uniquely using the analytic approach of Ref. [32], and we have

$$\Delta G_{\text{SE}}(0) = \Delta A_{60}^{\text{ana}}, \quad (1.106)$$

whereas for $Z = 1$, which is determined by numerical data,

$$\Delta G_{\text{SE}}(\alpha) \approx \Delta A_{60}^{\text{num}} + \alpha \Delta A_{70}, \quad (1.107)$$

with a possibly different limit $\Delta A_{60}^{\text{num}}$ as $Z \rightarrow 0$, and for $Z = 2$,

$$\Delta G_{\text{SE}}(2\alpha) \approx \Delta A_{60}^{\text{num}} + 2\alpha \Delta A_{70}, \quad (1.108)$$

where we ignore higher-order analytic terms. Hence, for $Z = 0$, we have

$$g(0) = \Delta G_{\text{SE}}(\alpha) - \Delta G_{\text{SE}}(0) = \Delta A_{60}^{\text{num}} - \Delta A_{60}^{\text{ana}} + \alpha [\Delta A_{70} + o(Z\alpha)]. \quad (1.109)$$

A possible inconsistency (nonvanishing $\Delta A_{60}^{\text{num}} - \Delta A_{60}^{\text{ana}}$) would influence the value of $g(0)$. For $Z = 1$, the value of g is determined solely by numerical data,

$$g(1) = \Delta G_{\text{SE}}(2\alpha) - \Delta G_{\text{SE}}(\alpha) = \alpha [\Delta A_{70} + o(Z\alpha)], \quad (1.110)$$

and for $Z = 2$, we have

$$g(2) = \Delta G_{\text{SE}}(3\alpha) - \Delta G_{\text{SE}}(2\alpha) = \alpha [\Delta A_{70} + o(Z\alpha)]. \quad (1.111)$$

Of course, analogous relations hold for $Z > 2$. This means that a meaningful comparison of the analytic and numerical approaches can be made by comparing the value $g(0)$, which is influenced by the term $\Delta A_{60}^{\text{num}} - \Delta A_{60}^{\text{ana}}$, to the other values $g(1), \dots, g(4)$, which are *independent* of the difference $\Delta A_{60}^{\text{num}} - \Delta A_{60}^{\text{ana}}$. We recall that the numerical data from Table 1.5 lead to the evaluation of the five values $g(0)$, $g(1)$, $g(2)$, $g(3)$ and $g(4)$. A plot of the function $g(Z)$ serves two purposes: (i) the values $g(1), \dots, g(4)$ should exhibit apparent convergence to some limiting value $\alpha \Delta A_{70}$ as $Z \rightarrow 0$, and this can be verified by inspection of the plot, and (ii) a discrepancy between the analytic and numerical approaches – as explained above – would result in a nonvanishing value for $\Delta A_{60}^{\text{num}} - \Delta A_{60}^{\text{ana}}$, and it would introduce an inconsistency between the trend in the values of $g(1), \dots, g(4)$, and the value of $g(0)$ [see Eq. (1.109)].

| Z | $F(1S_{1/2}, Z\alpha)$ | $F(2S_{1/2}, Z\alpha)$ | $F(2P_{1/2}, Z\alpha)$ | $F(2P_{3/2}, Z\alpha)$ |
|-----|------------------------------------|------------------------------------|------------------------------------|------------------------------------|
| 1 | 10.316 793 650(1) | 10.546 825 185(5) | −0.126 396 37(1) | 0.123 498 56(1) |
| 2 | 8.528 325 052(1) | 8.758 870 25(1) | −0.125 816 16(1) | 0.123 835 55(1) |
| 3 | 7.504 503 422(1) | 7.735 777 20(1) | −0.124 992 24(1) | 0.124 317 10(1) |
| 4 | 6.792 824 081(1) | 7.025 002 41(1) | −0.123 968 79(1) | 0.124 918 48(1) |
| 5 | 6.251 627 078(1) | 6.484 860 42(1) | −0.122 774 94(1) | 0.125 623 30(1) |
| Z | $G_{\text{SE}}(1S_{1/2}, Z\alpha)$ | $G_{\text{SE}}(2S_{1/2}, Z\alpha)$ | $G_{\text{SE}}(2P_{1/2}, Z\alpha)$ | $G_{\text{SE}}(2P_{3/2}, Z\alpha)$ |
| 1 | −30.290 24(2) | −31.185 15(9) | −0.973 5(2) | −0.486 5(2) |
| 2 | −29.770 967(5) | −30.644 66(5) | −0.949 40(5) | −0.470 94(5) |
| 3 | −29.299 170(2) | −30.151 93(2) | −0.926 37(2) | −0.456 65(2) |
| 4 | −28.859 222(1) | −29.691 27(1) | −0.904 12(1) | −0.443 13(1) |
| 5 | −28.443 372 3(8) | −29.255 033(8) | −0.882 478(8) | −0.430 244(8) |

Table 1.5: Numerical results for the scaled function F [defined in Eq. (1.1)] and the remainder function G_{SE} implicitly defined in Eq. (1.2).

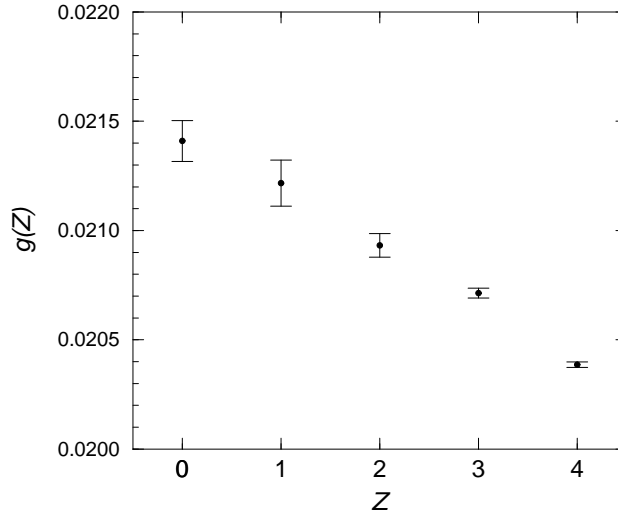


Figure 1.4: Plot of the function $g(Z)$ defined in Eq. (1.105) in the region of low nuclear charge. For the evaluation of the data point at $Z = 0$, a value of $A_{60}(1S_{1/2}) = -30.92415(1)$ is employed [9, 32, 88].

Among the different evaluations of A_{60} for the ground state, the result in [32] has the smallest quoted uncertainty. In Fig. 1.4 we display a plot of $g(Z)$ for low nuclear charge Z . A value of $A_{60}(1S_{1/2}) = A_{60}^{\text{ana}}(1S_{1/2}) = -30.92415(1)$ [9, 32, 88] is used in Fig. 1.4. The results indicate very good agreement between the numerical and analytic approaches to the Lamb shift in the low- Z region up to the level of a few Hz in frequency units for the low-lying atomic states (where n is the principal quantum number). The error bars represent the numerical uncertainty of the values in Table 1.5, which correspond to an uncertainty on the level of $1.0 \times Z^4$ Hz in frequency units.

Analytic work on the correction A_{60} has extended over three decades [32, 68, 69, 70, 71]. The complication arises that although the calculations are in general analytic, some remaining one-dimensional integrations could not be evaluated analytically because of the nature of the integrals [see e.g. Eq. (6.96) in [32]]. Therefore a step-by-step comparison of the analytic calculations is difficult. An additional difficulty is the isolation of those analytic terms which contribute in a given order in $Z\alpha$, i.e. the isolation of only those terms which contribute to A_{60} . The apparent consistency of the numerical and analytic data in Fig. 1.4 represents an independent consistency check on the rather involved analytic calculations.

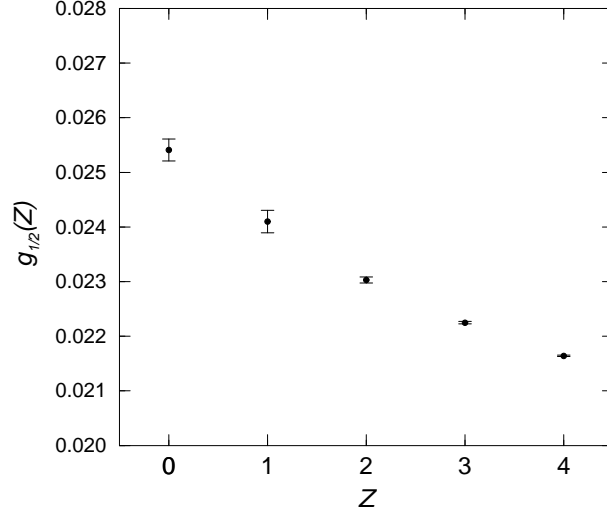


Figure 1.5: Comparison of numerical data and analytically evaluated higher-order binding corrections for the $2P_{1/2}$ state. We plot the function $g_{1/2}(Z)$ defined in Eq. (1.114) in the region of low Z . The numerical data appear to be consistent with the analytic result of $A_{60}(2P_{1/2}) = -0.99891(1)$ obtained in [1].

Our numerical results are not inconsistent with the analytic result [44] for a higher-order logarithm,

$$A_{71} = \pi \left(\frac{139}{64} - \ln 2 \right) = 4.65, \quad (1.112)$$

although they do not necessarily confirm it. As in [9], we obtain as an estimate $A_{71} = 5.5(1.0)$ (from the fit to the numerical data for both S states). Logarithmic terms corresponding to the probably nonvanishing A_{83} coefficient should be taken into account for a consistent fit of the corrections to G_{SE} . These highly singular terms are difficult to handle with a numerical fitting procedure. The terms A_{83} , A_{82} and A_{81} furnish three more free parameters for the numerical fit, where only five data points are available (in addition to the quantities A_{60} , A_{71} and A_{70} , which may also be regarded as free parameters for the fitting procedure). The determination of A_{60} by a fit from the numerical data is much more stable than the determination of the logarithmic correction A_{71} . We briefly note that our all-order evaluation essentially eliminates the uncertainty due to the unknown higher-order analytic terms. It is interesting to note that the same numerical methods are employed for both the S and P states in our all-order (in $Z\alpha$) calculation, whereas the analytic treatment of S and P states differs [1, 32].

The comparison of numerical and analytic result is much less problematic for P states, because the function G_{SE} is less singular [see Eqs. (1.4) and (1.6)]. For the 2P states, we observe that the function

$G_{\text{SE}}(2\text{P}_j, Z\alpha)$ has the same semi-analytic expansion about $Z\alpha = 0$ as the function $\Delta G_{\text{SE}}(Z\alpha)$ defined for S states in Eq. (1.100). We have

$$\begin{aligned} G_{\text{SE}}(2\text{P}_j, Z\alpha) = & A_{60}(2\text{P}_j) + (Z\alpha) A_{70}(2\text{P}_j) + (Z\alpha)^2 [A_{82}(2\text{P}_j) \ln^2(Z\alpha)^{-2} \\ & + A_{81}(2\text{P}_j) \ln(Z\alpha)^{-2} + A_{80}(2\text{P}_j) + o(Z\alpha)] . \end{aligned} \quad (1.113)$$

Hence, we plot the function

$$g_j(Z) = G_{\text{SE}}(2\text{P}_j, (Z+1)\alpha) - G_{\text{SE}}(2\text{P}_j, Z\alpha) \quad (1.114)$$

for $j = 1/2$ in the region of low Z , with the notion that an inconsistent analytic result for $A_{60}(2\text{P}_j)$ would lead to irregularity at $Z = 0$, in analogy with the S states. The numerical data shown in Fig. 1.5 appears to be consistent with the analytic results of

$$A_{60}(2\text{P}_{1/2}) = -0.998\,91(1) . \quad (1.115)$$

obtained in [1]. For the $2\text{P}_{3/2}$ state, see Fig. 6 of Ref. [12]. In this context it may be interesting to note that analytic results obtained in [1, 2] for the higher-order binding corrections to 2P, 3P and 4P states have recently been confirmed indirectly [89].

Chapter 2

Analytic Self–Energy Calculations for Excited States

2.1 Orientation

Analytic calculations of the one-loop self energy in bound systems have a long history, starting from Bethe’s seminal paper [33], and have meanwhile extended over more than five decades. The calculations are based on an expansion of the effect into powers of the parameter $Z\alpha$, where Z is the nuclear charge and α is the fine-structure constant (see e.g. [1, 2, 32, 43]). The expansion is semi-analytic, i.e. it involves powers of $Z\alpha$ and $\ln[(Z\alpha)^{-2}]$. Terms which are of higher than leading order in $Z\alpha$ are commonly referred to as the binding corrections (see also Ch. 3). A certain nonlogarithmic binding correction, known as the A_{60} -coefficient, has been of particular interest. For relevant formulas and definitions regarding A_{60} , we refer to Ch. 1, especially to Eqs. (1.1) – (1.6).

In this chapter, we present results of an analytic evaluation of higher-order binding corrections to the one-loop self energy for excited bound states of hydrogenlike systems. We focus on states with principal quantum numbers $n = 2 \dots 5$ and Dirac angular quantum numbers $\kappa = 1, -2, 2, \dots, 4, -5$. The current calculation represents a continuation of previous investigations on the subject [1, 2].

The improved results for A_{60} coefficients rely essentially on a more compact code for the analytic calculations, written in the computer-algebra package *Mathematica* [90], which enables the corrections to be evaluated semi-automatically. Intermediate expressions with some 10,000 terms are encountered, and the complexity of the calculations sharply increases with the principal quantum number n , and, as far as the complexity of the angular momentum algebra is concerned, with the orbital angular momentum $l = |\kappa + 1/2| - 1/2$ of the bound electron. Calculations were performed, in part, on IBM RISC/6000 workstations, both at the National Institute of Standards and Technology and at the Laboratoire Kastler–Brossel, and profited from the availability of 2 GigaBytes of Random Access Memory.

Of crucial importance was the development of convergence acceleration methods which were used extensively for the evaluation of remaining one-dimensional integrals which could not be done analytically. These integrals are analogous to expressions encountered in previous work [1, 2]. The numerically evaluated contributions involve slowly convergent hypergeometric series, and – in more extreme cases – infinite series over partial derivatives of hypergeometric functions, and generalizations of Lerch’s Φ transcendent [91, 92]. We have found the Combined Nonlinear–Condensation Transformation [23] to be a versatile method for the efficient numerical evaluation of the slowly convergent series encountered in the evaluation of the A_{60} -coefficients.

Results are given below for the A_{60} -coefficients with an absolute precision of 10^{-9} . As explained in detail in [1, 2, 32], the calculation of the one-loop self energy falls naturally into a high- and a low-energy part (F_H and F_L , respectively). In turn, the low-energy part can be separated naturally into the nonrelativistic dipole and the nonrelativistic quadrupole part, and into relativistic corrections to the current, to the hamiltonian, to the wavefunction, and to the energy of the bound state. For some states, severe numerical cancellations are observed between these (low-energy) contributions to the low-energy part of the self energy. In the final step of the calculation, we observe additional numerical

cancellations between the high- and the low-energy part for the finite contributions to A_{60} , beyond the necessary cancellation of the divergent contributions which depend on the scale-separation parameter ϵ ; this parameter and the mathematical method which is employed in the expansion of the self energy are described and explained in Sec. 2.2. For some of the investigated atomic states, the absolute magnitude of the A_{60} -coefficients is as small as 10^{-3} , although the largest single contribution is always on the order of 10^{-2} . This illustrates the cancellations between the finite contributions to A_{60} .

2.2 The epsilon-Method

We discuss here, by way of example, the ϵ method employed in the analytic calculation of the self energy in bound systems. This method is very suitable [1, 2, 32] for the separation of the two different energy scales for virtual photons: the nonrelativistic domain, in which the virtual photon assumes values of the order of the atomic binding energy, and the relativistic domain, in which the virtual photon assumes values of the order of the electron rest mass. Different approximation schemes and different asymptotic expansions are adequate for the two different domains. Without these approximations and expansions, the analytic evaluation of either the high- or the low-energy part would not be feasible. Therefore, the ϵ method is also used for the treatment of the highly excited atomic states which are the subject of (this part) of the thesis. At the same time, the model example discussed here is meant to illustrate the usefulness of the “ ϵ method” in a more general context.

We will consider here a model problem with one “virtual photon”. The separation into high- and low-energy photons necessitates the temporary introduction of a parameter ϵ ; the dependence on ϵ cancels when the high- and the low-energy parts are added together. We have,

$$\text{nonrelativistic domain} \ll \epsilon \ll \text{electron rest mass} \quad (2.1)$$

$$(Z\alpha)^2 m_e \ll \epsilon \ll m_e, \quad (2.2)$$

where α is the fine structure constant, and Z is the nuclear charge. The high-energy part is associated with photon energies $\omega > \epsilon$, and the low-energy part is associated with photon energies $\omega < \epsilon$.

In order to illustrate the procedure, we discuss a simple, one-dimensional example: the evaluation of

$$I(\beta) = \int_0^1 \sqrt{\frac{\omega^2 + \beta^2}{1 - \omega^2}} d\omega. \quad (2.3)$$

where the integration variable ω might be interpreted as the “energy” of a “virtual photon”. The integral I can be expressed in terms of special functions,

$$I(\beta) = \beta E\left(-\frac{1}{\beta^2}\right) = \beta \frac{\pi}{2} {}_2F_1\left(-\frac{1}{2}, \frac{1}{2}; 1; -\frac{1}{\beta^2}\right), \quad (2.4)$$

where E is the complete elliptic integral of the second kind, and ${}_2F_1$ denotes a hypergeometric function.

An alternative integral representation reads $I(\beta) = \int_0^{\pi/2} \sqrt{\beta^2 + \sin^2(\omega)} d\omega$.

The purpose of the calculation is to derive a semi-analytic expansion of $I(\beta)$ in powers of β and $\ln \beta$. The fine structure constant α takes the rôle of the expansion parameter β in actual calculations of the self energy. We discuss first the “high-energy part” of the calculation. It is given by the expression

$$I_H(\beta) = \int_\epsilon^1 \sqrt{\frac{\omega^2 + \beta^2}{1 - \omega^2}} d\omega. \quad (2.5)$$

For $\omega > \epsilon$, we may expand

$$\sqrt{\omega^2 + \beta^2} = \omega + \frac{\beta^2}{2\omega} + \frac{\beta^4}{8\omega^3} + \mathcal{O}(\beta^6), \quad (2.6)$$

but this expansion is not applicable in higher orders to the domain $0 < \omega < \epsilon$ because of the appearance of inverse powers of ω (analogous to an “infrared divergence” in QED).

The separation parameter ϵ acts as an infrared regulator. After expanding in β [see Eq. (2.6)], the resulting integrals in each order of β can be evaluated analytically. Subsequently, we expand every term in the

β -expansion in powers of ϵ up to the order ϵ^0 , i.e. we keep only the divergent and constant terms in ϵ . The result is

$$\begin{aligned}
I_H(\beta, \epsilon) &= 1 + \beta^2 \left\{ \frac{1}{2} \ln \left(\frac{2}{\epsilon} \right) + \mathcal{O}(\epsilon) \right\} \\
&+ \beta^4 \left\{ -\frac{1}{16\epsilon^2} - \frac{1}{16} \ln \left(\frac{2}{\epsilon} \right) + \frac{1}{32} + \mathcal{O}(\epsilon) \right\} \\
&+ \beta^6 \left\{ \frac{1}{64\epsilon^4} + \frac{1}{64\epsilon^2} + \frac{3}{128} \ln \left(\frac{2}{\epsilon} \right) - \frac{7}{512} + \mathcal{O}(\epsilon) \right\} \\
&+ \mathcal{O}(\beta^8).
\end{aligned} \tag{2.7}$$

Here, the “ \mathcal{O} ”-symbol identifies a contribution for which $\mathcal{O}(x)/x \rightarrow \text{const.}$ as $x \rightarrow 0$, whereas the “ \mathfrak{o} ”-symbol identifies the weaker requirement $\mathfrak{o}(x) \rightarrow 0$ as $x \rightarrow 0$; this is consistent with the standard notation (see e.g. [53]).

The contribution $I_H(\beta)$ corresponds to the “high-energy part” in an analytic calculation of the self energy, where the propagator of the bound electron is explicitly expanded in powers of the fine structure constant α . Now we turn to the “low-energy part”. The expression for the low-energy part ($0 < \omega < \epsilon$) reads

$$I_L(\beta) = \int_0^\epsilon \sqrt{\frac{\omega^2 + \beta^2}{1 - \omega^2}} d\omega. \tag{2.8}$$

The expansion (2.6) is not applicable in this energy domain; we therefore have to keep the numerator of the integrand $\sqrt{\omega^2 + \beta^2}$ in unexpanded form. However, we can expand the denominator $\sqrt{1 - \omega^2}$ of the integrand in powers of ω ; because $0 < \omega < \epsilon$ (with ϵ small), this expansion in ω is in fact an expansion in β – although the situation is somewhat problematic in the sense that every term in the ω -expansion gives rise to terms of arbitrarily high order in the β -expansion [see also Eq. (2.10) below].

The term $\sqrt{\omega^2 + \beta^2}$ is analogous to the Schrödinger–Coulomb propagator in the evaluation of the self energy – it has to be kept in an unexpanded form –, whereas the expansion

$$\frac{1}{\sqrt{1 - \omega^2}} = 1 + \frac{\omega^2}{2} + \frac{3}{8} \omega^4 + \mathcal{O}(\omega^6) \tag{2.9}$$

corresponds to the expansion into the $(Z\alpha)$ -expansion in the low-energy part.

Every term in the expansion (2.9) gives rise to arbitrarily high-order corrections in β , but it starts with the power $\omega^n \rightarrow \beta^{n+2}$. For example, we have for the leading term of order $\omega^0 = 1$ from Eq. (2.9),

$$\begin{aligned}
\int_0^\epsilon \sqrt{\omega^2 + \beta^2} d\omega &= \beta^2 \left\{ \frac{1}{2} \ln \left(\frac{2}{\beta} \epsilon \right) + \frac{1}{4} + \mathcal{O}(\epsilon) \right\} \\
&+ \beta^4 \left\{ \frac{1}{16\epsilon^2} + \mathcal{O}(\epsilon) \right\} + \beta^6 \left\{ -\frac{1}{64\epsilon^4} + \mathcal{O}(\epsilon) \right\} + \mathcal{O}(\beta^8).
\end{aligned} \tag{2.10}$$

Note that the terms generated in the orders β^4 and β^6 are needed to cancel divergent contributions in respective orders of β from the high-energy part given in Eq. (2.6). The term of order ω^2 from (2.9) results in

$$\begin{aligned}
\frac{1}{2} \int_0^\epsilon \omega^2 \sqrt{\omega^2 + \beta^2} d\omega &= \beta^4 \left\{ -\frac{1}{16} \ln \left(\frac{2}{\beta} \epsilon \right) + \frac{1}{64} + \mathcal{O}(\epsilon) \right\} \\
&+ \beta^6 \left\{ -\frac{1}{64\epsilon^2} + \mathcal{O}(\epsilon) \right\} + \mathcal{O}(\beta^8).
\end{aligned} \tag{2.11}$$

Altogether, we obtain for the low-energy part,

$$\begin{aligned}
I_L(\beta, \epsilon) &= \beta^2 \left\{ \frac{1}{2} \ln \left(\frac{2}{\beta} \epsilon \right) + \frac{1}{4} + \mathcal{O}(\epsilon) \right\} \\
&+ \beta^4 \left\{ \frac{1}{16 \epsilon^2} - \frac{1}{16} \ln \left(\frac{2}{\beta} \epsilon \right) + \frac{1}{64} + \mathcal{O}(\epsilon) \right\} \\
&+ \beta^6 \left\{ -\frac{1}{64 \epsilon^4} - \frac{1}{64 \epsilon^2} + \frac{3}{128} \ln \left(\frac{2}{\beta} \epsilon \right) - \frac{5}{512} + \mathcal{O}(\epsilon) \right\} \\
&+ \mathcal{O}(\beta^8 \ln \beta).
\end{aligned} \tag{2.12}$$

When the high-energy part (2.7) and the low-energy part (2.12) are added, the dependence on ϵ cancels, and we have

$$\begin{aligned}
I(\beta) &= I_H(\beta, \epsilon) + I_L(\beta, \epsilon) \\
&= 1 + \beta^2 \left\{ \frac{1}{2} \ln \left(\frac{4}{\beta} \right) + \frac{1}{4} \right\} + \beta^4 \left\{ -\frac{1}{16} \ln \left(\frac{4}{\beta} \right) + \frac{3}{64} \right\} \\
&+ \beta^6 \left\{ \frac{3}{128} \ln \left(\frac{4}{\beta} \right) - \frac{3}{128} \right\} + \mathcal{O}(\beta^8 \ln \beta).
\end{aligned} \tag{2.13}$$

In order to illustrate the analogy with the self energy calculation presented here, we would like to point out that the dependence on ϵ cancels out in the final result which is the sum of the high-energy part E_H given in Eq. (2.14) [for the two-loop case see Eq. (3.42)] and the low-energy part E_L in Eq. (2.15) [for the two-loop case see Eq. (3.58)].

2.3 Results for High- and Low-Energy Contributions

2.3.1 P_{1/2} states ($\kappa = 1$)

Here and in the following subsections, we present results which have been obtained for the high- and low-energy energy parts of the self energy or all states with principal quantum number $n = 2 \dots 5$ and orbital angular quantum number $l > 0$. These results, combined with numerical calculations for low-, intermediate and high nuclear charge, allow to reliably estimate quantum electrodynamic (QED) radiative corrections for any atomic state with principal quantum number $n \leq 5$. For the definition of the scaled self energy function F and of the analytic A -coefficients, see Eqs. (1.1) – (1.6). The results are given in terms of the expansion parameter $Z\alpha$ and the scale-separation parameter ϵ , whose rôle in the calculation is explained in Sec. 2.2.

For P_{1/2} states, we obtain for the following results for the high- and low-energy parts. The 2P_{1/2} high-energy part is:

$$F_H(2P_{1/2}) = -\frac{1}{6} + (Z\alpha)^2 \left[\frac{4177}{21600} - \frac{2}{9\epsilon} - \frac{103}{180} \ln(2\epsilon) \right], \tag{2.14}$$

2P_{1/2} low-energy part:

$$F_L(2P_{1/2}) = -\frac{4}{3} \ln k_0(2P) + (Z\alpha)^2 \left[-0.795\,649\,812(1) + \frac{2}{9\epsilon} + \frac{103}{180} \ln \left(\frac{\epsilon}{(Z\alpha)^2} \right) \right], \tag{2.15}$$

3P_{1/2} high-energy part:

$$F_H(3P_{1/2}) = -\frac{1}{6} + (Z\alpha)^2 \left[\frac{6191}{24300} - \frac{20}{81\epsilon} - \frac{268}{405} \ln(2\epsilon) \right], \quad (2.16)$$

3P_{1/2} low-energy part:

$$F_L(3P_{1/2}) = -\frac{4}{3} \ln k_0(3P) + (Z\alpha)^2 \left[-0.944\,288\,447(1) + \frac{20}{81\epsilon} + \frac{268}{405} \ln \left(\frac{\epsilon}{(Z\alpha)^2} \right) \right], \quad (2.17)$$

4P_{1/2} high-energy part:

$$F_H(4P_{1/2}) = -\frac{1}{6} + (Z\alpha)^2 \left[\frac{24409}{86400} - \frac{23}{90\epsilon} - \frac{499}{720} \ln(2\epsilon) \right], \quad (2.18)$$

4P_{1/2} low-energy part:

$$F_L(4P_{1/2}) = -\frac{4}{3} \ln k_0(4P) + (Z\alpha)^2 \left[-0.997\,810\,211(1) + \frac{23}{90\epsilon} + \frac{499}{720} \ln \left(\frac{\epsilon}{(Z\alpha)^2} \right) \right], \quad (2.19)$$

5P_{1/2} high-energy part:

$$F_H(5P_{1/2}) = -\frac{1}{6} + (Z\alpha)^2 \left[\frac{20129}{67500} - \frac{292}{1125\epsilon} - \frac{796}{1125} \ln(2\epsilon) \right], \quad (2.20)$$

5P_{1/2} low-energy part:

$$F_L(5P_{1/2}) = -\frac{4}{3} \ln k_0(5P) + (Z\alpha)^2 \left[-1.023\,991\,781(1) + \frac{292}{1125\epsilon} + \frac{796}{1125} \ln \left(\frac{\epsilon}{(Z\alpha)^2} \right) \right], \quad (2.21)$$

Here and in the following, $\ln k_0$ is the Bethe logarithm for which very accurate values are available [72, 73, 74, 75, 76, 77, 79].

2.3.2 P_{3/2} states ($\kappa = -2$)

The obtained results read as follows. The 2P_{3/2} high-energy part reads:

$$F_H(2P_{3/2}) = \frac{1}{12} + (Z\alpha)^2 \left[\frac{6577}{21600} - \frac{2}{9\epsilon} - \frac{29}{90} \ln(2\epsilon) \right], \quad (2.22)$$

2P_{3/2} low-energy part:

$$F_L(2P_{3/2}) = -\frac{4}{3} \ln k_0(2P) + (Z\alpha)^2 \left[-0.584\,516\,780(1) + \frac{2}{9\epsilon} + \frac{29}{90} \ln \left(\frac{\epsilon}{(Z\alpha)^2} \right) \right], \quad (2.23)$$

3P_{3/2} high-energy part:

$$F_H(3P_{3/2}) = \frac{1}{12} + (Z\alpha)^2 \left[\frac{67903}{194400} - \frac{20}{81\epsilon} - \frac{148}{405} \ln(2\epsilon) \right], \quad (2.24)$$

3P_{3/2} low-energy part:

$$F_L(3P_{3/2}) = -\frac{4}{3} \ln k_0(3P) + (Z\alpha)^2 \left[-0.693\,566\,427(1) + \frac{20}{81\epsilon} + \frac{148}{405} \ln \left(\frac{\epsilon}{(Z\alpha)^2} \right) \right], \quad (2.25)$$

4P_{3/2} high-energy part:

$$F_H(4P_{3/2}) = \frac{1}{12} + (Z\alpha)^2 \left[\frac{31399}{86400} - \frac{23}{90\epsilon} - \frac{137}{360} \ln(2\epsilon) \right], \quad (2.26)$$

4P_{3/2} low-energy part:

$$F_L(4P_{3/2}) = -\frac{4}{3} \ln k_0(4P) + (Z\alpha)^2 \left[-0.730\,579\,137(1) + \frac{23}{90\epsilon} + \frac{137}{360} \ln \left(\frac{\epsilon}{(Z\alpha)^2} \right) \right], \quad (2.27)$$

5P_{3/2} high-energy part:

$$F_H(5P_{3/2}) = \frac{1}{12} + (Z\alpha)^2 \left[\frac{199387}{540000} - \frac{292}{1125\epsilon} - \frac{436}{1125} \ln(2\epsilon) \right], \quad (2.28)$$

5P_{3/2} low-energy part:

$$F_L(5P_{3/2}) = -\frac{4}{3} \ln k_0(5P) + (Z\alpha)^2 \left[-0.747\,615\,653(1) + \frac{292}{1125\epsilon} + \frac{436}{1125} \ln \left(\frac{\epsilon}{(Z\alpha)^2} \right) \right]. \quad (2.29)$$

2.3.3 D_{3/2} states (kappa = 2)

The results obtained for states with $\kappa = 2$ read as follows. 3D_{3/2} high-energy part:

$$F_H(3D_{3/2}) = -\frac{1}{20} + (Z\alpha)^2 \left[-\frac{1721}{194400} - \frac{4}{405\epsilon} - \frac{4}{405} \ln(2\epsilon) \right], \quad (2.30)$$

3D_{3/2} low-energy part:

$$F_L(3D_{3/2}) = -\frac{4}{3} \ln k_0(3D) + (Z\alpha)^2 \left[0.021\,250\,354(1) + \frac{4}{405\epsilon} + \frac{4}{405} \ln \left(\frac{\epsilon}{(Z\alpha)^2} \right) \right], \quad (2.31)$$

4D_{3/2} high-energy part:

$$F_H(4D_{3/2}) = -\frac{1}{20} + (Z\alpha)^2 \left[-\frac{829}{86400} - \frac{1}{90\epsilon} - \frac{1}{90} \ln(2\epsilon) \right], \quad (2.32)$$

4D_{3/2} low-energy part:

$$F_L(4D_{3/2}) = -\frac{4}{3} \ln k_0(4D) + (Z\alpha)^2 \left[0.022\,882\,528(1) + \frac{1}{90\epsilon} + \frac{1}{90} \ln \left(\frac{\epsilon}{(Z\alpha)^2} \right) \right], \quad (2.33)$$

5D_{3/2} high-energy part:

$$F_H(5D_{3/2}) = -\frac{1}{20} + (Z\alpha)^2 \left[-\frac{35947}{3780000} - \frac{92}{7875\epsilon} - \frac{92}{7875} \ln(2\epsilon) \right], \quad (2.34)$$

5D_{3/2} low-energy part:

$$F_L(5D_{3/2}) = -\frac{4}{3} \ln k_0(5D) + (Z\alpha)^2 \left[0.023\,759\,683(1) + \frac{92}{7875\epsilon} + \frac{92}{7875} \ln \left(\frac{\epsilon}{(Z\alpha)^2} \right) \right]. \quad (2.35)$$

2.3.4 D_{5/2} states (kappa = -3)

For D_{5/2} states with Dirac quantum number $\kappa = -3$, the results read as follows. For the 3D_{5/2} high-energy part, we have:

$$F_H(3D_{5/2}) = \frac{1}{30} + (Z\alpha)^2 \left[\frac{371}{24300} - \frac{4}{405\epsilon} - \frac{4}{405} \ln(2\epsilon) \right], \quad (2.36)$$

3D_{5/2} low-energy part:

$$F_L(3D_{5/2}) = -\frac{4}{3} \ln k_0(3D) + (Z\alpha)^2 \left[0.019\,188\,397(1) + \frac{4}{405\epsilon} + \frac{4}{405} \ln \left(\frac{\epsilon}{(Z\alpha)^2} \right) \right], \quad (2.37)$$

4D_{5/2} high-energy part:

$$F_H(4D_{5/2}) = \frac{1}{30} + (Z\alpha)^2 \left[\frac{53}{2880} - \frac{1}{90\epsilon} - \frac{1}{90} \ln(2\epsilon) \right], \quad (2.38)$$

4D_{5/2} low-energy part:

$$F_L(4D_{5/2}) = -\frac{4}{3} \ln k_0(4D) + (Z\alpha)^2 \left[0.020\,710\,720(1) + \frac{1}{90\epsilon} + \frac{1}{90} \ln \left(\frac{\epsilon}{(Z\alpha)^2} \right) \right], \quad (2.39)$$

5D_{5/2} high-energy part:

$$F_H(5D_{5/2}) = \frac{1}{30} + (Z\alpha)^2 \left[\frac{3097}{157500} - \frac{92}{7875\epsilon} - \frac{92}{7875} \ln(2\epsilon) \right], \quad (2.40)$$

5D_{5/2} low-energy part:

$$F_L(5D_{5/2}) = -\frac{4}{3} \ln k_0(5D) + (Z\alpha)^2 \left[0.021\,511\,798(1) + \frac{92}{7875\epsilon} + \frac{92}{7875} \ln \left(\frac{\epsilon}{(Z\alpha)^2} \right) \right]. \quad (2.41)$$

2.3.5 F_{5/2} states (kappa = 3)

Now we turn our attention to F_{5/2} states. We have for the 4F_{5/2} high-energy part:

$$F_H(4F_{5/2}) = -\frac{1}{42} + (Z\alpha)^2 \left[-\frac{493}{235200} - \frac{1}{630\epsilon} - \frac{1}{630} \ln(2\epsilon) \right], \quad (2.42)$$

4F_{5/2} low-energy part:

$$F_L(4F_{5/2}) = -\frac{4}{3} \ln k_0(4F) + (Z\alpha)^2 \left[0.005\,523\,310(1) + \frac{1}{630\epsilon} + \frac{1}{630} \ln \left(\frac{\epsilon}{(Z\alpha)^2} \right) \right], \quad (2.43)$$

5F_{5/2} high-energy part:

$$F_H(5F_{5/2}) = -\frac{1}{42} + (Z\alpha)^2 \left[-\frac{2657}{1102500} - \frac{2}{1125\epsilon} - \frac{2}{1125} \ln(2\epsilon) \right], \quad (2.44)$$

5F_{5/2} low-energy part:

$$F_L(5F_{5/2}) = -\frac{4}{3} \ln k_0(5F) + (Z\alpha)^2 \left[0.006\,045\,398(1) + \frac{2}{1125\epsilon} + \frac{2}{1125} \ln \left(\frac{\epsilon}{(Z\alpha)^2} \right) \right], \quad (2.45)$$

2.3.6 F_{7/2} states (kappa = -4)

States with $\kappa = -4$ yield the following results. We obtain for the 4F_{7/2} state (high-energy part):

$$F_H(4F_{7/2}) = \frac{1}{56} + (Z\alpha)^2 \left[\frac{25357}{8467200} - \frac{1}{630\epsilon} - \frac{1}{630} \ln(2\epsilon) \right], \quad (2.46)$$

4F_{7/2} low-energy part:

$$F_L(4F_{7/2}) = -\frac{4}{3} \ln k_0(4F) + (Z\alpha)^2 \left[0.005\,180\,461(1) + \frac{1}{630\epsilon} + \frac{1}{630} \ln \left(\frac{\epsilon}{(Z\alpha)^2} \right) \right], \quad (2.47)$$

5F_{7/2} high-energy part:

$$F_H(5F_{7/2}) = \frac{1}{56} + (Z\alpha)^2 \left[\frac{774121}{211680000} - \frac{2}{1125\epsilon} - \frac{2}{1125} \ln(2\epsilon) \right], \quad (2.48)$$

5F_{7/2} low-energy part:

$$F_L(5F_{7/2}) = -\frac{4}{3} \ln k_0(5F) + \frac{2(Z\alpha)^2}{1125\epsilon} + (Z\alpha)^2 \left[0.005\,662\,248(1) + \frac{2}{1125} \ln \left(\frac{\epsilon}{(Z\alpha)^2} \right) \right]. \quad (2.49)$$

2.3.7 G_{7/2} states ($\kappa = 4$)

G_{7/2} and G_{9/2} states involve the most problematic angular momentum algebra of all atomic states considered here. We obtain,

$$F_H(5G_{7/2}) = -\frac{1}{72} + (Z\alpha)^2 \left[-\frac{4397}{6048000} - \frac{2}{4725\epsilon} - \frac{2}{4725} \ln(2\epsilon) \right], \quad (2.50)$$

and for the low-energy part,

$$F_L(5G_{7/2}) = -\frac{4}{3} \ln k_0(5G) + (Z\alpha)^2 \left[0.001\,834\,827(1) + \frac{2}{4725\epsilon} + \frac{2}{4725} \ln \left(\frac{\epsilon}{(Z\alpha)^2} \right) \right]. \quad (2.51)$$

2.3.8 G_{9/2} states ($\kappa = -5$)

We conclude by investigating G_{9/2} states, where the high-energy part reads ($n = 5$)

$$F_H(5G_{9/2}) = \frac{1}{90} + (Z\alpha)^2 \left[\frac{269}{283500} - \frac{2}{4725\epsilon} - \frac{2}{4725} \ln(2\epsilon) \right], \quad (2.52)$$

and the low-energy part reads,

$$F_L(5G_{9/2}) = -\frac{4}{3} \ln k_0(5G) + (Z\alpha)^2 \left[0.001\,757\,471(1) + \frac{2}{4725\epsilon} + \frac{2}{4725} \ln \left(\frac{\epsilon}{(Z\alpha)^2} \right) \right]. \quad (2.53)$$

2.4 Summary of Results

By adding the high- and low-energy parts given in Secs. 2.3.1 – 2.3.8, we obtain the following results for the self energy. For all atomic states, the dependence on the scale-separating parameter ϵ cancels when the low- and the high-energy parts are added, in agreement with the principal idea of the ϵ -method described in Sec. 2.2. The coefficients A_{40} , A_{61} and A_{60} can then be read off according to the definitions contained in Eqs. (1.1) – (1.6).

| $P_{1/2}$ state ($\kappa = 1$) | | | | | |
|----------------------------------|--|----------------|--------------------|----------------|-------------------|
| n | A_{40} | A_{40} (num) | A_{61} | A_{61} (num) | A_{60} (num) |
| 2 | $-\frac{1}{6} - \frac{4}{3} \ln k_0(2P)$ | -0.126 644 | $\frac{103}{108}$ | 0.572 222 | -0.998 904 402(1) |
| 3 | $-\frac{1}{6} - \frac{4}{3} \ln k_0(3P)$ | -0.115 746 | $\frac{268}{405}$ | 0.661 728 | -1.148 189 956(1) |
| 4 | $-\frac{1}{6} - \frac{4}{3} \ln k_0(4P)$ | -0.110 727 | $\frac{499}{720}$ | 0.693 056 | -1.195 688 142(1) |
| 5 | $-\frac{1}{6} - \frac{4}{3} \ln k_0(5P)$ | -0.107 954 | $\frac{796}{1125}$ | 0.707 556 | -1.216 224 512(1) |

Table 2.1: Results for $P_{1/2}$ states. The coefficients A_{40} and A_{61} are rational numbers; in the columns entitled “(num)”, we give the numerical values to six decimals. The A_{60} -coefficients in the last column constitute the main result of the investigation presented in the current chapter. As explained in Sec. 2.1, these coefficients involve numerical integrals which cannot be done analytically.

2.5 Typical Cancellations

As already emphasized in Sec. 2.1, severe numerical cancellations are encountered in the calculation of the A_{60} -coefficients. These cancellations will be illustrated here in Tables 2.8 and 2.9 for the $5G_{7/2}$ state.

| $P_{3/2}$ state ($\kappa = -2$) | | | | | |
|-----------------------------------|--|----------------|--------------------|----------------|-------------------|
| n | A_{40} | A_{40} (num) | A_{61} | A_{61} (num) | A_{60} (num) |
| 2 | $\frac{1}{12} - \frac{4}{3} \ln k_0(2P)$ | 0.123 355 | $\frac{29}{90}$ | 0.322 222 | -0.503 373 465(1) |
| 3 | $\frac{1}{12} - \frac{4}{3} \ln k_0(3P)$ | 0.134 254 | $\frac{148}{405}$ | 0.365 432 | -0.597 569 388(1) |
| 4 | $\frac{1}{12} - \frac{4}{3} \ln k_0(4P)$ | 0.139 273 | $\frac{137}{360}$ | 0.380 556 | -0.630 945 796(1) |
| 5 | $\frac{1}{12} - \frac{4}{3} \ln k_0(5P)$ | 0.142 046 | $\frac{426}{1125}$ | 0.387 556 | -0.647 013 509(1) |

Table 2.2: Analytic results for $P_{3/2}$ states.

| $D_{3/2}$ state ($\kappa = 2$) | | | | | |
|----------------------------------|---|----------------|-------------------|----------------|------------------|
| n | A_{40} | A_{40} (num) | A_{61} | A_{61} (num) | A_{60} (num) |
| 3 | $-\frac{1}{20} - \frac{4}{3} \ln k_0(3D)$ | -0.043 024 | $\frac{4}{405}$ | 0.009 877 | 0.005 551 575(1) |
| 4 | $-\frac{1}{20} - \frac{4}{3} \ln k_0(4D)$ | -0.041 012 | $\frac{1}{90}$ | 0.011 111 | 0.005 587 985(1) |
| 5 | $-\frac{1}{20} - \frac{4}{3} \ln k_0(5D)$ | -0.039 866 | $\frac{92}{7875}$ | 0.011 682 | 0.006 152 175(1) |

Table 2.3: Analytic results for $D_{3/2}$ states.

2.6 Observations

It is hoped that the analytic calculations described in the previous sections will be supplemented in the near future by a numerical treatment of the problem, which follows the lines indicated in Ch. 1. Work performed recently on relevant angular functions [93] is expected to become useful in that context. In order to facilitate the comparisons and consistency checks which will be of relevance for the numerical calculations, we report here on a number of observations which should facilitate the comparison of numerical and analytic approaches to the self energy problem. They are relevant for all atomic states under investigation here.

- (i) Our analytic calculations for the high-energy part establish the structure of nonvanishing A_{40} , A_{61} and A_{60} -coefficients for the states under investigation.

| $D_{5/2}$ state ($\kappa = -3$) | | | | | |
|-----------------------------------|--|----------------|-------------------|----------------|------------------|
| n | A_{40} | A_{40} (num) | A_{61} | A_{61} (num) | A_{60} (num) |
| 3 | $\frac{1}{30} - \frac{4}{3} \ln k_0(3D)$ | 0.040 310 | $\frac{4}{405}$ | 0.009 877 | 0.027 609 989(1) |
| 4 | $\frac{1}{30} - \frac{4}{3} \ln k_0(4D)$ | 0.042 321 | $\frac{1}{90}$ | 0.011 111 | 0.031 411 862(1) |
| 5 | $\frac{1}{30} - \frac{4}{3} \ln k_0(5D)$ | 0.043 468 | $\frac{92}{7875}$ | 0.011 682 | 0.033 077 571(1) |

Table 2.4: Analytic results for $D_{5/2}$ states.

| $F_{5/2}$ state ($\kappa = 3$) | | | | | |
|----------------------------------|---|----------------|------------------|----------------|------------------|
| n | A_{40} | A_{40} (num) | A_{61} | A_{61} (num) | A_{60} (num) |
| 4 | $-\frac{1}{42} - \frac{4}{3} \ln k_0(4F)$ | -0.021 498 | $\frac{1}{630}$ | 0.001 587 | 0.002 326 988(1) |
| 5 | $-\frac{1}{42} - \frac{4}{3} \ln k_0(5F)$ | -0.020 873 | $\frac{2}{1125}$ | 0.001 778 | 0.002 403 159(1) |

Table 2.5: Analytic results for $F_{5/2}$ states.

| $F_{7/2}$ state ($\kappa = -4$) | | | | | |
|-----------------------------------|--|----------------|------------------|----------------|------------------|
| n | A_{40} | A_{40} (num) | A_{61} | A_{61} (num) | A_{60} (num) |
| 4 | $\frac{1}{56} - \frac{4}{3} \ln k_0(4F)$ | 0.020 169 | $\frac{1}{630}$ | 0.001 587 | 0.007 074 960(1) |
| 5 | $\frac{1}{56} - \frac{4}{3} \ln k_0(5F)$ | 0.020 793 | $\frac{2}{1125}$ | 0.001 778 | 0.008 087 021(1) |

Table 2.6: Analytic results for $F_{7/2}$ states.

(ii) For a given κ quantum number, the coefficients increase in absolute magnitude with increasing principal quantum number n . This is the case for Bethe logarithms, for A_{61} coefficients and also for A_{60} coefficients. This behavior is consistent with the phenomenon that relativistic corrections to the self energy become more important as n increases.

(iii) For a given principal quantum number n , the coefficients decrease in absolute magnitude with increasing κ . As a function of the nuclear charge number Z , the plots of $F(Z\alpha)$ against Z should become “more flat” as κ increases for a given n [94].

(iv) The A_{61} coefficients, which represent the dominant relativistic correction to $F(Z\alpha)$, all have the same (positive) sign for states with κ quantum numbers $\kappa = 2, -3, 3, -4, 4, -5$. This “same-sign” pattern is also true of the A_{60} coefficients. Because A_{61} is the *dominant* correction in the order $(Z\alpha)^6$ due to the enhancement by the large logarithm, this observation explains why, in general, the qualitative dependence (on the nuclear charge number Z) of the self energy correction for the highly excited states is the same for the states with $\kappa = 2, -3, 3, -4, 4, -5$ (see [94]).

(v) A_{61} -coefficients are different for $P_{1/2}$ and $P_{3/2}$ states, but the spin dependence vanishes for higher

| $G_{7/2}$ state ($\kappa = 4$) | | | | | |
|----------------------------------|---|----------------|------------------|----------------|------------------|
| n | A_{40} | A_{40} (num) | A_{61} | A_{61} (num) | A_{60} (num) |
| 5 | $-\frac{1}{72} - \frac{4}{3} \ln k_0(5G)$ | -0.012 860 | $\frac{2}{4725}$ | 0.000 423 | 0.000 814 414(1) |

| $G_{9/2}$ state ($\kappa = -5$) | | | | | |
|-----------------------------------|--|----------------|------------------|----------------|------------------|
| n | A_{40} | A_{40} (num) | A_{61} | A_{61} (num) | A_{60} (num) |
| 5 | $\frac{1}{90} - \frac{4}{3} \ln k_0(5G)$ | 0.012 141 | $\frac{2}{4725}$ | 0.000 423 | 0.002 412 929(1) |

Table 2.7: Analytic results for $G_{7/2}$ and $G_{9/2}$ states.

| Contributions to the Low-Energy Part (5G _{7/2}) | |
|---|----------------------|
| A_{60} -contribution due to F_{nq} | 0.002 875 830 9(5). |
| A_{60} -contribution due to $F_{\delta\text{y}}$ | -0.001 083 109 4(5). |
| A_{60} -contribution due to $F_{\delta\text{H}}$ | -0.008 917 782 1(5). |
| A_{60} -contribution due to $F_{\delta\text{E}}$ | 0.004 920 556 0(5). |
| A_{60} -contribution due to $F_{\delta\phi}$ | 0.004 039 332 1(5). |
| A_{60} [from low-energy, cf. Eq. (2.51)] | 0.001 834 827(1) |

Table 2.8: As explained in Refs. [1, 2], the low-energy part of the self energy can be separated naturally into the nonrelativistic dipole term (which does not contribute to A_{60}), and into the following contributions: the nonrelativistic quadrupole part F_{nq} , the relativistic corrections to the current $F_{\delta\text{y}}$, and relativistic corrections to the hamiltonian $F_{\delta\text{H}}$, to the bound-state energy $F_{\delta\text{E}}$ and to the wavefunction $F_{\delta\phi}$. Observe that the total contribution to A_{60} to the low-energy part which read 0.001 834 827(1) is almost an order-of-magnitude smaller than the biggest individual contribution (from $F_{\delta\text{H}}$), due to mutual cancellations.

| | |
|---------------|------------------|
| $A_{60}(F_H)$ | -0.001 020 413 |
| $A_{60}(F_L)$ | 0.001 834 827(1) |
| A_{60} | 0.000 814 415(1) |

Table 2.9: An additional numerical cancellation occurs when the finite contributions to A_{60} originating from the low-energy part [$A_{60}(F_L)$, see Eq. (2.51)] and the high-energy part [$A_{60}(F_H)$, see Eq. (2.50)] are added. The result for the total A_{60} is also contained in Table 2.7.

orbital angular momentum L . Consequently, A_{61} -coefficients are the same e.g. for $D_{3/2}$ and $D_{5/2}$ states, or for $F_{5/2}$ and $F_{7/2}$ states etc. This can be easily checked against numerical results.

Preliminary results indicate satisfactory consistency between the analytic and numerical approaches to the self energy problem for highly excited states [95].

Chapter 3

The Two-Loop Self-Energy

3.1 Orientation

In the current Chapter, we investigate two-loop higher-order binding corrections to the fine structure, which contribute to the spin-dependent part of the Lamb shift. Our calculation focuses on the so-called “two-loop self energy” involving two virtual closed photon loops. For bound states, this correction has proven to be notoriously difficult to evaluate. The calculation of the binding corrections to the bound-state two-loop self energy is simplified by a separate treatment of hard and soft virtual photons. The two photon-energy scales are matched at the end of the calculation. We present results for the fine-structure difference of the two-loop self energy through the order of α^8 .

3.2 Introduction to the Two-Loop Self-Energy

As already discussed in Secs. 1.3.1 and 2.1 – 2.3, radiative corrections can be described – for atomic systems with low nuclear charge number – by a nonanalytic expansion in powers of the three parameters (i) α (the fine-structure constant), (ii) the product $Z\alpha$ (Z is the nuclear charge number), and (iii) the logarithm $\ln[(Z\alpha)^{-2}]$. The expansion in powers of α , which is the perturbation theory parameter in quantum electrodynamics (QED), corresponds to the number of loops in the diagrams. The bound-state effects are taken into account by the expansions in the two latter parameters (see also Ch. 2). Higher-order terms in the expansions in powers of $Z\alpha$ and $\ln[(Z\alpha)^{-2}]$ are referred to as the “binding corrections”. One of the historically most problematic sets of Feynman diagrams in the treatment of the Lamb shift for atomic systems has been the radiative correction due to two closed virtual-photon loops shown in Fig. 3.1.

Let us recall at this point that even the evaluation of higher-order binding corrections to the one-loop self energy – see also Ch. 2 –, which *a priori* should represent a less involved calculational challenge, has represented a problem for analytic evaluations for over three decades [1, 2, 9, 32, 70, 71, 96]. The energy shifts of the bound states due to the radiative corrections are conveniently expressed by expansion coefficients corresponding to the powers of $Z\alpha$ and $\ln[(Z\alpha)^{-2}]$; the naming convention is that the power of $Z\alpha$ and the power of the logarithm are indicated as indices to the analytic coefficients [see also Eq. (3.1)] below. Because the expansion in both the one-loop and the two-loop case starts with the fourth power of $Z\alpha$, the non-vanishing coefficients carry indices A_{kl} and B_{kl} for the one- and two-loop cases, respectively (with $k \geq 4$ – see [49, 97] for comprehensive reviews).

Logarithmic corrections with $l \geq 1$ can sometimes be inferred separately in a much simplified approach, e.g. by considering infrared divergent contributions to electron form factors. By contrast, the higher-order non-logarithmic coefficients represent a considerable calculational challenge. Realistically, i.e. with the help of current computer algebra systems [90], one can hope to evaluate non-logarithmic coefficients of sixth order in $Z\alpha$. Complete results for the one-loop higher-order correction A_{60} for S and P states have only been available recently [1, 2, 32]. Calculational difficulties have by now precluded a successful evaluation of the corresponding coefficient B_{60} for the two-loop effect. Ground-work for the evaluation of B_{60} was laid in [98]. Here, we are concerned with the evaluation of the fine-structure differences of the

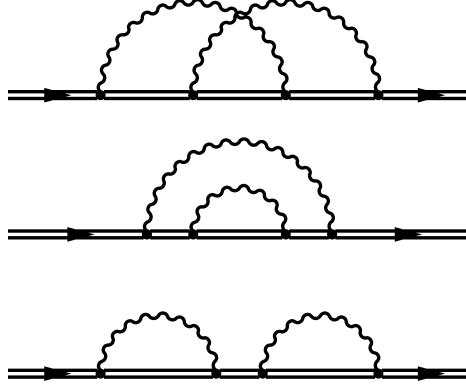


Figure 3.1: Feynman diagrams representing the two-photon electron self energy. The double line denotes the bound electron propagator. The arrow of time is from left to right.

logarithmic and non-logarithmic coefficients B_{6L} (where $L = 0, 1, 2$), i.e. with the $nP_{3/2}$ - $nP_{1/2}$ difference of these coefficients.

Using natural Gaussian units ($\hbar = c = \epsilon_0 = 1$), as it is customary for the current type of calculation, we write the two-photon self energy in the $Z\alpha$ -expansion for P states in terms of B -coefficients as

$$\Delta E_{\text{SE}} = \left(\frac{\alpha}{\pi}\right)^2 (Z\alpha)^4 \frac{m}{n^3} \left[B_{40} + (Z\alpha)^2 [B_{62} \ln^2(Z\alpha)^{-2} + B_{61} \ln(Z\alpha)^{-2} + B_{60}] + \mathcal{R} \right], \quad (3.1)$$

where the remainder \mathcal{R} is of order $\mathcal{O}(Z\alpha)^3$. Relevant Feynman diagrams are shown in Fig. 3.1.

Here, m denotes the electron mass (we write Eq. (3.1) in the non-recoil limit, i.e. for an infinite nuclear mass). The double logarithmic B_{62} -coefficient is spin-independent, so that we have $\Delta_{\text{fs}} B_{62} = 0$. Here, we evaluate the fine-structure differences

$$\Delta_{\text{fs}} B_{61} = B_{61}(nP_{3/2}) - B_{61}(nP_{1/2}),$$

$$\Delta_{\text{fs}} B_{60} = B_{60}(nP_{3/2}) - B_{60}(nP_{1/2}). \quad (3.2)$$

We follow the convention that $\Delta_{\text{fs}} X \equiv X(nP_{3/2}) - X(nP_{1/2})$ denotes the “fine-structure part” of a given quantity X . For $\Delta_{\text{fs}} B_{61}$ and $\Delta_{\text{fs}} B_{60}$, we provide complete results. It is perhaps worth noting that the two-loop self energy for bound states has represented a considerable challenge for theoretical evaluations. Our investigation represents a continuation of previous work on the two-loop problem (see e.g. [98, 99, 100, 101]). It is probably a triviality to express that technical difficulties in the calculation and its description in the following Sections cannot be avoided.

For the description of the self energy radiative effects – mediated by hard virtual photons –, we use the modified Dirac hamiltonian

$$H_{\text{D}}^{(m)} = \boldsymbol{\alpha} \cdot [\mathbf{p} - e F_1(\Delta) \mathbf{A}] + \beta m + e F_1(\Delta) \phi + F_2(\Delta) \frac{e}{2m} (\mathbf{i} \boldsymbol{\gamma} \cdot \mathbf{E} - \beta \boldsymbol{\sigma} \cdot \mathbf{B}), \quad (3.3)$$

which approximately describes an electron subject to an external scalar potential $\phi \equiv \phi(\mathbf{r})$ and an external vector potential $\mathbf{A} \equiv \mathbf{A}(\mathbf{r})$. This modified hamiltonian is still local in coordinate space. The Dirac matrices in (3.3) are to be understood in the standard (Dirac) representation [34] (in the sequel, we will also use the non-covariant notation $\beta \equiv \gamma^0$ and $\alpha^i \equiv \gamma^0 \gamma^i$).

The argument Δ of the electron form factors F_1 and F_2 in Eq. (3.3) is to be interpreted as a Laplacian operator acting on all quantities to the right (but not on the wave function of the bound electron in evaluating $H_D^{(m)}|\psi\rangle$). In momentum space, the action of the hamiltonian $H_D^{(m)}$ is described by the convolution $[H_D^{(m)}\psi](\mathbf{p}') = \int d^3p/(2\pi)^3 H_D^{(m)}(\mathbf{p}' - \mathbf{p}) \psi(\mathbf{p})$. The form factors – in momentum space – assume arguments according to the replacement $\Delta \rightarrow -q^2 \equiv -(\mathbf{p}' - \mathbf{p})^2$. In Eq. (3.3), radiative corrections are taken into account in the sense of an effective theory via the inclusion of the on-shell form factors F_1 and F_2 . Although the bound electron is not an on-shell particle, the modified hamiltonian (3.3) can still approximately account for significant radiative systems with low nuclear charge number Z . Of course, the hamiltonian (3.3) cannot offer a complete description of the bound electron. Recoil effects cannot be described by a one-particle equation *in principle*, and vacuum-polarization effects are not contained in Eq. (3.3). However, the effective description of self energy radiative corrections mediated by hard virtual photons given by Eq. (3.3) will turn out to be useful in the context of the current investigation of the two-loop self energy.

Both of the form factors F_1 and F_2 entering in Eq. (3.3) are infrared divergent, but this divergence is cut off in a natural way at the atomic binding energy scale $(Z\alpha)^2 m$. The fact that on-shell form factors can describe radiative corrections to the fine structure – mediated by high-energy virtual photons – has been demonstrated explicitly in [89]. The modified Dirac hamiltonian (3.3) and the associated modified Dirac equation have been introduced – in the one-loop approximation – in Ch. 7 of [34] [see for example Eqs. (7-77) and (7-103) *ibid.*]. The low-energy part of the calculation is carried out using nonrelativistic approximations in the spirit of the simplified treatment introduced in the previous one- and two-loop calculations [1, 2, 32, 98, 102]. This approach was inspired, in part, by various attempts to formulate simplified low-energy (“nonrelativistic”) approximations to quantum electrodynamics (“NRQED”), see e.g. [103, 104]. Both the high-energy and the low-energy contributions are matched at the separation scale ϵ whose rôle in the calculation is illustrated by the mathematical model example discussed in Sec. 2.2.

In a two-loop calculation, either of the two virtual photons may have a high or low energy as compared to the separation scale ϵ . *A priori*, this necessitates [98] a separation of the calculation into three different contributions: (i) both photon energies large, (ii) one photon with a large and one with a small energy, and (iii) both photons with small energies. For the particular problem at hand (the fine-structure differences of B_{61} and B_{60}), we are in the fortunate position that effects caused by hard virtual photons (i) are described by the modified Dirac hamiltonian (3.3), whereas the low-energy part discussed in Sec. 3.5 below comprises both remaining contributions (ii) and (iii).

We will continue by analyzing the two-loop form factors which enter into Eq. (3.3); these will be treated in Sec. 3.3. The calculation will be split into two parts: the high-energy part discussed in Sec. 3.4 and the low-energy part, which is treated along ideas introduced in [104] in Sec. 3.5.

3.3 Two-loop Form Factors

In order to analyze the modified Dirac hamiltonian (3.3) through two-loop order, we first have to investigate certain expansion coefficients of the electronic F_1 and F_2 form factors which are thoroughly discussed in the seminal papers [105, 106]. For the momentum transfer q^2 which is the argument of the two functions $F_1 \equiv F_1(q^2)$ and $F_2 \equiv F_2(q^2)$, we use the convention $q^2 = q_\mu q^\mu = (q^0)^2 - \mathbf{q}^2$. The variable t in [105, 106] is given as $t = q^2$. When we evaluate radiative corrections to the binding Coulomb field which is mediated by space-like virtual photons, we have $q^2 = -\mathbf{q}^2$ because for $q^0 = 0$. We use the conventions (see Eq. (1.2) in [105]):

$$F_1(t) = 1 + \sum_{n=1}^{\infty} \left(\frac{\alpha}{\pi}\right)^n F_1^{(2n)}(t), \quad F_2(t) = \sum_{n=1}^{\infty} \left(\frac{\alpha}{\pi}\right)^n F_2^{(2n)}(t). \quad (3.4)$$

One and two-loop effects are denoted by upper indices 2 and 4, respectively. This notation is motivated by the observation that two-loop effects are of forth order in the quantum electrodynamic interaction Lagrangian $-e\bar{\psi}\gamma^\mu A_\mu\psi$ (in the Furry picture, which is used for the description of bound states, the Coulomb interaction is taken out of the interaction Lagrangian).

There are two different points of view regarding the choice of diagrams to be included in the two-loop form factors, depending on whether the self energy vacuum polarization diagram Fig. 3.2 is included in

the calculation or not. We will discuss both cases and give results with and without the diagram shown in Fig. 3.2 taken into account.

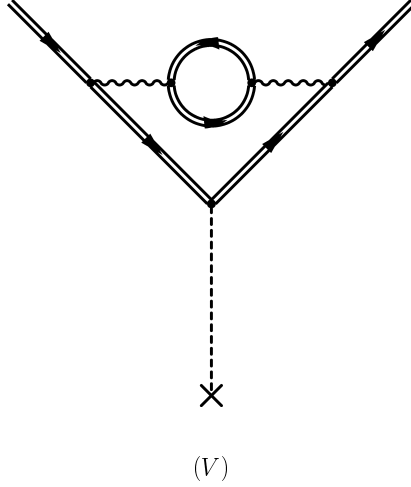


Figure 3.2: Combined self energy vacuum-polarization diagram (denoted “V” in the text).

First, we discuss results obtained for F_1 *including* the combined self energy vacuum polarization diagram. In this case, the known results for the slope $F_1'(0)$ and for $F_2(0)$, through two-loop order, read as follows. From Eq. (1.11) of [105], we have:

$$m^2 F_1'(0) = \frac{\alpha}{\pi} \left[-\frac{1}{3} \ln \left(\frac{\lambda}{m} \right) - \frac{1}{8} \right] + \left(\frac{\alpha}{\pi} \right)^2 \left[-\frac{4819}{5184} - \frac{49}{72} \zeta(2) + 3 \zeta(2) \ln 2 - \frac{3}{4} \zeta(3) \right], \quad (3.5)$$

where the forth-order coefficient has the numerical value

$$m^2 F_1'^{(4)}(0) = 0.469\,941\,487\,460. \quad (3.6)$$

According to Eq. (1.7) in [105], the value of $F_2(0)$, through two-loop order, reads

$$F_2(0) = \frac{1}{2} \frac{\alpha}{\pi} + \left(\frac{\alpha}{\pi} \right)^2 \left[\frac{197}{144} + \frac{1}{2} \zeta(2) - 3 \zeta(2) \ln 2 + \frac{3}{4} \zeta(3) \right], \quad (3.7)$$

where the two-loop coefficient has the numerical value

$$F_2^{(4)}(0) = -0.328\,478\,965\,579. \quad (3.8)$$

We now turn to the discussion of the slope $F_2'^{(4)}(0)$. In view of Eq. (1.20) of [105] (see also [107]), we have (up to two-loop order)

$$F_2(t) = \frac{\alpha}{\pi} \mathcal{F}_2^{(2)}(t) + \left(\frac{\alpha}{\pi} \right)^2 \left[\ln \frac{\lambda}{m} B(t) \mathcal{F}_2^{(2)}(t) + \mathcal{F}_2^{(4)}(t) \right], \quad (3.9)$$

where the coefficients \mathcal{F} are by definition infrared safe and

$$\mathcal{F}_2^{(2)}(0) = \frac{1}{2}, \quad B(t) = -\frac{t}{3m^2} - \frac{t^2}{20m^2} + \mathcal{O}(t^3). \quad (3.10)$$

Equations (3.9) and (3.10) uniquely determine the infrared divergent contribution to $F_2'^{(4)}(0)$. An analytic expressions for $\mathcal{F}_2^{(4)}(t)$, t spacelike, has recently been obtained [108, 109, 110, 111] in terms of harmonic

polylogarithms [112, 113]. As a byproduct, an analytic expression for the slope $\mathcal{F}_2^{\prime(4)}(0)$ was found. The result reads

$$m^2 F_2^{\prime(4)}(0) = -\frac{1}{6} \ln\left(\frac{\lambda}{m}\right) + m^2 \mathcal{F}_2^{\prime(4)}(0),$$

$$m^2 \mathcal{F}_2^{\prime(4)}(0) = \frac{1751}{2160} + \frac{13}{20} \zeta(2) - \frac{23}{10} \zeta(2) \ln 2 + \frac{23}{40} \zeta(3). \quad (3.11)$$

A numerical result for $\mathcal{F}_2^{\prime(4)}(0)$, complementing the above analytic expression, can easily be derived in combining Eq. (1.20), Eq. (1.30), and Eq. (3.2) in [105], as will be explained in the sequel. The dispersion relation (1.30) in [105] reads,

$$\text{Re } F_2(t) = -\frac{4m^2}{t-4m^2} F_2(0) + \frac{1}{\pi} \frac{t}{t-4m^2} P \int_{4m^2}^{\infty} \frac{dt'}{t'-t} \frac{t'-4m^2}{t'} \text{Im } F_2(t'), \quad (3.12)$$

where P denotes the Cauchy principal value. Equation (3.12) applies also if we single out the two-loop effect and differentiate at zero momentum transfer, and we obtain for the slope $F_2^{\prime(4)}(0)$ the relation

$$m^2 F_2^{\prime(4)}(0) = \frac{1}{4} F_2^{(4)}(0) + \frac{1}{4\pi} P \int_{4m^2}^{\infty} dt' \frac{4m^2 - t'}{t'^2} \text{Im } F_2^{\prime(4)}(t') = \frac{1}{4} F_2^{(4)}(0) + \mathcal{T}, \quad (3.13)$$

where $F_2^{(4)}(0)$ is given in Eq. (3.8). The second term on the right-hand side, denoted by \mathcal{T} , can be evaluated using the result for $\text{Im } F_2^{(4)}(x)$ presented in Eq. (3.2) in [105]; it reads

$$\mathcal{T} = -\int_0^1 dx \frac{(1-x)^3}{x(1+x)} \text{Im } F_2^{(4)}(x) = -\frac{1}{6} \ln\left(\frac{\lambda}{m}\right) + 0.030\,740\,507\,833(1). \quad (3.14)$$

Here, the last error is due to numerical integration, and use is made of the natural variable [105]

$$x = \frac{1 - \sqrt{1 - 4m^2/t}}{1 + \sqrt{1 - 4m^2/t}}. \quad (3.15)$$

In combining the result of Eq. (3.8) with Eqs. (3.13) and (3.14), the result $m^2 \mathcal{F}_2^{\prime(4)}(0) = -0.051\,379\,233\,561(1)$ is obtained which is in agreement with (3.11).

Now we will provide results for the form factors obtained *excluding* the self energy vacuum-polarization graph V shown in Fig. 3.2. These results refer to the pure two-photon self energy diagrams shown in Fig. 3.1. The two-loop self energy diagrams independently form a gauge-invariant set. They represent a historically problematic correction, and are the main subject of our investigation. The combined self energy vacuum-polarization diagram, according to Eqs. (1.9) and (1.10) in [106] – taking into account the subtracted dispersion relation (1.30) of [105] – leads to the following corrections:

$$F_1^{\prime(4),V}(0) = -\frac{1099}{1296} + \frac{77}{144} \zeta(2) = 0.031\,588\,972\,474,$$

$$F_2^{(4),V}(0) = \frac{119}{36} - 2\zeta(2) = 0.015\,687\,421\,859,$$

$$F_2^{\prime(4),V}(0) = \frac{311}{216} - \frac{7}{8} \zeta(2) = 0.000\,497\,506\,323. \quad (3.16)$$

For the pure self energy graphs, which we would like to denote by the symbol S , we therefore obtain the following results,

$$m^2 F_1'^{(4),S}(0) = -\frac{47}{576} - \frac{175}{144} \zeta(2) + 3 \zeta(2) \ln 2 - \frac{3}{4} \zeta(3) = 0.438\,352\,514\,986, \quad (3.17)$$

$$F_2^{(4),S}(0) = -\frac{31}{16} + \frac{5}{2} \zeta(2) - 3 \zeta(2) \ln 2 + \frac{3}{4} \zeta(3) = -0.344\,166\,387\,438, \quad (3.18)$$

$$\begin{aligned} m^2 F_2'^{(4),S}(0) &= -\frac{1}{6} \ln\left(\frac{\lambda}{m}\right) - \frac{151}{240} + \frac{61}{40} \zeta(2) - \frac{23}{10} \zeta(2) \ln 2 + \frac{23}{40} \zeta(3) \\ &= -\frac{1}{6} \ln\left(\frac{\lambda}{m}\right) - 0.051\,876\,739\,885 \equiv -\frac{1}{6} \ln\left(\frac{\lambda}{m}\right) + \mathcal{F}_2'^{(4),S}(0). \end{aligned} \quad (3.19)$$

where the latter equality defines $\mathcal{F}_2'^{(4),S}(0)$ in analogy with Eqs. (3.9) and (3.11).

3.4 High–Energy Part

Based on the modified Dirac hamiltonian (3.3), corrections to the energy of the bound Dirac particle can be inferred. We will refer to the energy corrections attributable to the F_1 and F_2 form factors as E_1 and E_2 , respectively. For E_1 , we have

$$E_1 = \langle [F_1(-\mathbf{q}^2) - 1] e \phi \rangle_{\text{fs}}, \quad (3.20)$$

where the index fs refers to the fine-structure terms, i.e. to the result obtained by subtracting the value of the matrix element for a $n\text{P}_{3/2}$ state from the value of the same matrix element evaluated on a $n\text{P}_{1/2}$ state. A matrix element $\langle A \rangle_{\text{fs}}$ of a given operator A is evaluated as

$$\langle A \rangle_{\text{fs}} \equiv \left\langle \psi_{n\text{P}_{3/2}} \left| A \right| \psi_{n\text{P}_{3/2}} \right\rangle - \left\langle \psi_{n\text{P}_{1/2}} \left| A \right| \psi_{n\text{P}_{1/2}} \right\rangle.$$

Note that in evaluating these matrix elements, ψ^+ (the hermitian conjugate of the Dirac wave function ψ) should be used (not the Dirac adjoint $\bar{\psi} = \psi^+ \gamma^0$). The Dirac wave functions ψ are expanded in powers of $(Z\alpha)$ up to the order relevant for the current investigation of two-loop effects. This expansion avoids potential problems associated with the logarithmic divergence of the Dirac wave function at the origin.

For E_1 , up to the order of $(Z\alpha)^6$, we have

$$E_1 = 4\pi Z\alpha F_1'^{(4)}(0) \left\langle \delta^{(3)}(\mathbf{r}) \right\rangle_{\text{fs}}. \quad (3.21)$$

For P states, the nonrelativistic (Schrödinger) wave function – the leading term in the $Z\alpha$ -expansion of the Dirac wave function – vanishes at $\mathbf{r} = 0$, but the first relativistic correction gives a finite contribution, resulting in

$$\langle \delta^{(3)}(\mathbf{r}) \rangle_{\text{fs}} = -\frac{n^2 - 1}{4n^5} (Z\alpha)^5 m^3. \quad (3.22)$$

This leads – again up to the order of $(Z\alpha)^6$ – to the following result for E_1 ,

$$E_1 = \left(\frac{\alpha}{\pi}\right)^2 \frac{(Z\alpha)^6}{n^3} \left[-F_1'^{(4)}(0) \frac{n^2 - 1}{n^2} \right] m^3. \quad (3.23)$$

Observe that the derivative of the F_1 form factor has a physical dimension of $1/m^2$ in natural units, giving the correct physical dimension for E_1 . The correction due to F_2 in (3.3) reads,

$$E_2 = \langle F_2(-\mathbf{q}^2) \frac{e}{2m} \mathbf{i} \boldsymbol{\gamma} \cdot \mathbf{E} \rangle_{\text{fs}}. \quad (3.24)$$

A particle in an external binding Coulomb field feels an electric field $\mathbf{E} = i(Ze)\mathbf{q}/\mathbf{q}^2$ – in momentum space – or $\mathbf{E} = -(Ze)\mathbf{r}/(4\pi r^3)$ in coordinate space. Vacuum polarization corrections to $\mathbf{E} = -(Ze)\mathbf{r}/(4\pi r^3)$ lead to higher-order effects. The correction E_2 splits up in a natural way into two contributions E_{2a} and E_{2b} which are associated with $F_2(0)$ and the slope $F_2'(0)$, respectively. E_{2a} reads

$$E_{2a} = \frac{Z\alpha}{2m} F_2^{(4)}(0) \left\langle -i \frac{\boldsymbol{\gamma} \cdot \mathbf{r}}{r^3} \right\rangle_{\text{fs}}. \quad (3.25)$$

The evaluation of the matrix element leads to

$$\left\langle -i \frac{\boldsymbol{\gamma} \cdot \mathbf{r}}{r^3} \right\rangle_{\text{fs}} = \left\{ \frac{(Z\alpha)^3}{n^3} + \left[\frac{487}{360} + \frac{5}{4n} - \frac{23}{10n^2} \right] \frac{(Z\alpha)^5}{n^3} \right\} m^2. \quad (3.26)$$

For the purpose of the current investigation, the $(Z\alpha)^6$ -component of E_{2a} is selected only:

$$E_{2a} = \left(\frac{\alpha}{\pi} \right)^2 \frac{(Z\alpha)^6}{n^3} \left[F_2^{(4)}(0) \left(\frac{487}{720} + \frac{5}{8n} - \frac{23}{20n^2} \right) \right] m. \quad (3.27)$$

The matrix element E_{2b} can be expressed as

$$E_{2b} = \frac{4\pi Z\alpha}{2m} F_2'^{(4)}(0) \langle \boldsymbol{\gamma} \cdot \mathbf{q} \rangle_{\text{fs}}. \quad (3.28)$$

A transformation into coordinate space leads to

$$\langle \boldsymbol{\gamma} \cdot \mathbf{q} \rangle_{\text{fs}} = i \left[\frac{\partial}{\partial \mathbf{x}} (\psi^+(\mathbf{x}) \boldsymbol{\gamma} \psi(\mathbf{x})) \right]_{x=0, \text{fs}} = -\frac{n^2 - 1}{\pi n^5} (Z\alpha)^5 m^4. \quad (3.29)$$

As a function of the principal quantum number n , the result for E_{2b} reads:

$$E_{2b} = \left(\frac{\alpha}{\pi} \right)^2 \frac{(Z\alpha)^6}{n^3} \left[-2 F_2'^{(4)}(0) \frac{n^2 - 1}{n^2} \right] m^3. \quad (3.30)$$

This result involves the infrared divergent slope of the F_2 form factor [see Eqs. (3.11) and (3.19)]. We are thus faced with the problem of matching the infrared divergence of the slope of the F_2 form factor, expressed in terms of the fictitious photon mass λ , with the usual (energy matching parameter) ϵ introduced originally in [32]. This can be done in two ways: (i) by matching the infrared divergence of the rate of soft bremsstrahlung, calculated with a fictitious photon mass λ , to a result of the same calculation, carried out with an explicit infrared cut-off ϵ for the photon energy. This way of calculation is described on pp. 361–362 of [34]. It leads to the result

$$\ln \frac{\lambda}{2\epsilon} = -\frac{5}{6}. \quad (3.31)$$

The matching procedure (ii) consists in a comparison of the result of the application of the formalism considered above, and its application to the high-energy part of the ground state Lamb shift, which is in leading order given by the infrared divergence of the F_1 form factor, and the result obtained by direct calculation of this high-energy part in a non-covariant formalism with an explicit energy cut-off ϵ , as it has been carried out in [32]. This second matching procedure leads to the following result – in agreement with (3.31) –,

$$\ln \frac{m}{\lambda} - \frac{3}{8} = \ln \frac{m}{2\epsilon} + \frac{11}{24}. \quad (3.32)$$

So, we are led to the replacement

$$-\ln \frac{\lambda}{m} \rightarrow \ln \frac{m}{2\epsilon} + \frac{5}{6} \quad (3.33)$$

A comparison with the results in Eqs. (3.11), (3.19), and (3.36) reveals that the logarithmic divergence for the fine-structure difference is given by a term

$$-\frac{n^2 - 1}{3n^2} \ln \frac{m}{2\epsilon}, \quad (3.34)$$

so that we may anticipate at this stage the result for $\Delta_{\text{fs}} B_{61}$,

$$\Delta_{\text{fs}} B_{61} = -\frac{n^2 - 1}{3n^2}. \quad (3.35)$$

Based on (3.30) and (3.33), we can express E_{2b} in terms of ϵ and $\mathcal{F}_2^{(4)}(0)$,

$$E_{2b} = \left(\frac{\alpha}{\pi}\right)^2 \frac{(Z\alpha)^6}{n^3} \left[-\frac{1}{3} \frac{n^2 - 1}{n^2} \ln \frac{m}{2\epsilon} - \left(\frac{5}{18} + 2 \mathcal{F}_2^{(4)}(0) m^2 \right) \frac{n^2 - 1}{n^2} \right] m. \quad (3.36)$$

There is a third correction due to the effect of *two* one-loop corrections on the electron vertices. Because we are only interested in the fine structure, we isolate the terms which are proportional to the spin-orbit coupling, and we obtain

$$E_3 = \left\langle [2F_2(0)] H_{\text{fs}} \left(\frac{1}{E - H} \right)' [2F_2(0)] H_{\text{fs}} \right\rangle_{\text{fs}}, \quad (3.37)$$

where

$$H_{\text{fs}} = \frac{Z\alpha}{4m^2 r^3} \boldsymbol{\sigma} \cdot \mathbf{L}, \quad (3.38)$$

and $1/(E - H)'$ is the nonrelativistic, spin-independent reduced Schrödinger–Coulomb Green function [114, 115]. The only spin-dependence in (3.37) occurs in the coupling $\boldsymbol{\sigma} \cdot \mathbf{L}$, and it can be taken into account by an overall factor,

$$\langle (\boldsymbol{\sigma} \cdot \mathbf{L})^2 \rangle_{\text{fs}} = -3. \quad (3.39)$$

We are therefore led to consider the “spin-independent version” of the matrix element which occurs in Eq. (3.37) and obtain the following result,

$$\left\langle \frac{Z\alpha}{4m^2 r^3} \left(\frac{1}{E - H} \right)' \frac{Z\alpha}{4m^2 r^3} \right\rangle_{\text{nP}} = \left(-\frac{227}{8640} - \frac{1}{96n} + \frac{1}{80n^2} \right) \frac{(Z\alpha)^6 m}{n^3}. \quad (3.40)$$

The spin-dependence can be easily restored by considering Eq. (3.39). The index “nP” in Eq. (3.40) means that the matrix element is evaluated with the nonrelativistic, spin-independent (Schrödinger) wave function. Alternatively, one may evaluate with either the $\text{nP}_{1/2}$ or the $\text{nP}_{3/2}$ Dirac wave function and expand up to the leading order in $(Z\alpha)$.

The evaluation of (3.40) can proceed e.g. by solving the differential equation which defines the correction to the wave function induced by H_{fs} , and subsequent direct evaluation of the resulting standard integrals using computer algebra [90]. The final result for E_3 reads,

$$E_3 = \left(\frac{\alpha}{\pi}\right)^2 \frac{(Z\alpha)^6}{n^3} \left[\frac{227}{2880} + \frac{1}{32n} - \frac{3}{80n^2} \right] m. \quad (3.41)$$

This concludes the discussion of the high-energy part. The final result for the high-energy part is

$$E_{\text{H}} = E_1 + E_{2a} + E_{2b} + E_3, \quad (3.42)$$

where E_1 , E_{2a} , E_{2b} , E_3 are given in Eqs. (3.23), (3.27), (3.36), (3.41), respectively.

3.5 Low–Energy Part

The low-energy part consists essentially of two contributions. Both effects, denoted here E_4 and E_5 , can be obtained by a suitable variation of the low-energy part of the *one-loop* self energy, by considering the spin-dependent effects introduced by a *further* one-loop electron anomalous magnetic moment interaction. The first of the two terms, E_4 , is caused by spin-dependent higher-order effects in the one-loop self energy, which receive additional corrections due to the anomalous magnetic moment of the electron. The second term, E_5 , is due to an anomalous magnetic moment correction to the electron transition current, which

can also be seen as a correction to the radiation field of the electron due to its anomalous magnetic moment.

The leading-order low-energy part (see [32]) reads

$$E_L = -\frac{2\alpha}{3\pi m} \int_0^\epsilon d\omega \omega \left\langle \phi \left| \mathbf{p} \frac{1}{H - (E - \omega)} \mathbf{p} \right| \phi \right\rangle. \quad (3.43)$$

In order to isolate the fine-structure effects, we should now consider corrections to the wave function, to the current, to the hamiltonian and to the energy of the bound state due to the spin-dependent relativistic (spin-orbit) hamiltonian

$$\mathcal{H} = F_2(0) \frac{e}{2m} \mathbf{i} \boldsymbol{\gamma} \cdot \mathbf{E} = \frac{\alpha(Z\alpha)}{4\pi m} \frac{-\mathbf{i} \boldsymbol{\gamma} \cdot \mathbf{r}}{r^3}. \quad (3.44)$$

The above hamiltonian \mathcal{H} is the last term in the modified Dirac hamiltonian [right-hand side of Eq. (3.3)], approximated for a particle bound in a Coulomb field with the F_2 form factor evaluated at zero momentum. The electric field \mathbf{E} in (3.44) corresponds to the binding Coulomb interaction. The hamiltonian (3.44) describes the modification of the spin-orbit interaction due to the anomalous magnetic moment of the electron.

The nonrelativistic limit of \mathcal{H} is the spin-orbit coupling H_{fs} given in Eq. (3.38), multiplied by a factor $2F_2^{(2)}(0) = \alpha/\pi$ (the additional factor 2 finds an explanation in [116]). The resulting hamiltonian

$$H_{\text{eff}} = \frac{\alpha}{\pi} H_{\text{fs}} = \frac{\alpha}{\pi} \frac{Z\alpha}{4m^2 r^3} \boldsymbol{\sigma} \cdot \mathbf{L} \quad (3.45)$$

takes into account magnetic vertex corrections in the framework of an effective theory. Denoting the variation of the expression (3.43) mediated by H_{eff} with the symbol δ_{eff} – in the spirit of the notation introduced in [98] –, we obtain the contribution

$$E_{4a} = \delta_{\text{eff}} \left\{ -\frac{2\alpha}{3\pi m} \int_0^\epsilon d\omega \omega \left\langle \phi \left| \mathbf{p} \frac{1}{H - (E - \omega)} \mathbf{p} \right| \phi \right\rangle \right\}. \quad (3.46)$$

Following the notation introduced in [1, 2], the contribution E_{4a} is the sum of the fine-structure effects created by the wave-function-correction $F_{\delta\phi}$, the first relativistic correction to the energy $F_{\delta E}$, and the correction due to the relativistic hamiltonian $F_{\delta H}$, each multiplied by a factor α/π . The final result for E_4 is

$$E_{4a} = \left(\frac{\alpha}{\pi} \right)^2 (Z\alpha)^4 \frac{m}{n^3} (\Delta_{\text{fs}} F_{\delta\phi} + \Delta_{\text{fs}} F_{\delta E} + \Delta_{\text{fs}} F_{\delta H}). \quad (3.47)$$

There is a further correction to the nonrelativistic effective coupling to the radiation field due to the “anomalous spin-orbit hamiltonian” (3.44). The correction, in the nonrelativistic limit, can be derived by considering a Foldy–Wouthuysen transformation which by definition diagonalizes the hamiltonian (3.44) in spinor space and also leads to corrections to the current according to

$$\alpha^i \rightarrow U \alpha^i U^{-1}, \quad U = \exp \left(-\mathbf{i} \frac{\beta \mathcal{H}}{2m} \right). \quad (3.48)$$

Here, β and α^i are standard Dirac matrices [34], i is a spatial index, and \mathcal{H} is given in (3.44). The calculation is carried out along ideas introduced in [1] and leads to the result

$$\delta \mathbf{j}_{4b} = \frac{\alpha}{\pi} \frac{Z\alpha}{2mr^3} \boldsymbol{\sigma} \times \mathbf{r}, \quad (3.49)$$

as a relativistic correction to the electron current which is simply α^i in the relativistic formalism and p^i/m in the leading nonrelativistic approximation. Again, following the notation introduced in [1, 2], the resulting additional contribution is

$$E_{4b} = \left(\frac{\alpha}{\pi} \right)^2 (Z\alpha)^4 \frac{m}{n^3} \Delta_{\text{fs}} F_{\delta y}. \quad (3.50)$$

The sum of (3.47) and (3.50) is just the $(Z\alpha)^6$ -component of the fine-structure difference of the one-loop self energy from [1, 2], multiplied by an additional factor α/π . It can also be written as

$$E_4 = E_{4a} + E_{4b} = \left(\frac{\alpha}{\pi} \right)^2 \frac{(Z\alpha)^6 m}{n^3} \left[-\frac{n^2 - 1}{3n^2} \ln \frac{2\epsilon}{(Z\alpha)^2 m} + \frac{n^2 - 1}{n^2} \Delta_{\text{fs}} \ell_4(n) \right], \quad (3.51)$$

where $\Delta_{\text{fs}}\ell_4(n)$ could be interpreted as a relativistic generalization of a Bethe logarithm, which is n -dependent. However, a significant numerical fraction of the n -dependence can be eliminated if the factor $(n^2 - 1)/n^2$ is taken out of the final result. The evaluation of $\Delta_{\text{fs}}\ell_4(n)$ has recently been performed in [117] with improved numerical methods (see e.g. [23]), and the following results have been obtained:

$$\begin{aligned}\Delta_{\text{fs}}\ell_4(2) &= 0.512\,559\,768(1), \\ \Delta_{\text{fs}}\ell_4(3) &= 0.511\,978\,815(1), \\ \Delta_{\text{fs}}\ell_4(4) &= 0.516\,095\,539(1), \\ \Delta_{\text{fs}}\ell_4(5) &= 0.519\,976\,941(1),\end{aligned}\tag{3.52}$$

where the uncertainty is due to numerical integration.

There is, as stated above, a further correction due to the explicit modification of the transition current due to the anomalous magnetic moment; it can be obtained through the replacement

$$\alpha^i \rightarrow \alpha^i + F_2(0) \frac{i\beta \sigma^{i\nu}}{2m} q_\nu\tag{3.53}$$

and must be considered in addition to the correction (3.48). A careful consideration of the nonrelativistic limit of this correction to the current, including retardation effects, leads to the result

$$\delta \mathbf{j}_5 = \frac{\alpha}{2\pi} \frac{Z\alpha}{2mr^3} \boldsymbol{\sigma} \times \mathbf{r}.\tag{3.54}$$

Consequently, we find that the correction is effectively $F_2(0)$ times the retardation corrections to the transition current $F_{\delta y}$ found in [1, 2]. We obtain

$$E_5 = \left(\frac{\alpha}{\pi}\right)^2 (Z\alpha)^4 \frac{m}{n^3} \frac{\Delta_{\text{fs}} F_{\delta y}}{2}.\tag{3.55}$$

In analogy with E_4 , this correction can favorably be rewritten as

$$E_5 = \left(\frac{\alpha}{\pi}\right)^2 \frac{(Z\alpha)^6 m}{n^3} \left[\frac{n^2 - 1}{n^2} \Delta_{\text{fs}}\ell_5(n) \right],\tag{3.56}$$

On the basis of [1, 2, 117], we obtain

$$\begin{aligned}\Delta_{\text{fs}}\ell_5(2) &= -0.173\,344\,868(1), \\ \Delta_{\text{fs}}\ell_5(3) &= -0.164\,776\,514(1), \\ \Delta_{\text{fs}}\ell_5(4) &= -0.162\,263\,216(1), \\ \Delta_{\text{fs}}\ell_5(5) &= -0.161\,165\,602(1).\end{aligned}\tag{3.57}$$

The final result for the low-energy part is

$$E_L = E_4 + E_5,\tag{3.58}$$

with E_4 and E_5 being given in Eqs. (3.51) and (3.56), respectively.

We can now understand why it was possible to join the two contributions with “mixed” and “low-and-low” energy virtual photons (ii) and (iii), which were discussed in Sec. 3.2, into a joint “low-energy part”. The reason is simple: The effective hamiltonian (3.45) has no infrared divergence, because it involves the low-energy limit of the magnetic form factor F_2 , which is infrared safe in one-loop order according to Eq. (3.9). Because the main contribution to the quantity $F_2(0)$ is caused by hard virtual photons, it is also justified to say that the contribution of “low-and-low” energy virtual photons vanishes at the order of interest for the current calculation (fine-structure difference). In higher-loop order, the further infrared divergence acquired by F_2 would lead to an infrared divergence in the effective hamiltonian constructed in analogy with Eq. (3.45); this infrared divergence would have to be attributed to a “mixed” contribution.

3.6 Results for the Two-Loop Corrections

We have obtained analytic results for higher-order correction to the two-loop self energy of P states in hydrogen-like systems. In our calculation, we have analyzed the electron form factors through two-loop order in Sec. 3.3, and we have split the calculation into a high-energy part with two hard virtual photons discussed in Sec. 3.4, and a low-energy part with at least one soft virtual photon analyzed in Sec. 3.5. The final result for the contribution to the fine-structure energy difference is obtained by adding the high-energy contributions $E_1 - E_3$ given in Eqs. (3.23), (3.27), (3.36), (3.41), and the low-energy effects E_4 and E_5 from Eqs. (3.51) and (3.56). The dependence on ϵ cancels out in the final result which is the sum of the high-energy part E_H given in Eq. (3.42) and the low-energy part E_L defined in Eq. (3.58). This is also evident when considering explicitly the Eqs. (3.36) and (3.51). The final results for the analytic coefficients of order $\alpha^2(Z\alpha)^6$ read

$$\Delta_{\text{fs}}B_{61} = -\frac{n^2 - 1}{3n^2}. \quad (3.59)$$

[see also Eq. (3.35)] and

$$\begin{aligned} \Delta_{\text{fs}}B_{60} = & \left(\frac{227}{2880} + \frac{1}{32n} - \frac{3}{80n^2} \right) + F_2^{(4),S}(0) \left(\frac{487}{720} + \frac{5}{8n} - \frac{23}{20n^2} \right) \\ & + \frac{n^2 - 1}{n^2} \left[- \left(F_1'^{(4),S}(0) + 2\mathcal{F}_2'^{(4),S}(0) \right) m^2 - \frac{5}{18} + \Delta_{\text{fs}}\ell_4(n) + \Delta_{\text{fs}}\ell_5(n) \right], \end{aligned} \quad (3.60)$$

where explicit numerical results for $F_1'^{(4),S}(0)$, $F_2'^{(4),S}(0)$ and $\mathcal{F}_2'^{(4),S}(0)$ can be found in Eqs. (3.17), (3.18) and (3.19), respectively. This result refers to the pure self energy diagrams in Fig. 3.1. The result reads numerically for the principal quantum numbers $n = 2-5$,

$$\Delta_{\text{fs}}B_{60}(2) = -0.361\,196\,470(1), \quad (3.61)$$

$$\Delta_{\text{fs}}B_{60}(3) = -0.411\,156\,068(1), \quad (3.62)$$

$$\Delta_{\text{fs}}B_{60}(4) = -0.419\,926\,624(1), \quad (3.63)$$

$$\Delta_{\text{fs}}B_{60}(5) = -0.419\,832\,876(1). \quad (3.64)$$

If it is desired to add in the combined self energy vacuum-polarization diagram from Fig. 3.2, then the form-factor results from Eqs. (3.6), (3.8) and (3.11) instead of the pure self energy results given in Eqs. (3.17), (3.18) and (3.19) have to be used in evaluating (3.60). When including the combined self energy vacuum-polarization diagram from Fig. 3.2, there is no further low-energy contribution, so that the alternative set of numerical values for the form factors from Eqs. (3.6), (3.8) and (3.11) fully takes into account the additional effect of the diagram in Fig. 3.1 on the fine-structure in the order of $\alpha^2(Z\alpha)^6$.

Chapter 4

Spinless Particles in Bound–State Quantum Electrodynamics

4.1 Orientation

We describe in this Chapter a simplified derivation of the relativistic corrections of order α^4 for a bound system consisting of two spinless particles. We devote special attention to ponium, the bound system of two oppositely charged pions. The leading quantum electrodynamic (QED) correction to the energy levels is of the order of α^3 and due to electronic vacuum polarization. We analyze further corrections due to the self energy of the pions, and due to recoil effects, and we give a complete result for the scalar-QED leading logarithmic corrections which are due to virtual loops involving only the scalar constituent particles (the pions); these corrections are of order $\alpha^5 \ln \alpha$ for S states.

4.2 Introduction to Spinless QED and Ponium

Exotic bound systems like ponium [118, 119] (the bound system of two oppositely charged pions) offer interesting possibilities for studies of fundamental properties of quantum mechanical bound states: the interplay between strong-interaction corrections and quantum electrodynamic corrections is of prime interest, and the small length scales characteristic of the heavy particles make it possible to explore effects of the virtual excitations of the quantum fields in previously unexplored kinematical regimes [3, 4, 6]. We do not wish to hide the fact that any potential high-precision experiments in this area are faced with various experimental difficulties. Our calculations address QED corrections to the spectrum of bound systems whose constituent particles are spinless; relativistic corrections to the decay lifetime of ponium have recently been discussed in [120] in the context of the DIRAC experiment at CERN.

Here, we report on results regarding the spectrum of a bound system consisting of two spinless particles. We apply the simplified calculational scheme employed in [40] for the relativistic and recoil corrections to a bound system of two “non-Dirac” particles to the case of two interacting spinless particles (see Sec. 4.3). We then recall known results on leading-order vacuum polarization corrections in Sec. 4.4 and clarify the relative order-of-magnitude of the one- and two-loop electronic vacuum polarization, the relativistic and recoil corrections and the self energies in ponium (also in Sec. 4.4). We then provide an estimate for the self energy in Sec. 4.5, and we analyze the leading recoil correction of order α^5 (the Salpeter correction) which leads us to complete results for the scalar-QED logarithmic corrections of order $\alpha^5 \ln \alpha$.

4.3 Breit hamiltonian for Spinless Particles

We start from the Lagrangian for a charged spinless field coupled to the electromagnetic field [see equations (6-50) – (6-51b) of [34]],

$$\mathcal{L}(x) = [(\partial_\mu - ieA_\mu) \phi^*(x)] (\partial^\mu + ieA^\mu) \phi(x) - m^2 \phi^*(x) \phi(x) - \frac{1}{4} F_{\mu\nu}(x) F^{\mu\nu}(x), \quad (4.1)$$

where the field strength tensor $F_{\mu\nu}$ reads $F_{\mu\nu}(x) = \partial_\mu A_\nu(x) - \partial_\nu A_\mu(x)$. We use natural Gaussian units with $\hbar = c = \epsilon_0 = 1$. The transition current for a free spinless particle ($A^\mu = 0$) can be inferred from (4.1); it reads in momentum space

$$j^\mu(p', p) = \phi^*(p') (p'^\mu + p^\mu) \phi(p). \quad (4.2)$$

This current now has to be expressed in terms of nonrelativistic wave functions. Specifically, the j^0 -component has to reproduce the normalization of the nonrelativistic (Schrödinger) wave function. By contrast, according to Eq. (4.2) the zero-component of the current reads $2m \phi^* \phi$ in the nonrelativistic limit $p^0 \rightarrow m, p^0 \rightarrow m$. The nonrelativistic wave functions are normalized according to

$$\int d^3x \phi_S^*(\mathbf{x}) \phi_S(\mathbf{x}) = 1. \quad (4.3)$$

It is therefore evident that we cannot simply associate the relativistic wave function ϕ with ϕ_S ; rather, we should define according to Eqs. (13) – (14) of [40]

$$\phi(\mathbf{p}) = \frac{\phi_S(p^0, \mathbf{p})}{\sqrt{2p^0}}, \quad (4.4)$$

where $p^0 = \sqrt{\mathbf{p}^2 + m^2} \approx m$ is the energy of the free nonrelativistic particle (in deriving low-energy effective interactions, one always expands about *free*-particle amplitudes; all interactions are treated as perturbations; note the analogy to nonrelativistic QED – NRQED – for spinor particles [104]). The Klein–Gordon current, in the presence of external fields, reads in contrast to (4.2)

$$j^\mu(p', p) = \phi^*(p') (p'^\mu + p^\mu - 2eA^\mu) \phi(p). \quad (4.5)$$

The zero-component of this current can be interpreted as a charge density, which is not necessarily positive definite. Questions related to the normalization of the Klein–Gordon wave functions in this case are discussed in detail in [121, 122, 123, 124].

In terms of the Schrödinger wave function, the current is given as

$$j^0(\mathbf{p}', \mathbf{p}) = \phi_S^*(\mathbf{p}') \phi_S(\mathbf{p}), \quad (4.6)$$

$$j^i(\mathbf{p}', \mathbf{p}) = \phi_S^*(\mathbf{p}') \frac{p^i + p'^i}{2m} \phi_S(\mathbf{p}), \quad (4.7)$$

where m is the mass of the particle. The atomic momenta p^i and p'^i in Eq. (4.7) are of order $Z\alpha$. As shown below, interactions involving the spatial components j^i of the transition current give rise to relativistic contributions of order $(Z\alpha)^4$ to the spectrum. This is exactly the order of magnitude that is the subject of the current investigation. Therefore, although Eq. (4.7) is only valid up to corrections of relative order $(Z\alpha)^2$, these can be neglected because the further corrections contribute to the energy levels at the order of $(Z\alpha)^6$. Specifically, we can expect corrections proportional to $(p^i p^2)$ to the current j^i when a systematic expansion of the nonrelativistic current is performed; these terms are analogous to those obtained for relativistic corrections to the current of spinor particles which can be obtained via a Foldy–Wouthuysen transformation [1, 125].

In the following, the index S on the wave function will be dropped, and the nonrelativistic amplitudes describing the two interacting particles (with electric charges e_1 and e_2) will be denoted as ϕ_1 and ϕ_2 , respectively. Following [40], the Breit hamiltonian $U(\mathbf{p}_1, \mathbf{p}_2, \mathbf{q})$ in momentum space is related to the invariant scattering amplitude M and to the photon propagator $D_{\mu\nu}(q)$ in the following way [see also equation (83,8) in [126]]:

$$\begin{aligned} M &= e_1 e_2 j_1^\mu(\mathbf{p}'_1, \mathbf{p}_1) D_{\mu\nu}(\mathbf{q}) j_2^\nu(\mathbf{p}'_2, \mathbf{p}_2) \\ &= -\phi_1^*(\mathbf{p}'_1) \phi_2^*(\mathbf{p}'_2) \left[\frac{e_1 e_2}{q^2} + U(\mathbf{p}_1, \mathbf{p}_2, \mathbf{q}) \right] \phi_1(\mathbf{p}_1) \phi_2(\mathbf{p}_2) \end{aligned} \quad (4.8)$$

where $\mathbf{q} = \mathbf{p}'_2 - \mathbf{p}_2 = -(\mathbf{p}_1 - \mathbf{p}'_1)$. We employ a Coulomb-gauge photon propagator,

$$D_{00}(\mathbf{q}) = -\frac{1}{\mathbf{q}^2}, \quad D_{ij}(\mathbf{q}) = -\frac{1}{\mathbf{q}^2 - \omega^2} \left[\delta^{ij} - \frac{q^i q^j}{\mathbf{q}^2} \right] \approx -\frac{1}{\mathbf{q}^2} \left[\delta^{ij} - \frac{q^i q^j}{\mathbf{q}^2} \right], \quad (4.9)$$

where we can neglect the energy of the virtual photon in D_{ij} for the derivation of next-to-leading order relativistic corrections. The invariant scattering amplitude M then reads

$$\begin{aligned} \frac{M}{e_1 e_2} &= -\phi_1^*(\mathbf{p}'_1) \phi_2^*(\mathbf{p}'_2) \frac{1}{\mathbf{q}^2} \phi_1(\mathbf{p}_1) \phi_2(\mathbf{p}_2) \\ &+ \phi_1^*(\mathbf{p}'_1) \phi_2^*(\mathbf{p}'_2) \left[\frac{p_1^i + p_1'^i}{2m_1} \frac{p_2^j + p_2'^j}{2m_2} \frac{1}{\mathbf{q}^2} \left[\delta^{ij} - \frac{q^i q^j}{\mathbf{q}^2} \right] \right] \phi_1(\mathbf{p}_1) \phi_2(\mathbf{p}_2). \end{aligned} \quad (4.10)$$

We therefore identify

$$\begin{aligned} U(\mathbf{p}_1, \mathbf{p}_2, \mathbf{q}) &= -\frac{e_1 e_2}{4m_1 m_2} \frac{(2p_1^i - q^i)(2p_2^j + q^j)}{\mathbf{q}^2} \left[\delta^{ij} - \frac{q^i q^j}{\mathbf{q}^2} \right] \\ &= -\frac{e_1 e_2}{4m_1 m_2} \left\{ \frac{(2\mathbf{p}_1 - \mathbf{q}) \cdot (2\mathbf{p}_2 + \mathbf{q})}{\mathbf{q}^2} \right. \\ &\quad \left. - \frac{(2\mathbf{p}_1 \cdot \mathbf{q} - \mathbf{q}^2)(2\mathbf{p}_2 \cdot \mathbf{q} + \mathbf{q}^2)}{\mathbf{q}^4} \right\}. \\ &= -\frac{e_1 e_2}{m_1 m_2} \left[\frac{\mathbf{p}_1 \cdot \mathbf{p}_2}{\mathbf{q}^2} - \frac{(\mathbf{p}_1 \cdot \mathbf{q})(\mathbf{p}_2 \cdot \mathbf{q})}{\mathbf{q}^4} \right]. \end{aligned} \quad (4.11)$$

We now transform to the center-of-mass frame in which $\mathbf{p}_1 = -\mathbf{p}_2 = \mathbf{p}$, so that the expression for $U(\mathbf{p}_1, \mathbf{p}_2, \mathbf{q})$ becomes even simpler,

$$U(\mathbf{p}, -\mathbf{p}, \mathbf{q}) = \frac{e_1 e_2}{m_1 m_2} \left[\frac{\mathbf{p}^2}{\mathbf{q}^2} - \frac{(\mathbf{p} \cdot \mathbf{q})^2}{\mathbf{q}^4} \right]. \quad (4.12)$$

The formula (83,13) of [126] can now be employed in evaluating the Fourier transform,

$$\int \frac{d^3 q}{(2\pi)^3} \exp(i\mathbf{q} \cdot \mathbf{r}) \frac{4\pi(\mathbf{a} \cdot \mathbf{q})(\mathbf{b} \cdot \mathbf{q})}{\mathbf{q}^4} = \frac{1}{2r} \left[\mathbf{a} \cdot \mathbf{b} - \frac{(\mathbf{a} \cdot \mathbf{r})(\mathbf{b} \cdot \mathbf{r})}{r^2} \right]. \quad (4.13)$$

The Breit hamiltonian, which we would like to denote by H_B , is obtained by adding to the Fourier transform of (4.12) the relativistic correction to the kinetic energy. Denoting with $\hat{\mathbf{p}} = -i\partial/\partial\mathbf{x}$ the momentum operator in the coordinate-space representation, we obtain

$$H_B(\mathbf{r}, \hat{\mathbf{p}}) = -\frac{\hat{\mathbf{p}}^4}{8m_1^3} - \frac{\hat{\mathbf{p}}^4}{8m_2^3} + \frac{e_1 e_2}{8\pi r} \frac{\hat{\mathbf{p}}^2}{m_1 m_2} + \frac{e_1 e_2}{8\pi r^3} \frac{\mathbf{r} \cdot (\mathbf{r} \cdot \hat{\mathbf{p}}) \hat{\mathbf{p}}}{m_1 m_2}. \quad (4.14)$$

In the order of $(Z\alpha)^4$, there is no contribution due to virtual annihilation for spinless particles; corrections of this type would enter only for positronium and dimuonium [6] because they are caused by the spin-dependent part of the transition current [see Eqs. (83,20) and (82,22) of [126]], which is absent for spinless particles. For S states, virtual annihilation is altogether prohibited by angular momentum conservation.

The matrix elements of the Breit hamiltonian (4.14) for spinless particles can be evaluated on nonrelativistic bound states via computational techniques outlined in Sec. A3 of Ch. 1 of [116]. For $m_1 = m_2 = m$ and $e_1 e_2 = -4\pi Z\alpha$, we obtain

$$E_B = -\frac{(Z\alpha)^2 m}{4n^2} - \frac{(Z\alpha)^4 m}{2n^3} \left[\frac{1}{2l+1} - \frac{1}{4} \delta_{l0} - \frac{11}{32n} \right] \quad (4.15)$$

as the Breit energy for the energy levels of the bound system of two spinless particles, including relativistic corrections of order $(Z\alpha)^4$. Here, we keep Z as a parameter which denotes the nuclear charge number in a bound system. Of course, for two particles each carrying an elementary charge, Z has to be set to unity. The fine-structure constant is denoted by α . The result (4.15) agrees with previous calculations [40, 127, 128, 129, 130, 131], notably with Eq. (38) of [129].

It is instructive to compare the result (4.15) with the known result for a single-particle system of mass $m/2$ satisfying the Klein–Gordon equation, bound to a nucleus with charge Ze . According to Eq. (2-86) of [34], we obtain the “Klein–Gordon energy” (KG)

$$E_{\text{KG}} = -\frac{(Z\alpha)^2 m}{4n^2} - \frac{(Z\alpha)^4 m}{2n^3} \left[\frac{1}{2l+1} - \frac{3}{8n} \right]. \quad (4.16)$$

The two results (4.15) and (4.16) are manifestly different in the order of $(Z\alpha)^4$.

From (4.14) we conclude that the zitterbewegung term is absent for spinless particles. However, this statement is in need of further explanation because a considerable variety of physical interpretations exists in the literature with regard to the zitterbewegung term. We briefly expand: The Dirac α -matrices fulfill $\alpha = i[H_D, x]$ (H_D is the Dirac hamiltonian) as the relativistic generalization of the velocity operator. By contrast, in the nonrelativistic formalism, we have the analogous relation $p/m = i[H_S, x]$ where H_S is the Schrödinger hamiltonian. Since the α -matrices have eigenvalues ± 1 , the magnitude of the velocity of the electron – at face value – is equal to the velocity of light at any given instant. On p. 106 of [132], it is argued that “the explanation for this fact is that the electron carries out a fast irregular motion (“zitterbewegung”) – which is responsible for the spin – whereas the mean velocity is given by the momentum \mathbf{p}/m ”. Note that the introduction of the Dirac matrix formalism is necessitated by the need to describe the internal degrees of freedom of the particle – the spin. On p. 71 of [34], it is shown that the zitterbewegung term can be traced back to the positional fluctuations $\langle \delta \mathbf{r}^2 \rangle \sim 1/m^2$ of the electron, and a connection is drawn to the Darwin term which results naturally in the context of the Foldy–Wouthuysen transformed Dirac hamiltonian. On pp. 117–118 of [133] and p. 62 of [34], it is argued that the momentum \mathbf{p} of a Dirac wave packet can be associated in a natural way with the group velocity, but that in addition to the group velocity term, there exist highly oscillatory terms which represent the zitterbewegung. Similarly, on pp. 139–140 of [133], it is shown that the zitterbewegung term can also be interpreted as arising from the interaction of the atomic electron with virtual electron-positron pairs created in the Coulomb field of the nucleus. This virtual electron-positron pair-creation is subject to the uncertainty principle and can occur only for time intervals of the order of $\Delta t \sim \hbar/(2mc^2)$ (where we temporarily restore the factor \hbar). At the time the original atomic electron fills up the vacated negative-energy state (the bound-electron wave-function has negative-energy components), the escalated electron (which forms part of the virtual pair) is at most a distance $c\Delta t \sim 1/m$ away from the original electron. This distance is precisely of the order of magnitude of the fluctuations of the electron coordinate and consistent with the discussion on p. 71 of [34]. All these interpretations elucidate different aspects of the same problem.

In the context of the Breit hamiltonian, we would like to adhere to the definition that the zitterbewegung term is the term of order $(Z\alpha)^4$ in the Breit hamiltonian generated by a contribution which is manifestly proportional of $\delta(\mathbf{r})$ in coordinate space (or a constant in momentum space). Such a term is absent in the result (4.14). For spin-1/2 particles, such a term is generated by the multiplication of the photon propagator (proportional to $1/\mathbf{q}^2$) with the zero-component of the transition current which is given for a spin-1/2 particle as [see equation (4) of [40]]

$$\bar{u}' \gamma^0 \bar{u} = w^* \left(1 - \frac{\mathbf{q}^2}{8m^2} + \frac{i \boldsymbol{\sigma} \cdot \mathbf{p}' \times \mathbf{p}}{4m^2} \right) w. \quad (4.17)$$

Here, u is the bispinor amplitude for the bound particle, and w is the bound-state Schrödinger wave function related by

$$u = \begin{pmatrix} \left(1 - \frac{\mathbf{p}^2}{8m^2} \right) w \\ \frac{\boldsymbol{\sigma} \cdot \mathbf{p}}{2m} w \end{pmatrix} \quad (4.18)$$

according to equation (3) of [40]. One might wonder why a term proportional to δ_{l0} , apparently generated by a δ -function in coordinate space, prevails in the Breit energy (4.15). This term arises naturally when

evaluating a matrix element of the structure $\langle \phi_S | (\mathbf{r} \cdot (\mathbf{r} \cdot \hat{\mathbf{p}}) \hat{\mathbf{p}}) / r^3 | \phi_S \rangle$ (last term of equation (4.14)) on the nonrelativistic wave function ϕ_S and should *not* be associated with the zitterbewegung.

Vacuum polarization corrections and the self energy, as well as corrections due to the strong interaction, are not included in (4.15). These corrections will be discussed in the two following sections.

4.4 Vacuum Polarization Effects

As pointed out by various authors (e.g. [5, 7, 134, 135, 136, 137, 138]), the electronic vacuum polarization enters already at the order of α^3 [more precisely, $\alpha(Z\alpha)^2$] in bound systems with spinless particles, because the spinless particles are much heavier than the electron, which means that the Bohr radius of the bound system is roughly of the same order of magnitude as the Compton wavelength of the electron. The Compton wavelength of the electron, however, is the fundamental length scale at which the charge of any bound particle is screened by the electronic vacuum polarization.

The vacuum polarization (VP) correction to energy levels has been evaluated [5, 6, 134, 136, 137, 138] with nonrelativistic wave functions. We recall that the leading-order VP correction (due to the Uehling potential) can be expressed as

$$\Delta E = \langle \psi | V_U | \psi \rangle = \frac{\alpha}{\pi} C_E E_\psi, \quad (4.19)$$

where

$$E_\psi = -\frac{(Z\alpha)^2 m}{4n^2} \quad (4.20)$$

is the Schrödinger binding energy for a two-body system with two particles each of mass m [first term on the right-hand side of (4.15)]. For the C_E coefficients, we recall the following known results [6, 136, 137],

$$C_E(1S) = 0.22, \quad C_E(2S) = 0.10. \quad (4.21)$$

Two-loop vacuum polarization effects enter at a relative order α^2 in ponium and are therefore of the same order of magnitude as the relativistic corrections mediated by the Breit interaction (discussed in Sec. 4.3). The self energy correction which is discussed in the following section is even smaller, but of considerable theoretical interest.

4.5 Effects due to Scalar QED

As shown in [102], the leading logarithmic correction to the self energy can be obtained, in nonrelativistic approximation, from second-order perturbation theory based on nonrelativistic quantum electrodynamics [104] (see also [103]). We will investigate here, in a systematic way, the leading logarithms generated for S states by self energy and relativistic-recoil effects (the so-called Salpeter correction), and show that these are spin-independent.

The quantized electromagnetic field is [see Eq. (5) of [102]],

$$\mathbf{A}(\mathbf{r}) = \sum_{\lambda=1,2} \int \frac{d^3k}{\sqrt{(2\pi)^3} 2k} \epsilon_\lambda(\mathbf{k}) \left[a_{\mathbf{k},\lambda}^+ \exp(-i\mathbf{k} \cdot \mathbf{r}) + a_{\mathbf{k},\lambda} \exp(i\mathbf{k} \cdot \mathbf{r}) \right], \quad (4.22)$$

and the nonrelativistic interaction hamiltonian for an atomic system with two spinless particles (charges e_1 and e_2 and masses m_1 and m_2) reads

$$H_I = -\frac{e_1}{m_1} \mathbf{p}_1 \cdot \mathbf{A}(\mathbf{r}_1) + \frac{e_1^2}{2m_1} \mathbf{A}(\mathbf{r}_1)^2 - \frac{e_2}{m_2} \mathbf{p}_2 \cdot \mathbf{A}(\mathbf{r}_2) + \frac{e_2^2}{2m_2} \mathbf{A}(\mathbf{r}_2)^2. \quad (4.23)$$

For two spin-1/2 particles, the terms

$$-\frac{e_1}{m_1} \boldsymbol{\sigma}_1 \cdot \mathbf{B}(\mathbf{r}_1) - \frac{e_2}{m_2} \boldsymbol{\sigma}_2 \cdot \mathbf{B}(\mathbf{r}_2) \quad (4.24)$$

have to be added to H_I [see Eq. (7) of [102]]. We will carry out the calculations for the general case of one particle of charge $e_1 = e$ and the other having a charge $e_2 = -Ze$ (we follow the convention of [34]

that for hydrogen, e is the physical charge of the electron, i.e. $e = -|e|$). The unperturbed hamiltonian of the system of the two particles and the electromagnetic field reads [see e.g. Eq. (6) of [102]],

$$H_0 = \frac{\mathbf{p}_1^2}{2m_1} + \frac{\mathbf{p}_2^2}{2m_2} - \frac{Z\alpha}{r} + \sum_{\lambda=1,2} \int d^3k k a_{k,\lambda}^+ a_{k,\lambda}. \quad (4.25)$$

where $\mathbf{r} = \mathbf{r}_1 - \mathbf{r}_2$. The eigenstates of the “atomic part” H_0^A of this hamiltonian in the center-of-mass system $\mathbf{p}_1 + \mathbf{p}_2 = 0$ are the nonrelativistic Schrödinger–Coulomb wave functions for a reduced mass $m_r = m_1 m_2 / (m_1 + m_2)$ [here, the “atomic part” H_0^A excludes the photon field, i.e. the last term of (4.25)]. We denote $\mathbf{p} \equiv \mathbf{p}_1 = -\mathbf{p}_2$.

Given that the first-order perturbation $\langle \phi_S | H_I | \phi_S \rangle$ vanishes, the second-order perturbation yields the dominant nonvanishing perturbation. When evaluated on an atomic state, it is given by

$$\delta E_{SE} = \langle \phi_S | H_I \frac{1}{H_0 - E_S} H_I | \phi_S \rangle. \quad (4.26)$$

The interaction hamiltonian (4.23) gives rise to QED corrections that involve both particles (in the current context, these are recoil corrections involving the product $e_1 e_2$), and also to terms which involve only a single particle and are proportional to e_1^2 or e_2^2 . The latter effects correspond to the self-energies of the two particles.

The low-energy part of the self energy in leading order [32] can be inferred directly from (4.26), and it can be seen that the spin-dependent parts from (4.24) vanish in leading order in the $(Z\alpha)$ -expansion [102]:

$$E_L = -\frac{e_1^2}{6\pi^2} \int_0^\epsilon dk k \left\langle \phi \left| \frac{\mathbf{p}}{m_1} \frac{1}{H_0^A - (E_S - k)} \frac{\mathbf{p}}{m_1} \right| \phi \right\rangle + (e_1 \leftrightarrow e_2, m_1 \leftrightarrow m_2). \quad (4.27)$$

where

$$E_S = -\frac{(Z\alpha)^2 m_r}{2n^2} \quad (4.28)$$

is the Schrödinger energy (m_r in the reduced mass of the atomic system under investigation). Starting from the *spin-independent* expression (4.27), it is now relatively straightforward to show that the leading “self energy logarithm” for S states is given by

$$\delta E_{SE} \approx \frac{4 \ln(Z\alpha)^{-2}}{3\pi n^3} \delta_{l0} \left[\alpha (Z\alpha)^4 \frac{m_r^3}{m_1^2} + Z (Z\alpha)^5 \frac{m_r^3}{m_2^2} \right]. \quad (4.29)$$

This result is by consequence spin-independent. The derivation is simplified when using the ϵ -method developed and used in various bound-state calculations [1, 2, 32]. The two terms in square brackets in (4.29) correspond to the two self-energies of the two constituent particles with charges $e_1 = e$ and $e_2 = -Ze$ and masses m_1 and m_2 , respectively. It has been pointed out [97] that in contrast to the self energy corrections, the vacuum polarization corrections given in Eq. (4.21) must not be double-counted. The “double-counting” of self energy corrections (and lack of it in the vacuum-polarization case) finds a natural explanation in our formalism: whereas the vacuum-polarization correction mainly leads to a modification of the $1/r$ -type Coulomb attraction in (4.25) within a nonrelativistic effective theory, the structure of the interaction hamiltonian (4.23) implies the existence of the *two* self-energies of the *two* constituent particles of the atomic system.

It might be instructive to point out that the formula (4.29) is consistent with Welton’s argument for estimating the self energy of a bound particle which is based on analyzing the influence of the fluctuating electromagnetic field [a detailed discussion is given on pp. 80–82 of [34]]. For a system with two particles of equal mass $m_1 = m_2 = m$, we have $m_r = m/2$.

The leading-order recoil correction (Salpeter correction) can also be inferred from the interaction hamiltonian (4.23) via second-order perturbation theory, by “picking up” terms that involve products $e_1 e_2$. It has been shown in [102] that the leading *logarithm* (for S states) of the Salpeter correction is spin-independent (just like the leading logarithm of the self energy correction). The Salpeter correction is usually referred to as a relativistic recoil (RR) correction. By following [102], we obtain for the leading logarithm of this effect

$$\delta E_{RR} \approx \frac{2(Z\alpha)^5}{3\pi n^3} \delta_{l0} \ln \left(\frac{1}{Z\alpha} \right) \frac{m_r^3}{m_1 m_2}. \quad (4.30)$$

This correction involves only the products $e_1 e_2 = -4\pi Z\alpha$ and can therefore be written as a function of $Z\alpha$ alone.

For ponium, we have $Z = 1$, $m_1 = m_2 = m = m_\pi$, $m_r = m_\pi/2$. The leading logarithmic correction from scalar QED for ponium in the order of $\alpha^5 \ln \alpha$ is obtained by adding the corrections (4.29) and (4.30),

$$\delta E_{\log} = \delta E_{\text{SE}} + \delta E_{\text{RR}} = \frac{3}{4} \frac{\alpha^5}{\pi n^3} \ln \left(\frac{1}{\alpha} \right) m_\pi. \quad (4.31)$$

The non-logarithmic term of order α^5 is spin-dependent, and its evaluation requires a relativistic treatment of the self energy of a bound spinless particle; such a calculation would be of considerable theoretical interest, but the size of the effect for ponium, which is roughly two orders of α smaller than the leading vacuum polarization correction, precludes experimental verification in the near future. However, we would like to point out here that a fully relativistic treatment of this problem, including a detailed discussion of the renormalization of the self energy of the spinless particle, has not yet been accomplished. Scalar QED is a renormalizable theory [34].

The dominance of vacuum polarization over the self energy in ponium is expressed, in particular, by the fact that even *two-loop* vacuum polarization of order α^4 has a stronger effect on the spectrum of ponium than the leading logarithm from Eq. (4.31) according to Ref. [17], and that the strong-interaction correction of order α^3 [139] has to be well understood before any experimental verification of (4.31) appears feasible. Finally, we remark that for a manifestly non-elementary particle like the pion which has a finite charge radius, form-factor corrections have to be taken into account.

Chapter 5

QED Calculations: A Summary

Calculations in the area of bound-state quantum electrodynamics have a long history, starting with Hans Bethe's first evaluation of the hydrogen Lamb shift [33]. Since then, the field has developed considerably, and the immense progress in high-resolution spectroscopy (for a recent culmination of the activities, see [42]) has necessitated the inclusion of higher- and higher-order corrections into the theoretical framework, leading to increased complexity of the theoretical calculations. Why should such an effort be carried out? A more accurate understanding of the QED corrections is of crucial importance for the determination of the fundamental constants and the test of quantum electrodynamics. The theory of the QED bound states can, at little risk to over-statement, be described as one of the most developed theories in all of physics. It combines the intricacies of quantum field theory (divergences, renormalization) with the experimental possibilities implied by the accuracy of high-resolution spectroscopy.

For decades, there has been a tremendous amount of work on analytic self-energy calculations, notably on the coefficient A_{60} for S states. However, an accurate comparison of the analytic results to numerical data was impossible, simply because no numerical data were available in the region of low nuclear charge. The semi-analytic expansion in $Z\alpha$ is in part problematic because there is evidence that it may represent a divergent series. This argument may be based in part on the analogy between Figs. 5.1 and 5.2, and on the observed rapid growth of the analytic self energy coefficients (A_{40} is of order one for S states, A_{50} is about 10, and the magnitude of A_{60} is as large as 30). The QED effective action gives rise to a divergent asymptotic expansion in appropriately defined effective coupling parameters. It is therefore *a priori* difficult to associate a finite remainder to a truncated series that involves all known (but disregards the unknown) analytic coefficients.

The results reported here in Ch. 1 answer this conceptual question in the following way: the semi-analytic expansion in powers of $Z\alpha$ is in full agreement with the obtained numerical results. We may therefore conclude that the semi-analytic expansion probably gives rise to a generalized asymptotic series whose remainder is of the order of the first neglected semi-analytic term as $Z\alpha \rightarrow 0$. Therefore, we may assume that a truncated semi-analytic expansion in powers of $Z\alpha$ leads to reliable theoretical predictions in the realm of low nuclear charge numbers Z . However, although the numerical results confirm the validity of the semi-analytic expansion in this Z -region, they also show the limitations of this approach: much more accurate results are obtainable by numerical calculations. The accuracy on the level of 1 Hz for atomic hydrogen reported in Ch. 1 would have involved analytic terms of an excessively high order in $Z\alpha$ [approximately $\alpha(Z\alpha)^9$], and the multitude and complexity of terms would have been a severe obstacle for analytic calculations in this order of $Z\alpha$. In general, the related activities have recently sparked a rather broad interest in the numerical calculation of relativistic, QED self energy and two-body corrections at low Z and the comparison of analytic and numerical results [87, 140, 141, 142, 143, 144, 145, 146, 147, 148, 149, 150, 151].

We have described in Ch. 1 a nonperturbative evaluation of the one-photon self energy in hydrogenlike ions with low nuclear charge numbers $Z = 1$ to 5. The general outline of our approach is discussed in Sec. 1.3. In Sec. 1.4, the numerical evaluation of the low-energy part (generated by virtual photons of low energy) is described. In Sec. 1.5, we discuss the numerical evaluation of the high-energy part, which is generated by high-energy virtual photons and contains the formally infinite contributions, which are removed by the renormalization. Sec. 1.5 also contains a brief discussion of the convergence acceleration methods

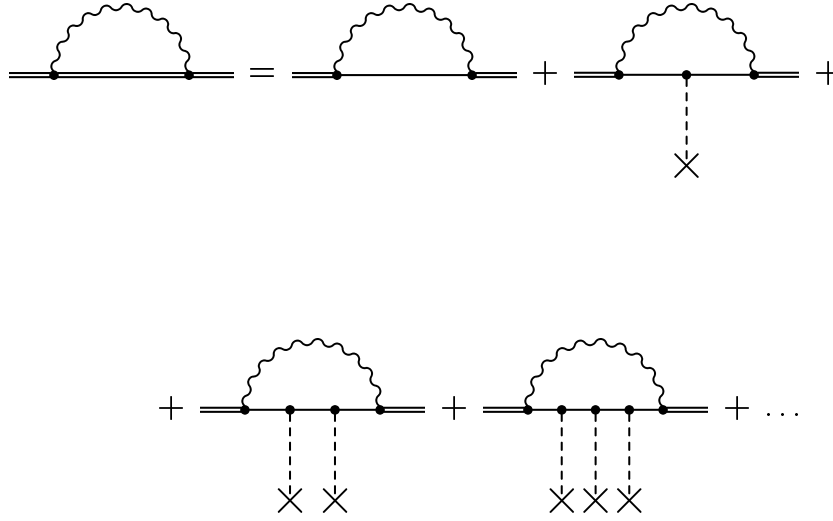


Figure 5.1: Expansion of the bound electron self energy in powers of the binding Coulomb field. The dashed lines denote Coulomb photons, the crosses denote the interaction with the (external) binding field. Each interaction with the binding Coulomb field gives rise to a higher-order term in the $Z\alpha$ -expansion.

as employed in the current evaluation. We discuss in Sec. 1.6 the comparison of analytic and numerical data for K- and L-shell states in the region of low Z . The main results of the current investigation are contained in Table 1.5: numerical data, nonperturbative in $Z\alpha$, for the scaled function F and the self energy remainder function G_{SE} for K- and L-shell states at low nuclear charge. The numerical accuracy of our data is 1 Hz or better in frequency units for 1S, 2S and both 2P states in atomic hydrogen.

Still, calculations within the semi-analytic expansion in addition to the numerical calculations (a kind of “dual strategy”) remain important. They serve as a confirmation and check for currently available and future numerical approaches. In general, in view of the complexity of the calculations, an independent check is always *highly* desirable. For the two-loop effect, the $(Z\alpha)$ -expansion converges more rapidly than for the one-loop effect in absolute frequency units because of the additional radiative factor α/π which decreases the overall size of the effect (see Ch. 3).

It is hoped that the analytic calculations reported in Ch. 3 for low nuclear charge number Z will be supplemented in the future by an accurate numerical treatment of the two-loop self energy problem (see also related recent work in the high- Z region, Refs. [13, 151, 152]). This presupposes that the considerable numerical problems in the domain of small nuclear charge could be solved by adequate numerical methods, and that the further problem of the increased computational demand of the two-loop effect in comparison to the one-loop problem [9, 12] can be tackled – possibly by massively parallel computer architectures. Note, however, that the most accurate theoretical predictions could only be reached in combining numerical and analytic results. The reason is the following: All numerical calculations are performed in the non-recoil limit which is the limit of infinite nuclear mass. This is not quite sufficient for an accurate theoretical treatment because the self energy of a bound-state depends genuinely on the ratio of the orbiting particle to the nuclear mass – an effect beyond the recoil correction. For example, the argument of the logarithms in Eqs. (1.2) and (3.1) should be replaced according to $\ln[(Z\alpha)^{-2}] \rightarrow \ln[\sigma(Z\alpha)^{-2}]$, where $\sigma = m/m_r$ and m_r is the reduced mass [97]. The possibility to include these tiny, but important effects

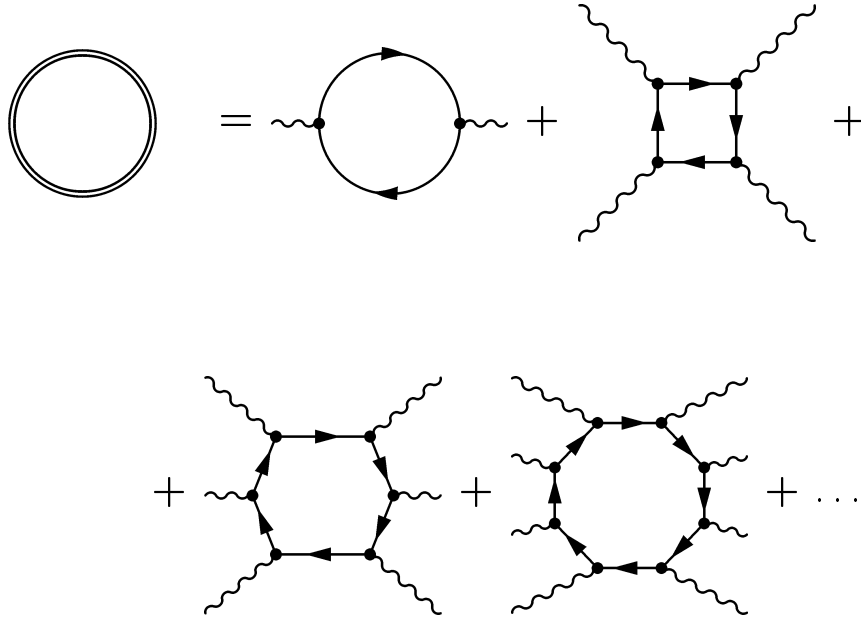


Figure 5.2: Expansion of the QED effective action in powers of the external field. As discussed in Sec. 8.3.2, the resulting asymptotic series in powers of the coupling is divergent.

depends crucially on a reliable knowledge of the analytic coefficients *in combination* with an accurate numerical treatment of the problem (see also the discussion in Sec. 2.6).

The analytic results can be used to obtain improved theoretical predictions for the hydrogenic fine structure as compared to the previous order- α^7 -calculations [1, 2], because they remove the principal theoretical uncertainty in the order of α^8 due to the problematic two-loop self energy which is represented diagrammatically in Fig. 3.1. Our calculation in Ch. 3 illustrates the usefulness of the simplified effective treatments of two-loop effects in the analytic approach based on the modified Dirac hamiltonian (3.3) and the “ ϵ method”. This aspect highlights, as we believe, the need for systematic, simplified treatments of higher-order radiative corrections in bound systems.

In Ch. 3, we primarily address spin-dependent effects in one-electron (hydrogenlike) systems. However, the same effects also contribute to the fine-structure splitting in two-electron (heliumlike) systems. There is currently remarkable interest in improved measurements of the fine-structure splitting in helium and heliumlike atomic systems with low nuclear charge [36, 37, 38, 39]. The effects addressed here contribute to the fine-structure splitting in helium on the level of 100 Hz, which is not much smaller than the current experimental accuracy of about 1 kHz, and allows for an estimate of uncalculated higher-order contributions.

All analytic calculations rely on the separation of the virtual photon energy into high- and low-energy energy regions via a parameter ϵ . This separation is illustrated in Sec. 2.2. For two-photon problems, four energy regions result from such a separation, but for the one-photon problem discussed in Ch. 2, one separation parameter ϵ is sufficient. We present in Ch. 2 analytic calculations for excited atomic states based on the semi-analytic $Z\alpha$ -expansion. These may be complemented in the near future by numerical results [95]. We discuss some intricacies of the analytic treatment of highly excited atomic states in Sec. 2.1. Results for the individual contributions are presented in Subsections 2.3.1 – 2.3.8 and summarized in Sec. 2.4. Final values of the analytic coefficients can be found in Tables 2.1 – 2.7. The characteristic numerical cancellations between individual contributions are described in Sec. 2.5. Finally, in Sec. 2.6, we describe a number of observations regarding the dependence of the A_{61} and the

A_{60} -coefficients on the quantum numbers of the atomic state.

All of the above calculations are related to the bound electron, which is a spin-1/2 particle. In nature, particles with different spin quantum numbers exist, and these, too, can form bound systems. The spin-dependence of the corrections is a conceptually interesting issue that forms the subject of Ch. 4. This interest is sparked by the projected DIRAC experiment at CERN where the bound system of two oppositely charged pions (“pionium”) will be studied. Notably, even the relativistic corrections for a bound two-body system consisting of spinless particles are different for spinless particles than for particles with nonvanishing spin. They are given by a generalized Breit hamiltonian that we discuss in Sec. 4.3. There, we present a simplified derivation for the relativistic and recoil corrections of order α^4 to a bound state of two spinless particles. The results agree with previous calculations [129]. As evident from equation (4.14), the zitterbewegung term is absent in a bound system of two spinless particles.

The self energy is suppressed in systems with spinless particles in comparison to the vacuum polarization effect as discussed in Secs. 4.4 and 4.5, because the lightest known spinless particle is much heavier than the electron, which implies that the vacuum polarization effect is larger by two orders of $Z\alpha$ than the self energy in bound systems of spinless particles. We provide a complete result for the leading scalar-QED correction of order $\alpha^5 \ln \alpha$ in Sec. 4.5. A list of further QED corrections to the 1S level of pionium, including two-loop vacuum polarization, finite-size corrections and other effects, can be found in [17].

To conclude this Chapter, we would like to mention the complementarity of the high-precision calculations and experiments at low nuclear charge and the strong-field calculations and related experiments at high nuclear charge numbers. While an accuracy [42] of one part in 10^{14} currently appears to be out of reach for hydrogenlike Uranium [153], the experiments on highly charged ions have meanwhile attained a precision where a detailed understanding of the nuclear structure and shape is necessary in order to describe QED effects rigorously [154].

Bound systems described by quantum electrodynamics belong to the most accurately understood physical systems today. They convey a certain esthetic appeal because the apparent simplicity of the two- and three-particle systems gives rise to a large number of conceptual as well as calculational difficulties when a thorough understanding is sought in higher orders of perturbation theory.

Part II

Convergence Acceleration and Divergent Series

Chapter 6

Introduction to Convergence Acceleration and Divergent Series in Physics

The second part of this thesis will be concerned with convergence acceleration methods and with the summation of divergent series. In theoretical physics, we often encounter sequences of numbers, either as a result of perturbation theory or as partial sums of an infinite series defining a physical quantity, whose numerical properties are disfavoured: in many cases, the sequences converge so slowly that they are numerically useless. In other cases, the sequences do not converge at all, and yet we know – or assume – that the sequences are associated, nevertheless, to the physical quantity in question, for example in the form of a divergent asymptotic expansion.

Let us consider the case where the sequence $\{s_n\}_{n=0}^{\infty}$ under investigation is given by partial sums of an infinite series,

$$s_n = \sum_{k=0}^n a_k. \quad (6.1)$$

We assume, furthermore, that the a_k are real (this condition will be relaxed in the sequel).

(i) Let us assume that the sequence $\{s_n\}_{n=0}^{\infty}$ is *convergent*. The purpose of convergence acceleration is to convert $\{s_n\}_{n=0}^{\infty}$ into a new sequence $\{s'_n\}_{n=0}^{\infty}$ with hopefully better numerical properties. If we denote the limit of the sequence by s , that is $s \equiv \lim_{n \rightarrow \infty} s_n$, then the rate of convergence is obviously increased if

$$\lim_{n \rightarrow \infty} \frac{s'_n - s}{s_n - s} = 0. \quad (6.2)$$

(ii) Alternatively, let us assume that the sequence $\{s_n\}_{n=0}^{\infty}$ is *divergent*. The purpose of the resummation is to determine the generalized limit (or antilimit) of the sequence. The following question immediately arises: how is it possible to associate a finite generalized limit with a divergent series. L. Euler wrote in a letter to Goldbach (1745): “Summa cuiusque seriei est valor expressionis illius finitae, ex cuius evolutione illa series oritur.”, which means: the generalized limit of any divergent series is the value of the particular characteristic finite expression, whose expansion gives rise to the divergent series. This is still the main notion of resummation today: Given a divergent series, to “reconstruct” *a posteriori* the function whose expansion gave rise to the divergent series, with a suitable mathematical resummation method.

We illustrate this idea with a trivial example: A divergent series can be generated, e.g., by expanding the function $f(z) = 1/(1+z) \sim \sum_{j=0}^{\infty} (-z)^j$ at $z = 1$ in powers of z . The partial sums of the resulting divergent series read

$$s_n = \sum_{j=0}^n (-1)^j = \begin{cases} 1 & \text{for } n \text{ even} \\ 0 & \text{for } n \text{ odd} \end{cases}. \quad (6.3)$$

The resulting sequence, which is $1, 0, 1, 0, \dots$, can be identified as originating from the discussed function by expansion at unit argument, and its antilimit is therefore $1/2$. Since this argument may not sound

convincing, let us briefly indicate that the result may also be obtained by imposing the postulate that the antilimit of the sum of two divergent series should be the sum of the two antilimits each. Then, it is easy to derive (by inspection) that the antilimit a of the series $\sum_{j=0}^{\infty} (-1)^j$ should fulfill $1 - a = a$, and thus $a = 1/2$ (again). A more formal investigation of this series and its resummation can be found in [155] [see Eq. (1.1.1) and the instructive discussion on the p. 6 *ibid.*]. It is probably a triviality to express that the most familiar resummation methods like the Euler transformation, Padé approximants and recently developed nonlinear sequence transformations of the Levin–Weniger type all convert the divergent sequence $1, 0, 1, 0, \dots$ to the convergent sequence $1/2, 1/2, 1/2, 1/2, \dots$, in mutual agreement. Some of these resummation methods are discussed in the sequel, and we also refer the reader to the seminal review [156]. It has been stressed in J. E. Littlewood’s introduction to [155] that the subject of divergent series is in no way “mystical or unrigorous”.

Fundamental differences exist between nonalternating series (without loss of generality we can assume $a_k > 0 \forall k$ in that case), and strictly alternating series $a_k = (-1)^k b_k$ where $b_k > 0 \forall k$ (mixed forms will also be discussed in the sequel). The acceleration of the convergence and the summation of divergent *nonalternating* series has been historically problematic.

For example, it has been known for a long time that the acceleration of nonalternating slowly convergent series can be highly unstable numerically (see [156] and references therein). Likewise, the summation of nonalternating factorially divergent series has represented a considerable problem, because the series are typically non–Borel summable (see [157, 158, 159, 160] for suitable generalizations of the concept of Borel summability which provide solutions for large classes of problems of practical interest).

Recently, considerable progress has been achieved for the nonalternating case, and we will describe some of the relevant applications. For the acceleration of convergence of nonalternating series, new powerful algorithms have been devised [23], and generalizations of the Borel summation process have led to promising results in the case of nonalternating factorially divergent series [25, 27, 28].

One would intuitively assume that the perturbation series, even if it is divergent, should be associated to the physical quantity of interest in a more or less unique way. Unfortunately, many divergent series and the associated physical observables (e.g., energy levels as a function of the coupling strength) fail to fulfill the Carleman criterion [161] which guarantees that an asymptotic series can be uniquely associated to a given mathematical function. It appears that some ambiguity has to be accepted as far as the connection between perturbation theory and physical quantities is concerned, although some attempts have been made to resolve ambiguities in particular cases (see e.g. [162]).

For completeness, we give here the Carleman criterion which guarantees that there is a one-to-one correspondence between a function and its associated asymptotic series (see for example [163], Theorems XII.17 – XII.19 and the definition on p. 43 in [164], p. 410 in [165], or the comprehensive and elucidating review [166]):

Carleman Criterion. Let $f(z)$ be a function which is analytic in the interior and continuous on a sectorial region $\mathcal{S} = \{z | |\arg(z)| \leq k\pi/2 + \epsilon, 0 < |z| < R\}$ of the complex plane for some $\epsilon > 0$. Let the function f have an asymptotic expansion $f(z) \sim \sum_{n=0}^{\infty} c_n z^n$ (for $z \rightarrow 0$). The function f obeys a strong asymptotic condition (of order k) if there are suitable positive constants C and σ such that $|f(z) - \sum_{n=0}^m c_n z^n| \leq C \sigma^{m+1} [k(m+1)! |z|^{m+1}]$ holds for all m and for all $z \in \mathcal{S}$. The validity of such a condition implies that the function $f(z)$ is uniquely determined by its asymptotic series.

Typically, nonalternating factorially divergent series which entail nonperturbative (imaginary) contributions do not fulfill the Carleman condition. This failure gives rise to the inevitable ambiguities.

Even the generalized Borel resummation methods introduced in [157, 158, 159, 160] cannot provide conclusive answers for all possible physical scenarios. One highly problematic application is given by the quantum-mechanical double-well oscillator. The perturbation series for the ground state (as well as for any other unperturbed state) is divergent. Yet it is known that the ground state splits into two states of opposite parity when the second minimum of the potential approaches the first from infinity [167, 168]. The interesting observation is that two distinct quantum states are described by one and the same perturbation series. The energy difference is nonperturbative in the coupling and cannot be inferred *in*

principle from perturbation theory. The problem has been the subject of intensive discussion [169, 170, 171, 172, 173, 174]. The resulting multi-instanton expansion has recently found a more mathematically motivated explanation in the theory of resurgent functions [175, 176, 177].

We conclude this introduction by expressing that convergence acceleration and resummation methods cannot be separated. The connection can be seen as follows. We consider the remainders $r_n \equiv s_n - s$, i.e. the difference of the element s_n of the sequence and the limit s . The acceleration of convergence is achieved by eliminating, as far as possible, the remainders r_n from a necessarily finite set of input data $\{s_n\}_{n=0}^m$, in order to obtain a better estimate s'_m to s than the obvious estimate which would be provided by s_m . Clearly, the “elimination of remainders” is a concept which can be transported to the case of a divergent series. The only difference is that for a convergent series, $r_n \rightarrow 0$ as $n \rightarrow \infty$, whereas for a divergent series, $\lim_{n \rightarrow \infty} r_n$ does not exist. Otherwise, the concept of the elimination of remainders is the same for both cases.

Returning to our (simple) example, it is intuitively obvious that a method which helps to eliminate the remainders

$$r_n = \sum_{j=n+1}^{\infty} (-z)^j = \frac{(-z)^{n+1}}{1+z} \quad (6.4)$$

inside the circle of convergence $|z| < 1$, could be suitable to accomplish an analogous elimination of the r_n if z assumes values *outside* of the domain of convergence of the series $\sum_{j=0}^{\infty} (-z)^j$ because the mathematical structure of the expression which defines r_n does not change. These entirely heuristic considerations will be illustrated and explained in the sequel.

Chapter 7

Convergence Acceleration

7.1 The Concept of Convergence Acceleration

7.1.1 A Brief Survey

We intend to give a brief overview of the convergence acceleration methods used in this Thesis, without any claim for completeness or comprehensiveness with regard to currently known convergence acceleration techniques. Indeed, excellent textbooks (e.g. [178, 179, 180]) and review articles [156, 181, 182, 183, 184] on the subject are available. Here, we focus on aspects of the methods which will become useful for the applications discussed in later Chapters of the Thesis.

This brief introduction is structured as follows: After a discussion of basic concepts (Secs. 7.1.2 and 7.1.3), we introduce Padé approximants (one of *the* standard mathematical tools for extrapolation and convergence acceleration) in Sec. 7.1.4. Next, we discuss nonlinear sequence transformations in Sec. 7.1.5. Both of these convergence acceleration methods are much more powerful and much more numerically stable in the case of alternating input series than in the case of input series whose terms have the same sign (nonalternating series). We conclude in Sec. 7.1.6 with a discussion of the recently proposed [23] combined nonlinear-condensation transformation (CNCT) which provides an efficient algorithm in the historically problematic case of *nonalternating* input series.

Before we start the discussion of Padé approximants and nonlinear sequence transformations, we would like to mention that a large number of other convergence acceleration methods exist which have all been documented in the literature: examples include the Euler transformation, Aitken's Δ^2 process, the iterated Δ^2 process, and Richardson extrapolation which can be implemented using Wynn's rho algorithm, and its iterations. Last, but not least, we mention the Euler–Maclaurin sum formula. The interested reader will find related information e.g. in Chs. 5 and 6 of [156], App. E.2 of [43], and in Eq. (3.6.28) ff. of [185].

Concerning the mutual differences between the Padé method (Sec. 7.1.4) and nonlinear sequence transformations (Sec. 7.1.5), we would like to expand: Given a formal series

$$\mathcal{P}(z) = \sum_{j=0}^{\infty} c_j z^j \quad (7.1)$$

as input, the Padé method produces rational approximants which depend exclusively on a finite subset of the coefficients $\{c_j\}_{j=0}^{\infty}$, which in turn determine the partial sums of (7.1). Nonlinear sequence transformations require, in addition to the partial sums of (7.1), also explicit remainder estimates, i.e. estimates for the remainder $\sum_{j=n+1}^{\infty} c_j z^j$ which remains after the summation of the first n terms of (7.1).

Thus, the remainder estimates introduce additional degrees of freedom in the construction of sequence transformations as compared to Padé approximants. As pointed out in [26], one may draw an analogy between sequence transformations and Padé approximants on the one hand and the Gaussian integration and the Simpson rule on the other hand; the variable integration nodes and weight factors of the Gaussian integration yield additional degrees of freedom which may be used in order to construct a potentially much more powerful algorithm for numerical integration.

Except for the additional degrees of freedom, nonlinear sequence transformations have additional advantages. For example, the delta transformation to be discussed in Sec. 7.1.5 gave very good results in the case of the sextic anharmonic oscillator, and there is strong numerical evidence that it is able to sum the extremely violently divergent perturbation series for the octic anharmonic oscillator [186]. By contrast, as discussed in [186], Padé approximants are apparently not powerful enough to sum divergent series whose coefficients diverge like $(2n)!$ or even $(3n)!$. These observations stimulated research on sequence transformations considerably. The rapid progress in this field is convincingly demonstrated by the large number of monographs [180, 187, 188, 189, 190, 191, 192, 193, 194, 195] and review articles [156, 196, 197, 198] which appeared in recent years.

7.1.2 The Forward Difference Operator

An essential ingredient in the construction of sequence transformations, both for convergence acceleration and for the resummation of divergent series, is the (forward) difference operator. We define the difference operator Δ acting on the sequence $\{s_n\}_{n=0}^{\infty}$:

$$\Delta : \{s_n\}_{n=0}^{\infty} \rightarrow \{(\Delta s)_n\}_{n=0}^{\infty}, \quad (\Delta s)_n \equiv s_{n+1} - s_n, \quad (7.2)$$

The n th element of the sequence $\{(\Delta s)_n\}_{n=0}^{\infty}$ is given by $(\Delta s)_n = s_{n+1} - s_n$. This way of writing the n th element of the *transformed* sequence stresses the fact that $(\Delta s)_n$ is to be regarded as an element of some new sequence. However, the brackets are often left out, and we write

$$\Delta s_n \equiv s_{n+1} - s_n = (\Delta s)_n. \quad (7.3)$$

An important relation is,

$$(\Delta^k s)_n = (-1)^k \sum_{j=0}^k (-1)^j \binom{k}{j} s_{n+j}. \quad (7.4)$$

Again, we identify

$$\Delta^k s_n \equiv (\Delta^k s)_n. \quad (7.5)$$

The k th power of the difference operator plays a crucial rule in constructing sequence transformations.

7.1.3 Linear and Logarithmic Convergence

As already stressed in Ch. 6, the main notion of convergence acceleration is to extract information “hidden in trailing digits” from a necessarily finite number of sequence elements, in order to convert a sequence $\{s_n\}_{n=0}^{\infty}$ into a new sequence $\{s'_n\}_{n=0}^{\infty}$ with hopefully better numerical properties.

We briefly recall the notion of logarithmic convergence and the difficulties associated with the acceleration of the convergence of nonalternating series. Let a sequence $\{s_n\}_{n=0}^{\infty}$ fulfill the asymptotic condition

$$\lim_{n \rightarrow \infty} \frac{s_{n+1} - s}{s_n - s} = \rho, \quad (7.6)$$

where $s = s_{\infty}$ is the limit of the sequence as $n \rightarrow \infty$. If $\rho > 1$, then the sequence $\{s_n\}_{n=0}^{\infty}$ is divergent. For $\rho = 1$, the sequence may either be convergent or divergent. A convergent sequence with $\rho = 1$ is called *logarithmically convergent* (if $\rho < 1$, the series is called *linearly convergent*). Let us further assume that the elements of the sequence $\{s_n\}_{n=0}^{\infty}$ in Eq. (7.6) represent partial sums

$$s_n = \sum_{k=0}^n a(k) \quad (7.7)$$

of an infinite series. Here, we will almost exclusively investigate slowly convergent nonalternating sequences $\{s_n\}_{n=0}^{\infty}$ whose elements are all real and positive (for these sequences, $0 < \rho \leq 1$). In the case of slow convergence, ρ is either very close or equal to unity.

As observed by many authors (e.g. [156]), the acceleration of the convergence of nonalternating sequences is a potentially unstable numerical process. The reason is the following: A sequence transformation can

only accelerate convergence if it succeeds in extracting additional information about the index-dependence of the truncation errors

$$r_n = s_n - s \quad (7.8)$$

from a necessarily finite set of partial sums $\{s_n\}_{n=0}^k$ of the input series. Normally, this is done by forming arithmetic expressions involving higher weighted differences of the s_n . The calculation of higher weighted differences is a potentially unstable process which can easily lead to a serious loss of numerical significance due to cancellation if the input data all have the same sign.

We had mentioned in Ch. 6 that the rate of convergence can be said to be increased if the transformed sequence elements $\{s'_n\}_{n=0}^\infty$ and the input data $\{s_n\}_{n=0}^\infty$ fulfill [see also Eq. (6.2)]

$$\lim_{n \rightarrow \infty} \tau_n \equiv \lim_{n \rightarrow \infty} \frac{s'_n - s}{s_n - s} = 0, \quad (7.9)$$

where we implicitly define the τ_n . Let us assume that the input sequence $\{s_n\}_{n=0}^\infty$ is logarithmically convergent and that the transformed sequence $\{s'_n\}_{n=0}^\infty$ is linearly convergent with $\lim_{n \rightarrow \infty} (s'_{n+1} - s)/(s'_n - s) = \rho' < 1$ [see Eq. (7.6) and the definition of logarithmic convergence]. Then

$$\lim_{n \rightarrow \infty} \frac{\tau_{n+1}}{\tau_n} \equiv \lim_{n \rightarrow \infty} \frac{s'_{n+1} - s}{s'_n - s} \frac{s_n - s}{s_{n+1} - s} = \rho' < 1, \quad (7.10)$$

so that $\lim_{n \rightarrow \infty} \tau_n = 0$, and the rate of convergence is increased [according to the definition of convergence acceleration in Eq. (7.9)].

7.1.4 The Standard Tool: Padé Approximants

The Padé approximation produces a rational approximation to the original input series; this approximation is given by the ratio of two polynomials. The $[l/m]$ Padé approximant to a series $\mathcal{P}(z)$,

$$\mathcal{P}(z) = \sum_{j=0}^{\infty} c_j z^j, \quad (7.11)$$

is given by the ratio of two polynomials $P_l(z)$ and $Q_m(z)$ of degree l and m , respectively:

$$[l/m]_{\mathcal{P}}(z) = \frac{P_l(z)}{Q_m(z)} = \frac{p_0 + p_1 z + \dots + p_l z^l}{q_0 + q_1 z + \dots + q_m z^m}. \quad (7.12)$$

The polynomials $P_l(z)$ and $Q_m(z)$ are constructed so that the Taylor expansion of the Padé approximation Eq. (7.12) agrees with the original input series Eq. (7.11) up to the order of $l + m$

$$\mathcal{P}(z) - [l/m]_{\mathcal{P}}(z) = O(z^{l+m+1}). \quad (7.13)$$

In other words, the Padé approximant $[l/m]_{\mathcal{P}}(z)$ reproduces upon re-expansion the first $l + m + 1$ (c_0, \dots, c_{l+m}) coefficients of the input series.

Usually the normalization condition is chosen such as q_0 is one. Hence there are $l + m + 1$ equations to determine the coefficients of $P_l(z)$ and $Q_m(z)$. In most cases it is quite unattractive to solve this system of equations. A more attractive *recursive* prescription for the evaluation of Padé approximants is the ϵ -algorithm given by the formulas [199]

$$\begin{aligned} \epsilon_{-1}^{(n)} &= 0, \quad \epsilon_0^{(n)} = s_n, \\ \epsilon_{k+1}^{(n)} &= \epsilon_{k-1}^{(n+1)} + 1/[\epsilon_k^{(n+1)} - \epsilon_k^{(n)}] \end{aligned} \quad (7.14)$$

for k and n integer. The ϵ -algorithm is discussed in [199], and a detailed discussion of its implementation can be found in [156]. If the input data $\epsilon_0^{(n)} = s_n$ are the partial sums

$$s_n = \sum_{j=0}^n c_j z^j \quad (7.15)$$

of the power series Eq. (7.11), then the elements $\epsilon_{2k}^{(n)}$ of the two-dimensional table of transformations produce Padé approximants according to

$$\epsilon_{2k}^{(n)} = [n + k/k]_P(z). \quad (7.16)$$

The elements with odd lower subscripts $\epsilon_{2k+1}^{(n)}$ of the table of transformations are only auxiliary quantities. In practical applications (see e.g. Tables 1 – 3 of [24]), the epsilon algorithm can be used for evaluation of the following staircase sequence in the Padé table:

$$[0/0], [1/0], [1/1], [2/1], \dots, [\nu/\nu], [\nu + 1/\nu], [\nu + 1/\nu + 1], \dots \quad (7.17)$$

Because of Eq. (7.16) this corresponds to the sequence

$$\epsilon_0^{(0)}, \epsilon_0^{(1)}, \epsilon_2^{(0)}, \epsilon_2^{(1)}, \epsilon_4^{(0)}, \epsilon_4^{(1)}, \epsilon_6^{(0)}, \dots, \epsilon_{2\nu}^{(0)}, \epsilon_{2\nu}^{(1)}, \epsilon_{2\nu+2}^{(0)}, \dots, \quad (7.18)$$

which can be written as $\{\epsilon_{2\lfloor \nu/2 \rfloor}^{(\nu-2\lfloor \nu/2 \rfloor)}\}_{\nu=0}^\infty$. Here $\lfloor \nu/2 \rfloor$ denotes the integral part of $\nu/2$, which is the largest integer μ satisfying $\mu \leq \nu/2$. With this notation the Padé sequence in Eq. (7.17) can also be written as $\{[\nu - \lfloor \nu/2 \rfloor / \lfloor \nu/2 \rfloor]_P(z)\}_{\nu=0}^\infty$.

Modern computer algebra packages [90] contain built-in routines for the evaluation of Padé approximants. While these are computationally less effective than the epsilon algorithm, they are more flexible with regard to the degree of the numerator and denominator polynomials. In particular, the sequence allow for the evaluation of the sequence of lower-diagonal Padé approximants of the form $\{[\lfloor \nu/2 \rfloor / \nu - \lfloor \nu/2 \rfloor]_P(z)\}_{\nu=0}^\infty$.

As already mentioned in Sec. 7.1.1, it is a typical feature of all algorithms for Padé approximants that the coefficients c_0, c_1, \dots, c_{l+m} of the formal power series (7.11) suffice to determine $[l/m]_P(g)$ completely. No additional information is needed. At first sight, this seems to be very advantageous. However, there are situations in which this apparent advantage becomes a disadvantage. For instance, the truncation error of an asymptotic power series which has the Stieltjes property is for real argument bounded in magnitude by the first term not included in the partial sum (see Example 9.3 on p. 92 of [91]). Accordingly, the truncation error of a strictly alternating divergent hypergeometric series ${}_2F_0(\alpha, \beta; -x)$ with $\alpha, \beta, x > 0$, which provides a good mathematical model for many divergent perturbation expansions, is bounded in magnitude by the first term not included in the partial sum. In addition, the truncation error and the first term not included in the partial sum have the same sign (see Theorem 5.12-5 of [200]). In principle, this information should be very helpful in summation processes. Unfortunately, Padé approximants are not able to profit from it. This greatly reduces their efficiency if a divergent hypergeometric series ${}_2F_0$ of that kind or a divergent perturbation series of a similar type is to be summed.

7.1.5 Nonlinear Sequence Transformations

A sequence transformation \mathcal{T} is a rule which converts a slowly convergent or divergent sequence $\{s_n\}_{n=0}^\infty$ whose elements may be the partial sums $s_n = \sum_{k=0}^n a_k$ [see Eq. (6.1)] of an infinite series, into a new sequence $\{s'_n\}_{n=0}^\infty$ with hopefully better numerical properties. Padé approximants, which were discussed in Section 7.1.4, are special sequence transformations since they transform the partial sums of a formal power series (7.11) into a doubly indexed sequence of rational approximants (7.17). In the current Section, alternative transformations will be discussed.

Let us now assume that the sequence $\{s_n\}_{n=0}^\infty$ of partial sums of an infinite series diverges but can be summed to its generalized limit s . Then the sequence elements s_n can for all integers $n \geq 0$ be partitioned into the generalized limit s and remainders r_n :

$$s_n = s + r_n. \quad (7.19)$$

If $\{s_n\}_{n=0}^\infty$ diverges, then the remainders r_n do not vanish as $n \rightarrow \infty$. A divergent sequence would be summed to its generalized limit s if the remainders r_n could somehow be eliminated from the sequence elements s_n . For a slowly convergent sequence, one can hope to accelerate convergence by eliminating approximations to the r_n obtained from a finite set of sequence elements which are used as input data for the transformation.

The sequence $\{s_n\}_{n=0}^\infty$ is transformed into a new sequence $\{s'_n\}_{n=0}^\infty$, whose elements can for all $n \geq 0$ be partitioned into the generalized limit s of the original sequence and a transformed remainder r'_n :

$$s'_n = s + r'_n. \quad (7.20)$$

This approximative elimination process can be termed successful if the transformed remainders r'_n either vanish as $n \rightarrow \infty$ (in the case of a divergent input sequence where the r_n do not vanish at all as $n \rightarrow \infty$), or if the r'_n vanish faster than the original remainders r_n as $n \rightarrow \infty$ [in the case of a slowly convergent input sequence, see also Eq. (7.9)]. A *sequence transformation* is a rule which transforms a slowly convergent or divergent sequence $\{s_n\}_{n=0}^\infty$ into a new sequence $\{s'_n\}_{n=0}^\infty$ with hopefully better numerical properties.

However, the truncation errors of a divergent series can depend on n in a very complicated way. Consequently, the direct elimination of approximations to r_n from s_n can be very difficult. A considerable simplification can often be achieved by means of a suitable reformulation. Let us consider the following model sequence (see Section 3.2 of [156]):

$$\tilde{s}_n = \tilde{s} + \omega_n z_n. \quad (7.21)$$

Here, ω_n is a *remainder estimate*, which has to be chosen according to some rule and which may depend on n in a very complicated way, and z_n is a *correction term*, which should be chosen in such a way that it depends on n in a relatively smooth way. Moreover, the products $\omega_n z_n$ should be capable of producing sufficiently accurate approximations to the actual remainders r_n of the sequence to be transformed.

The principal advantage of this approach is that now only the correction terms $\{z_n\}_{n=0}^\infty$ have to be determined. The subsequent elimination of $\omega_n z_n$ from s_n is often much easier than the direct elimination of approximations to r_n from s_n . The use of remainder estimates $\{\omega_n\}_{n=0}^\infty$ is also an efficient way of incorporating *additional* information about the remainders into the summation scheme.

The model sequence (7.21) has another undisputable advantage: There is a *systematic* way of constructing a sequence transformation which is exact for this model sequence. Let us assume that a *linear* operator \hat{T} can be found which annihilates the correction term z_n . Then, a sequence transformation, which is exact for the model sequence (7.21), can be constructed quite easily. Just apply \hat{T} to $[\tilde{s}_n - \tilde{s}]/\omega_n = z_n$. Since \hat{T} annihilates z_n according to $\hat{T}(z_n) = 0$ and is by assumption linear, we find that the following sequence transformation \mathcal{T} is *exact* for the model sequence (7.21) (see Eq. (3.2-11) of [156]):

$$\mathcal{T}(\tilde{s}_n, \omega_n) = \frac{\hat{T}(\tilde{s}_n/\omega_n)}{\hat{T}(1/\omega_n)} = \tilde{s}. \quad (7.22)$$

Simple and yet very powerful sequence transformations are obtained if the annihilation operators are based upon the finite difference operator Δ defined in Sec. 7.1.2. A polynomial $P_{k-1}(n)$ of degree $k-1$ in n is annihilated by the k -th power of Δ . Thus, we now assume that the correction terms $\{z_n\}_{n=0}^\infty$ can be chosen in such a way that multiplication of z_n by some suitable quantity $w_k(n)$ yields a polynomial $P_{k-1}(n)$ of degree $k-1$ in n :

$$w_k(n) z_n = P_{k-1}(n). \quad (7.23)$$

Since $\Delta^k P_{k-1}(n) = 0$, the weighted difference operator $\hat{T} = \Delta^k w_k(n)$ annihilates z_n , and the corresponding sequence transformation (7.22) is given by the ratio

$$\mathcal{T}_k^{(n)}(w_k(n)|s_n, \omega_n) = \frac{\Delta^k \{w_k(n)s_n/\omega_n\}}{\Delta^k \{w_k(n)/\omega_n\}}. \quad (7.24)$$

A number of sequence transformations can be obtained by specializing $w_k(n)$. For instance, $w_k(n) = (n + \beta)^{k-1}$ with $\beta > 0$ yields Levin's sequence transformation [201]:

$$\begin{aligned} \mathcal{L}_k^{(n)}(\beta, s_n, \omega_n) &= \frac{\Delta^k \{(n + \beta)^{k-1} s_n/\omega_n\}}{\Delta^k \{(n + \beta)^{k-1}/\omega_n\}} \\ &= \frac{\sum_{j=0}^k (-1)^j \binom{k}{j} \frac{(\beta + n + j)^{k-1}}{(\beta + n + k)^{k-1}} \frac{s_{n+j}}{\omega_{n+j}}}{\sum_{j=0}^k (-1)^j \binom{k}{j} \frac{(\beta + n + j)^{k-1}}{(\beta + n + k)^{k-1}} \frac{1}{\omega_{n+j}}}. \end{aligned} \quad (7.25)$$

We follow the notation of [156]. The subscript k denotes the *order* of the transformation, and n denotes the starting index (the initial element) of the input data. Observe that the $k+1$ sequence elements s_n, \dots, s_{n+k} and the $k+1$ remainder estimates $\omega_n \dots \omega_{n+k}$ are needed for the computation of the transformation $\mathcal{L}_k^{(n)}$. The shift parameter β has to be positive in order to admit $n = 0$ in (7.25). In most practical applications, it is observed that any choice other than $\beta = 1$ does not lead to a significant improvement of the rate of convergence, and therefore the choice $\beta = 1$ is standard [156].

The notation $\mathcal{L}_k^{(n)}(\beta, s_n, \omega_n)$ is in need of a certain further explanation. As explained above, n represents the initial element of the sequence $\{s_n\}_{n=0}^\infty$ used in the evaluation of the transform. The specification of s_n as the second argument of $\mathcal{L}_k^{(n)}(\beta, s_n, \omega_n)$ is therefore redundant as far as the index n is concerned, because n already appears as an upper index in $\mathcal{L}_k^{(n)}$. The arguments s_n (and ω_n) are to be interpreted as follows: they rather specify the initial element s_n and the initial remainder estimate ω_n which have to be used in the calculation of the right-hand side of (7.25). Of course, the evaluation of $\mathcal{L}_k^{(n)}(\beta, s_n, \omega_n)$ requires the $k+1$ sequence elements $\{s_n, \dots, s_{n+k}, s_{n+k}\}$ as input. The knowledge of the “post-initial” elements $\{s_{n+1}, \dots, s_{n+k}\}$ is implicitly assumed in writing the definition (7.25).

According to Smith and Ford, who had investigated the performance of sequence transformations for a wide range of test problems [202, 203], Levin’s transformation is among the most powerful and most versatile sequence transformations that are currently known.

We can also assume that the unspecified weights $w_k(n)$ in (7.24) are Pochhammer symbols according to $w_k(n) = (n + \beta)_{k-1} = \Gamma(n + \beta + k - 1)/\Gamma(n + \beta)$ with $\beta > 0$. This yields the delta transformation (see Eq. (8.2-7) of [156]):

$$\begin{aligned} \mathcal{S}_k^{(n)}(\beta, s_n, \omega_n) &= \frac{\Delta^k \{(n + \beta)_{k-1} s_n / \omega_n\}}{\Delta^k \{(n + \beta)_{k-1} / \omega_n\}} \\ &= \frac{\sum_{j=0}^k (-1)^j \binom{k}{j} \frac{(\beta + n + j)_{k-1}}{(\beta + n + k)_{k-1}} \frac{s_{n+j}}{\omega_{n+j}}}{\sum_{j=0}^k (-1)^j \binom{k}{j} \frac{(\beta + n + j)_{k-1}}{(\beta + n + k)_{k-1}} \frac{1}{\omega_{n+j}}}. \end{aligned} \quad (7.26)$$

As in the case of Levin’s transformation, the most obvious choice for the shift parameter is $\beta = 1$.

The numerator and denominator sums in (7.25) and (7.26) can be computed more effectively with the help of the three-term recursions [see Eq. (7.2-8) of [156]]:

$$L_{k+1}^{(n)}(\beta) = L_k^{(n+1)}(\beta) - \frac{(\beta + n + k)(\beta + n + k)^{k-1}}{(\beta + n + k + 1)^k} L_k^{(n)}(\beta), \quad (7.27)$$

and (see Eq. (8.3-7) of [156])

$$S_{k+1}^{(n)}(\beta) = S_k^{(n+1)}(\beta) - \frac{(\beta + n + k)(\beta + n + k - 1)}{(\beta + n + 2k)(\beta + n + 2k - 1)} S_k^{(n)}(\beta). \quad (7.28)$$

The initial values $L_0^{(n)}(\beta) = S_0^{(n)}(\beta) = s_n / \omega_n$ and $L_0^{(n)}(\beta) = S_0^{(n)}(\beta) = 1 / \omega_n$ produce the numerator and denominator sums, respectively, of $\mathcal{L}_k^{(n)}(\beta, s_n, \omega_n)$ and $\mathcal{S}_k^{(n)}(\beta, s_n, \omega_n)$.

Let us assume that the terms a_k in (6.1) are strictly alternating, i.e. $a_k = (-1)^k b_k$ with $b_k > 0$. In this case, the first term $(-1)^{n+1} b_{n+1}$ not included in the partial sum $s_n = \sum_{k=0}^n (-1)^k b_k$ is the best *simple* estimate for the truncation error. This corresponds to the remainder estimate

$$\omega_n = (-1)^{n+1} b_{n+1} = \Delta s_n, \quad (7.29)$$

which was proposed by Smith and Ford [202]. The use of this remainder estimate in (7.25) and (7.26)

yields the following sequence transformations [Eqs. (7.3-9) and (8.4-4) of [156]]:

$$\begin{aligned}
d_k^{(n)}(\beta, s_n) &= \mathcal{L}_k^{(n)}(\beta, s_n, \Delta s_n) \\
&= \frac{\sum_{j=0}^k (-1)^j \binom{k}{j} \frac{(\beta + n + j)^{k-1}}{(\beta + n + k)^{k-1}} \frac{s_{n+j}}{\Delta s_{n+j}}}{\sum_{j=0}^k (-1)^j \binom{k}{j} \frac{(\beta + n + j)^{k-1}}{(\beta + n + k)^{k-1}} \frac{1}{\Delta s_{n+j}}}, \tag{7.30}
\end{aligned}$$

$$\begin{aligned}
\delta_k^{(n)}(\beta, s_n) &= \mathcal{S}_k^{(n)}(\beta, s_n, \Delta s_n) \\
&= \frac{\sum_{j=0}^k (-1)^j \binom{k}{j} \frac{(\beta + n + j)_{k-1}}{(\beta + n + k)_{k-1}} \frac{s_{n+j}}{\Delta s_{n+j}}}{\sum_{j=0}^k (-1)^j \binom{k}{j} \frac{(\beta + n + j)_{k-1}}{(\beta + n + k)_{k-1}} \frac{1}{\Delta s_{n+j}}}. \tag{7.31}
\end{aligned}$$

Alternative remainder estimates for the sequence transformations (7.25) and (7.26) were discussed in Sections 7 and 8 of [156] or in [204, 205].

A final word on sequence transformations: It is observed that sequence transformations constructed according to (7.31) often lead to much better numerical results than better known convergence accelerators like the Euler transformation, Wynn's epsilon or rho algorithms, or Aitken's Δ^2 process [156]. In particular, there is overwhelming empirical evidence that $d_k^{(n)}$ and $\delta_k^{(n)}$ work very well in the case of convergent or divergent alternating series for instance as they occur in special function theory [23, 156, 180, 201, 202, 203, 206, 207, 208, 209, 210] or in perturbation theory [186, 207, 208, 211, 212, 213, 214, 215, 216, 217]. Only for some special model problems could rigorous convergence proofs be obtained (see [218] or Sections 13 and 14 of [156]). No general convergence proof is known for delta transformation $\delta_k^{(n)}$ as well as their parent transformations $\mathcal{L}_k^{(n)}$ and $\mathcal{S}_k^{(n)}$. In view of the partially unsatisfactory situation concerning the availability of mathematical proof, we have carried out high-precision studies of the convergence of sequence transformations of the type (7.31), in part using multi-precision arithmetic (see Sec. 7.2.2). In the absence of a rigorous proof, one of the concerns which may be raised against the convergence of the transforms (7.31) is a plausible asymptotic nature of the sequence of transforms. In our numerical experiments, we found no indication of asymptotic behaviour. The rate of convergence of the transforms remained constant, and we observed apparent convergence up to 430 decimal figures (see Sec. 7.2.2 below). In the absence of rigorous proof and the presence of considerable numerical evidence for the computational usefulness of sequence transformations of the type (7.31), we believe that experimental mathematics may give some hints at the theoretical soundness of the concepts involved.

7.1.6 The Combined Nonlinear–Condensation Transformation (CNCT)

We assume the series $\sum_{k=0}^{\infty} a_k$ is slowly convergent and nonalternating, i.e. $a_k > 0 \forall k$. In order to make the notation of involved subscripts more clear, we temporarily identify $a_k \equiv a(k)$. Following Van Wijngaarden [219], we transform the nonalternating input series

$$\sum_{k=0}^{\infty} a(k), \quad a(k) \geq 0, \tag{7.32}$$

whose partial sums are given by (7.7), into an alternating series $\sum_{j=0}^{\infty} (-1)^j \mathbf{A}_j$. After the first step of the transformation, the limit of the input series is recovered according to

$$\sum_{k=0}^{\infty} a(k) = \sum_{j=0}^{\infty} (-1)^j \mathbf{A}_j. \tag{7.33}$$

The quantities \mathbf{A}_j are defined according to

$$\mathbf{A}_j = \sum_{k=0}^{\infty} \mathbf{b}_k^{(j)}, \quad (7.34)$$

where

$$\mathbf{b}_k^{(j)} = 2^k a(2^k (j+1) - 1). \quad (7.35)$$

Obviously, the terms \mathbf{A}_j defined in Eq. (7.34) are all positive if the terms $a(k)$ of the original series are all positive. The \mathbf{A}_j are referred to as the *condensed series* [23], and the series $\sum_{j=0}^{\infty} (-1)^j \mathbf{A}_j$ is referred to as the *transformed alternating series*, or alternatively as the *Van Wijngaarden transformed series*.

The construction of the condensed series reminds one of Cauchy's condensation theorem (see e.g. p. 28 of Ref. [220] or p. 121 of Ref. [221]). Given a nonalternating series $\sum_{k=0}^{\infty} a(k)$ with terms that satisfy $|a(k+1)| < |a(k)|$, Cauchy's condensation theorem states that $\sum_{k=0}^{\infty} a(k)$ converges if and only if the first condensed sum \mathbf{A}_0 defined according to Eq. (7.34) converges.

The summation over k in Eq. (7.34) does not pose numerical problems. Specifically, it can be easily shown in many cases of practical importance that the convergence of $\sum_{k=0}^{\infty} \mathbf{b}_k^{(j)}$ (in k) is linear even if the convergence of $\sum_{k=0}^{\infty} a(k)$ is only logarithmic. We will illustrate this statement by way of two examples.

Example 1: a logarithmically convergent input series whose terms behave asymptotically as $a(k) \sim k^{-1-\epsilon}$ with $\epsilon > 0$. In this case, the partial sums

$$\mathbf{A}_j^{(n)} = \sum_{k=0}^n \mathbf{b}_k^{(j)} \quad (7.36)$$

converge linearly with

$$\lim_{n \rightarrow \infty} \frac{\mathbf{A}_j^{(n+1)} - \mathbf{A}_j}{\mathbf{A}_j^{(n)} - \mathbf{A}_j} = \frac{1}{2^\epsilon (j+1)^{1+\epsilon}} < 1, \quad a(k) \sim k^{-1-\epsilon}, \quad k \rightarrow \infty. \quad (7.37)$$

Example 2: a series with $a(k) \sim k^\beta r^k$ where $0 < r < 1$ and β real. Here, we have $\rho = r < 1$, and the series is (formally) linearly convergent. However, slow convergence may result if ρ is close to one. In this case, the condensed series are very rapidly convergent,

$$\lim_{n \rightarrow \infty} \frac{\mathbf{A}_j^{(n+1)} - \mathbf{A}_j}{\mathbf{A}_j^{(n)} - \mathbf{A}_j} = 0, \quad a(k) \sim k^\beta r^k, \quad k \rightarrow \infty. \quad (7.38)$$

Therefore, when summing over k in evaluating the condensed series according to Eq. (7.34), it is in many cases sufficient to evaluate the condensed series by adding the terms successively, and no further acceleration of the convergence is required.

As shown in [23, 222], the condensation transformation defined according to Eqs (7.33)–(7.35) is essentially a reordering of the terms of the input series $\sum_{k=0}^{\infty} a(k)$. Furthermore, Daniel was able to show (see the Corollary on p. 92 of Ref. [222]) that for nonalternating convergent series whose terms decrease in magnitude ($|a(k)| > |a(k+1)|$), the equality (7.33) holds. This formally justifies the correctness of the condensation transformation defined according to Eqs. (7.33) – (7.35).

Note that the property

$$\mathbf{A}_{2j-1} = \frac{1}{2} [\mathbf{A}_{j-1} - a_{j-1}], \quad (j = 1, 2, \dots), \quad (7.39)$$

derived in [222], facilitates the numerical evaluation of a set of condensed series, by reducing the evaluation of condensed series of odd index to a trivial computation.

In the second step of the CNCT, the convergence of the Van Wijngaarden transformed series $\sum_{j=0}^{\infty} (-1)^j \mathbf{A}_j$ on the right-hand side of Eq. (7.33) is accelerated by a suitable nonlinear sequence transformation. We start from the partial sums

$$\mathbf{S}_n = \sum_{j=0}^n (-1)^j \mathbf{A}_j \quad (7.40)$$

of the Van Wijngaarden transformed series.

We use the partial sums \mathbf{S}_n defined in Eq. (7.40) as input data for the delta transformation (7.31). This leads to the CNC transforms

$$\mathcal{T}_{\text{CNC}}(n) = \delta_n^{(0)}(1, \mathbf{S}_0) . \quad (7.41)$$

which require as input the elements $\{\mathbf{S}_0, \dots, \mathbf{S}_n, \mathbf{S}_{n+1}\}$ of the Van Wijngaarden transformed series.

7.2 Applications of Convergence Acceleration Methods

7.2.1 Applications in Statistics and Applied Biophysics

Several slowly convergent series of the type considered in this Section of the Thesis define special functions that have important uses in statistics, namely the Riemann zeta, generalized zeta, Jonquière functions and Lerch's transcendent (see [92] for definitions and some properties of these functions). Discrete distributions are related to these functions by associating probability mass functions (p.m.f.s) with the terms of the particular infinite series defining the special functions. In turn, the normalization constants of the p.m.f.s are associated with the sums of the series.

Consider a discrete distribution with the p.m.f.

$$\Pr[X = n] = c p(n; \theta) \quad (7.42)$$

and with support of all nonnegative integers $n = 0, 1, \dots$, where θ is a (vector of) parameter(s) and c is a constant. The probability over the set of all outcomes is unity:

$$\sum_{n=0}^{\infty} \Pr[X = n] = 1 , \quad (7.43)$$

from which we obtain the normalization constant

$$c^{-1} = \sum_{n=0}^{\infty} p(n; \theta) \quad (7.44)$$

(in statistics, the random variable is usually denoted by the symbol n , whether continuous or discrete, but we will denote it here by the symbol n in order to follow the usual notation used in the treatment of special functions). Thus we expect the sum in Eq. (7.44) to exist and to converge to a finite value. In the sequel, we consider several related discrete distributions. The Zipf distribution has the p.m.f.

$$p_x = c \frac{1}{n^s} \quad (7.45)$$

with support of all positive integers $n = 1, 2, \dots$. The normalization constant (7.44) is then

$$c^{-1} = \zeta(s) = \sum_{n=1}^{\infty} \frac{1}{n^s} , \quad (7.46)$$

where $s > 1$, which is immediately recognized as the Dirichlet series for the Riemann zeta function [Eq. (1) on p. 32 of Ref. [92]]. Basic properties of the Zipf distribution can be found in [223].

The Zipf–Mandelbrot distribution [224] is the generalization of the Zipf distribution that adds a constant to the ranks n and has the p.m.f.

$$p_x = c \frac{1}{(n + v)^s} \quad (7.47)$$

with the support of all nonnegative integers $n = 0, 1, \dots$. The normalization constant (7.44) is then

$$c^{-1} = \zeta(s, v) = \sum_{n=0}^{\infty} \frac{1}{(n + v)^s} , \quad (7.48)$$

where $v \neq 0, -1, \dots$. The sum (7.48) is recognized as the generalized zeta function [Eq. (1) on p. 24 of Ref. [92]].

Further, the p.m.f.

$$p_x = c \frac{z^n}{n^s} \quad (7.49)$$

with the support of all positive integers $n = 1, 2, \dots$ defines the Good distribution [225]. The constant (7.44) is then

$$c^{-1} = F(z, s) = \sum_{n=1}^{\infty} \frac{z^n}{n^s}, \quad (7.50)$$

where $|z| < 1$, which is recognized as the Jonquière's function [Eq. (14) on p. 30 of Ref. [92]; see also [226]]. Important properties of the Good distribution were derived in [227, 228].

In biophysics, one is interested in establishing the statistical structure of DNA and RNA sequences. Indeed, an interest in statistical compositions of DNA and protein sequences originated shortly after the discovery that the nucleotide sequences of RNA uniquely determines the amino-acid sequence of the proteins. An early analysis was performed in [229], where it was observed that the distributions of relative abundances of amino-acids and nucleotides were nonrandom, i.e. deviated from models assuming uniform distribution of different words in any given text. Zipf distributions and related generalizations proved to be very useful in further studies [230, 231, 232].

A formal generalization of the Zipf, the Zipf–Mandelbrot and the Good distributions is possible upon realizing that the Riemann zeta, the generalized zeta and the Jonquière functions constitute special cases of the Lerch transcendent which is defined by the following series

$$\Phi(z, s, v) = \sum_{n=0}^{\infty} \frac{z^n}{(n+v)^s}, \quad (7.51)$$

where $|z| < 1$ and $v \neq 0, -1, \dots$ [Eq. (1) on p. 27 of Ref. [92]]. We use here the nonstandard notation of a dummy index n in order to highlight the connection with statistical theory. The relations between $\Phi(z, s, v)$ and $\zeta(s)$, $\zeta(s, v)$ and $F(z, s)$ can be obtained by considering appropriate limits if $\Phi(z, s, v)$ (e.g., by letting z and/or v to 0 and/or 1), and by making use of the following functional relation [Eq. (2) on p. 27 of Ref. [92]]

$$\Phi(z, s, v) = z^m \Phi(z, s, m+v) + \sum_{n=0}^{m-1} \frac{z^n}{(n+v)^s}. \quad (7.52)$$

In particular, Eq. (7.52) with $m = 1$ can be used to evaluate sums that start from $n = 1$ rather than from $n = 0$:

$$\sum_{n=1}^{\infty} \frac{z^n}{(n+v)^s} = z \Phi(z, s, 1+v) \quad (7.53)$$

In Tab. 7.1, we have summarized the relations between the different statistical distributions and their defining special functions. The table illustrates the fact that the three distributions, Zipf (Zeta), Zipf–Mandelbrot (Generalized zeta) and Good (Jonquière), are special cases of the Lerch distribution, and that their properties can be expressed in terms of Lerch's transcendent with special values of parameters.

We have found that the application of the combined nonlinear-condensation transformation (CNCT) described in detail in Sec. 7.1.6 is very suitable for the accelerated evaluation of the Lerch transcendent (7.51) in the nonalternating case ($z > 0$). Details of the implementation, both in C and *Mathematica* [90], are discussed in [30, 31]. For $z < 0$, the series (7.51) is alternating. In this case, the direct application of the delta transformation (7.31) leads to an efficient calculational scheme [31]. A C code for the Lerch transcendent is available [233, 234].

7.2.2 An Application in Experimental Mathematics

We would like to begin this section by quoting [235]: “In April 1993, Enrico Au–Yeung, an undergraduate at the University of Waterloo, brought to the attention of the author's [David Bailey's] colleague Jonathan

| Distribution (related function) | Support | p.m.f. | c^{-1} |
|---------------------------------------|---------------|--------------------|-------------------------------|
| Zipf (zeta function) | $1, 2, \dots$ | $c n^{-s}$ | $\zeta(s) = \Phi(1, s, 1)$ |
| Zipf–Mandelbrot (generalized zeta) | $0, 1, \dots$ | $c(n+v)^{-s}$ | $\zeta(s, v) = \Phi(1, s, v)$ |
| Good (Jonquière function) | $1, 2, \dots$ | $c z^n n^{-s}$ | $F(z, s) = z \Phi(z, s, 1)$ |
| Lerch (Lerch’s transcendent) | $0, 1, \dots$ | $c z^n (n+v)^{-s}$ | $\Phi(z, s, v)$ |

Table 7.1: Interrelationships between distributions defined by Riemann zeta, generalized zeta, Jonquière and Lerch functions.

Borwein the curious fact that

$$\sum_{k=1}^{\infty} \left(1 + \frac{1}{2} + \dots + \frac{1}{k}\right)^2 k^{-2} = 4.59987\dots \approx \frac{17}{4} \zeta(4) = \frac{17\pi^2}{360}, \quad (7.54)$$

based on a computation of 500,000 terms. Borwein’s reaction was to compute the value of this constant to a higher level of precision in order to dispel this conjecture. Surprisingly, his computation to 30 digits affirmed it. [David Bailey] then computed this constant to 100 decimal digits, and the above equality was still affirmed.” Many formulas similar to (7.54) have subsequently been established by rigorous proof [236].

With the help of a multiprecision system [235, 237, 238] and the CNCT, we have verified (7.54) “experimentally” to a couple of hundred decimals. The calculation will be sketched in the following. Using the definition

$$\bar{b}(k) = \left(1 + \frac{1}{2} + \dots + \frac{1}{k}\right)^2 k^{-2}, \quad (7.55)$$

we rewrite (7.54) as follows,

$$\begin{aligned} \sum_{k=0}^{\infty} \bar{b}(k) &= \sum_{k=0}^{\infty} \left(\sum_{j=0}^k \frac{1}{j+1} \right)^2 (k+1)^{-2} \\ &= \sum_{k=0}^{\infty} \left(\frac{\psi(k+2) + C}{k+1} \right)^2, \end{aligned} \quad (7.56)$$

where C is the *Euler-Mascheroni* constant $C = 0.577\,215\dots$, and $\psi(z)$ is the logarithmic derivative of the Gamma function [91, 92],

$$\psi(z) = \frac{d}{dz} \ln \Gamma(z). \quad (7.57)$$

With the help of the relation

$$\sum_{k=0}^{\infty} \frac{\psi(k+2)}{(k+1)^2} = 2\zeta(3) - C\zeta(2), \quad (7.58)$$

the conjecture (7.54) can be rewritten as

$$\sum_{k=0}^{\infty} \left(\frac{\psi(k+2)}{k+1} \right)^2 = \frac{17}{4} \zeta(4) - 4C\zeta(3) + C^2\zeta(2). \quad (7.59)$$

We proceed to calculate numerically, to high precision, the infinite sum

$$\sum_{k=0}^{\infty} \bar{a}(k), \quad \bar{a}(k) = \left(\frac{\psi(k+2)}{k+1} \right)^2, \quad (7.60)$$

using the CNC transformation.

In order to establish the rate of convergence of (7.60), we investigate the asymptotic behaviour of the $\bar{a}(k)$ as $k \rightarrow \infty$. The logarithm of the Gamma function can be expanded into an asymptotic series [see Eq. (4.03) on p. 294 of [91]]:

$$\ln \Gamma(z) = \left(z - \frac{1}{2} \right) \ln z - z + \frac{1}{2} \ln(2\pi) + \sum_{s=1}^{m-1} \frac{\mathcal{B}_{2s}}{2s(2s-1)z^{2s-1}} + R_m(z), \quad (7.61)$$

where

$$R_m(z) = \int_0^{\infty} \frac{\mathcal{B}_{2m} - \mathcal{B}_{2m}(x - \llbracket x \rrbracket)}{2m(x+z)^{2m}} dx. \quad (7.62)$$

Here, $\llbracket x \rrbracket$ is the integral part of x , i.e., the largest integer m satisfying $m \leq x$, $\mathcal{B}_k(x)$ is a Bernoulli polynomial defined by the generating function [see Eq. (1.06) on p. 281 of Ref. [91]]:

$$\frac{t \exp(xt)}{\exp(t) - 1} = \sum_{m=0}^{\infty} \mathcal{B}_m(x) \frac{t^m}{m!}, \quad |t| < 2\pi, \quad (7.63)$$

and

$$\mathcal{B}_m = \mathcal{B}_m(0) \quad (7.64)$$

is a Bernoulli number (p. 281 of Ref. [91]). The following asymptotic relation for $\psi(z)$ follows:

$$\psi(z) = \ln z - \frac{1}{2z} - \sum_{s=1}^{m-1} \frac{\mathcal{B}_{2s}}{2sz^{2s}} + \mathcal{O}\left(\frac{1}{z^{2m}}\right). \quad (7.65)$$

The leading asymptotics of the remainder of the sum (7.60) after adding $N-1$ terms can thus be derived easily. We have for large k ,

$$\bar{a}(k) \sim \frac{\ln(k+2)^2}{(k+1)^2} - \frac{\ln(k+2)}{(k+1)^2(k+2)} - \frac{\ln(k+2)}{6(k+1)^2(k+2)^2} + \mathcal{O}\left(\frac{1}{k^4}\right), \quad k \rightarrow \infty. \quad (7.66)$$

Based on these formulas, the remainder of the sum (7.60), for large N , can be written as

$$\sum_{k=N}^{\infty} \bar{a}(k) \sim \frac{\ln^2 N}{N} + \frac{\ln N}{N} + \frac{1}{N} + \mathcal{O}\left(\frac{\ln^2 N}{N^2}\right). \quad (7.67)$$

Here, the Euler-Maclaurin formula [Eqs. (2.01) and (2.02) on p. 285 of Ref. [91]] has been used in order to convert the sum over the $\bar{a}(k)$ in the asymptotic regime of large k [see Eq. (7.66)] into an integral plus correction terms. In order to calculate (7.59) to an accuracy of 200 decimals, Eq. (7.67) says that we would be required to add on the order of 10^{205} terms. Without the use of convergence acceleration methods, this would represent a formidable computational task.

Using the CNCT, it is easy to calculate the sum (7.59) to 200 digits, based on multiprecision arithmetic [235] and a Linux personal computer, within a few hours. We obtain for the 246th and the 247th CNC transform defined according to Eq. (7.41),

$$\begin{aligned}\mathcal{T}_{\text{CNC}}(246) = & 2.37254\ 51620\ 38445\ 67035\ 68130\ 69148\ 85258\ 25756\ 18499\ 54254 \\ & 97013\ 57806\ 20011\ 72404\ 62937\ 46020\ 32218\ 23862\ 67095\ 00004 \\ & 69194\ 36541\ 28946\ 10390\ 15116\ 52595\ 90270\ 23975\ 58737\ 74256 \\ & 23420\ 48480\ 95165\ 00802\ 19816\ 35378\ 76591\ 98589\ 60393\ 32103, \quad (7.68)\end{aligned}$$

and

$$\begin{aligned}\mathcal{T}_{\text{CNC}}(247) = & 2.37254\ 51620\ 38445\ 67035\ 68130\ 69148\ 85258\ 25756\ 18499\ 54254 \\ & 97013\ 57806\ 20011\ 72404\ 62937\ 46020\ 32218\ 23862\ 67095\ 00004 \\ & 69194\ 36541\ 28946\ 10390\ 15116\ 52595\ 90270\ 23975\ 58737\ 74256 \\ & 23420\ 48480\ 95165\ 00802\ 19816\ 35378\ 76591\ 98589\ 60393\ 32112. \quad (7.69)\end{aligned}$$

The apparent convergence to 200 decimals can be verified against the right-hand side of Eq. (7.59). Of course, the right-hand side of Eq. (7.59), which involves only rationals, zeta functions and the Euler–Mascheroni constant,

$$\frac{17}{4} \zeta(4) - 4C \zeta(3) + C^2 \zeta(2),$$

can be easily evaluated to 200 decimals using known algorithms which are included in computer algebra systems [90].

The evaluation of the terms $\bar{a}(k)$ proceeds as follows. For *small* index k , it is easy to write a recursion relation relating $\bar{a}(k)$ and $\bar{a}(k+1)$ based on the (trivial) recursion for the ψ function,

$$\psi(k+1) = \psi(k) + \frac{1}{k}. \quad (7.70)$$

For *large* index k , the asymptotic formula (7.65) can be used in order to calculate the ψ function to high precision. The point at which index one may switch from the recursion to the asymptotic method depends on how many explicit values for Bernoulli numbers are available to the machine. We use the first values for the first 60 Bernoulli numbers, to 250 decimals, for our calculation. We switch from one method to the other when the index k of $\bar{a}(k)$ has reached a value of 500.

With 84 308 $\bar{a}(k)$ terms evaluated (out of which 1364 by recursion and 82944 by the asymptotic method), we evaluate the first 247 transforms with the results presented above in Eqs. (7.68) and (7.69). If the terms of the series (7.54) were added on a term-by-term basis, then about 10^{205} would be required for an accuracy of 200 decimals in the final result. The reduction of this number to roughly 84 000 corresponds to an acceleration of the convergence by roughly 200 orders of magnitude. We have also carried out, using enhanced precision, a calculation to 430 decimals, involving about 500 CNC transformations and arithmetic with 600 decimal figures. These evaluations not only confirm the conjecture (7.59) to high precision, but they also represent one of the most accurate experimental verifications of the convergence properties of the delta transformation (7.31) today. Moreover, it is observed that the rate of convergence of the CNC transforms, which is approximately one decimal figure per transformation, remains constant over a wide range of transformation orders. This observed behaviour is consistent with linear convergence [$\rho \approx 0.1$ in Eq. (7.6)] in higher transformation orders. By contrast, the series (7.59) is only logarithmically convergent. This corresponds to convergence acceleration according to the definition (7.9).

7.2.3 Other Applications of the CNCT

We would like to mention the existing applications in the domain of quantum electrodynamic bound-state calculations (see [9, 12, 43] and Ch. 1 of this Thesis). Another existing application concerns the quantum electrodynamic effective action (see Ref. [20]).

J. Becher [239] has investigated the applicability of the combined nonlinear-condensation transformation to series of the form

$$R_p(x) = \sum_{k=0}^{\infty} \frac{x^{2k+1}}{(2k+1)^p}, \quad (7.71)$$

as well as

$$T_p(x, b) = \sum_{k=0}^{\infty} \frac{1}{(2k+1)^p} \frac{\cosh(2k+1)x}{\cosh(2k+1)b}, \quad (7.72)$$

and

$$U_p(x, b) = \sum_{k=0}^{\infty} \frac{1}{(2k+1)^p} \frac{\cosh(2k+1)x}{\sinh(2k+1)b}. \quad (7.73)$$

Series of this type occur naturally in the context of plate contact problems with periodic boundary conditions [240]. The arguments p , x and b are real and positive for cases of practical relevance. For $x \approx b$ and $p \approx 1$, the series T_p and U_p are very slowly convergent. In App. A.2 of [239], it is demonstrated by way of numerical example that the CNCT is able to efficiently accelerate the convergence of these series in problematic parameter regions.

In the numerical calculations, it is necessary to evaluate terms with large index k . This can lead to numerical overflow because of the large arguments of the hyperbolic functions. Clearly, representations like

$$T_p(x, b) = \sum_{k=0}^{\infty} \frac{e^{(2k+1)(x-b)}}{(2k+1)^p} \frac{1 + e^{-2x(2k+1)}}{1 + e^{-2b(2k+1)}} \quad (7.74)$$

provide a solution for this problem.

Let us recall that considerable effort has been invested in the development of efficient numerical methods for the evaluation of the series (7.71) – (7.73) [241, 242, 243, 244, 245]. These alternative methods make intensive use of special properties of the series. They involve integral transformations and infinite series over numerical integral [244], and they make use of special properties of Legendre’s chi-function [243] which is related to the functions (7.71) – (7.73).

A further application of convergence acceleration methods discussed by J. Becher [239] is the calculation of the incomplete Gamma function $\Gamma(0, x)$ whose asymptotic expansion for large argument reads

$$\Gamma(0, x) \sim \frac{e^{-x}}{x} \sum_{n=0}^{\infty} (-1)^n \frac{n!}{x^n}, \quad x \rightarrow \infty \dots \quad (7.75)$$

It is observed (see App. A.3 *ibid.*) that the divergent asymptotic series of this function for large positive argument can be resummed effectively using the delta transformation, without any recourse to the CNCT.

7.3 Conclusions and Outlook for Convergence Acceleration

We have discussed several applications of the convergence acceleration methods introduced in Sec. 7.1: in statistical physics (Sec. 7.2.1), in experimental mathematics (Sec. 7.2.2), and other applications, mainly in the evaluation of special functions (Sec. 7.2.3). Specifically, it is observed that a combination of the methods introduced in Secs. 7.1.5 and 7.1.6 leads to an efficient calculational scheme for the Lerch transcendent Φ defined in Eq. (7.51). This special function provides a generalization of several kinds of probability density functions which are of significance for the statistical analysis of DNA sequences (see Table 7.1).

Other applications can be envisaged: For example, the evaluation of generalized hypergeometric functions – notably of two-variable hypergeometric functions (Appell functions) F_1 and F_2 [246] – has been historically problematic. In the recent investigation [247], the evaluation of $F_1(\alpha, \beta_1, \beta_2, \gamma; x, y)$ is considered:

The algorithm consists in two steps: (i) the sophisticated use of analytic continuations to map the point (x, y) into the convergence region of the defining hypergeometric series of the Appell function, and (ii) the computation of the Appell function within the region of convergence. The analytic continuations give rise – in addition to F_1 functions of transformed argument – to the G_2 function, which can in turn be written in terms of Appell’s F_2 function. This implies that numerical methods also have to be devised for the F_2 function. The second step of the algorithm described in [247] is the actual numerical calculation of the Appell function(s) (F_1 and F_2) within the region of convergence. This calculation proceeds by investigating the criterion $t_0 = \max(|x|, |y|) < 0.5$. If the criterion is fulfilled, then both the F_1 and the F_2 are evaluated by single-index series expansions in terms of ${}_2F_1$ ’s, for example employing the formula [248, 249]

$$F_1(\alpha, \beta_1, \beta_2, \gamma; x, y) = \sum_{r=0}^{\infty} \frac{(\alpha)_r (\beta_1)_r (\beta_2)_r (\gamma - \alpha)_r}{(\gamma + r - 1)_r (\gamma)_{2r} r!} \times {}_2F_1(\alpha + r, \beta_1 + r, \gamma + 2r, x) {}_2F_1(\alpha + r, \beta_2 + r, \gamma + 2r, y). \quad (7.76)$$

If the criterion is not fulfilled, the authors resort to the solution of a third-order differential equation for the evaluation of the Appell function [starting from the point $(x, y) = (0, 0)$ where F_1 vanishes]. It appears possible that an application of convergence acceleration algorithms to the series (7.76) could lead to an efficient calculational scheme in the problematic case $t_0 > 0.5$ where the authors of [247] had to resort to an integration of a third-order differential equation.

Possible improvements over existing algorithms concern “multi-stage transformations”. For example, it was observed in [26] that the rate of convergence of the output data resulting from Borel summation (see Sec. 8.2.2) of a specific divergent series describing the quantum electrodynamic effective action could be further accelerated by using two iterations of the epsilon algorithm [defined in Eq. 7.14], i.e. by evaluating Padé approximants to the Padé approximants of the Borel transforms (in this sequence). Iterated forms of a number of convergence accelerators have been discussed in [156]. In general, the iteration of suitable convergence accelerators depends on a thorough analysis of the remainder structure resulting from previous “stages” of the transformation, and it is not *a priori* guaranteed that a “multi-stage transformation” with only *one* iterated algorithm will help. In principle, the use of iterated algorithms can only be helpful when the evaluation of the sequence transforms or Padé approximants is computationally cheap in comparison to the evaluation of further terms of the input sequence which could potentially be used to calculate higher-order terms in a single-stage transformation process.

Chapter 8

Divergent Series

8.1 Introduction to Divergent Series in Physics

The observation that many perturbation series encountered in quantum mechanics and quantum field theory are divergent, sparked the development of large-order perturbation theory [250]. This subject is inherently connected to the resummation of divergent series, and with the development of appropriate numerical methods which exploit all available information contained in a necessarily finite number of perturbative coefficients. Of prime importance in this context is the Borel method to be discussed in Sec. 8.2.2.

As already stressed in Ch. 8, there are connections between the convergence acceleration methods discussed in Ch. 7 and the resummation methods discussed in the current Chapter. Specifically, the methods introduced in Secs. 7.1.4 and 7.1.5 will be used below in Sec. 8.3.2 in the context of the resummation of the divergent perturbation series for the QED effective action.

Essentially, we will consider four physical applications of resummation methods: (i) the energy displacement of a hydrogen atom in a background electric field, including the autoionization width (Sec. 8.2), (ii) zero-dimensional field theories (Sec. 8.3.1), (iii) the QED effective Lagrangian for background magnetic and electric fields (Sec. 8.3.2), and (iv) the energy levels of the double-well potential which receive nonperturbative contributions from multi-instanton effects (Sec. 8.3.3).

Several important aspects and basic concepts connected with divergent series and the large-order behavior of perturbation theory can be illustrated by investigating the (divergent) perturbation series of the Stark effect [251]. This effect, which is also known as the LoSurdo–Stark effect in view of the existence of the investigation [252]), describes the energy displacement of a hydrogen atom in a static external electric field and can be expressed as a perturbation series (power series) in the electric field strength.

The first nonvanishing perturbation (in atomic units) is the second-order effect

$$F^2 \sum_{m \neq 1S} \frac{\langle \phi_{1S} | z | \phi_m \rangle \langle \phi_m | z | \phi_{1S} \rangle}{E_{1S} - E_m},$$

where the sum over m runs over the entire spectrum, including the continuum, but excluding the 1S ground state, and E_m is the nonrelativistic (Schrödinger) energy of the m th state. A well known, but perhaps surprising result says that the coefficients of the terms of order F^4 , F^6 , F^8 , ... grow so rapidly that the series in F ultimately diverges, irrespective of how small the field strength is. The convergence radius of the factorially divergent perturbation series is zero. The perturbation series for the Stark effect [251, 252] can be formulated to arbitrarily high order [253]. The perturbative coefficients grow factorially in absolute magnitude [254]. The perturbation series is a divergent, asymptotic expansion in the electric field strength F , i.e. about zero electric field. This means that the perturbative terms at small coupling first decrease in absolute magnitude up to some minimal term. After passing through the minimal term, the perturbative terms increase again in magnitude, and the series ultimately diverges.

By the use of a *resummation* method, it is possible to assign a finite value to an otherwise divergent series, and various applications of resummation methods in mathematics and physics have been given,

e.g., in [24, 156, 165, 179, 255]. When a divergent series is resummed (cf. Ch. 6), the superficial precision limit set by the minimal term can be overcome, and more accurate results can be obtained as compared to the optimal truncation of the perturbation series. However, the resummation of the relevant divergent series is problematic in the considered case, because the Borel transform, from which the physically correct, finite result is obtained by evaluating a *generalized* Borel integral – see Eq. (8.11) in Sec. 8.2.2 below –, exhibits a rich singularity structure in the complex plane. The perturbation series is formally not Borel summable.

The Stark effect and its associated divergent perturbative expansion including the nonperturbative, non-analytic imaginary contributions have attracted considerable attention, both theoretically and experimentally [157, 253, 254, 256, 257, 258, 259, 260, 261, 262, 263, 264, 265, 266, 267, 268, 269, 270, 271, 272, 273, 274, 275, 276, 277, 278, 279, 280, 281, 282, 283, 284, 285, 286]. Experiments have been performed in field strengths up to a couple of MV/cm [287, 288, 289, 290].

Rather mathematically motivated investigations regarding the Borel summability of the divergent perturbation series for the Stark effect were performed in [265] and [159], and it was established that the perturbation series of the Stark effect is Borel summable in the distributional sense (for the definition of “distributional Borel summability” we refer to [158]).

In comparison to the previous investigation [157], we use here an optimized resummation method that combines an analytic continuation of the Borel transform with Padé approximants in the conformal variable and the explicit use of the “leading renormalon pole”. All of these methods will be described in Secs. 8.2.2 and 8.2.3. These optimized Borel transforms represent an alternative to so-called order-dependent mappings which have been discussed intensively in the literature [291, 292, 293, 294].

After the discussion of the Stark effect (Secs. 8.2.2 – 8.2.4), we turn our attention to the resummation of the divergent perturbation series for zero-dimensional field theories (Sec. 8.3.1), to the QED effective action (Sec. 8.3.2), and to the double-well potential (Sec. 8.3.3).

8.2 The Stark Effect: A Paradigmatic Example

8.2.1 Perturbation Series for the Stark Effect

In the presence of an electric field, the $SO(4)$ symmetry of the hydrogen atom is broken, and parabolic quantum numbers n_1 , n_2 and m are used for the classification of the atomic states [168]. For the Stark effect, the perturbative expansion of the energy eigenvalue $E(n_1, n_2, m, F)$ reads [see Eq. (59) of [253]],

$$E(n_1, n_2, m, F) \sim \sum_{N=0}^{\infty} E_{n_1 n_2 m}^{(N)} F^N, \quad (8.1)$$

where F is the electric field strength. For $N \rightarrow \infty$, the leading large-order factorial asymptotics of the perturbative coefficients have been derived in [269] as

$$E_{n_1 n_2 m}^{(N)} \sim A_{n_1 n_2 m}^{(N)} + (-1)^N A_{n_2 n_1 m}^{(N)}, \quad N \rightarrow \infty, \quad (8.2)$$

where $A_{n_i n_j m}^{(N)}$ is given as an asymptotic series,

$$A_{n_i n_j m}^{(N)} \sim K(n_i, n_j, m, N) \sum_{k=0}^{\infty} a_k^{n_i n_j m} (2n_j + m + N - k)!. \quad (8.3)$$

The quantities $a_k^{n_i n_j m}$ are constants. The K -coefficients in Eq. (8.3) are given by

$$K(n_i, n_j, m, N) = - [2\pi n^3 n_j! (n_j + m)!]^{-1} \exp \{3(n_i - n_j)\} 6^{2n_j + m + 1} (3n^3/2)^N. \quad (8.4)$$

Here, the principal quantum number n as a function of the parabolic quantum numbers n_1 , n_2 and m is given by [see Eq. (65) in [253]]

$$n = n_1 + n_2 + |m| + 1. \quad (8.5)$$

According to Eq. (8.2), the perturbative coefficients $E_{n_1 n_2 m}^{(N)}$, for large order $N \rightarrow \infty$ of perturbation theory, can be written as a sum of a nonalternating factorially divergent series [first term in Eq. (8.2)]

and of an alternating factorially divergent series [second term in Eq. (8.2)]. Because the $a_k^{n_i n_j m}$ in Eq. (8.3) are multiplied by the factorial $(2n_i + m + N - k)!$, we infer that for large perturbation theory order N , the term related to the $a_0^{n_i n_j m}$ coefficient ($k = 0$) dominates. Terms with $k \geq 1$ are suppressed in relation to the leading term by a relative factor of $1/N^k$ according to the asymptotics

$$\frac{(2n_j + m + N - k)!}{(2n_j + m + N)!} \sim \frac{1}{N^k} \left[1 + \mathcal{O}\left(\frac{1}{N}\right) \right] \quad (8.6)$$

for $N \rightarrow \infty$. The leading ($k = 0$)-coefficient has been evaluated in [254] as

$$a_0^{n_i n_j m} = 1. \quad (8.7)$$

According to Eqs. (8.2), (8.3) and (8.7), for states with $n_1 < n_2$, the nonalternating component of the perturbation series dominates in large order of perturbation theory, whereas for states with $n_1 > n_2$, the alternating component is dominant as $N \rightarrow \infty$. For states with $n_1 = n_2$, the odd- N perturbative coefficients vanish [269], and the even- N coefficients necessarily have the same sign in large order [see Eq. (8.2)]. According to Eq. (8.2), there are subleading divergent nonalternating contributions for states with $n_1 > n_2$, and there exist subleading divergent alternating contributions for states with $n_1 < n_2$. This complicates the resummation of the perturbation series.

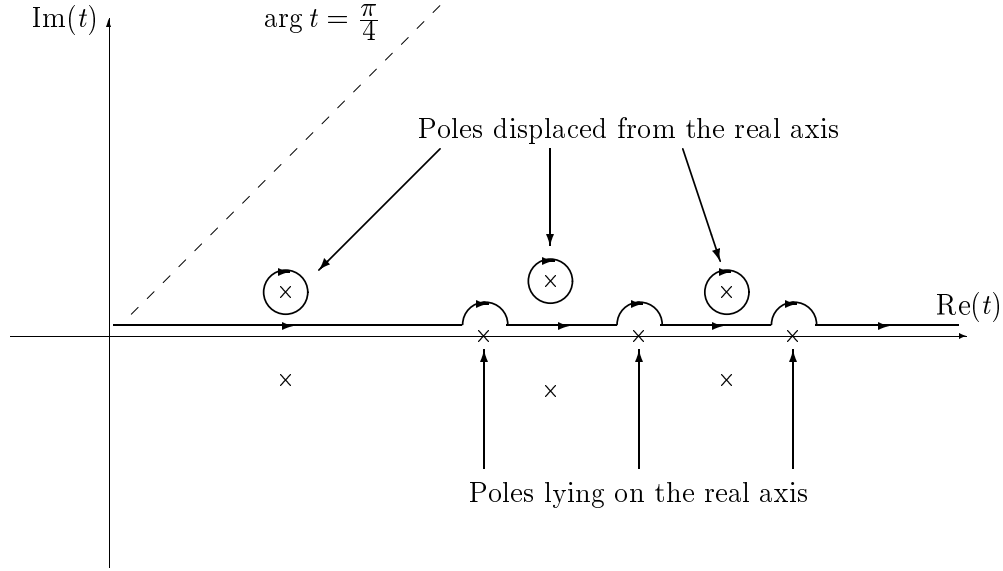


Figure 8.1: Integration contour C_{+1} for the evaluation of the generalized Borel integral defined in Eq. (8.11). Poles displaced from the real axis are evaluated as full poles, whereas those poles which lie on the real axis are treated as half poles.

8.2.2 Borel–Padé Resummation

The resummation of the perturbation series (8.1) by a combination of the Borel transformation and Padé approximants proceeds as follows. First we define the parameter

$$\lambda = 2 \max(n_1, n_2) + m + 1. \quad (8.8)$$

The large-order growth of the perturbative coefficients [see Eqs. (8.2) and (8.3)] suggests the definition of the (generalized) Borel transform [see Eq. (4) in [26]]

$$\begin{aligned}
E_B(z) &\equiv E_B(n_1, n_2, m, z) \\
&= \mathcal{B}^{(1, \lambda)} [E(n_1, n_2, m); z] \\
&= \sum_{N=0}^{\infty} \frac{E_{n_1 n_2 m}^{(N)}}{\Gamma(N + \lambda)} z^N,
\end{aligned} \tag{8.9}$$

where we consider the argument z of $E_B(z)$ as a complex variable and λ is defined in Eq. (8.8). The additive constant (in this case λ) in the argument of the Gamma function is chosen in accordance with the notion of an “asymptotically improved” resummation (see also [26]). It is observed that the additive constant λ can be shifted by a small integer without affecting the convergence of the Borel resummed series. Because the perturbative coefficients $E_{n_1 n_2 m}^{(N)}$ diverge factorially in absolute magnitude, the Borel transform $E_B(z)$ has a finite radius of convergence about the origin. The evaluation of the (generalized) Laplace–Borel integral [see Eq. (8.11) below] therefore requires an analytic continuation of $E_B(z)$ beyond the radius of convergence. The “classical” Borel integral is performed in the z -range $z \in (0, \infty)$, i.e. along the positive real axis [see e.g. Eqs. (8.2.3) and (8.2.4) of [165]]. It has been suggested in [295] that the analytic continuation of (8.9) into regions where F retains a nonvanishing, albeit infinitesimal, imaginary part can be achieved by evaluating Padé approximants. Using the first $M+1$ terms in the power expansion of the Borel transform $E_B(z)$, we construct the Padé approximant [we follow the notation of [179], see also Eq. (7.12)]

$$\mathcal{P}_M(z) = \left[\llbracket M/2 \rrbracket / \llbracket (M+1)/2 \rrbracket \right]_{E_B} (z), \tag{8.10}$$

where $\llbracket x \rrbracket$ denotes the largest positive integer smaller than x . We then evaluate the (modified) Borel integral along the integration contour C_{+1} shown in Fig. 8.1 in order to construct the transform $\mathcal{T}E_M(F)$ where

$$\mathcal{T}E_M(F) = \int_{C_{+1}} dt t^{\lambda-1} \exp(-t) \mathcal{P}_M(F t). \tag{8.11}$$

The successive evaluation of transforms $\mathcal{T}E_M(F)$ in increasing transformation order M is performed, and the apparent convergence of the transforms is examined. This procedure is illustrated in Tables I and II of [25].

The contour C_{+1} is supposed to encircle all poles at $t = z_i$ in the upper right quadrant of the complex plane with $\arg z_i < \pi/4$ in the mathematically negative sense. That is to say, the contribution of all poles z_i with $\text{Re } z_i > 0$, $\text{Im } z_i > 0$ and $\text{Re } z_i > \text{Im } z_i$,

$$-2\pi i \sum_i \text{Res}_{t=z_i} t^{\lambda-1} \exp(-t) \mathcal{P}_M(F t),$$

is added to the principal value (P.V.) of the integral (8.11) carried out in the range $t \in (0, \infty)$. We have,

$$\begin{aligned}
\mathcal{T}E_M(F) &= (\text{P.V.}) \int_0^\infty dt t^{\lambda-1} \exp(-t) \mathcal{P}_M(F t) \\
&\quad - 2\pi i \sum_i \text{Res}_{t=z_i} t^{\lambda-1} \exp(-t) \mathcal{P}_M(F t).
\end{aligned} \tag{8.12}$$

The principal-value prescription [first term in Eq. (8.12)] for the evaluation of the Laplace–Borel integral has been recommended in [295, 296]. This prescription leads to a real (rather than complex) result for the energy shift and cannot account for the width of the quasistationary state. The additional pole contributions [second term in Eq. (8.12)] are responsible for complex-valued (imaginary) corrections which lead, in particular, to the decay width.

By contour integration (Cauchy Theorem) and Jordan's Lemma, one can show that the result obtained along C_{+1} is equivalent to an integration along the straight line with $\arg z = \pi/4$,

$$\mathcal{T}E_M(F) = c^\lambda \int_0^\infty dt t^{\lambda-1} \exp(-ct) \mathcal{P}_M(F ct) \quad (8.13)$$

where $c = \exp(i\pi/4)$. This contour has been used in [157] (see also p. 815 in [297]). The exponential factor $\exp(-ct)$ and the asymptotic behavior of the Padé approximant $\mathcal{P}_M(F ct)$ as $t \rightarrow \infty$ together ensure that the integrand falls off sufficiently rapidly so that the Cauchy Theorem and Jordan's Lemma can be applied to show the equivalence of the representations (8.12) and (8.13).

The representation (8.13) illustrates the fact that the integration in the complex plane along C_{+1} analytically continues the resummed result in those cases where the evaluation of the standard Laplace–Borel integral is not feasible due to poles on the real axis. The representations (8.11) and (8.12) serve to clarify the rôle of the additional terms which have to be added to the result obtained by the principal-value prescription in order to obtain the full physical result, including the nonperturbative, nonanalytic contributions. Note that, as stressed in [25], the pole contributions in general do not only modify the imaginary, but also the real part of the resummed value for the perturbation series.

Formally, the limit of the sequence of the $\mathcal{T}E_M(F)$ as $M \rightarrow \infty$, provided it exists, yields the nonperturbative result inferred from the perturbative expansion (8.1),

$$\lim_{M \rightarrow \infty} \mathcal{T}E_M(F) = E(F) \equiv E(n_1, n_2, m, F). \quad (8.14)$$

Because the contour C_{+1} shown in Fig. 8.1 extends into the complex plane, the transforms $\mathcal{T}E_M(F)$ acquire an imaginary part even though the perturbative coefficients in Eq. (8.1) are real.

In the context of numerical analysis, the concept of incredulity [298] may be used for the analysis of the convergence of the transforms $\mathcal{T}E_M(F)$ of increasing order M . If a certain number of subsequent transforms exhibit apparent numerical convergence within a specified relative accuracy, then the calculation of transforms is stopped, and the result of the last calculated transformation is taken as the numerical limit of the series under investigation. It has been observed in [25, 295] that for a number of physically relevant perturbation series, the apparent numerical convergence of the transforms (8.11), with increasing transformation order, leads to the physically correct results.

It is observed that the rate of convergence of the transforms (8.11) can be enhanced if instead of the unmodified Padé approximants (8.10) leading “renormalon” poles are explicit used for the construction of modified approximants. For the ground state, this entails the following replacement in Eq. (8.11):

$$\mathcal{P}_M(z) \rightarrow \mathcal{P}'_M(z),$$

where

$$\mathcal{P}'_M(z) = \frac{1}{1-z^2} \left[\left\lfloor \frac{M+4}{2} \right\rfloor \middle/ \left\lfloor \frac{M-3}{2} \right\rfloor \right]_{E'_B(\zeta)}(z), \quad (8.15)$$

where $E'_B(\zeta) = (1 - \zeta^2) E_B(\zeta)$. For the excited state with quantum numbers $n_1 = 3$, $n_2 = 0$ and $m = 1$, we replace

$$\mathcal{P}_M(z) \rightarrow \mathcal{P}''_M(z),$$

where

$$\mathcal{P}''_M(z) = \frac{1}{1-z} \left[\left\lfloor \frac{M+2}{2} \right\rfloor \middle/ \left\lfloor \frac{M-1}{2} \right\rfloor \right]_{E''_B}(z), \quad (8.16)$$

where $E''_B(\zeta) = (1 - \zeta^2) E_B(\zeta)$. The resummation method by a combination of Borel and Padé techniques – current Section – will be referred to as “method I” in the sequel.

8.2.3 Doubly–Cut Borel Plane

According to Eqs. (8.2) and (8.3), the perturbative coefficient $E_{n_1 n_2 m}^{(N)}$, for large N , can be written as the sum of an alternating and of a nonalternating divergent series. In view of Eqs. (8.4) and (8.7), we conclude that the series defined in Eq. (8.9),

$$E_B(z) = \sum_{N=0}^{\infty} \frac{E_{n_1 n_2 m}^{(N)}}{\Gamma(N + \lambda)} z^N,$$

has a radius of convergence

$$s = \frac{2}{3n^3} \quad (8.17)$$

about the origin, where n is the principal quantum number [see Eq. (8.5)]. Therefore, the function

$$\mathcal{E}_B(w) = \sum_{N=0}^{\infty} \frac{E_{n_1 n_2 m}^{(N)} s^N}{\Gamma(N + \lambda)} w^N, \quad (8.18)$$

has a unit radius of convergence about the origin. It is not *a priori* obvious if the points $w = -1$ and $w = +1$ represent isolated singularities or branch points. The asymptotic properties (8.2) and (8.3) together with Eq. (8.6) suggest that the points $w = -1$ and $w = +1$ do not constitute poles of finite order. We observe that the leading factorial growth of the perturbative coefficients in large perturbation order N is divided out in the Borel transform (8.18), which is a sum over N . The perturbative coefficient $E_{n_1 n_2 m}^{(N)}$ can be written as an asymptotic series over k [see Eq. (8.3)]. We interchange the order of the summations over N and k , we use Eq. (8.6) and take advantage of the identity

$$\sum_{N=0}^{\infty} \frac{w^N}{N^k} = \text{Li}_k(w). \quad (8.19)$$

The Borel transform $\mathcal{E}_B(w)$ can then be written as a sum over terms of the form $T_k(w)$ where for $k \rightarrow \infty$,

$$T_k(w) \sim C(n_i, n_j, m) a_k^{n_i n_j m} \text{Li}_k(w). \quad (8.20)$$

The coefficient $C(n_i, n_j, m)$ is given by

$$C(n_i, n_j, m) = - [2\pi n^3 n_j! (n_j + m)!]^{-1} \exp \{3(n_i - n_j)\} 6^{2n_j + m + 1}. \quad (8.21)$$

These considerations suggest that the points $w = -1$ and $w = +1$ represent essential singularities (in this case, branch points) of the Borel transform $\mathcal{E}_B(w)$ defined in Eq. (8.18). For the analytic continuation of $\mathcal{E}_B(w)$ by conformal mapping, we write w as

$$w = \frac{2y}{1 + y^2} \quad (8.22)$$

(this conformal mapping preserves the origin of the complex plane). Here, we refer to w as the Borel variable, and we call y the conformal variable. We then express the M th partial sum of (8.18) as

$$\begin{aligned} \mathcal{E}_B^M(w) &= \sum_{N=0}^M \frac{E_{n_1 n_2 m}^{(N)} s^N}{\Gamma(N + \lambda)} w^N \\ &= \sum_{N=0}^M C_N y^N + \mathcal{O}(y^{M+1}), \end{aligned} \quad (8.23)$$

where the coefficients C_N are uniquely determined [see, e.g., Eqs. (36) and (37) of [299]]. We define the partial sum of the Borel transform, re-expanded in terms of the conformal variable y , as

$$\mathcal{E}'_B^M(y) = \sum_{N=0}^M C_N y^N. \quad (8.24)$$

We then evaluate (lower-diagonal) Padé approximants to the function $\mathcal{E}'_B^M(y)$,

$$\mathcal{E}''_B^M(y) = \left[\llbracket M/2 \rrbracket / \llbracket (M+1)/2 \rrbracket \right]_{\mathcal{E}'_B^M}(y). \quad (8.25)$$

We define the following transforms,

$$\mathcal{T}'' E_M(F) = s^\lambda \int_{C_{+1}} dw w^{\lambda-1} \exp(-w) \mathcal{E}''_B^M(y(w)). \quad (8.26)$$

At increasing M , the limit as $M \rightarrow \infty$, provided it exists, is then again assumed to represent the complete, physically relevant solution,

$$E(F) = \lim_{M \rightarrow \infty} \mathcal{T}'' E_M(F). \quad (8.27)$$

We do not consider the question of the existence of this limit here (for an outline of questions related to these issues we refer to [300]; potential problems at excessively strong coupling are discussed in Sec. IIC of [301]).

Inverting Eq. (8.22) yields [see Eq. (8.26)]

$$y(w) = \frac{\sqrt{1+w} - \sqrt{1-w}}{\sqrt{1+w} + \sqrt{1-w}}. \quad (8.28)$$

The conformal mapping given by Eqs. (8.22) and (8.28) maps the doubly cut w -plane with cuts running from $w = 1$ to $w = \infty$ and $w = -1$ to $w = -\infty$ unto the unit circle in the complex y -plane (i.e., it is a surjective mapping). The cuts themselves are mapped to the edge of the unit circle in the y -plane.

In comparison to the investigations [299] and [300], we use here a different conformal mapping defined in Eqs. (8.22) and (8.28) which reflects the different singularity structure in the complex plane [cf. Eq. (27) in [299]]. We also mention the application of Padé approximants for the numerical improvement of the conformal mapping performed according to Eq. (8.25). In comparison to [27], where the additional Padé-improvement in the conformal variable is also used, we perform here the analytic continuation by a mapping whose structure reflects the *double* cuts suggested by the asymptotic properties of the perturbative coefficients given in Eqs. (8.2), (8.3) and (8.6) [cf. Eq. (5) in [27]].

The method introduced in this Section will be referred to as “method II”. One goal of the current investigation is to contrast and compare the two methods I and II. A comparison of different approaches to the resummation problem for series with both alternating and nonalternating divergent components appears useful, in part because the conformal mapping (without further Padé improvement) has been recommended for the resummation of quantum chromodynamic perturbation series [299, 300].

8.2.4 Numerical Calculations for the Stark Effect

In this section, the numerical results based on the resummation methods introduced in Secs. 8.2.2 and 8.2.3 are presented. Before we describe the calculation in detail, we should note that relativistic corrections to both the real and the imaginary part of the energy contribute at a relative order of $(Z\alpha)^2$ compared to the leading nonrelativistic effect which is treated here (and in the previous work on the subject, see e.g. [157, 269]). Therefore, the theoretical uncertainty due to relativistic effects can be estimated to be, at best, 1 part in 10^4 (for an outline of the relativistic and quantum electrodynamic corrections in hydrogen see [1, 2, 48, 49, 50, 51, 302]). Measurements in very high fields are difficult [287]. At the achievable field strengths to date (less than 0.001 a.u. or about 5 MV/cm), the accuracy of the theoretical prediction exceeds the experimental precision, and relativistic effects do not need to be taken into account.

The perturbative coefficients $E_{n_1 n_2 m}^{(N)}$ defined in Eq. (8.1) for the energy shift can be inferred, to arbitrarily high order, from the Eqs. (9), (13–15), (28–33), (59–67) and (73) in [253]. The atomic unit system is used in the sequel, as is customary for this type of calculation [253, 259, 262, 264]. The unit of energy is $\alpha^2 m_e c^2 = 27.211 \text{ eV}$ where α is the fine structure constant, and the unit of the electric field is the field strength felt by an electron at a distance of one Bohr radius a_{Bohr} to a nucleus of elementary charge, which is $1/(4\pi\epsilon_0) (e/a_{\text{Bohr}}^2) = 5.142 \times 10^3 \text{ MV/cm}$ (here, ϵ_0 is the permittivity of the vacuum).

We consider the resummation of the divergent perturbative expansion (8.1) for two states of atomic hydrogen. These are the ground state ($n_1 = n_2 = m = 0$) and an excited state with parabolic quantum numbers $n_1 = 3$, $n_2 = 0$, $m = 1$. We list here the first few perturbative coefficients for the states under investigation. For the ground state, we have (in atomic units),

$$E_{000}(F) = -\frac{1}{2} - \frac{9}{4} F^2 - \frac{3555}{64} F^4 - \frac{2512779}{512} F^6 - \frac{13012777803}{16384} F^8 + \dots \quad (8.29)$$

The perturbation series for the state $n_1 = 3$, $n_2 = 0$, $m = 1$ is alternating, but has a subleading nonalternating component [see Eq. (8.2)]. The first perturbative terms read

$$E_{301}(F) = -\frac{1}{50} + \frac{45}{2} F - \frac{31875}{2} F^2 + \frac{54140625}{4} F^3 - \frac{715751953125}{16} F^4 + \dots \quad (8.30)$$

Note that for $F = 0$, the unperturbed nonrelativistic energy is recovered, which is $-1/(2n^2)$ in atomic units. In contrast to the real perturbative coefficients, the energy pseudoeigenvalue (resonance) $E(n_1, n_2, m, F)$ has a real and an imaginary component,

$$E(n_1, n_2, m, F) = \text{Re } E_{n_1 n_2 m}(F) - \frac{i}{2} \Gamma_{n_1 n_2 m}(F), \quad (8.31)$$

where $\Gamma_{n_1 n_2 m}(F)$ is the autoionization width.

Using a computer algebra system [90], the first 50 nonvanishing perturbative coefficients are evaluated for the ground state, and for the state with parabolic quantum numbers $n_1 = 3$, $n_2 = 0$, $m = 1$, we evaluate the first 70 nonvanishing perturbative coefficients. The apparent convergence of the transforms defined in Eqs. (8.11) and (8.26) in higher order is examined. In the case of the Borel–Padé transforms defined in Eq. (8.11), use is made of the replacements in Eqs. (8.15) and (8.16) [“leading renormalon poles are being put in by hand”]. This procedure leads to the numerical results listed in Tables 8.1 and 8.2. The numerical error of our results is estimated on the basis of the highest and lowest value of the four highest-order transforms.

An important result of the comparison of the methods introduced in Secs. 8.2.2 and 8.2.3 is the following: Both methods appear to accomplish a resummation of the perturbation series to the physically correct result. Method I (Borel+Padé with leading renormalon poles, see Sec. 8.2.2) and method II (Borel+Padé-improved conformal mapping, see Sec. 8.2.3) appear to lead to results of comparable accuracy.

To date, a rigorous theory of the performance of the resummation methods for divergent series of the type discussed in this work (with alternating and nonalternating components) does not exist. The *logarithmic* singularities introduced by the branch points of higher-order polylogarithms [see the index k in Eq. (8.19)] are difficult to approximate with the rational functions employed in the construction of Padé approximants. A solution to the problem of approximating the logarithmic singularities, based on finite number of perturbative coefficients, would probably lead to further optimization of the rate of convergence of the transformed series. Within the current scheme of evaluation, the problematic logarithmic singularities may be responsible, at least in part, for certain numerical instabilities at higher transformation order, e.g. in the result for $\mathcal{T}''E_{70}(F = 2.1393 \times 10^{-4})$ in Eq. (8.32) below.

For the atomic state with quantum numbers $n_1 = 3$, $n_2 = 0$ and $m = 1$, the evaluation of the transforms $\mathcal{TE}_M(F)$ defined in Eq. (8.11) (method I) and of the transforms $\mathcal{T}''E_M(F)$ defined in Eq. (8.26) (method II) in transformation order $M = 67, 68, 69, 70$ for a field strength of $F = 2.1393 \times 10^{-4}$. Method I leads to the following results,

$$\begin{aligned} \mathcal{TE}_{67}(F = 2.1393 \times 10^{-4}) &= -0.015\,860\,468\,199\,2 - i\,0.529\,048 \times 10^{-6}, \\ \mathcal{TE}_{68}(F = 2.1393 \times 10^{-4}) &= -0.015\,860\,468\,200\,9 - i\,0.529\,047 \times 10^{-6}, \\ \mathcal{TE}_{69}(F = 2.1393 \times 10^{-4}) &= -0.015\,860\,468\,198\,9 - i\,0.529\,048 \times 10^{-6}, \\ \mathcal{TE}_{70}(F = 2.1393 \times 10^{-4}) &= -0.015\,860\,468\,194\,5 - i\,0.529\,015 \times 10^{-6}. \end{aligned} \quad (8.32)$$

Method II yields the following data,

$$\begin{aligned} \mathcal{T}''E_{67}(F = 2.1393 \times 10^{-4}) &= -0.015\,860\,468\,200\,4 - i\,0.529\,047 \times 10^{-6}, \\ \mathcal{T}''E_{68}(F = 2.1393 \times 10^{-4}) &= -0.015\,860\,468\,200\,3 - i\,0.529\,047 \times 10^{-6}, \\ \mathcal{T}''E_{69}(F = 2.1393 \times 10^{-4}) &= -0.015\,860\,468\,200\,4 - i\,0.529\,047 \times 10^{-6}, \\ \mathcal{T}''E_{70}(F = 2.1393 \times 10^{-4}) &= -0.015\,860\,468\,203\,3 - i\,0.529\,046 \times 10^{-6}. \end{aligned} \quad (8.33)$$

Numerical results obtained by resummation are presented in Tables 8.1 and 8.2 for a variety of field strengths and for the two atomic states under investigation here.

| F (a.u.) | $\text{Re } E_{000}(F)$ | $\Gamma_{000}(F)$ |
|------------|------------------------------------|-------------------------------------|
| 0.04 | $-0.503\,771\,591\,013\,654\,2(5)$ | $3.892\,699\,990(1) \times 10^{-6}$ |
| 0.06 | $-0.509\,203\,451\,088(2)$ | $5.150\,775\,0(5) \times 10^{-4}$ |
| 0.08 | $-0.517\,560\,50(5)$ | $4.539\,63(5) \times 10^{-3}$ |
| 0.10 | $-0.527\,419\,3(5)$ | $1.453\,8(5) \times 10^{-2}$ |
| 0.12 | $-0.537\,334(5)$ | $2.992\,7(5) \times 10^{-2}$ |
| 0.16 | $-0.555\,24(5)$ | $7.131(5) \times 10^{-2}$ |
| 0.20 | $-0.570\,3(5)$ | $1.212(5) \times 10^{-1}$ |
| 0.24 | $-0.582\,6(1)$ | $1.767(5) \times 10^{-1}$ |
| 0.28 | $-0.591\,7(5)$ | $2.32(3) \times 10^{-1}$ |
| 0.32 | $-0.600(5)$ | $2.92(3) \times 10^{-1}$ |
| 0.36 | $-0.604(5)$ | $3.46(3) \times 10^{-1}$ |
| 0.40 | $-0.608(5)$ | $4.00(5) \times 10^{-1}$ |

Table 8.1: Real and imaginary part of the energy pseudoeigenvalue $E_{000}(F)$ for the ground state of atomic hydrogen (parabolic quantum numbers $n_1 = 0, n_2 = 0, m = 0$).

| F (a.u.) | $\text{Re } E_{301}(F)$ | $\Gamma_{301}(F)$ |
|-------------------------|------------------------------------|--------------------------------|
| 1.5560×10^{-4} | $-0.016\,855\,237\,140\,761\,7(5)$ | $0.421\,683(5) \times 10^{-9}$ |
| 1.9448×10^{-4} | $-0.016\,179\,388\,257\,0(5)$ | $0.143\,773(5) \times 10^{-6}$ |
| 2.1393×10^{-4} | $-0.015\,860\,468\,20(1)$ | $0.105\,09(5) \times 10^{-5}$ |
| 2.5282×10^{-4} | $-0.015\,269\,293(1)$ | $0.176\,39(5) \times 10^{-4}$ |
| 2.9172×10^{-4} | $-0.014\,742\,60(3)$ | $0.999\,96(9) \times 10^{-4}$ |
| 3.3061×10^{-4} | $-0.014\,260\,2(3)$ | $0.295\,4(2) \times 10^{-3}$ |

Table 8.2: Real part and imaginary part of the energy pseudoeigenvalue $E_{301}(F)$ for the excited state with parabolic quantum numbers $n_1 = 3, n_2 = 0, m = 1$. The field strength F is given in atomic units.

| n | s_n | $[\nu - \llbracket \nu/2 \rrbracket / \llbracket \nu/2 \rrbracket]$ | $\delta_n^{(0)}(1, s_0)$ |
|-------|-------------------------------|---|--------------------------|
| 1 | -2 | -0.455 882 352 941 | <u>0.837 837 837 838</u> |
| 2 | 50.5 | 0.011 324 180 660 | <u>0.652 631 578 947</u> |
| 3 | -1 682 | 0.225 195 251 591 | <u>0.613 275 696 169</u> |
| 4 | 82 777.375 | 343 344 968 231 | <u>0.609 400 007 774</u> |
| 5 | $-5.373\,298 \times 10^6$ | 0.416 165 471 150 | <u>0.612 698 290 875</u> |
| ... | ... | ... | ... |
| 60 | $5.492\,129 \times 10^{151}$ | <u>0.619 816 798 266</u> | <u>0.620 282 559 592</u> |
| 61 | $-5.272\,807 \times 10^{154}$ | 0.619 846 730 800 | <u>0.620 282 559 593</u> |
| 62 | $5.146\,602 \times 10^{157}$ | <u>0.619 874 504 158</u> | <u>0.620 282 559 594</u> |
| 63 | $-5.105\,759 \times 10^{160}$ | <u>0.619 900 292 634</u> | <u>0.620 282 559 594</u> |
| 64 | $5.146\,926 \times 10^{163}$ | <u>0.619 924 254 847</u> | <u>0.620 282 559 595</u> |
| 65 | $-5.270\,772 \times 10^{166}$ | <u>0.619 946 535 301</u> | <u>0.620 282 559 595</u> |
| 66 | $5.481\,925 \times 10^{169}$ | <u>0.619 967 265 778</u> | <u>0.620 282 559 595</u> |
| 67 | $-5.789\,242 \times 10^{172}$ | <u>0.619 986 566 577</u> | <u>0.620 282 559 595</u> |
| 68 | $6.206\,411 \times 10^{175}$ | <u>0.620 004 547 622</u> | <u>0.620 282 559 595</u> |
| 69 | $-6.752\,937 \times 10^{178}$ | <u>0.620 004 547 622</u> | <u>0.620 282 559 595</u> |
| 70 | $7.455\,631 \times 10^{181}$ | <u>0.619 986 566 577</u> | <u>0.620 282 559 595</u> |
| exact | 0.620 282 559 595 | 0.620 282 559 595 | 0.620 282 559 595 |

Table 8.3: Evaluation of the perturbation series for $Z(\Phi)$ [zero-dimensional ϕ^4 -theory, see Eq. (8.34)] for $g = 1$. The s_n are the partial sums of the divergent asymptotic series (8.35), the Padé approximants $[\nu - \llbracket \nu/2 \rrbracket / \llbracket \nu/2 \rrbracket]$ are calculated according to Eq. (7.13), and the delta transforms are evaluated according to Eq. (7.31).

8.3 Further Applications of Resummation Methods

8.3.1 Zero-Dimensional Theories with Degenerate Minima

We consider the generating functional in a zero-dimensional theory (in this case, the usual path integral reduces to an ordinary integral). First, we briefly consider the Φ^4 -theory in zero dimensions [see Eq. (9-177) ff. in [34]]; the generating functional reads

$$Z(\Phi) = \int_{-\infty}^{\infty} \frac{d\Phi}{\sqrt{2\pi}} \exp \left[-\frac{1}{2} \Phi^2 - g \Phi^4 \right]. \quad (8.34)$$

The strictly alternating divergent asymptotic expansion in powers of g for $g \rightarrow 0$ reads,

$$Z(\Phi) \sim \sum_{N=0}^{\infty} \frac{4^N \Gamma(2N + 1/2)}{\sqrt{\pi} \Gamma(N + 1)} (-g)^N. \quad (8.35)$$

On using the known asymptotics valid for $N \rightarrow \infty$, which in this case yield the “large-order” asymptotics of the perturbative coefficients,

$$\frac{\Gamma(2N + 1/2)}{\Gamma(N + 1)} \sim \frac{4^N}{\sqrt{2\pi}} \Gamma(N) \left[1 + \mathcal{O} \left(\frac{1}{N} \right) \right] \quad (8.36)$$

it is easy to explicitly establish the factorial divergence of the series (see also p. 888 of [297]). The generating functional in zero dimensions has been proposed as a paradigmatic example for the divergence of perturbation theory in higher order. It can be resummed easily to the nonperturbative result; in particular it is manifestly Borel summable, and no singularities are present on the positive real axis. Specifically, in Table 8.2.4, we consider the resummation of the series (8.35) by Padé approximants (Sec. 7.1.4) and delta transformations (Sec. 7.1.5). The rapid rate of convergence due to the delta transformations in comparison to the Padé approximants is obvious; this finding is consistent with the results of Ref. [24].

Complications are introduced by degenerate minima. As a second example, we consider the modified generating functional [compare with Eq. (2.6) on p. 15 of [250] and with Eq. (40.1) on p. 854 of [297]]:

$$\begin{aligned} Z'(\Phi) &= \int_{-\infty}^{\infty} \frac{d\Phi}{\sqrt{2\pi}} \exp \left[-\frac{1}{2} \Phi^2 (1 - \sqrt{g} \Phi)^2 \right] \\ &= \int_{-\infty}^{\infty} \frac{d\Phi}{\sqrt{2\pi}} \exp \left[-\frac{1}{2} \Phi^2 + \sqrt{g} \Phi^3 - \frac{1}{2} g \Phi^4 \right]. \end{aligned} \quad (8.37)$$

The expansion of the exponential in powers of the coupling g leads to a divergent asymptotic series,

$$\begin{aligned} Z'(\Phi) &= \sum_{N=0}^{\infty} \frac{1}{N!} \int_{-\infty}^{\infty} \frac{d\Phi}{\sqrt{2\pi}} e^{-1/2 \Phi^2} \left(\sqrt{g} \Phi^3 - \frac{1}{2} g \Phi^4 \right)^N \\ &= \sum_{N=0}^{\infty} \int_{-\infty}^{\infty} \frac{d\Phi}{\sqrt{2\pi}} e^{-1/2 \Phi^2} \sum_{j=0}^N \frac{(-1)^j}{\Gamma(2N-j+1)} \\ &\quad \times \binom{2N-j}{j} (\sqrt{g} \phi^3)^{2(N-j)} \left(\frac{g \phi^4}{2} \right)^j \\ &= \sum_{N=0}^{\infty} 2\sqrt{\pi} \frac{(-1)^N C_{2N}^{N+1/2}(1)}{\Gamma(N-1/2)} g^N \\ &= \sum_{N=0}^{\infty} \frac{8^N \Gamma(2N+1/2)}{\sqrt{\pi} \Gamma(N+1)} g^N, \end{aligned} \quad (8.38)$$

where $C_M^N(x)$ denotes a Gegenbauer (ultraspherical) polynomial. Note that terms of half-integer power of g entail an odd power of the field and vanish after integration. The first few terms of the asymptotic expansion read,

$$\begin{aligned} Z'(\Phi) &= 1 + 6g + 210g^2 + 13860g^3 \\ &\quad + 1351350g^4 + 174594420g^5 \\ &\quad + 28109701620g^6 + 5421156741000g^7 \\ &\quad + 1218404977539750g^8 + \mathcal{O}(g^9). \end{aligned} \quad (8.39)$$

For the perturbative coefficients

$$C_N = \frac{8^N \Gamma(2N + 1/2)}{\sqrt{\pi} \Gamma(N + 1)}, \quad (8.40)$$

we establish the following asymptotics,

$$C_N \sim \frac{1}{\pi\sqrt{2}} N^{-1} 32^N \Gamma(N + 1). \quad (8.41)$$

Due to the nonalternating character of the expansion (8.38), it is not Borel summable in the ordinary sense. Rather, it is Borel summable in the distributional sense [158, 159]. Here, we present numerical evidence supporting the summability of the divergent expansion (8.39) based on a finite number of perturbative coefficients. The final integration is carried out along the contour C_0 introduced in [25] [see also Eq. (8.44) below]. The same contour has also been used for the resummation of divergent perturbation series describing renormalization group (anomalous dimension) γ functions [27]. As explained in [25], the integration along C_0 , which is based on the mean value of the results obtained above and below the real axis, leads to a *real* final result if all perturbative coefficients are real.

| M | partial sum | $\mathcal{T}Z_M(g = 0.01)$ |
|-------|-------------------|----------------------------|
| 2 | 1.081 000 | 1.102 326 |
| 3 | 1.094 860 | 1.096 141 |
| 4 | 1.108 373 | 1.089 875 |
| 5 | 1.125 832 | 1.090 695 |
| 6 | 1.153 942 | 1.092 000 |
| 7 | 1.208 154 | 1.091 596 |
| 8 | 1.329 994 | 1.091 389 |
| 9 | 1.642 718 | 1.091 553 |
| 10 | 2.545 239 | 1.091 545 |
| 11 | 5.438 230 | 1.091 503 |
| 12 | 1.5×10^1 | 1.091 525 |
| 13 | 5.5×10^1 | 1.091 527 |
| 14 | 2.2×10^2 | 1.091 519 |
| 15 | 9.5×10^2 | 1.091 523 |
| 16 | 4.5×10^3 | 1.091 523 |
| 17 | 2.2×10^4 | 1.091 521 |
| 18 | 1.2×10^5 | 1.091 522 |
| 19 | 6.9×10^5 | 1.091 522 |
| 20 | 4.1×10^6 | 1.091 522 |
| exact | 1.091 522 | 1.091 522 |

Table 8.4: Resummation of the asymptotic series for the generating functional of a zero-dimensional theory with degenerate minima given in Eqs. (8.38) and (8.39). We have $g = 0.01$. Results in the third column are obtained by the method indicated in Eq. (8.44) along the integration contour C_0 (see [25]). The partial sums in the second column are obtained from the asymptotic series (8.38).

In particular, the resummation of the divergent expansion (8.39) is accomplished as follows. We first define the Borel transform of the generating functional by [see Eq. (4) in [26] and the discussion after

Eq. (8.9)]

$$\begin{aligned} Z'_B(z) &\equiv \mathcal{B}^{(1,1)}[Z'; z] \\ &= \sum_{N=0}^{\infty} \frac{C_N}{\Gamma(N+1)} z^N. \end{aligned} \quad (8.42)$$

Padé approximants to this Borel transform are evaluated,

$$\mathcal{P}'_M(z) = \left[\llbracket M/2 \rrbracket / \llbracket (M+1)/2 \rrbracket \right]_{Z'_B} (z), \quad (8.43)$$

where $\llbracket x \rrbracket$ denotes the largest positive integer smaller than x . We then evaluate the (modified) Borel integral along the integration contour C_0 introduced in [25]; specifically we define the transform $\mathcal{TZ}_M(g)$

$$\mathcal{TZ}_M(g) = \int_{C_0} dt \exp(-t) \mathcal{P}'_M(gt). \quad (8.44)$$

In this case, poles above and below the real axis must be considered, and the final result involves no imaginary part. The particular case of $g = 0.01$ is considered. Values for the partial sums of the perturbation series (8.39) and the transforms defined in Eq. (8.44) are shown in Tab. 8.4. The transforms exhibit apparent convergence to 6 decimal places in 20th order, whereas the partial sums of the perturbation series diverge. Between the second and forth term of the perturbation series, (the forth term constitutes the minimal term), the partial sums provide approximations to the exact result. It might seem surprising that the minimal term in the perturbative expansion is reached already in forth order, although the coupling assumes the small value $g = 0.01$. This behavior immediately follows from the large geometric factor in Eq. (8.41) which leads to a “resultative coupling strength parameter” of $g_{\text{res}} = 0.32$. “Nonperturbative effects” of the order of $\exp(-1/g_{\text{res}})$ provide a fundamental limit to the accuracy obtainable by optimal truncation of the perturbation series; this is consistent with the numerical data in Table 8.4.

We have also investigated the resummation of the divergent series (8.39) via a combination of a conformal mapping and Padé approximants in the conformal variable. The situation is analogous to the Stark effect: Results are consistent than those presented in Table 8.4 obtained by the “pure” Borel–Padé and in this case slightly more accurate. The radius of convergence of the Borel transform $Z'_B(z)$ defined in Eq. (8.42) is $s = 1/32$ [cf. Eq. (8.17) for the Stark effect], and the appropriate conformal mapping in this case reads

$$w = \frac{4y}{(1+y)^2} \quad (8.45)$$

[cf. Eq. (8.22)]. The inverse reads

$$y(w) = \frac{1 - \sqrt{1-w}}{1 + \sqrt{1-w}}$$

[cf. Eq. (8.28)]. The conformal mapping (8.45) maps the complex w -plane with a cut along $(1, \infty)$ unto the unit circle in the complex y -plane. While the zero-dimensional model example given in Eq. (8.37) does not exhibit all problematic features of degenerate anharmonic double-well oscillators, certain analogies can be established; these comprise in particular the need to evaluate the mean value of Borel transforms above and below the real axis (see also [27]).

8.3.2 The Effective Action as a Divergent Series

Maxwell’s equations receive corrections from virtual excitations of the charged quantum fields (notably electrons and positrons). This leads to interesting effects [303, 304]: light-by-light scattering, photon splitting, modification of the speed of light in the presence of strong electromagnetic fields, and – last, but not least – pair production.

When the heavy degrees of freedom are integrated out (in this case, the “heavy particles” are the electrons and positrons), an effective theory results. The corrections can be described by an effective interaction, the so-called quantum electrodynamic (QED) effective Lagrangian. The dominant effect for electromagnetic

fields that vary slowly with respect to the Compton wavelength (frequencies $\omega \ll 2m c^2/\hbar$) is described by the one-loop quantum electrodynamic effective (so-called “Heisenberg–Euler”) Lagrangian which is known to all orders in the electromagnetic field [304, 305, 306, 307, 308, 309].

The Heisenberg–Euler Lagrangian $\Delta\mathcal{L}$, which constitutes a quantum correction to the Maxwell Lagrangian, is usually expressed as a one-dimensional proper-time integral [see e.g. Eq. (3.43) in [304],

$$\Delta\mathcal{L} = -\frac{e^2}{8\pi^2} \lim_{\epsilon, \eta \rightarrow 0^+} \int_{i\eta}^{\infty+i\eta} \frac{ds}{s} e^{-(m^2-i\epsilon)s} \left[ab \coth(eas) \cot(ebs) - \frac{a^2-b^2}{3} - \frac{1}{(es)^2} \right]. \quad (8.46)$$

To clarify the notation, we introduce the well-known Lorentz invariants \mathcal{F} and \mathcal{G} which are given by

$$\mathcal{F} = \frac{1}{4} F_{\mu\nu} F^{\mu\nu} = \frac{1}{2} (\mathbf{B}^2 - \mathbf{E}^2) = \frac{1}{2} (a^2 - b^2), \quad (8.47)$$

$$\mathcal{G} = \frac{1}{4} F_{\mu\nu} (*F)^{\mu\nu} = -\mathbf{E} \cdot \mathbf{B} = \pm ab, \quad (8.48)$$

where \mathbf{E} and \mathbf{B} are the electric and magnetic field strengths, $F_{\mu\nu}$ is the field strength tensor, and $(*F)^{\mu\nu}$ denotes the dual field strength tensor $(*F)^{\mu\nu} = (1/2) \epsilon^{\mu\nu\rho\sigma} F_{\rho\sigma}$. By a and b we denote the *secular invariants*,

$$\begin{aligned} a &= \sqrt{\sqrt{\mathcal{F}^2 + \mathcal{G}^2} + \mathcal{F}}, \\ b &= \sqrt{\sqrt{\mathcal{F}^2 + \mathcal{G}^2} - \mathcal{F}}. \end{aligned} \quad (8.49)$$

These Lorentz invariants are referred to as secular invariants because they emerge naturally as eigenvalues of the field strength tensor; these eigenvalues are conserved under proper Lorentz transformations of the field strength tensor. There are connections between the different representations [304]: If the relativistic invariant \mathcal{G} is positive, then it is possible to transform to a Lorentz frame in which \mathbf{E} and \mathbf{B} are *antiparallel*. In the case $\mathcal{G} < 0$, it is possible to choose a Lorentz frame in which \mathbf{E} and \mathbf{B} are *parallel*. Irrespective of the sign of \mathcal{G} we have in the specified frame

$$a = |\mathbf{B}| \quad \text{and} \quad b = |\mathbf{E}| \quad \text{if and only if} \quad \mathbf{B} \text{ is (anti-)parallel to } \mathbf{E}. \quad (8.50)$$

In any case, because a and b are positive definite, we have

$$ab = |\mathbf{E} \cdot \mathbf{B}| > 0 \quad \text{for any Lorentz frame and } \mathcal{G} \neq 0, \quad (8.51)$$

which clarifies the sign ambiguity in (8.48). We give in (8.47) and (8.48) seemingly redundant definitions, but it will soon become apparent that each of the alternative “points of view” has its applications. The Maxwell Lagrangian is given by

$$\mathcal{L}_{\text{cl}} = -\mathcal{F} = -\frac{1}{4} F_{\mu\nu} F^{\mu\nu} = \frac{1}{2} (\mathbf{E}^2 - \mathbf{B}^2) = \frac{1}{2} (b^2 - a^2). \quad (8.52)$$

As it is obvious from Eq. (8.46), the correction $\Delta\mathcal{L}$ to the Maxwell Lagrangian is conveniently written in terms of the secular invariants a and b .

It was observed as early as 1956 [310] that the quantum correction (8.46), when expressed as a perturbation series in the usual QED perturbation theory parameter $\alpha = e^2/(4\pi)$, constitutes a divergent series. This divergent character of the QED perturbative expansion is supported by Lipatov’s argument based on a saddle-point expansion of the generating functional [311, 312, 313], and explicit estimates for the large-order (factorially divergent) behaviour of the QED perturbative coefficients have been obtained in [314, 315]. Recently, the divergent character of the large-order behaviour of perturbative expansions in quantum field theory has found an exquisite confirmation in explicit 30-loop calculations of renormalization group γ functions in a six-dimensional ϕ^3 theory, and in a Yukawa theory [316, 317].

Here, we will study the divergent series generated by expanding the effective action (8.46) in powers of e^2 . We will distinguish the cases of a magnetic and an electric background fields. We start with a magnetic field of strength B in which case the effective action reads

$$S_B \equiv \Delta\mathcal{L}(E=0, B) = -\frac{e^2 B^2}{8\pi^2} \int_0^\infty \frac{ds}{s^2} \left\{ \coth s - \frac{1}{s} - \frac{s}{3} \right\} \exp\left(-\frac{m_e^2}{eB} s\right) \quad (8.53)$$

[put $a = B$, $b = 0$ in Eq. (8.46)]. The nonperturbative results in Eq. (8.53) can be expanded in powers of the effective coupling

$$g_B = \frac{e^2 B^2}{m_e^4}. \quad (8.54)$$

This results in the divergent asymptotic series

$$\begin{aligned} S_B &\sim -\frac{2e^2 B^2}{\pi^2} g_B \sum_{n=0}^{\infty} \frac{(-1)^{n+1} 4^n |\mathcal{B}_{2n+4}|}{(2n+4)(2n+3)(2n+2)} g_B^n \\ &= -\frac{2e^2 B^2}{\pi^2} g_B \left[-\frac{1}{720} + \frac{1}{1260} g_B - \frac{1}{630} g_B^2 \right. \\ &\quad \left. + \dots - 2.33 \times 10^{107} g_B^{50} + \dots \right] \end{aligned} \quad (8.55)$$

for $g_B \rightarrow 0$. Here, $|\mathcal{B}_{2n+4}|$ denotes the *modulus* of the $(2n+4)$ th Bernoulli number. The Bernoulli numbers alternate in sign,

$$\text{sign}(\mathcal{B}_{2n+4}) = (-1)^{n+1}. \quad (8.56)$$

The expansion coefficients

$$c_n = \frac{(-1)^{n+1} 4^n |\mathcal{B}_{2n+4}|}{(2n+4)(2n+3)(2n+2)} \quad (8.57)$$

obviously display an alternating sign pattern and grow factorially in absolute magnitude,

$$c_n \sim \frac{(-1)^{n+1}}{8} \frac{\Gamma(2n+2)}{\pi^{2n+4}} \left(1 + \mathcal{O}(2^{-(2n+4)}) \right) \quad (8.58)$$

for $n \rightarrow \infty$.

The series (8.55) is an alternating series. In [163, 255, 310], it was shown that the series (8.55) is Borel summable. A further expansion of the perturbative coefficients c_n for large n is carried out in [255] in order to perform the Borel summation; this analysis follows the asymptotic expansion in Eq. (8.58) above, and higher-order terms in the asymptotics of the coefficients for large n are also used. Here we consider the resummation of the divergent series (8.55) with the help of rational approximants which use as input data only a *finite* number of perturbation theory coefficients in *numerical* form. Specifically, we use Padé approximants defined in Eq. (7.12) and discussed in Sec. 7.1.4 and the nonlinear sequence transformations d and δ defined in Eqs. (7.30) and (7.31), respectively. The nonlinear transformations were discussed in Sec. 7.1.5.

The transformations are applied to the divergent perturbation series Eq. (8.55), the transforms are calculated with the help of the recurrence relations (7.27) and (7.28). The evaluations presented in Tables 8.5 and 8.6 are carried out for values $g_B = 1/10$, $g_B = 1$ and $g_B = 10$ of the expansion parameter g_B defined in Eq. (8.54). The first column in the tables contains the index n , the second column contains the partial sums of the input series and in the last three columns are the results of the Padé Approximation, the d-transformation and the delta-transformation.

The data in the tables is presented to a numerical accuracy of 10^{-9} . The convergence of the transforms is indicated by underlining those decimal places which appear to have converged to the nonperturbative result. The numerical data in the Tables 8.5 and 8.6 indicate that the most favourable numerical results are obtained with the Weniger delta-transformation. For the numerical calculations, exact rational arithmetics was used [90]. Numerical experiments for g_B larger than 1 (not shown) and data presented in [24] indicate that the Weniger delta transformation appears to resum the divergent series (8.55) at least up to $g_B = 200$, and to arbitrary precision. The other resummation prescriptions – Padé, and the Levin d-transformation – *fail* in this domain of strong coupling.

In the case of a background electric field, Eq. (8.46) yields the following expression

$$S_E \equiv \Delta \mathcal{L}(E, B = 0) = \frac{e^2 E^2}{8\pi^2} \int_0^\infty \frac{ds}{s^2} \left\{ \coth s - \frac{1}{s} - \frac{s}{3} \right\} \exp \left(-i \frac{(m_e - i\epsilon)^2}{e E} s \right). \quad (8.59)$$

| n | s_n | $[\nu - \llbracket \nu/2 \rrbracket / \llbracket \nu/2 \rrbracket]$ | $d_n^{(0)}(1, s_0)$ | $\delta_n^{(0)}(1, s_0)$ |
|-------|-----------------------|---|-----------------------|--------------------------|
| 1 | <u>-0.209</u> 523 809 | <u>-0.209</u> 523 809 | <u>-0.211</u> 640 211 | <u>-0.211</u> 640 211 |
| 2 | <u>-0.212</u> 063 492 | <u>-0.211</u> 640 211 | <u>-0.211</u> 342 466 | <u>-0.211</u> 342 466 |
| 3 | <u>-0.210</u> 986 050 | <u>-0.211</u> 306 990 | <u>-0.211</u> 403 608 | <u>-0.211</u> 400 530 |
| 4 | <u>-0.211</u> 771 470 | <u>-0.211</u> 415 931 | <u>-0.211</u> 392 250 | <u>-0.211</u> 393 488 |
| 5 | <u>-0.210</u> 896 256 | <u>-0.211</u> 382 773 | <u>-0.211</u> 393 652 | <u>-0.211</u> 393 513 |
| 6 | <u>-0.212</u> 279 564 | <u>-0.211</u> 397 516 | <u>-0.211</u> 393 776 | <u>-0.211</u> 393 695 |
| 7 | <u>-0.209</u> 336 271 | <u>-0.211</u> 391 398 | <u>-0.211</u> 393 631 | <u>-0.211</u> 393 675 |
| 8 | <u>-0.217</u> 447 776 | <u>-0.211</u> 394 638 | <u>-0.211</u> 393 677 | <u>-0.211</u> 393 670 |
| 9 | <u>-0.189</u> 339 933 | <u>-0.211</u> 393 026 | <u>-0.211</u> 393 673 | <u>-0.211</u> 393 671 |
| 10 | <u>-0.308</u> 952 549 | <u>-0.211</u> 393 982 | <u>-0.211</u> 393 670 | <u>-0.211</u> 393 671 |
| exact | -0.211 393 671 | -0.211 393 671 | -0.211 393 671 | -0.211 393 671 |

Table 8.5: Evaluation of the perturbation series for S_B given in Eq. (8.53) for $g_B = 1/10$. Results are given in terms of the scaled function \bar{S}_B given by $S_B = 10^{-2} \times (-e^2 B^2)/(8\pi^2) \times \bar{S}_B$. The performance of three different resummation methods is compared: in the second column, Padé approximants are used. In the third column, we list results obtained using the Levin transformation defined in Eq. (7.30), whereas in the last column, the delta transformation (7.31) is employed. The apparent convergence is indicated by underlining the decimal figures that have stabilized in increasing transformation order.

In analogy to the expansion parameter for the magnetic case from Eq. (8.54), we can define the effective coupling as

$$g_E = \frac{e^2 E^2}{m_e^4}. \quad (8.60)$$

The expansion of the effective action in powers of g_E leads to the formal power series

$$\begin{aligned}
S_E &\sim -\frac{2e^2 E^2}{\pi^2} g_E \sum_{n=0}^{\infty} \frac{4^n |\mathcal{B}_{2n+4}|}{(2n+4)(2n+3)(2n+2)} g_E^n \\
&= -\frac{2e^2 E^2}{\pi^2} g_E \left[\frac{1}{720} + \frac{1}{1260} g_E + \frac{1}{630} g_E^2 \right. \\
&\quad \left. + \dots + 2.33 \times 10^{107} g_E^{50} + \dots \right]. \quad (8.61)
\end{aligned}$$

The perturbation series is nonalternating. Because the remainder estimate $\omega_n = a_{n+1}$ [see Eq. (7.29)] is in general not valid for nonalternating series, we cannot assume that any of the previously discussed resummation methods (Padé, or the delta or d-transformation) are able to resum the perturbation series Eq. (8.61). This is confirmed by the explicit numerical data presented in Table 8.3.2.

There exists a “nonperturbative” imaginary part for the uniform background electric field which is *a priori* not contained in the perturbation series whose coefficients are all real and positive [see Eq. (8.61)]. The imaginary part can be directly inferred from Eq. (8.59) by residue calculus, the result is [34, 255]

$$\text{Im } S_E = \frac{e^2 E^2}{8\pi^3} \sum_{n=1}^{\infty} \frac{1}{n^2} \exp\left(-\frac{n\pi m_e^2}{eE}\right). \quad (8.62)$$

The characteristic factor

$$\exp\left(-\frac{1}{g_E}\right) \quad (8.63)$$

| n | s_n | $[\nu - \llbracket \nu/2 \rrbracket / \llbracket \nu/2 \rrbracket]$ | $d_n^{(0)}(1, s_0)$ | $\delta_n^{(0)}(1, s_0)$ |
|-------|------------------------------|---|-----------------------|--------------------------|
| 1 | <u>-0.095 238 095</u> | <u>-0.095 238 095</u> | <u>-0.179 894 179</u> | <u>-0.179 894 179</u> |
| 2 | <u>-0.349 206 349</u> | <u>-0.179 894 179</u> | <u>-0.159 879 642</u> | <u>-0.159 879 642</u> |
| 3 | <u>-0.728 234 728</u> | <u>-0.143 682 906</u> | <u>-0.164 402 059</u> | <u>-0.163 671 330</u> |
| 4 | <u>-7.125 955 525</u> | <u>-0.171 471 152</u> | <u>-0.165 580 804</u> | <u>-0.164 993 772</u> |
| 5 | 80.395 411 995 | <u>-0.154 744 471</u> | <u>-0.164 224 936</u> | <u>-0.164 738 292</u> |
| ... | ... | ... | ... | ... |
| 15 | $2.034\,128 \times 10^{18}$ | <u>-0.163 152 747</u> | <u>-0.164 599 332</u> | <u>-0.164 598 912</u> |
| 16 | $-2.179\,139 \times 10^{20}$ | <u>-0.165 362 567</u> | <u>-0.164 598 614</u> | <u>-0.164 598 919</u> |
| 17 | $2.630\,171 \times 10^{22}$ | <u>-0.163 457 086</u> | <u>-0.164 599 763</u> | <u>-0.164 598 928</u> |
| 18 | $-3.552\,782 \times 10^{24}$ | <u>-0.165 217 014</u> | <u>-0.164 599 218</u> | <u>-0.164 598 935</u> |
| 19 | $5.338\,753 \times 10^{26}$ | <u>-0.163 675 239</u> | <u>-0.164 599 045</u> | <u>-0.164 598 938</u> |
| 20 | $-8.876\,881 \times 10^{28}$ | <u>-0.165 109 383</u> | <u>-0.164 598 656</u> | <u>-0.164 598 939</u> |
| 21 | $1.625\,237 \times 10^{31}$ | <u>-0.163 836 808</u> | <u>-0.164 598 854</u> | <u>-0.164 598 939</u> |
| 22 | $-3.262\,042 \times 10^{33}$ | <u>-0.165 027 568</u> | <u>-0.164 599 254</u> | <u>-0.164 598 939</u> |
| 23 | $7.148\,693 \times 10^{35}$ | <u>-0.163 959 721</u> | <u>-0.164 599 016</u> | <u>-0.164 598 939</u> |
| 24 | $-1.704\,211 \times 10^{38}$ | <u>-0.164 963 933</u> | <u>-0.164 598 550</u> | <u>-0.164 598 939</u> |
| 25 | $4.404\,583 \times 10^{40}$ | <u>-0.164 055 347</u> | <u>-0.164 598 862</u> | <u>-0.164 598 939</u> |
| exact | -0.164 598 939 | -0.164 598 939 | -0.164 598 939 | -0.164 598 939 |

Table 8.6: Evaluation of the perturbation series for S_B given in Eq. (8.53) for $g_B = 1$. Results are given in terms of the scaled function \bar{S}_B given by $S_B = 10^{-1} \times (-e^2 B^2)/(8\pi^2) \times \bar{S}_B$. The apparent convergence is indicated by underlining the decimal figures that have stabilized in increasing transformation order.

is nonperturbative since Eq. (8.62) has an essential singularity in the limit $g_E \rightarrow 0$, and it is reminiscent of characteristic expressions occurring in the description of quantum mechanical tunneling processes (see p. 195 in [34]). In our context, the imaginary part (8.62) describes the pair production in an electric background field. As is well known, the vacuum in very strong electric fields becomes unstable with regard to particle-antiparticle pair production (see also the elucidating discussion in [303]).

Spontaneous pair production becomes considerable only in strong external electric fields. Ordinary field strengths are much smaller than the critical field E_{crit} for which

$$\frac{e E_{\text{crit}}}{m_e^2} = 1. \quad (8.64)$$

The critical field strength E_{crit} can be written (including \hbar and c) as the ratio of the rest mass of the electron to the characteristic length scale which is set by the Compton wavelength of the electron:

$$E_{\text{crit}} = \frac{m_e c^2}{e\hbar/m_e c} = \frac{m_e^2 c^3}{e\hbar} \sim 10^{16} \frac{\text{V}}{\text{cm}}. \quad (8.65)$$

This critical field strengths are comparable to those felt by an electron in a hydrogenlike atom whose nucleus has the charge $Z \approx 137$.

Nonalternating divergent perturbation series require considerable effort in their resummation. It has been shown in [25] that a generalized Borel-Padé method can be used to reconstruct the imaginary part of the full nonperturbative result. This method depends on the special integration contours in the complex plane, introduced in Secs. 8.2.2 and 8.2.3. In Table 8.8, we present results for the generalized Borel transforms constructed according to Eqs. (1) – (6) of [25].

| n | s_n | $[\nu - \llbracket \nu/2 \rrbracket / \llbracket \nu/2 \rrbracket]$ | $d_n^{(0)}(1, s_0)$ | $\delta_n^{(0)}(1, s_0)$ |
|-----|---------------------------------|---|---------------------|--------------------------|
| 1 | −0.349 206 349 | −0.349 206 349 | −0.095 238 095 | −0.095 238 095 |
| 2 | −0.603 174 603 | −0.095 238 095 | −0.406 735 069 | −0.406 735 069 |
| 3 | −1.680 615 680 | −0.270 879 691 | −0.187 029 818 | −0.221 607 947 |
| 4 | −9.534 805 934 | 0.130 519 638 | −6.833 824 219 | −0.003 699 447 |
| 5 | −97.056 173 456 | −0.227 975 543 | −0.305 826 743 | −0.718 038 750 |
| ... | ... | ... | ... | ... |
| 20 | −8.984 372 007 $\times 10^{28}$ | −0.345 709 493 | −0.214 873 519 | −0.213 414 911 |
| 21 | −1.643 099 018 $\times 10^{31}$ | 0.132 431 882 | −0.045 964 685 | −0.148 354 420 |
| 22 | −3.294 725 508 $\times 10^{33}$ | −0.328 142 128 | −1.274 287 822 | −0.037 304 526 |
| 23 | −7.214 261 175 $\times 10^{35}$ | 0.248 593 926 | −0.358 736 820 | −0.367 757 660 |
| 24 | −1.718 574 682 $\times 10^{38}$ | −0.313 562 944 | −0.237 543 483 | −1.233 623 635 |
| 25 | −4.438 810 865 $\times 10^{40}$ | 0.434 092 399 | −0.109 659 997 | −0.499 971 155 |

Table 8.7: *Failure* of the evaluation of the perturbation series for S_E (electric background field) given in Eq. (8.59) for $g_E = 1$. Results are given in terms of the scaled function \bar{S}_E given by $S_E = 10^{-1} \times (-e^2 E^2)/(8\pi^2) \times \bar{S}_E$. Observe the apparent lack of convergence.

As for the complex resonances of the Stark effect (see the numerical results in Sec. 8.2.4), it is possible to reconstruct the nonperturbative imaginary part (pair production rate) from the purely real perturbative coefficients in Eq. (8.61).

8.3.3 The Double-Well Problem

We discuss in the current section specific results, recently obtained in [29], for the quantum-mechanical double-well problem and the related multi-instanton expansion. The energy levels of the double-well potential receive, beyond perturbation theory, contributions which are non-analytic in the coupling strength; these are related to instanton effects. For example, the separation between the energies of odd- and even-parity states is given at leading order by the one-instanton contribution, which, in the path integral formalism, corresponds to a tunneling of the particle from one minimum of the potential to the other minimum. In order to determine the energies (of individual levels as well as the separations) more accurately, multi-instanton configurations have also to be taken into account. The multi-instanton configurations describe a particle that tunnels between the minima more than once. For even instantons, the particle returns to the minimum from which it started the motion.

For the double-well problem, the energy eigenvalues of the states at nonvanishing coupling $g \neq 0$ cannot *in principle* be obtained by analytic continuation from the unperturbed situation at vanishing coupling $g = 0$ because a potential with degenerate minima introduces a degeneracy in the spectrum: for any *one* unperturbed state, *two* states emerge when the perturbation is switched on. These two states are separated by an energy shift which is nonperturbative and nonanalytic in the coupling, i.e. vanishing to any order in perturbation theory. Therefore, the two states are described by the same perturbation series and yet differ in their energy by instanton contributions. Specifically, we consider the case of the double-well potential with the hamiltonian

$$H = -\frac{g}{2} \frac{\partial^2}{\partial q^2} + \frac{1}{g} V(q), \quad V(q) = \frac{1}{2} q^2 (1 - q)^2. \quad (8.66)$$

Of course, the alternative formulation $H = -\partial^2/\partial q^2 + \frac{1}{2} q^2 (1 - \sqrt{g}q)^2$ gives rise to the same energy levels, but the form (8.66) illustrates that the coupling plays the formal rôle of \hbar . The hamiltonian (8.66) can be obtained from $H = -\partial^2/\partial q^2 + \frac{1}{2} q^2 (1 - \sqrt{g}q)^2$ by the scaling $q \rightarrow q/\sqrt{g}$. It has been

| n | partial sum | $\mathcal{T}S_n(g_E)$ |
|-------|---------------|---|
| 2 | 0.001 146 032 | $0.001\,144\,848 + i\,7.70 \times 10^{-17}$ |
| 3 | 0.001 146 705 | $0.001\,146\,639 + i\,8.22 \times 10^{-11}$ |
| 4 | 0.001 146 951 | $0.001\,147\,113 + i\,3.54 \times 10^{-8}$ |
| 5 | 0.001 147 087 | $0.001\,147\,264 + i\,1.93 \times 10^{-8}$ |
| 6 | 0.001 147 195 | $0.001\,147\,173 + i\,3.15 \times 10^{-7}$ |
| 7 | 0.001 147 310 | $0.001\,147\,113 + i\,2.58 \times 10^{-7}$ |
| 8 | 0.001 147 469 | $0.001\,147\,162 + i\,2.30 \times 10^{-7}$ |
| 9 | 0.001 147 743 | $0.001\,147\,165 + i\,2.63 \times 10^{-7}$ |
| 10 | 0.001 148 327 | $0.001\,147\,144 + i\,2.53 \times 10^{-7}$ |
| 11 | 0.001 149 825 | $0.001\,147\,157 + i\,2.46 \times 10^{-7}$ |
| 12 | 0.001 154 375 | $0.001\,147\,155 + i\,2.56 \times 10^{-7}$ |
| 13 | 0.001 170 560 | $0.001\,147\,151 + i\,2.51 \times 10^{-7}$ |
| 14 | 0.001 237 137 | $0.001\,147\,156 + i\,2.51 \times 10^{-7}$ |
| 15 | 0.001 550 809 | $0.001\,147\,153 + i\,2.53 \times 10^{-7}$ |
| 16 | 0.003 228 880 | $0.001\,147\,154 + i\,2.51 \times 10^{-7}$ |
| 17 | 0.013 345 316 | $0.001\,147\,154 + i\,2.52 \times 10^{-7}$ |
| 18 | 0.081 610 937 | $0.001\,147\,153 + i\,2.52 \times 10^{-7}$ |
| 19 | 0.594 142 371 | $0.001\,147\,154 + i\,2.52 \times 10^{-7}$ |
| 20 | 4.852 426 276 | $0.001\,147\,154 + i\,2.52 \times 10^{-7}$ |
| exact | 0.001 147 154 | $0.001\,147\,154 + i\,2.52 \times 10^{-7}$ |

Table 8.8: Resummation of the asymptotic series for the QED effective action (8.61) in a constant background electric field for $g_E = 0.05$. Results in the third column are obtained by the method discussed in Secs. 8.2.2 and 8.2.3 along the integration contour C_{+1} (see Fig. 8.1). The partial sums in the second column are obtained from the asymptotic series (8.61).

conjectured [171, 172, 173, 174] that an asymptotic expansion for the energy eigenvalue can be obtained by finding a solution to the equation

$$\frac{1}{\sqrt{2\pi}} \Gamma\left(\frac{1}{2} - D(E, g)\right) \left(-\frac{2}{g}\right)^{D(E, g)} \exp[-A(E, g)/2] = \pm i, \quad (8.67)$$

which can be understood as a modified Bohr-Sommerfeld quantization condition. The plus and minus signs apply to even- and odd-parity states, respectively. The conjecture (8.67), whose validity has been proven in [176], has found a natural explanation in the framework of Ecalle's theory of resurgent functions [175, 177, 318]. The functions $D(E, g)$, $A(E, g)$ constitute power series in both variables. The function $D(E, g)$ describes the perturbative expansion; its evaluation is discussed in [171, 174]. The first terms read

$$D(E, g) = E + g \left(3E^2 + \frac{1}{4}\right) + g^2 \left(35E^3 + \frac{25}{4}E\right) + \mathcal{O}(g^2). \quad (8.68)$$

The ground and the first excited state are both described by the same perturbation series which can be found by inverting the equation $D(E, g) = 1/2$. When the energy is expressed in terms of the naive perturbation series in g , the function $[D(E, g) - N - 1/2]$ then vanishes in any order of perturbation theory, i.e. in all orders in g . Here, N is the quantum number of the unperturbed state which is a

harmonic oscillator eigenstate. The function $A(E, g)$ essentially describes instanton contributions [174]; its first terms read

$$A(E, g) = \frac{1}{3g} + g \left(17E^2 + \frac{19}{12} \right) + g^2 \left(227E^3 + \frac{187}{4}E \right) + \mathcal{O}(g^2). \quad (8.69)$$

A solution to the equation (8.67) can be found by systematically expanding the energy eigenvalue $E(g)$ in powers of g and in the two quantities

$$\lambda(g) = \ln \left(-\frac{2}{g} \right) \quad \text{and} \quad \xi(g) = \frac{\exp[-1/(6g)]}{\sqrt{\pi g}}. \quad (8.70)$$

Terms of order $\xi(g)^n$ belong to the n -instanton contribution. The energy eigenvalue for nonvanishing perturbation $g \neq 0$ can be described by two quantum numbers: the unperturbed quantum number N and the positive or negative parity of the state. We have (the upper index denotes the instanton order)

$$E_{N,\pm}(g) = \sum_{n=0}^{\infty} E_{N,\pm}^{(n)}(g) \quad (8.71)$$

where the perturbation series (zero-instanton contribution) is given as

$$E_{N,\pm}^{(0)}(g) = \sum_{K=0}^{\infty} E_{N,K}^{(0)} g^K, \quad (8.72)$$

where the right-hand side is parity independent. For $n > 0$, the instanton contribution reads

$$E_{N,\pm}^{(n)}(g) = \left(\frac{2}{g} \right)^{Nn} \xi(g)^n \sum_{k=0}^{n-1} \lambda(g)^k \sum_{l=0}^{\infty} \epsilon_{nkl}^{(N,\pm)} g^l. \quad (8.73)$$

The lower indices n , k and l of the ϵ coefficients denote the instanton order, the power of the logarithm and the power of g , respectively. Some of the results that will be used in the sequel read,

$$\epsilon_{100}^{(0,+)} = -\epsilon_{100}^{(0,-)} = -1, \quad \epsilon_{101}^{(0,+)} = -\epsilon_{101}^{(0,-)} = \frac{71}{12},$$

$$\epsilon_{101}^{(0,+)} = -\epsilon_{101}^{(0,-)} = \frac{6299}{288}, \quad \epsilon_{210}^{(0,+)} = \epsilon_{210}^{(0,-)} = 1,$$

$$\epsilon_{211}^{(0,+)} = \epsilon_{211}^{(0,-)} = -\frac{53}{6}, \quad \epsilon_{212}^{(0,+)} = \epsilon_{212}^{(0,-)} = -\frac{1277}{72},$$

$$\epsilon_{200}^{(0,+)} = \epsilon_{200}^{(0,-)} = \gamma, \quad \epsilon_{201}^{(0,+)} = \epsilon_{201}^{(0,-)} = -\frac{23}{2} - \frac{53}{6}\gamma,$$

$$\epsilon_{202}^{(0,+)} = \epsilon_{202}^{(0,-)} = \frac{13}{12} - \frac{1277}{72}\gamma, \quad (8.74)$$

where $\gamma = 0.57221 \dots$ is Euler's constant. Odd-instanton contributions have opposite sign for opposite-parity states and are responsible, in particular, for the energy difference of the ground state with quantum numbers $(0, +)$ and the first excited state with quantum numbers $(0, -)$. The dominant contribution to the separation of the two lowest energy levels is given by the one-instanton contribution:

$$E_{0,-}(g) - E_{0,+}(g) \sim 2\xi(g) \left(1 - \frac{71}{12}g - \frac{6299}{288}g^2 + \mathcal{O}(g^3) \right) + \mathcal{O}(\xi(g)^3). \quad (8.75)$$

By contrast, even-instanton contributions have like sign for opposite-parity states and are responsible, in particular, for the displacement of the mean value $(1/2)[E_{0,-}(g) + E_{0,+}(g)]$ from the value of the generalized Borel sum of the perturbation series $\mathcal{B} \left(\sum_{K=0}^{\infty} E_{0,K}^{(0)} g^K \right)$ (for the evaluation of the generalized Borel

sum of a nonalternating divergent series, see Sec. 8.3.1). The dominant contribution to the displacement comes from the two-instanton effect, and we have

$$\begin{aligned} & \frac{1}{2} [E_{0,-}(g) + E_{0,+}(g)] - \text{Re} \left\{ \mathcal{B} \left(\sum_{K=0}^{\infty} E_{0,K}^{(0)} g^K \right) \right\} \sim \\ & \xi(g)^2 \left\{ \ln \left(\frac{2e^\gamma}{g} \right) + g \left[-\frac{53}{6} \ln \left(\frac{2e^\gamma}{g} \right) - \frac{23}{2} \right] + g^2 \left[-\frac{1277}{72} \ln \left(\frac{2e^\gamma}{g} \right) + \frac{13}{12} \right] + \mathcal{O}(g^3 \ln(g)) \right\} \\ & + \mathcal{O}(\xi(g)^4). \end{aligned} \quad (8.76)$$

The function [172]

$$\Delta(g) = 4 \frac{\frac{1}{2} [E_{0,-}(g) + E_{0,+}(g)] - \text{Re} \left\{ \mathcal{B} \left(\sum_{K=0}^{\infty} E_{0,K}^{(0)} g^K \right) \right\}}{[E_{0,-}(g) - E_{0,+}(g)]^2 \ln \left(\frac{2e^\gamma}{g} \right)} \quad (8.77)$$

relates the multi-instanton contributions to the energy eigenvalues, which can be evaluated numerically, and to the (generalized) Borel sum of the perturbation series which is evaluated by analytic continuation of the integration path into the complex plane (see [297]). The calculation of $\Delta(g)$ at small coupling is problematic because of severe numerical cancellations. From the equations (8.75), (8.76) and (8.77), we obtain the following asymptotics for $\Delta(g)$,

$$\begin{aligned} \Delta(g) \sim & 1 + g \left[\frac{71}{6} + \left(-\frac{53}{6} \ln \left(\frac{2e^\gamma}{g} \right) - \frac{23}{2} \right) / \ln \left(\frac{2e^\gamma}{g} \right) \right] \\ & + g^2 \left[\frac{10711}{72} + \left(\frac{1277}{72} \ln \left(\frac{2e^\gamma}{g} \right) - \frac{13}{12} \right) / \ln \left(\frac{2e^\gamma}{g} \right) \right] + \mathcal{O}(g^3). \end{aligned} \quad (8.78)$$

If we additionally perform an expansion in inverse powers of $\ln(2/g)$ and keep only the first few terms in $\{1/\ln(2/g)\}$ in each term in the g -expansion, the result reads

$$\begin{aligned} \Delta(g) \sim & 1 + 3g - \frac{23}{2} \frac{g}{\ln(2/g)} \left[1 - \frac{\gamma}{\ln(2/g)} + \frac{\gamma^2}{\ln^2(2/g)} + \mathcal{O} \left(\frac{1}{\ln^3(2/g)} \right) \right] + \frac{53}{2} g^2 \\ & - 135 \frac{g^2}{\ln(2/g)} \left[1 - \frac{\gamma}{\ln(2/g)} + \frac{\gamma^2}{\ln^2(2/g)} + \mathcal{O} \left(\frac{1}{\ln^3(2/g)} \right) \right] + \mathcal{O}(g^3). \end{aligned} \quad (8.79)$$

The higher-order corrections, which are only logarithmically suppressed with respect to the leading terms $1 + 3g$, change the numerical values quite significantly, even at small coupling. In Table 8.9 we present numerical results for the function $\Delta(g)$ at small coupling; these are in agreement with the first few asymptotic terms listed in equation (8.78) up to numerical accuracy. Of course, for strong coupling, significant deviations from the leading asymptotics must be expected due to higher-order effects; these are indeed observed. For example, at $g = 0.1$ the numerically determined value reads $\Delta(0.1) = 0.87684(1)$ whereas the first asymptotic terms given in equation (8.78) sum up to a numerical value of 0.86029.

The higher-order corrections to the two-instanton effect are related to the corrections to the leading factorial growth of the perturbative coefficients. This can be seen by expressing that the imaginary part of the perturbation series, when continued analytically from negative to positive coupling, has to cancel with the imaginary part of the two-instanton contribution which is generated by the logarithms $\ln(-2/g)$. The corrections of order $g \ln(-2/g)$ and $g^2 \ln(-2/g)$ yield the $1/K$ - and $1/K^2$ -corrections to the leading factorial growth of the perturbative coefficients. From the results for $\epsilon_{21j}^{(0,\pm)}$ ($j = 0, 1, 2$) given in equation (8.74), we obtain

$$E_{0,K}^0 \sim -\frac{3^{K+1} K!}{\pi} \left[1 - \frac{53}{18} \frac{1}{K} - \frac{1277}{648} \frac{1}{K^2} + \mathcal{O} \left(\frac{1}{K^3} \right) \right]. \quad (8.80)$$

Table 8.9: Comparison of numerical values for the function $\Delta(g)$ defined in equation (8.77) in the region of small coupling to values obtained by calculating the first few terms in its asymptotic expansion given in (8.78).

| coupling g | 0.005 | 0.006 | 0.007 | 0.008 | 0.009 |
|--------------------|-----------|-----------|------------|------------|------------|
| $\Delta(g)$ num. | 1.0063(5) | 1.0075(5) | 1.00832(5) | 1.00919(5) | 1.00998(5) |
| $\Delta(g)$ asymp. | 1.00640 | 1.00739 | 1.00832 | 1.00919 | 1.01001 |

The analytic results should be checked against explicit values of the perturbative coefficients. We have determined the first 200 perturbative coefficients $E_{0,K}^{(0)}$ ($K = 0, \dots, 200$) of the perturbation in the form of rational numbers, i.e. to formally infinite numerical accuracy. This allows to verify the $1/K$ - and $1/K^2$ -corrections to the leading factorial growth in equation (8.80) to high accuracy, for example by employing Richardson extrapolation [319]. Using the 160th through the 200th perturbation coefficient as input data for the Richardson algorithm, the coefficients of the leading, of the $1/K$ -subleading and of the $1/K^2$ suppressed corrections are found to be consistent with the analytic results given in equation (8.80) up to a relative numerical accuracy of 10^{-26} , 10^{-23} and 10^{-20} , respectively. For completeness, we give here the numerical values of the 198th through the 200th perturbative coefficients, to 30 decimals. These read:

$$\begin{aligned}
E_{0,198}^{(0)} &= -5.50117\,76962\,88587\,93527\,75694\,38632 \times 10^{464}, \\
E_{0,199}^{(0)} &= -3.28445\,39841\,65780\,00616\,21912\,32835 \times 10^{467}, \\
E_{0,200}^{(0)} &= -1.97082\,14193\,09543\,76979\,53006\,07410 \times 10^{470}.
\end{aligned} \tag{8.81}$$

Values for all 200 coefficients are available [234].

It is an interesting consequence of the expansion (8.71) that the energy difference ($E_{0,-} - E_{0,+}$), at small coupling, is described to high accuracy by the one-instanton contribution ($n = 1$ in equation (8.73)). For $g = 0.001$, we obtain to 180 decimals,

$$\begin{aligned}
E_{0,+}(0.001) &= 0. \quad 49899\,54548\,62109\,17168\,91308\,39481\,92163\,68209\,47240 \\
&\quad 20809\,66532\,93278\,69722\,01391\, \underline{15135\,28505\,38294\,45798} \\
&\quad \underline{45759\,95999\,06739\,55175\,84722\,67802\,81306\,96906\,01325} \\
&\quad \underline{25943\,77289\,94365\,88255\,24440\,17437\,12789\,27978\,99793},
\end{aligned} \tag{8.82}$$

whereas

$$\begin{aligned}
E_{0,-}(0.001) &= 0. \quad 49899\,54548\,62109\,17168\,91308\,39481\,92163\,68209\,47240 \\
&\quad 20809\,66532\,93278\,69722\,01391\, \underline{29839\,92959\,55803\,70812} \\
&\quad \underline{27749\,92448\,48259\,36743\,64757\,68328\,84835\,35511\,34663} \\
&\quad \underline{06309\,82331\,51885\,23308\,08622\,84780\,52722\,10103\,67282}.
\end{aligned} \tag{8.83}$$

Decimals which differ in the two energy levels are underlined. The results have been obtained by lattice extrapolation using a modified Richardson algorithm which is constructed according to ideas outlined

in [156]. Calculations were performed on IBM RISC/6000 workstations while making extensive use of multiprecision libraries [235, 237, 238]. We define $\mathcal{P}_M(g)$ as the M th partial sum of the one-instanton contribution $E_{0,-}^{(1)}(g) - E_{0,+}^{(1)}(g)$,

$$\mathcal{P}_M(g) = 2\xi(g) \sum_{j=0}^M \epsilon_{10j}^{(0,-)} g^j. \quad (8.84)$$

Using exact rational expressions for the coefficients $\epsilon_{10j}^{(0,-)}$ ($j \leq 141$), we obtain

$$\begin{aligned} \mathcal{P}_{140}(0.001) \times 10^{71} = \\ 1.47046\,44541\,75092\,50138\,19899\,64494\,15198\,15678\,00350\,05260\,35283 \\ 86053\,33378\,03660\,50415\,75193\,50528\,41826\,73433\,99328\,21246\,74888, \end{aligned} \quad (8.85)$$

$$\begin{aligned} \mathcal{P}_{141}(0.001) \times 10^{71} = \\ 1.47046\,44541\,75092\,50138\,19899\,64494\,15198\,15678\,00350\,05260\,35283 \\ 86053\,33378\,03660\,50415\,75193\,50528\,41826\,73433\,99328\,21246\,74887. \end{aligned} \quad (8.86)$$

These values are in excellent agreement with the numerically determined energy difference (see the results presented above in equations (8.82) and (8.83))

$$\begin{aligned} [E_{0,-}(0.001) - E_{0,+}(0.001)] \times 10^{71} = \\ 1.47046\,44541\,75092\,50138\,19899\,64494\,15198\,15678\,00350\,05260\,35283 \\ 86053\,33378\,03660\,50415\,75193\,50528\,41826\,73433\,99328\,21246\,74887. \end{aligned} \quad (8.87)$$

The first 70 decimals in equations (8.82) and (8.83) are the same because the one-instanton contribution is of the order of 1.4×10^{-71} . The accuracy to which the one-instanton contribution describes the energy difference $E_{0,-}(0.001) - E_{0,+}(0.001)$ is limited by the three-instanton effect which for $g = 0.001$ is of the order of 8×10^{-212} . Note that the two-instanton effect (which for $g = 0.001$ is of the order of 4×10^{-142}) does not limit the accuracy to which the one-instanton contribution describes the energy difference because it has the same sign for opposite-parity states.

We have demonstrated that the behavior of the characteristic function $\Delta(g)$ defined in equation (8.77) at small coupling is consistent with higher-order corrections to the one- and two-instanton contributions, specifically with the instanton expansion of the energy levels governed by the equations (8.71) and (8.73), with the assumption that the instanton contributions given by equation (8.73) should be Borel summed, with the explicit results for the higher-order coefficients listed in (8.74) and the analytically derived asymptotics for the function $\Delta(g)$ given in equation (8.78). The corrections of relative order $1/K^m$ to the leading factorial growth of the perturbative coefficients – see equation (8.80) – are consistent with the analytically evaluated $g^m \ln(-2/g)$ -corrections to the two-instanton effect and with the explicit values for the first 200 terms in the perturbation series (8.72). The nonperturbative energy difference $E_{0,-}(g) - E_{0,+}(g)$ at small coupling g is described, to high accuracy, by the one-instanton contribution only.

8.4 Divergent Series: Some Conclusions

A priori, it may seem rather unattractive to assume that the quantum electrodynamic perturbation series may be divergent even after the regularization and the renormalization. However, as shown by explicit

nontrivial 30-loop calculations of renormalization group γ functions in a six-dimensional ϕ^3 theory, and in a Yukawa theory (presented recently in [316, 317]), we believe that the ultimate divergence of the perturbative expansion can be regarded as a matter-of-fact, clearly demonstrated by explicit high-order calculations. Therefore, it appears meaningful to explore the physical implications of this divergence.

We have discussed four physical applications of resummation methods for divergent series: (i) the energy displacement of a hydrogen atom in a background electric field (Sec. 8.2.4), (ii) zero-dimensional (model) field theories (Sec. 8.3.1), (iii) the QED effective Lagrangian (Sec. 8.3.2), and (iv) the energy levels of the double-well potential (Sec. 8.3.3). The mathematical structure of these problems can be characterized as follows, in the order of increasing complexity:

- The QED effective Lagrangian for a background magnetic field, expressed as a perturbation series in α , is manifestly Borel summable [163, 255, 310], and the nonperturbative result can be inferred by a number of different resummation methods, as discussed in Sec. 8.3.2.
- The QED effective Lagrangian for a background electric field, as well as the perturbation series for a hydrogen atom in an electric field, is not Borel summable. The same applies to the perturbation series for a zero-dimensional field theory with degenerate minima. However, these three problems admit a treatment according to the concept of *generalized* (distributional) Borel summability [158]. Numerical results (see [25, 28] and Secs. 8.2.4 and 8.3.2) confirm the distributional Borel summability, and the use of additional asymptotic information about the perturbative coefficients [“leading renormalon poles”, see Eqs. (8.15) and (8.16) in Sec. 8.2.2] accelerates the convergence of the Borel-transformed perturbation series.
- The double-well potential represent a very problematic case: the full nonperturbative solution to the eigenvalue problem cannot be obtained *in principle* from perturbation theory. The reason is the following: the perturbation introduces an additional degeneracy in the spectrum: each unperturbed level splits into *two* energy levels when the perturbation is nonvanishing. Both of these levels are described by one and the same naive perturbation series (see Sec. 8.3.3). The energy difference is nonperturbative and nonanalytic in the coupling strength, and finds an explanation in the theory of instantons.

For the Stark effect and the QED effective Lagrangian (electric field), the existence of nonperturbative contributions is intimately linked with the failure of the Carleman criterion (see for example [163], Theorems XII.17 and XII.18 and the definition on p. 43 in [164], p. 410 in [165], Ch. 6 of this Thesis or the elucidating discussion in Ref. [166]). The Carleman criterion determines, roughly speaking, if nonanalytic contributions exist for a given effect which is described by a specified perturbation series. In this sense, the divergence of the perturbative expansion is physically important: for the QED effective action, it allows for the existence of nonanalytic, nonperturbative contributions like the pair-production amplitude which is not contained in the real perturbation series (8.61) and cannot be obtained on the basis of perturbation theory alone.

Also, we would like to illustrate here the utility of resummation methods in those cases where perturbation theory breaks down at large coupling. As explained in Secs. 8.2.4, 8.3.1 and 8.3.2, even in situations where the perturbation series diverges strongly, it can still be used to obtain meaningful physical results if it is combined with a suitable resummation method. In a relatively weak field, it is possible to obtain more accurate numerical results by resummation than by optimal truncation of the perturbation series (see also [25]). In a strong field, it is possible to obtain physically correct results by resummation even though the perturbation series diverges strongly (see the discussion in Sec. 8.2.4 and the data in Tables 8.1, 8.2 and 8.4). By resummation, the perturbation series which is inherently a weak-coupling expansion can be given a physical interpretation even in situations where the coupling is large. Returning to the analogy to quantum field theory, one might be tempted to suggest that physically complete results can in many cases be obtained after regularization, renormalization *and* resummation.

Can the full nonperturbative result (for energy levels etc.) be inferred in *all* cases by a resummation of the divergent perturbation series? The answer is, unfortunately, no. This is demonstrated in Sec. 8.3.3 by way of example. In theories with degenerate minima (such as the double-well problem), corrections to energy levels are caused by so-called instanton contributions that follow naturally by an expansion of the path integral around nontrivial saddle points. The n -instanton contribution is characterized by a nonperturbative factor $\xi(g)^n$ where [see Eq. (8.70)] $\xi(g) = \exp[-1/(6g)]/\sqrt{\pi g}$, and g is the coupling. The

expansion of $\xi(g)$ in powers of g vanishes in all orders of g . The nonperturbative energy splitting between even- and odd-parity states is investigated by considering the function $\Delta(g)$ defined in Eq. (8.77). This function would vanish if the generalized Borel sum of the perturbation series could reproduce energy levels exactly. However, it does not vanish, as demonstrated by the data in Tab. 8.9 (the numerical data can be interpreted naturally by considering so-called two-instanton effects). At the same time, in a zero-dimensional theory with degenerate minima (considered in Sec. 8.3.1), resummation is successful *despite* the existence of a nontrivial saddle point. The reason for the success of the resummation in this model problem appears to lie in the fact that no degeneracies are introduced by the additional saddle point. The perturbation series determines the generating functional uniquely, which is not the case in the double-well potential where two distinct energy levels (of opposite parity) share the same perturbation series. This intriguing situation will warrant further investigation in the near future.

Chapter 9

Conclusions

We proceed to the interpretation of the results obtained in this Thesis, which has a dual subject: “quantum electrodynamic bound-state calculations and large-order perturbation theory”.

The significance of quantum electrodynamics as one of the most appealing physical theories (a “jewel” of theoretical physics according to Richard Feynman) does not require any further explanation. The esthetic appeal of bound-state quantum electrodynamics stems from the accuracy of the experimental verifications, the significance of the theory for the determination of the fundamental constants, and the conceptual complexity of the calculations which derives from the apparent simplicity of the physical systems under study, when an accurate understanding is required in higher orders of perturbation theory. However, the divergence of the perturbative expansion in large orders, which persists even after the regularization and renormalization, raises fundamental questions regarding the internal consistency of the theoretical predictions. The problems associated with the divergence of the perturbative expansion do not only plague quantum electrodynamics, but even occur in ordinary quantum mechanical perturbation theory. This Thesis is divided into two Parts, which represent two attempts to advance our understanding of the higher-order corrections as well as of the conceptual questions raised by the divergence of the perturbative expansion.

In the first Part, we discussed aspects of certain quantum electrodynamic bound-state calculations, which have been carried out over the past years. Not all of these calculations [1, 2, 3, 4, 5, 6, 7, 8, 9, 10, 11, 12, 13, 14, 15, 16, 17, 18] could be described in full detail. Both the experimental accuracy as well as the accuracy of the theoretical calculations have improved dramatically in recent years [42]. On the theoretical side, the calculations at low nuclear charge number may be based on either of two methods: the analytic approach that is based on the $Z\alpha$ -expansion and the numerical approach in which all electron propagators are kept in exact relativistic form. Progress has been achieved due to advances in the analytic approach that profit from an adequate formulation of the problem, and due to the development of numerical techniques which have led to the highly accurate numerical evaluation of QED corrections in the realm of low nuclear charge number. This has led to the favourable situation where analytic and numerical calculations can be checked against each other. In view of the complexity of the calculations and their importance for the determination of the fundamental constants [86], the existence of independent cross-checks for the calculations is highly desirable.

Numerical calculations at low Z have been made possible by convergence acceleration methods described in the second Part of this Thesis (notably by the combined nonlinear-condensation transformation). These techniques have led to the solution of the severe numerical difficulties associated with the singularity of the propagators for equal radial arguments, and to a reduction in computing time by three orders of magnitude. Results obtained for the one-photon self energy are several orders of magnitude more accurate than previous calculations of the effect. They represent the first *direct* evaluations of the one-loop self energy at the nuclear charge numbers $Z = 1$ and $Z = 2$, which are of crucial importance for precision spectroscopy (atomic hydrogen and hydrogenlike helium).

The analytic calculations of the one-loop self energy for higher excited states will be complemented in the near future by numerical calculations based on the new techniques [95], leading to a cross-check of the type mentioned above. Severe difficulties associated with the multitude of analytic terms due to the more complicated wavefunctions of the highly excited states and the associated angular momentum algebra have been a problem for self energy calculations in this area.

The calculations for the bound-state two-loop self energy report on the first evaluation of the highly problematic nonlogarithmic higher-order two-loop binding correction B_{60} . Let us recall that analytic work on the corresponding A_{60} correction for the less involved one-loop problem has extended over three decades [32, 68, 69, 70, 71]. The development of analytic methods for the evaluation of B_{60} leads to an improved understanding of the scaling of the two-loop effect at low Z and will enable a detailed comparison of analytic and possibly available numerical results for the two-loop effect in the future. At the same time, these results lead to improved predictions for the hydrogen and helium fine structure.

The spin-dependence of quantum electrodynamic corrections is a conceptually important issue. We focus on spinless particles and present a simplified derivation of the generalized Breit hamiltonian for a system of two spinless particles. Although scalar QED is a renormalizable theory, we found the issue of bound-state calculations within this theory insufficiently addressed in the literature. Our calculations for the leading-order self energy and the relativistic recoil correction are the first corrections of the “self energy type” to be evaluated within bound-state QED involving only scalar particles.

As a further application, we would like to mention the recent investigation [18].

In the second Part of the Thesis, we investigate convergence acceleration and resummation methods for divergent series. The convergence acceleration techniques address the fundamental problem of the acceleration of a slowly convergent, nonalternating series. Severe numerical instabilities associated with the formation of higher-order weighted differences for nonalternating series have been a major obstacle for algorithms that try to accomplish this task. The methods find applications in areas as diverse as DNA sequence analysis and experimental mathematics.

Recent highly nontrivial 30-loop calculations [316, 317] have convincingly demonstrated the divergence of the perturbative expansions in quantum field theory originally conjectured by Dyson [320]. We discuss nonlinear sequence transformations as an alternative to the “usual” Borel method for the resummation of divergent series that result from perturbative expansions in quantum field theory. These transformations have favourable asymptotic properties and lead in many cases to better numerical results than Padé approximants. We also discuss generalizations of the Borel method which lead to consistent results even if the full, nonperturbative physical energy level or vacuum-to-vacuum amplitude acquires an imaginary part due to quantum mechanical tunneling. This imaginary part, which represents the autoionization decay width (Stark effect) and the electron-positron pair-production amplitude (in the case of the QED effective action), can be derived starting only from the real (not complex!) perturbative coefficients. In the double-well problem, the situation is different. Even- and odd-parity states acquire an energy separation which is nonperturbative and nonanalytic in the coupling strength and is an effect which *in principle* cannot be derived from perturbation theory alone. The energy separation is given by so-called multi-instantons which follow naturally from a path integral representation of the partition function and correspond to configurations where the particle tunnels repeatedly between the two minima of the double-well potential. The results lead to a better understanding of the energy shifts due to multi-instanton effects, by evaluating higher-order corrections to the two-instanton effect, and they also lead to an accurate verification of the instanton expansion via a comparison to numerically determined energy levels.

The common theme of all investigations discussed in is to *explore the predictive limits of quantum theory*. It has been the aim of this Thesis to present results for some of the essential QED corrections which influence the spectrum of bound systems and are of current experimental interest, as well as to work towards a solution of the questions regarding the predictive limits of field theories set by the ultimate divergence of the perturbative expansion. Certain methods developed along this endeavour have meanwhile found applications in other areas (applied biophysics and mathematics).

Bibliography

- [1] U. D. Jentschura and K. Pachucki, Phys. Rev. A **54**, 1853 (1996).
- [2] U. D. Jentschura, G. Soff, and P. J. Mohr, Phys. Rev. A **56**, 1739 (1997).
- [3] U. D. Jentschura, G. Soff, V. G. Ivanov, and S. G. Karshenboim, Phys. Rev. A **56**, 4483 (1997).
- [4] S. G. Karshenboim, U. D. Jentschura, V. G. Ivanov, and G. Soff, Phys. Lett. B **424**, 397 (1998).
- [5] U. D. Jentschura, G. Soff, V. Ivanov, and S. G. Karshenboim, Phys. Lett. A **241**, 351 (1998).
- [6] S. G. Karshenboim, V. G. Ivanov, U. D. Jentschura, and G. Soff, Zh. Éksp. Teor. Fiz. **113**, 409 (1998), [JETP **86**, 226 (1998)].
- [7] S. G. Karshenboim, U. D. Jentschura, V. G. Ivanov, and G. Soff, Eur. Phys. J. D **2**, 209 (1998).
- [8] I. F. Ginzburg, U. D. Jentschura, S. G. Karshenboim, F. Krauss, V. G. Serbo, and G. Soff, Phys. Rev. C **58**, 3565 (1998).
- [9] U. D. Jentschura, P. J. Mohr, and G. Soff, Phys. Rev. Lett. **82**, 53 (1999).
- [10] U. D. Jentschura, P. J. Mohr, and G. Soff, in *AIP Conf. Proc. 457*, edited by D. H. E. Dubin and D. Schneider (A. I. P., Woodbury, NY, 1999), p. 40.
- [11] U. D. Jentschura, P. J. Mohr, and G. Soff, IEEE Trans. Instrum. Meas. **48**, 186 (1999).
- [12] U. D. Jentschura, P. J. Mohr, and G. Soff, Phys. Rev. A **64**, 042512 (2001).
- [13] I. A. Goidenko, L. N. Labzowsky, A. V. Nefiodov, U. D. Jentschura, G. Plunien, S. Zschocke, and G. Soff, Phys. Scr. T **92**, 426 (2001).
- [14] G. Soff, I. Bednyakov, T. Beier, F. Erler, I. A. Goidenko, U. D. Jentschura, L. N. Labzowsky, A. V. Nefiodov, G. Plunien, R. Schützhold, and S. Zschocke, Hyp. Int. **132**, 75 (2001).
- [15] U. D. Jentschura, P. J. Mohr, and G. Soff, Hyp. Int. **132**, 373 (2001).
- [16] U. D. Jentschura and K. Pachucki, J. Phys. A **35**, 1927 (2002).
- [17] U. D. Jentschura, G. Soff, and P. J. Indelicato, J. Phys. B **35**, 2459 (2002).
- [18] U. D. Jentschura and I. Nandori, Phys. Rev. A **66**, 022114 (2002).
- [19] J. Urban, F. Krauss, U. Jentschura, and G. Soff, Nucl. Phys. B **523**, 40 (1998).
- [20] U. D. Jentschura, H. Gies, S. R. Valluri, D. R. Lamm, and E. J. Weniger, Can. J. Phys. **80**, 267 (2002).
- [21] I. Nandori, K. Sailer, U. D. Jentschura, and G. Soff, J. Phys. G **28**, 607 (2002).
- [22] D. R. Lamm, S. R. Valluri, U. D. Jentschura, and E. J. Weniger, Phys. Rev. Lett. **88**, 089101 (2002).
- [23] U. D. Jentschura, P. J. Mohr, G. Soff, and E. J. Weniger, Comput. Phys. Commun. **116**, 28 (1999).

- [24] U. D. Jentschura, J. Becher, E. J. Weniger, and G. Soff, Phys. Rev. Lett. **85**, 2446 (2000).
- [25] U. D. Jentschura, Phys. Rev. D **62**, 076001 (2000).
- [26] U. D. Jentschura, E. J. Weniger, and G. Soff, J. Phys. G **26**, 1545 (2000).
- [27] U. D. Jentschura and G. Soff, J. Phys. A **34**, 1451 (2001).
- [28] U. D. Jentschura, Phys. Rev. A **64**, 013403 (2001).
- [29] U. D. Jentschura and J. Zinn-Justin, J. Phys. A **34**, L253 (2001).
- [30] U. D. Jentschura, S. V. Aksenov, P. J. Mohr, M. A. Savageau, and G. Soff, in *Proceedings of the Nanotech 2003 Conference (Vol. 2)*, see also e-print math.NA/0202009 (Computational Publications, Boston, 2003), pp. 535–537.
- [31] S. V. Aksenov, M. A. Savageau, U. D. Jentschura, J. Becher, G. Soff, and P. J. Mohr, Comput. Phys. Commun. **150**, 1 (2003).
- [32] K. Pachucki, Ann. Phys. (N.Y.) **226**, 1 (1993).
- [33] H. A. Bethe, Phys. Rev. **72**, 339 (1947).
- [34] C. Itzykson and J. B. Zuber, *Quantum Field Theory* (McGraw-Hill, New York, NY, 1980).
- [35] B. de Beauvoir, F. Nez, L. Julien, B. Cagnac, F. Biraben, D. Touahri, L. Hilico, O. Acef, A. Clairon, and J. J. Zondy, Phys. Rev. Lett. **78**, 440 (1997).
- [36] E. G. Myers and M. R. Tabbutt, Phys. Rev. A **61**, 010501 (1999).
- [37] E. G. Myers, H. S. Margolis, J. K. Thompson, M. A. Farmer, J. D. Silver, and M. R. Tabbutt, Phys. Rev. Lett. **82**, 4200 (1999).
- [38] C. H. Storry, M. C. George, and E. A. Hessels, Phys. Rev. Lett. **84**, 3274 (2000).
- [39] M. C. George, L. D. Lombardi, and E. A. Hessels, Phys. Rev. Lett. **87**, 173002 (2001).
- [40] K. Pachucki and S. G. Karshenboim, J. Phys. B **28**, L221 (1995).
- [41] T. Udem, A. Huber, B. Gross, J. Reichert, M. Prevedelli, M. Weitz, and T. W. Hänsch, Phys. Rev. Lett. **79**, 2646 (1997).
- [42] M. Niering, R. Holzwarth, J. Reichert, P. Pokasov, T. Udem, M. Weitz, T. W. Hänsch, P. Lemonde, G. Santarelli, M. Abgrall, P. Laurent, C. Salomon, and A. Clairon, Phys. Rev. Lett. **84**, 5496 (2000).
- [43] U. D. Jentschura, Ph. D. thesis, Dresden University of Technology; published as “Quantum Electrodynamical Radiative Corrections in Bound Systems”, *Dresdner Forschungen: Theoretische Physik, Band 2* (w.e.b. Universitätsverlag, Dresden, 1999).
- [44] S. G. Karshenboim, Z. Phys. D **39**, 109 (1997).
- [45] T. W. Hänsch, private communication (2000).
- [46] C. L. Cesar, D. G. Fried, T. C. Killian, A. D. Polcyn, J. C. Sandberg, I. A. Yu, T. J. Greytak, D. Kleppner, and J. M. Doyle, Phys. Rev. Lett. **77**, 255 (1996).
- [47] T. C. Killian, D. G. Fried, L. Willmann, D. Landhuis, S. C. Moss, T. J. Greytak, and D. Kleppner, Phys. Rev. Lett. **81**, 3807 (1998).
- [48] W. R. Johnson and G. Soff, At. Data Nucl. Data Tables **33**, 405 (1985).
- [49] P. J. Mohr, G. Plunien, and G. Soff, Phys. Rep. **293**, 227 (1998).
- [50] P. J. Mohr, in *Atomic, Molecular, and Optical Physics Handbook*, edited by G. W. F. Drake (A. I. P., Woodbury, NY, 1996), pp. 341–351.

- [51] M. I. Eides, H. Grotch, and V. A. Shelyuto, Phys. Rep. **342**, 63 (2001).
- [52] E. T. Whittaker and G. N. Watson, *A course of modern analysis* (Cambridge University Press, Cambridge, UK, 1944).
- [53] H. Erdelyi, *Asymptotic Expansions* (Dover, New York, NY, 1987).
- [54] R. P. Feynman, Phys. Rev. **74**, 1430 (1948).
- [55] R. P. Feynman, Phys. Rev. **76**, 769 (1949).
- [56] J. B. French and V. F. Weisskopf, Phys. Rev. **75**, 1240 (1949).
- [57] N. M. Kroll and W. E. Lamb, Phys. Rev. **75**, 388 (1949).
- [58] J. Schwinger, Phys. Rev. **75**, 898 (1949).
- [59] H. Fukuda, Y. Miyamoto, and S. Tomonaga, Prog. Theor. Phys. (Kyoto) **4**, 47 (1949).
- [60] M. Baranger, Phys. Rev. **84**, 866 (1951).
- [61] R. Karplus, A. Klein, and J. Schwinger, Phys. Rev. **86**, 288 (1952).
- [62] M. Baranger, H. A. Bethe, and R. P. Feynman, Phys. Rev. **92**, 482 (1953).
- [63] H. M. Fried and D. R. Yennie, Phys. Rev. **112**, 1391 (1958).
- [64] H. M. Fried and D. R. Yennie, Phys. Rev. Lett. **4**, 583 (1960).
- [65] A. J. Layzer, Phys. Rev. Lett. **4**, 580 (1960).
- [66] A. J. Layzer, J. Math. Phys. **2**, 292 (1961).
- [67] A. J. Layzer, J. Math. Phys. **2**, 308 (1961).
- [68] G. W. Erickson and D. R. Yennie, Ann. Phys. (N.Y.) **35**, 271 (1965).
- [69] G. W. Erickson and D. R. Yennie, Ann. Phys. (N.Y.) **35**, 447 (1965).
- [70] G. W. Erickson, Phys. Rev. Lett. **27**, 780 (1971).
- [71] J. Sapirstein, Phys. Rev. Lett. **47**, 1723 (1981).
- [72] S. Klarsfeld and A. Maquet, Phys. Lett. B **43**, 201 (1973).
- [73] H. A. Bethe, L. M. Brown, and J. R. Stehn, Phys. Rev. **77**, 370 (1950).
- [74] J. M. Harriman, Phys. Rev. **101**, 594 (1956).
- [75] C. Schwartz and J. J. Tieman, Ann. Phys. (N.Y.) **6**, 178 (1959).
- [76] M. Lieber, Phys. Rev. **174**, 2037 (1968).
- [77] R. W. Huff, Phys. Rev. **186**, 1367 (1969).
- [78] G. W. Erickson, J. Phys. Chem. Ref. Data **6**, 831 (1977).
- [79] G. W. F. Drake and R. A. Swainson, Phys. Rev. A **41**, 1243 (1990).
- [80] P. J. Mohr, Phys. Rev. A **46**, 4421 (1992).
- [81] P. J. Mohr, Ann. Phys. (N.Y.) **88**, 26 (1974).
- [82] P. J. Mohr, Ann. Phys. (N.Y.) **88**, 52 (1974).
- [83] P. J. Mohr, Phys. Rev. A **26**, 2338 (1982).
- [84] P. J. Mohr, Radiative Corrections in Hydrogen-like Systems, PhD thesis, University of California, Berkeley (1973).

- [85] P. J. Mohr and Y. K. Kim, Phys. Rev. A **45**, 2727 (1992).
- [86] P. J. Mohr and B. N. Taylor, Rev. Mod. Phys. **72**, 351 (2000).
- [87] A. V. Manohar and I. W. Stewart, Phys. Rev. Lett. **85**, 2248 (2000).
- [88] The numerical value of $A_{60} = -30.924\,15(1)$ has been obtained by K. Pachucki after reevaluation of certain poorly convergent one-dimensional numerical integrals in his calculation [32].
- [89] K. Pachucki, J. Phys. B **32**, 137 (1999).
- [90] S. Wolfram, *Mathematica-A System for Doing Mathematics by Computer* (Addison-Wesley, Reading, MA, 1988).
- [91] F. W. J. Olver, *Asymptotics and Special Functions* (Academic Press, New York, NY, 1974).
- [92] H. Bateman, *Higher Transcendental Functions* (McGraw-Hill, New York, NY, 1953), Vol. 1.
- [93] E.-O. Le Bigot, P. Indelicato, and P. J. Mohr, Phys. Rev. A **64**, 052508 (2001).
- [94] P. Indelicato and P. J. Mohr, Hyp. Int. **114**, 147 (1998).
- [95] E.-O. Le Bigot and P. Indelicato, private communication (2002).
- [96] G. W. Erickson and D. R. Yennie, Ann. Phys. (N.Y.) **35**, 271, 447 (1965).
- [97] J. Sapirstein and D. R. Yennie, in *Quantum Electrodynamics*, Vol. 7 of *Advanced Series on Directions in High Energy Physics*, edited by T. Kinoshita (World Scientific, Singapore, 1990), pp. 560–672.
- [98] K. Pachucki, Phys. Rev. A **63**, 042503 (2001).
- [99] T. Appelquist and S. J. Brodsky, Phys. Rev. A **2**, 2293 (1970).
- [100] K. Pachucki, Phys. Rev. Lett. **72**, 3154 (1994).
- [101] M. I. Eides and V. A. Shelyuto, Phys. Rev. A **52**, 954 (1995).
- [102] K. Pachucki, J. Phys. B **31**, 5123 (1998).
- [103] I. Białynicki-Birula, in *Quantum Electrodynamics and Quantum Optics*, edited by A. O. Barut (Plenum, New York, 1984), pp. 41–61.
- [104] W. E. Caswell and G. P. Lepage, Phys. Lett. B **167**, 437 (1986).
- [105] E. Remiddi, Nuovo Cim. A **11**, 825 (1972).
- [106] E. Remiddi, Nuovo Cim. A **11**, 865 (1972).
- [107] D. R. Yennie, S. C. Frautschi, and H. Suura, Ann. Phys. (N.Y.) **13**, 379 (1961).
- [108] P. Mastrolia and E. Remiddi, private communication (2001).
- [109] R. Bonciani, P. Mastrolia, and E. Remiddi, Nucl. Phys. B **661**, 289 (2003).
- [110] P. Mastrolia and E. Remiddi, Nucl. Phys. B **664**, 341 (2003).
- [111] R. Bonciani, P. Mastrolia, and E. Remiddi, Nucl. Phys. B **676**, 399 (2004).
- [112] E. Remiddi and J. A. M. Vermaseren, Int. J. Mod. Phys. A **15**, 725 (2000).
- [113] T. Gehrmann and E. Remiddi, Comput. Phys. Commun. **141**, 296 (2001).
- [114] R. A. Swainson and G. W. F. Drake, J. Phys. A **24**, 79 (1991).
- [115] R. A. Swainson and G. W. F. Drake, J. Phys. A **24**, 95 (1991).
- [116] H. A. Bethe and E. E. Salpeter, *Quantum Mechanics of One- and Two-Electron Atoms* (Springer, Berlin, 1957).

- [117] U. D. Jentschura, E.-O. Le Bigot, P. Indelicato, P. J. Mohr, and G. Soff, Phys. Rev. Lett. **90**, 163001 (2003).
- [118] L. G. Afanasyev, A. S. Chvyrov, O. E. Gorchakov, M. A. Ivanov, V. V. Karpukhin, A. V. Kolomyichenko, V. I. Komarov, V. V. Kruglov, A. V. Kuptsov, L. L. Nemenov, M. V. Nikitin, Z. P. Pustynnik, A. V. Kulikov, S. V. Trusov, V. V. Yazkov, G. G. Mkrtchyan, and A. P. Kurov, Phys. Lett. B **308**, 200 (1993).
- [119] L. G. Afanasyev, A. S. Chvyrov, O. E. Gorchakov, V. V. Karpukhin, A. V. Kolomyichenko, V. I. Komarov, V. V. Kruglov, A. V. Kuptsov, L. L. Nemenov, M. V. Nikitin, Z. P. Pustynnik, A. V. Kulikov, S. V. Trusov, and V. V. Yazkov, Phys. Lett. B **308**, 478 (1994).
- [120] A. Heim, K. Hencken, D. Trautmann, and G. Baur, J. Phys. B **34**, 3763 (2001).
- [121] A. Klein and J. Rafelski, Phys. Rev. D **11**, 300 (1975).
- [122] M. Bawin and J. P. Lavine, Phys. Rev. D **12**, 1192 (1975).
- [123] A. Klein and J. Rafelski, Phys. Rev. D **12**, 1194 (1975).
- [124] W. Fleischer and G. Soff, Z. Naturforschung **101**, 703 (1984).
- [125] G. Lach and K. Pachucki, Phys. Rev. A **64**, 042510 (2001).
- [126] V. B. Berestetskii, E. M. Lifshitz, and L. P. Pitaevskii, *Quantenelektrodynamik (Band IV der Lehrbuchreihe über Theoretische Physik von L. D. Landau und E. M. Lifshitz)*, 7 ed. (Akademie-Verlag, Berlin, 1991).
- [127] W. A. Barker and F. N. Glover, Phys. Rev. **99**, 317 (1955).
- [128] E. Brezin, C. Itzykson, and J. Zinn-Justin, Phys. Rev. D **1**, 2349 (1969).
- [129] A. Nandy, Phys. Rev. D **5**, 1531 (1972).
- [130] D. A. Owen, Found. Phys. **24**, 273 (1994).
- [131] M. Halpert and D. A. Owen, J. Phys. G **20**, 51 (1994).
- [132] W. Heitler, *Quantum Theory of Radiation* (Oxford University Press, New York, 1950).
- [133] J. J. Sakurai, *Advanced Quantum Mechanics* (Addison-Wesley, Reading, MA, 1967).
- [134] G. Pustovalov, Zh. Éksp. Teor. Fiz. **32**, 1519 (1957), [JETP **5**, 1234 (1957)].
- [135] E. Borie and G. A. Rinker, Rev. Mod. Phys. **54**, 67 (1982).
- [136] D. Eiras and J. Soto, Phys. Rev. Lett. **491**, 101 (2000).
- [137] D. Eiras and J. Soto, Phys. Rev. D **61**, 114027 (2000).
- [138] P. Labelle and K. Buckley, e-print hep-ph/9804201.
- [139] J. Gasser, V. E. Lyubovitskij, A. Rusetzky, and A. Gall, Phys. Rev. D **64**, 016008 (2001).
- [140] A. N. Artemyev, V. M. Shabaev, and V. A. Yerokhin, Phys. Rev. A **52**, 1884 (1995).
- [141] A. N. Artemyev, V. M. Shabaev, and V. A. Yerokhin, J. Phys. B **28**, 5201 (1995).
- [142] V. M. Shabaev, A. N. Artemyev, T. Beier, and G. Soff, J. Phys. B **31**, L337 (1998).
- [143] V. M. Shabaev, A. N. Artemyev, T. Beier, G. Plunien, V. A. Yerokhin, and G. Soff, Phys. Rev. A **57**, 4235 (1998).
- [144] K. Pachucki and H. Grotch, Phys. Rev. A **51**, 1854 (1995).
- [145] A. S. Yelkhovsky, JETP **86**, 472 (1998).

- [146] T. Beier and G. Soff, Z. Phys. D **8**, 129 (1988).
- [147] S. M. Schneider, W. Greiner, and G. Soff, J. Phys. B **26**, L529 (1993).
- [148] S. G. Karshenboim, JETP **76**, 541 (1993), [ZhETF **103**, 1105 (1993)].
- [149] I. Goidenko, L. Labzowsky, A. Nefiodov, G. Plunien, and G. Soff, Phys. Rev. Lett. **83**, 2312 (1999).
- [150] S. Mallampalli and J. Sapirstein, Phys. Rev. Lett. **80**, 5297 (1998).
- [151] V. A. Yerokhin, Phys. Rev. A **62**, 012508 (2000).
- [152] V. A. Yerokhin and V. M. Shabaev, Phys. Rev. A **64**, 062507 (2001).
- [153] T. Stöhlker, P. H. Mokler, F. Bosch, R. W. Dunford, F. Franzke, O. Klepper, C. Kozhuharov, T. Ludziejewski, F. Nolden, H. Reich, P. Rymuza, Z. Stachura, M. Steck, P. Swiat, and A. Warczak, Phys. Rev. Lett. **85**, 3109 (2000).
- [154] P. J. Mohr and G. Soff, Phys. Rev. Lett. **70**, 158 (1993).
- [155] G. H. Hardy, *Divergent Series* (Clarendon Press, Oxford, UK, 1949).
- [156] E. J. Weniger, Comput. Phys. Rep. **10**, 189 (1989).
- [157] V. Franceschini, V. Grecchi, and H. J. Silverstone, Phys. Rev. A **32**, 1338 (1985).
- [158] E. Caliceti, V. Grecchi, and M. Maioli, Commun. Math. Phys. **104**, 163 (1986).
- [159] E. Caliceti, V. Grecchi, and M. Maioli, Commun. Math. Phys. **157**, 347 (1993).
- [160] E. Caliceti, J. Phys. A **33**, 3753 (2000).
- [161] T. Carleman, *Les Fonctions Quasi-Analytiques* (Gauthiers-Villars, Paris, 1926).
- [162] J. L. Kneur and D. Reynaud, e-print hep-th/0111120.
- [163] S. Graffi, V. Grecchi, and B. Simon, Phys. Lett. B **32**, 631 (1970).
- [164] M. Reed and B. Simon, *Methods of Modern Mathematical Physics IV: Analysis of Operators* (Academic Press, New York, 1978).
- [165] C. M. Bender and S. A. Orszag, *Advanced Mathematical Methods for Scientists and Engineers* (McGraw-Hill, New York, NY, 1978).
- [166] J. Fischer, Int. J. Mod. Phys. A **12**, 3625 (1997).
- [167] L. D. Landau and E. M. Lifshitz, *Quantum Mechanics* (Volume 3 of the Course of Theoretical Physics) (Pergamon Press, London, 1958).
- [168] L. D. Landau and E. M. Lifshitz, *Quantenmechanik (Band III der Lehrbuchreihe über Theoretische Physik von L. D. Landau und E. M. Lifshitz)* (Akademie-Verlag, Berlin, 1979).
- [169] E. Caliceti, V. Grecchi, and M. Maioli, Commun. Math. Phys. **113**, 625 (1988).
- [170] E. Caliceti, V. Grecchi, and M. Maioli, Commun. Math. Phys. **176**, 1 (1996).
- [171] J. Zinn-Justin, J. Math. Phys. **22**, 511 (1981).
- [172] J. Zinn-Justin, Nucl. Phys. B **192**, 125 (1981).
- [173] J. Zinn-Justin, Nucl. Phys. B **218**, 333 (1983).
- [174] J. Zinn-Justin, J. Math. Phys. **25**, 549 (1984).
- [175] F. Pham, *Resurgence, Quantized Canonical Transformation and Multi-Instanton*, Algebraic Analysis, vol. II (1988); C. R. Acad. Sci. Paris **309**, 999 (1989).

- [176] E. Delabaere and H. Dillinger, Ph.D. thesis, University of Nice, Nice, 1991 (unpublished).
- [177] B. Candelpergher, J. C. Nosmas, and F. Pham, *Approche de la Résurgence* (Hermann, Paris, 1993).
- [178] G. A. Baker, *Essentials of Padé approximants* (Academic Press, New York, 1975).
- [179] G. A. Baker and P. Graves-Morris, *Padé Approximants*, 2nd ed. (Cambridge University Press, Cambridge, 1996).
- [180] C. Brezinski and M. Redivo-Zaglia, *Extrapolation Methods* (North-Holland, Amsterdam, 1991).
- [181] G. A. Baker, Adv. Theor. Phys. **1**, 1 (1965).
- [182] *The Padé Approximant in Theoretical Physics*, edited by G. A. Baker and J. L. Gammel (Academic Press, New York, 1970).
- [183] J. L. Basdevant, Fortschr. Physik **20**, 283 (1972).
- [184] G. A. Baker, *Quantitative theory of critical phenomena* (Academic Press, San Diego, 1990).
- [185] M. Abramowitz and I. A. Stegun, *Handbook of Mathematical Functions*, 10 ed. (National Bureau of Standards, Washington, D. C., 1972).
- [186] E. J. Weniger, J. Čížek, and F. Vinette, J. Math. Phys. **34**, 571 (1993).
- [187] C. Brezinski, *Padé-type Approximation and General Orthogonal Polynomials* (Birkhäuser, Basel, 1980).
- [188] C. Brezinski, *Accélération de la Convergence en Analyse Numérique* (Springer, Berlin, 1977).
- [189] C. Brezinski, *Algorithmes d'Accélération de la Convergence – Étude Numérique* (Editions Technip, Paris, 1978).
- [190] C. Brezinski, *Projection Methods for Systems of Equations* (Elsevier, Amsterdam, 1997).
- [191] J.-P. Delahaye, *Sequence Transformations* (Springer, Berlin, 1988).
- [192] C. B. Liem, T. Lü, and T. M. Shih, *The Splitting Extrapolation Method* (World Scientific, Singapore, 1995).
- [193] G. I. Marchuk and V. V. Shaidurov, *Difference Methods and Their Extrapolations* (Springer, New York, 1983).
- [194] G. Walz, *Asymptotics and Extrapolation* (Akademie-Verlag, Berlin, 1996).
- [195] J. Wimp, *Sequence Transformations and Their Applications* (Academic Press, New York, NY, 1981).
- [196] C. Brezinski, J. Comput. Appl. Math. **12–13**, 19 (1985).
- [197] D. S. Gaunt and A. J. Guttmann, in *Phase Transitions and Critical Phenomena 3*, edited by C. Domb and M. S. Green (Academic Press, London, 1974), p. 181.
- [198] A. J. Guttmann, in *Phase Transitions and Critical Phenomena*, edited by C. Domb and J. L. Lebowitz (Academic Press, London, 1989), pp. 3–234.
- [199] P. Wynn, Math. Tables Aids Comput. **10**, 91 (1956).
- [200] B. C. Carlson, *Special Functions of Applied Mathematics* (Academic Press, New York, 1977).
- [201] D. Levin, Int. J. Comput. Math. B **3**, 371 (1973).
- [202] D. A. Smith and W. F. Ford, SIAM J. Numer. Anal. **16**, 223 (1979).
- [203] D. A. Smith and W. F. Ford, Math. Comput. **38**, 481 (1982).
- [204] E. J. Weniger, in *Nonlinear Numerical Methods and Rational Approximation*, edited by A. Cuyt (Kluwer, Dordrecht, 1994), Vol. II, pp. 269–282.

- [205] H. H. H. Homeier and E. J. Weniger, *Comput. Phys. Commun.* **92**, 1 (1995).
- [206] E. J. Weniger, *Comput. Phys.* **10**, 496 (1996).
- [207] E. J. Weniger, *J. Comput. Appl. Math.* **32**, 291 (1990).
- [208] E. J. Weniger and J. Čížek, *Comput. Phys. Commun.* **59**, 471 (1990).
- [209] D. Roy, R. Bhattacharya, and S. Bhowmick, *Comput. Phys. Commun.* **93**, 159 (1996).
- [210] R. Bhattacharya, D. Roy, and S. Bhowmick, *Comput. Phys. Commun.* **101**, 213 (1997).
- [211] E. J. Weniger, *Phys. Rev. A* **56**, 5165 (1997).
- [212] E. J. Weniger, *Numer. Algor.* **3**, 477 (1992).
- [213] E. J. Weniger, J. Čížek, and F. Vinette, *Phys. Lett. A* **156**, 169 (1991).
- [214] E. J. Weniger, *Int. J. Quantum Chem.* **57**, 265 (1996).
- [215] E. J. Weniger, *Ann. Phys. (N.Y.)* **246**, 133 (1996).
- [216] E. J. Weniger, *Phys. Rev. Lett.* **77**, 2859 (1996).
- [217] D. Roy, R. Bhattacharya, and S. Bhowmick, *Comput. Phys. Commun.* **113**, 131 (1998).
- [218] A. Sidi, *J. Comput. Appl. Math.* **7**, 37 (1981).
- [219] A. van Wijngaarden, in *Cursus: Wetenschappelijk Rekenen B, Process Analyse* (Stichting Mathematisch Centrum, Amsterdam, 1965), pp. 51–60.
- [220] T. J. Bromwich, *An Introduction to the Theory of Infinite Series*, 3 ed. (Chelsea, New York, NY, 1991).
- [221] K. Knopp, *Theorie und Anwendung der unendlichen Reihen* (Springer, Berlin, 1964).
- [222] J. W. Daniel, *Math. Comput.* **23**, 91 (1969).
- [223] N. L. Johnson, S. Kotz, and A. W. Kemp, *Univariate discrete distributions, Wiley series in probability and mathematical statistics* (J. Wiley & Sons, New York, 1992).
- [224] B. B. Mandelbrot, *The fractal geometry of nature* (W. H. Freeman, San Francisco, 1983).
- [225] I. J. Good, *Biometrika* **40**, 237 (1953).
- [226] C. Truesdell, *Ann. Math.* **46**, 144 (1945).
- [227] K. B. Kulasekera and D. W. Tonkyn, *Commun. Stat. Sim.* **21**, 499 (1992).
- [228] L. G. Doray and A. Luong, *Commun. Stat. Sim.* **26**, 1075 (1997).
- [229] G. Gamow and M. Yčas, *Proc. Natl. Acad. Sci. USA* **41**, 1011 (1955).
- [230] R. N. Mantegna, S. V. Buldyrev, A. L. Goldberger, S. Havlin, C. K. Peng, M. Simons, and H. E. Stanley, *Phys. Rev. Lett.* **73**, 3169 (1994).
- [231] A. K. Konopka and C. Martindale, *Science* **268**, 789 (1995).
- [232] C. Martindale and A. K. Konopka, *Computers Chem.* **20**, 35 (1996).
- [233] S. V. Aksenov, internet homepage:
<http://aksenov.freeshell.org/>.
- [234] See the URL <http://tqd1.physik.uni-freiburg.de/~ulj>.
- [235] D. H. Bailey, *A Fortran-90 based multiprecision system*, NASA Ames Tech. Rep. RNR-94-013.
- [236] D. H. Bailey, J. M. Borwein, and R. Girgensohn, *Exp. Math.* **3**, 17 (1994).

- [237] D. H. Bailey, *A portable high performance multiprecision package*, NASA Ames Tech. Rep. RNR-90-022.
- [238] D. H. Bailey, ACM Trans. Math. Soft. **19**, 288 (1993).
- [239] J. Becher, *Master Thesis: Numerical Convergence Acceleration Techniques and Their Application in Theoretical Physics (in German)*.
Available at <http://www.physik.tu-dresden.de/publik/diplom.htm#Dipl.ITP>
(Technische Universität Dresden, 1999, unpublished).
- [240] J. P. Dempsey, L. M. Keer, N. B. Patel, and M. L. Glasser, ASME J. Appl. Mech. **51**, 324 (1984).
- [241] D. A. Macdonald, Math. Comput. **66**, 1619 (1997).
- [242] P. Baratella and R. Gabutti, J. Comput. Appl. Math. **62**, 181 (1995).
- [243] J. Boersma and J. P. Dempsey, Math. Comput. **59**, 157 (1992).
- [244] W. Gautschi, Math. Comput. **57**, 325 (1991).
- [245] K. M. Dempsey, D. Liu, and J. P. Dempsey, Math. Comput. **55**, 693 (1990).
- [246] P. Appell and J. K. de Fariet, *Fonctions Hypergéométriques et Hypersphériques Polynômes d'Hermite* (Gauthiers-Villars, Paris, 1926).
- [247] F. D. Colavecchia, G. Gasaneo, and J. E. Miraglia, Comput. Phys. Commun. **138**, 29 (2001).
- [248] J. L. Burchnall and T. W. Chaundy, Quart. J. Math. (Oxford) **11**, 248 (1940).
- [249] J. L. Burchnall and T. W. Chaundy, Quart. J. Math. (Oxford) **12**, 112 (1941).
- [250] J. C. LeGuillou and J. Zinn-Justin, *Large-Order Behaviour of Perturbation Theory* (North-Holland, Amsterdam, 1990).
- [251] J. Stark, Berl. Ber. **1913**, 932 (1913).
- [252] A. LoSurdo, Atti R. Accad. Lincei **22**, 664 (1913).
- [253] H. Silverstone, Phys. Rev. A **18**, 1853 (1978).
- [254] L. Benassi, V. Grecchi, E. Harrell, and B. Simon, Phys. Rev. Lett. **42**, 704 (1979).
- [255] G. V. Dunne and T. M. Hall, Phys. Rev. D **60**, 065002 (1999).
- [256] H. S. Silverstone and P. M. Koch, J. Phys. B **12**, L537 (1979).
- [257] J. R. Oppenheimer, Phys. Rev. **31**, 66 (1928).
- [258] M. H. Alexander, Phys. Rev. **178**, 34 (1969).
- [259] M. Hehenberger, H. V. McIntosh, and E. Brändas, Phys. Rev. A **10**, 1494 (1974).
- [260] N. A. Gushina and V. K. Nikulin, Chem. Phys. **10**, 23 (1975).
- [261] P. Froelich and E. Brändas, Phys. Rev. A **12**, 1 (1975).
- [262] R. J. Damburg and V. V. Kolosov, J. Phys. B **9**, 3149 (1976).
- [263] T. Yamabe, A. Tachibana, and H. J. Silverstone, Phys. Rev. A **16**, 877 (1977).
- [264] R. J. Damburg and V. V. Kolosov, J. Phys. B **11**, 1921 (1978).
- [265] S. Graffi and V. Grecchi, Commun. Math. Phys. **62**, 83 (1978).
- [266] I. W. Herbst and B. Simon, Phys. Rev. Lett. **41**, 67 (1978).
- [267] L. Benassi, V. Grecchi, E. Harrell, and B. Simon, Phys. Rev. Lett. **42**, 1430 (Erratum) (1979).

- [268] R. J. Damburg and V. V. Kolosov, J. Phys. B **12**, 2637 (1979).
- [269] H. Silverstone, B. G. Adams, J. Čížek, and P. Otto, Phys. Rev. Lett. **43**, 1498 (1979).
- [270] J. E. Avron, B. G. Adams, J. Čížek, M. Clay, M. L. Glasser, P. Otto, J. Paldus, and E. Vrscay, Phys. Rev. Lett. **43**, 691 (1979).
- [271] B. G. Adams, J. E. Avron, J. Čížek, P. Otto, J. Paldus, R. K. Moats, and H. J. Silverstone, Phys. Rev. A **21**, 1914 (1980).
- [272] L. Benassi and V. Grecchi, J. Phys. B **13**, 911 (1980).
- [273] E. Luc-Koenig and A. Bachelier, J. Phys. B **13**, 1743 (1980).
- [274] E. Luc-Koenig and A. Bachelier, J. Phys. B **13**, 1769 (1980).
- [275] H. J. Silverstone, E. Harrell, and C. Grot, Phys. Rev. A **24**, 1925 (1981).
- [276] A. Maquet, S. I. Chu, and W. P. Reinhardt, Phys. Rev. A **27**, 2946 (1983).
- [277] D. Farrelly and W. P. Reinhardt, J. Phys. B **16**, 2103 (1983).
- [278] W. L. Glab, K. Ng, D. Yao, and M. H. Nayfeh, Phys. Rev. A **31**, 3677 (1985).
- [279] V. V. Kolosov, J. Phys. B **20**, 2359 (1987).
- [280] V. V. Kolosov, J. Phys. B **22**, 833 (1989).
- [281] G. Alvarez and H. J. Silverstone, Phys. Rev. Lett. **63**, 1364 (1989).
- [282] G. Alvarez, R. J. Damburg, and H. J. Silverstone, Phys. Rev. A **44**, 3060 (1991).
- [283] F. M. Fernández, J. Phys. A **25**, 495 (1992).
- [284] C. A. Nicolaides and S. I. Themelis, Phys. Rev. A **45**, 349 (1992).
- [285] G. Alvarez and H. J. Silverstone, Phys. Rev. A **50**, 4679 (1994).
- [286] J. Zamastil, J. Čížek, and L. Skála, Phys. Rev. Lett. **84**, 5683 (2000).
- [287] P. M. Koch, Phys. Rev. Lett. **41**, 99 (1978).
- [288] T. Bergeman, C. Harvey, K. B. Butterfield, H. C. Bryant, D. A. Clark, P. A. M. Gram, D. MacArthur, M. Davis, J. B. Donahue, J. Dayton, and W. W. Smith, Phys. Rev. Lett. **53**, 775 (1984).
- [289] W. L. Glab and M. N. Nayfeh, Phys. Rev. A **31**, 530 (1985).
- [290] H. Rottke and K. H. Welge, Phys. Rev. A **33**, 301 (1986).
- [291] R. Seznec and J. Zinn-Justin, J. Math. Phys. **20**, 1398 (1979).
- [292] J. C. LeGuillou and J. Zinn-Justin, Ann. Phys. (N.Y.) **147**, 57 (1983).
- [293] R. Guida, K. Konishi, and H. Suzuki, Ann. Phys. (N.Y.) **241**, 152 (1995).
- [294] R. Guida, K. Konishi, and H. Suzuki, Ann. Phys. (N.Y.) **249**, 109 (1996).
- [295] M. Pindor, e-print hep-th/9903151.
- [296] P. A. Rączka, Phys. Rev. D **43**, R9 (1991).
- [297] J. Zinn-Justin, *Quantum Field Theory and Critical Phenomena*, 3rd ed. (Clarendon Press, Oxford, 1996).
- [298] A. van Wijngaarden, B.I.T. **6**, 66 (1966).
- [299] I. Caprini and J. Fischer, Phys. Rev. D **60**, 054014 (1999).

- [300] I. Caprini and J. Fischer, Phys. Rev. D **62**, 054007 (2000).
- [301] J. C. LeGuillou and J. Zinn-Justin, Phys. Rev. B **21**, 3976 (1980).
- [302] V. B. Berestetskii, E. M. Lifshitz, and L. P. Pitaevskii, *Quantenelektrodynamik (Band IVb der Lehrbuchreihe über Theoretische Physik von L. D. Landau und E. M. Lifshitz)*, 1 ed. (Akademie-Verlag, Berlin, 1973).
- [303] W. Greiner and J. Reinhardt, *Quantum Electrodynamics* (Springer, New York, 1992).
- [304] W. Dittrich and H. Gies, *Probing the Quantum Vacuum – Tracts in Physics Vol. 166* (Springer, Berlin, Heidelberg, New York, 2000).
- [305] W. Heisenberg and H. Euler, Z. Phys. **98**, 714 (1936).
- [306] V. Weisskopf, Dan. Mat. Fys. Medd. **14**, 1 (1936).
- [307] J. Schwinger, Phys. Rev. **82**, 664 (1951).
- [308] Z. Białynicka-Birula and I. Białynicki-Birula, Phys. Rev. D **2**, 2341 (1970).
- [309] W. Dittrich and M. Reuter, *Effective Lagrangians in Quantum Electrodynamics – Lecture Notes in Physics Vol. 220* (Springer, Berlin, Heidelberg, New York, 1985).
- [310] V. I. Ogievetsky, Proc. Acad. Sci. USSR **109**, 919 (1956), [in Russian].
- [311] L. N. Lipatov, Pis'ma Zh. Éksp. Teor. Fiz. **24**, 179 (1976), [JETP Lett. **24**, 157 (1976)].
- [312] L. N. Lipatov, Zh. Éksp. Teor. Fiz. **71**, 2010 (1976), [JETP **44**, No. 6 (1977)].
- [313] L. N. Lipatov, Zh. Éksp. Teor. Fiz. **72**, 411 (1977), [JETP **45**, 216 (1977)].
- [314] C. Itzykson, G. Parisi, and J. B. Zuber, Phys. Rev. D **16**, 996 (1977).
- [315] R. Balian, C. Itzykson, J. B. Zuber, and G. Parisi, Phys. Rev. D **17**, 1041 (1978).
- [316] D. Broadhurst and D. Kreimer, Phys. Lett. B **475**, 63 (2000).
- [317] D. Broadhurst and D. Kreimer, Nucl. Phys. B **600**, 403 (2001).
- [318] L. Boutet de Monvel (Ed.), *Méthodes Résurgentes* (Hermann, Paris, 1994).
- [319] L. F. Richardson, Phil. Trans. Roy. Soc. London A **226**, 229 (1927).
- [320] F. J. Dyson, Phys. Rev. **85**, 32 (1952).

DANKSAGUNG

Herrn Prof. Dr. Gerhard Soff möchte ich sehr herzlich für die immerwährende Unterstützung meiner Arbeit danken und dabei die vielen hilfreichen Diskussionen nicht unerwähnt lassen. Sein nie nachlassendes Interesse an den zu untersuchenden Fragestellungen, seine Hilfsbereitschaft sowie die vielfache Unterstützung meiner Forschungsaktivitäten in Rat und Tat haben wesentlich zum Gelingen dieser Arbeit beigetragen.

Weiterhin gilt mein Dank allen Kollegen aus der Arbeitsgruppe “Theorie der Hadronen und Kerne” am Institut für Theoretische Physik der Technischen Universität Dresden. Die freundliche Atmosphäre am Institut hat sich sehr positiv auf das Gelingen der vielfältigen Forschungsprojekte ausgewirkt. In diesem Zusammenhang möchte ich besonders den Institutssekretärinnen G. Schädlich, G. Latus und U. Wächtler an dieser Stelle recht herzlich danken.

Es ist mir eine besondere Freude, die wissenschaftlichen Kooperations-Partner an dieser Stelle zu erwähnen, mit denen ich das Vergnügen und das Glück hatte, im Laufe der Arbeiten zusammenzukommen. Die Diskussionen waren Anlaß zu höchster intellektueller Freude und trugen wesentlich zum Genuß der wissenschaftlichen Arbeit bei. Man könnte behaupten, ein wichtiger Aspekt Wissenschaft werde in guter Näherung gerade durch die Diskussion und den sozialen Prozeß des Austauschs der Gedanken *definiert*, und/oder der Austausch der Gedanken *sei* die Wissenschaft. Erwähnt seien an dieser Stelle Frau Prof. Dr. Emanuela Caliceti, Herr Prof. Dr. Victor Elias, Herr Dr. Holger Gies, Herr Prof. Dr. Vincenzo Grechi, Herr Prof. Dr. Barry R. Holstein, Herr Prof. Dr. Paul J. Indelicato, Herr Dr. F. Krauss, Herr Prof. Dr. Darrell R. Lamm, Herr Dr. Michael Meyer-Hermann, Herr Dr. Peter J. Mohr, Herr Priv.-Doz. Dr. Krzysztof Pachucki, Herr Priv.-Doz. Dr. Günter Plunien, Herr Prof. Dr. Vladimir M. Shabaev, Herr Prof. Dr. Sreeram Valluri, Herr Priv.-Doz. Dr. Ernst Joachim Weniger, Herr Dr. Vladimir A. Yerokhin, sowie in besonderem Maße Herr Prof. Dr. Jean Zinn-Justin.

Herrn Dr. J. Sims vom National Institute of Standards and Technology sei herzlich gedankt für seine Hilfe bei der Entwicklung von parallelen Rechenprogrammen mit Hilfe des MPI Message Passing Interface.

Besonderer Dank gilt auch meinen Eltern für wichtige Unterstützung und Hilfe. Schließlich gilt Sabine mein ganz besonderer Dank für Ihre immerwährende Unterstützung, ihre Geduld und ihre Hingabe.

This work is based on a Habilitation Thesis which was submitted to the University of Technology, Dresden, on 26 June 2002. It was defended on 14 April 2003. The current version is not identical to the habilitation thesis submitted to Dresden University of Technology; it contains hyperreferences and updates, and in addition a number of typographical errors present in the original Thesis have been eliminated. Numerical results in Eqs. (2.14)–(2.53) are in agreement with recently available data as reported in [U. D. Jentschura, E.-O. Le Bigot, P. Indelicato, P. J. Mohr and G. Soff, Asymptotic Properties of Self-Energy Coefficients, e-print physics/0304042, Phys. Rev. Lett. **90**, 163001 (2003), and E.-O. Le Bigot, U. D. Jentschura, P. Indelicato, P. J. Mohr and G. Soff, e-print physics/0304068, Phys. Rev. A **68**, 042101 (2003)]. A number of biographic references (e.g. [30, 31, 109, 110, 111, 117]) have been updated, and some section headings have been edited in order to be conformal with the hypertext standard for electronic documents (mathematical expressions cannot be used within pdf-bookmarks).

This thesis is the third in the traditional threefold sequence “diploma(master)–dissertation(PhD)–habilitation” that is being followed in Continental Europe. Copies of the author’s PhD thesis are available as U. D. Jentschura, “Quantum Electrodynamical Radiative Corrections in Bound Systems (Dresdner Forschungen: Theoretische Physik, Band 2)”, w.e.b. Universitätsverlag, Dresden, 1999 (ISBN: 3-933592-65-8), 225 pages (address of w.e.b. Publishers: Bergstraße 78, 01069 Dresden, Germany, world-wide web address: <http://www.web-univerlag.de>, electronic-mail address: mail@web-univerlag.de). This habilitation thesis is also available – in the form of a book – from Shaker Verlag GmbH, Postfach 101818, 52018 Aachen, Germany (world-wide web address: <http://www.shaker.de>, electronic-mail address: info@shaker.de). Further inquiries and questions are always welcome (email: jentschura@physik.uni-freiburg.de or U. D. Jentschura, Physikalisches Institut, Universität Freiburg, Hermann-Herder-Straße 3, 79104 Freiburg im Breisgau, Germany).